DTIC
ELECTE
DEC 2 3 1993
A

EVALUATION OF MODERATE ANGLE OF ATTACK ROLL
OF A
DUAL ENGINE, THRUST VECTORING AIRCRAFT
USING QUANTITATIVE FEEDBACK THEORY

THESIS

Kevin E. Boyum
Captain, USAF

AFIT/GE/ENG/93D-01

93-30961

93 12 22 085

DEPARTMENT OF THE AIR FORCE
AIR UNIVERSITY

AIR FORCE INSTITUTE OF TECHNOLOGY

Wright-Patterson Air Force Base, Ohio

AFIT/GE/ENG/93D-01

DTIC
ELECTE
DEC 23 1993
S
A

**EVALUATION OF MODERATE ANGLE OF ATTACK ROLL
OF A
DUAL ENGINE, THRUST VECTORING AIRCRAFT
USING QUANTITATIVE FEEDBACK THEORY**

THESIS

Kevin E. Boyum
Captain, USAF

AFIT/GE/ENG/93D-01

DTIC QUALITY INSPECTED 3

Approved for public release; distribution unlimited

EVALUATION OF A MODERATE ANGLE OF ATTACK ROLL

OF A

DUAL ENGINE, THRUST VECTORING AIRCRAFT

USING QUANTITATIVE FEEDBACK THEORY

THESIS

Presented to the Faculty of the Graduate School of Engineering

of the Air Force Institute of Technology

Air University

In Partial Fulfillment of the

Requirements for the Degree of

Master of Science in Electrical Engineering

Kevin E. Boyum, B.S.E.E.

Captain, USAF

December 1993

Acknowledgments

I would like to thank Dr. Meir Pachter and Dr. Constantine Houpis for their guidance and continued support throughout this thesis. I feel fortunate to have had the opportunity to work with them both for the past year and a half, and to have gained valuable insight into the finer elements of flight control theory. I am also greatly indebted to Stu Sheldon and Steve Rasmusson of the Flight Dynamics Directorate for providing me with the computational resources required for this thesis, as well as invaluable advice. Rich Sating, your MIMO QFT Cad Package has been an indispensabie tool in the thesis, as was Bob's Btocl.

Most importantly, I would like to thank my best friend, fellow student, and wife, Beth, for her continued support, patience and prayers throughout this endeavor. I love you very much, Beth.

Finally, I believe that very little is accomplished in this world without the prayers of family and friends -- thanks to all of you who remembered me in your prayers to our Lord and Savior, Jesus Christ.

<div align="right">Kevin E. Boyum</div>

Table of Contents

List of Figures

List of Tables

Abstract

This thesis develops an innovative approach to the design of a flight control system for performing the large-amplitude velocity vector roll maneuver at high angles of attack (AOAs). A six degree of freedom aircraft model is developed from the fundamental nine-state equations of motion using a modified linearization technique. The MIMO (multiple-input multiple-output) Quantitative Feedback Theory (QFT) robust control design technique is then used to jointly address the system nonlinearities present in this maneuver and the changes in the system parameters due to changes in flight condition, treating them as structured uncertainty in the design of a three-axis rate-commanded control system. The development of a weighting matrix, based on the fundamentals of the aileron-rudder interconnect, aids in this design process. Nonlinear six degree-of-freedom closed-loop control system simulations demonstrate the accuracy of the developed models, the validity of the QFT designed compensator and prefilter, and the successful initiation and arrest of the velocity vector roll maneuver.

EVALUATION OF MODERATE ANGLE OF ATTACK ROLL

OF A

DUAL ENGINE, THRUST VECTORING AIRCRAFT

USING QUANTITATIVE FEEDBACK THEORY

1. Introduction

The combat performance of a fighter aircraft is typically gauged by the aircraft's turning capabilities, which are dictated by the structural and aerodynamic angle of attack (AOA) limits of the aircraft. The designers of today's high performance research and fighter aircraft have significantly extended the structural limits through the use of advanced metallic and composite materials, and are now focusing on the AOA limits of these aircraft. Advanced control hardware, such as thrust vectoring nozzles, have been introduced to provide more control authority at high AOAs, and research has now turned toward the design of flight control systems which can take advantage of this advanced hardware to control high AOA flight. Within the past three years, research aircraft have performed loaded roll maneuvers at AOAs as high as fifty degrees, compared to the previous limits of approximately twenty-five degrees [27]. This performance increase does not, however, come without a price; the flight control systems required to control these aircraft at higher AOAs have become increasingly large and complex. Therefore, to allow for continued performance increases, designers are strongly motivated to explore alternate design techniques which may reduce flight control system complexity without sacrificing performance.

1.1. Background

The flight envelope of a typical high performance fighter aircraft, as shown in Fig. 1, bounds the region of flight for that aircraft. At any operating point within this envelope, a highly coupled, nonlinear, time-varying set of equations, called the equations of motion (EOM), describe the motion of the aircraft.

The coefficients of these EOM exhibit large variations as the operating point changes within the aircraft flight envelope. Theoretically, a different set of equations describes the motion of the aircraft at each operating point within the flight envelope. However, practical flight control design requires specified performance throughout most, if not all, of the flight envelope, and the designer would therefore require an infinite number of operating points. Since this is not mathematically tractable, the designer typically splits the flight envelope into regions of flight, as shown in Fig. 1, and identifies several operating points in each region to serve as the basis of the flight control design.

As the aircraft's flight envelope expands, the number of operating points must also increase. This is especially true in high AOA flight, where the aircraft dynamics change significantly with only a slight change in AOA. To properly account for these changes using the point design methods, the number of operating points in the high AOA region of the flight envelope must increase significantly. The flight control system must be able to manage the transition from one of these operating points to the next, and then be able to manage the structured uncertainty associated with all the operating points in between the design points. In other words, it must provide robust compensation over the entire range of structured parameter uncertainty. The linear multivariable design methods used today do not do this well.
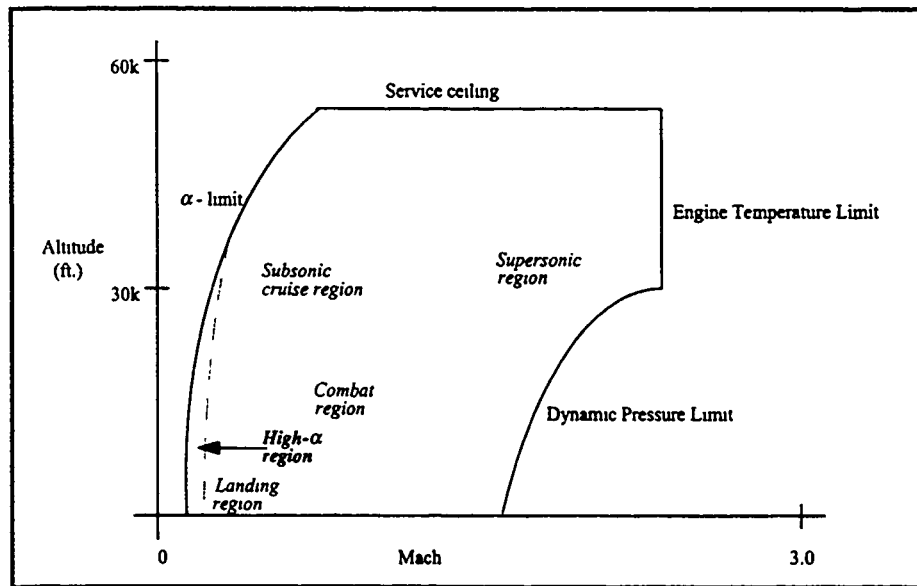
Figure 1. Flight Envelope of a High-Performance Aircraft

2

This is not, unfortunately, the whole story. To use the linear multivariable design techniques at each of the aforementioned operating points, the designer must extract a linear model of the aircraft from the nonlinear EOM. Using standard linearization techniques, this linear model is valid for small perturbations about the *trim* condition at that particular flight condition (F.C.). At most operating points within the flight envelope this linear model provides sufficient fidelity for control system design. In the high AOA region of the flight envelope, however, the robustness of this linear model is significantly reduced due to the highly nonlinear, coupled nature of the EOM at high AOAs. Even very small departures from a high AOA trim condition can violate the integrity of the conventionally obtained linearized model. Designing for *maneuvers* at high AOAs therefore requires a robust control design technique, rendering the linear multivariable point design techniques nearly useless.

For this reason, flight control designers are investigating alternative design techniques for the high AOA region of flight. Enns, et al., [9, 4, 28] have adopted a nonlinear design technique called dynamic inversion which essentially inverts the dynamic nonlinear EOM in order to generate the actuator commands required for desired rates of change of the state variables. The resulting design is a full-envelope control law requiring no gain scheduling. However, the resulting control system requires that the entire aerodynamic data base be stored in the flight control system memory, therefore requiring more memory space than a gain scheduled flight control law! Buffington, et al., [3] are employing a variation of the dynamic inversion method, using dynamic inversion for an inner-loop design. The Mu-synthesis H_∞ design technique is then used to design an outer-loop in an effort to improve the robustness of the design. Finally, Chiang, et al., [5] are attempting to use the linear H_∞ design technique for particular maneuvers.

This thesis introduces an innovative approach to the design of flight control systems for high AOA maneuvering. Quantitative Feedback Theory (QFT), developed by Dr. Isaac Horowitz, is a feedback control design technique capable of guaranteeing *a priori* specified performance in a large problem class where the structured plant parameter variation is uncertain but bounded. By bounding the variations in the aircraft parameters throughout a large amplitude maneuvers at high AOAs, over several F.C.s, the QFT design technique could potentially be used to synthesize a single fixed feedback control law to control an

3

aircraft throughout the maneuvers, *and also* operate over a range of F.C.s, rather than at just one operating point in the flight envelope. In this thesis, QFT is used both to address this uncertainty and to attack the nonlinearities inherent to the high AOA flight regime.

1.2. QFT History

QFT has been shown to provide guaranteed control system performance for a large class of systems with highly uncertain plants (structured plant parameter uncertainty) [8, 15]. The designer can specify the allowable range of system response and, with knowledge only of the range of variation in the plant's parameters, synthesize the compensator required to guarantee the *a priori* specified system performance. This differs from other point design techniques in that every operating point falling within the bounded range of plant variation will have the desired response characteristics, not just the finite number designed for in the point design techniques. In other words, only QFT provides robust compensation over the entire range of structured parameter uncertainty.

In flight control system design, the designer usually has multiple control inputs and multiple outputs to be controlled. This type of system is defined as a multiple-input multiple-output (MIMO) system. In 1963, Dr. Horowitz presented, for the first time, a technique capable of synthesizing a design around uncertain MIMO system plants [13]. This was the first formulation of the QFT family of design techniques. Considerable work in multivariable control system design both preceded and followed the publication of this book, but dealt with design synthesis in cases where the system plant was *known*, that is point designs. In 1979, Dr. Horowitz presented a simpler multivariable design technique, based on his earlier work, for designing feedback around highly uncertain plants [14, 16]. It is now well known as QFT. The essential features of the QFT control design paradigm are [15]:

- It is a frequency domain technique

- The MIMO solution is reduced to a set of multiple-input single-output (MISO) equivalent problems

- The design is tuned to the extent of the structured uncertainty and performance tolerances established *a priori*. Hence, it is quantitative in nature.

4

QFT is particularly attractive for the MIMO control system design case since the design problem can be decomposed into more tractable MISO cases where the design execution is performed on single loop equivalent systems [14]. A quick look at the complexity of even a 3-dimensional MIMO problem shows vividly the significance of this capability.

QFT was, in spite of its demonstrated merit, almost immediately criticized for its inherent non-optimality and overdesign. Dr. Horowitz admitted from the start that the method made no optimality claim [14, 16]. He was quick to point out though that "the technique guarantees a satisfactory design ... by a comparatively straightforward systematic procedure" and no other design technique could make that claim [29].

In later work in 1982, Dr. Horowitz improved his formulation of QFT and proposed a method to reduce the inherent overdesign by making use of the fact that there is some correlation in the uncertainties between the elements of the system plant [15]. Knowledge of this correlation allows the designer to further reduce the loop design bandwidth and thus the overdesign of the final design solution. This improved formulation of the QFT, referred to as Method Two, is presently being used extensively for flight control system design problems at the Air Force Institute of Technology (AFIT). It has been applied quite successfully to a number of very different design problems and aircraft. The following partial list enumerates some of the AFIT thesis efforts in QFT flight control research.

- Arnold -- *FCS Reconfiguration Using QFT* [2]

- Clough -- *Reconfiguration for a STOL Aircraft Using QFT* [6]

- Hamilton -- *QFT Digital Controller for an Unmanned Research Vehicle* [12]

- Migyanko -- *Integrated Flight/Propulsion Control for a STOL Aircraft Using QFT* [18]

- Russell -- *Analog QFT Design for the KC-135* [23]

- Schneider -- *AFTI/F-16 FCS Design Using Digital QFT* [26]

- Wheaton -- *Automatic FCS Design for an Unmanned Research Vehicle using Digital QFT* [29]

QFT is applied to square ($l = m$) system plants with l inputs and m outputs. In flight control design, the designer typically has more control inputs than outputs to be controlled ($l > m$), and a decision must be made as to how to use the extra inputs. This is always the case, regardless of the design technique employed [29]. For the QFT design problem, a $l x m$ weighting matrix W can be used to blend the l inputs into m general inputs. Obviously, the formation of the $m x m$ effective QFT plant (PW) produces a variation of the original system plant and thus proper selection of the weighting matrix is critical in maintaining the integrity of the original plant. A further consideration on the weighting matrix selection is that the determinant of the resulting $m x m$ effective plant is *preferably* minimum-phase (m.p.)or, in other words, the determinant must have no zeros located in the right half s-plane. *Preferably* m.p. implies that certain non-minimum phase (n.m.p.) characteristics can be dealt with.

In one of the first digital QFT flight control system designs, Maj. Arnold used a W matrix of plus ones, zeros, and minus ones whose elements were assigned based solely on physical insight and on the particular aircraft-specific control knowledge [2]. Later, Capt. Clough adjusted the magnitudes of the elements to other than ones and zeros in his W matrix using basically a trial and error procedure. Lt. Hamilton [12] made good progress at identifying some possible analytic approaches to improving the W matrix by a trial and error selection process. The weighting matrix selection for QFT compatibility is probably the single most important part of the overall design effort [20].

1.3. Problem

The high AOA, large-amplitude maneuver to be considered in this thesis is the velocity vector (or stability axis) roll. The velocity vector of an aircraft represents the speed and direction of the center of gravity of the aircraft at any instant in time, and the AOA of an aircraft is defined as the angle included between the aircraft's velocity vector and the aircraft's body x-axis, as shown in Fig. 2. A high AOA velocity vector roll can therefore be defined as the rotation of an aircraft about the axis formed by the aircraft's velocity vector. This maneuver is extremely difficult to control for several reasons. First, an aircraft's control surface deflections, and the adverse yaw phenomenon due to these deflections, provide

6

moments primarily about the aircraft body axes rather than the stability axes. As the aircraft's AOA increases from near zero, the control surfaces' effectiveness decreases (due to the aerodynamics and the seperation of the body and stability axes) and the requirement for control surface management becomes an increasingly difficult, and critical, task. The pitching moment induced by high roll rates creates additional difficulties in controlling the velocity vector roll. Because much of the aircraft's weight is located fore and aft of the center of gravity, normal acceleration tends to draw the nose and tail of the aircraft farther from the axis of rotation, resulting in a positive pitch rate and an increase in AOA. Perhaps the most significant difficulty in designing a controller for a high AOA velocity vector roll is accounting for the nonlinearities introduced into the system by the maneuver itself. These nonlinearities must be present in the aircraft model that is to be used in the control system design. Thus, standard linear aircraft models and standard flight control design techniques that hinge on the seperation of the longitudinal and lateral/directional channels cannot be used.

The purpose of this thesis is therefore three-fold: 1) explore the nonlinearities of a thirty-degree AOA velocity vector roll, 2) develop an aircraft model which accurately represents these nonlinearities, and, using QFT, 3) design a flight control system to control the thrust vectored F-18 High Angle of Attack Research Vehicle (HARV) aircraft through the velocity vector roll maneuver over a range of F.C.s.
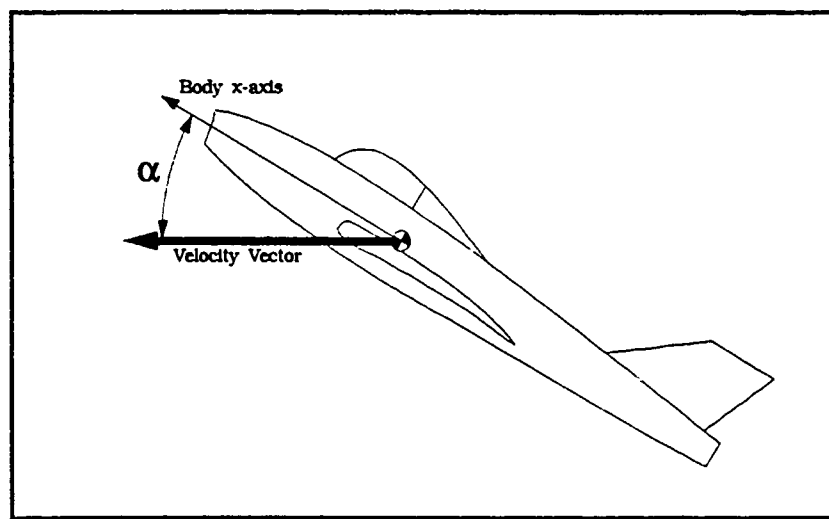
Figure 2. Aircraft Velocity Vector and Angle of Attack (α)

1.4. Scope

This thesis focuses on the development of an aircraft model suitable for velocity vector roll control system analysis and design, and on the design of the flight control system using QFT. Special emphasis is placed on the nonlinear aspects of this design. Therefore, the other source of parameter variation in the QFT model, the range of F.C.s within the high AOA region of the flight envelope, is limited to one AOA, viz., thirty degrees. At this AOA, trim conditions at various altitudes, and therefore at different speeds, can then serve as the source of F.C. parameter variation in the QFT model. Issues associated with the implementation of the flight control system, such as the development of a discrete-time controller, are not addressed in this thesis.

1.5. Approach

The use of the QFT design technique allows both changes in F.C. within the high AOA region of the flight envelope and nonlinearities introduced by the velocity vector roll maneuver to be treated as structured parameter variations (bounded uncertainties). Because the flight envelope region in which high AOA flight can occur is relatively small, and the F.C.s are limited to one AOA, only modest changes in the system parameters due to changes in F.C. are expected. However, the nonlinearities due to large excursions in roll rate and in bank angle throughout the velocity vector roll may not be as well behaved. Therefore, the first phase of this thesis is the development of an aircraft model suitable for a rather unconventional velocity vector roll control system design.

This model can be realized in two steps. First, the full state, nonlinear EOM are partially linearized so that only the nonlinearities due to large excursions in roll rate and in bank angle throughout a velocity vector roll remain. This implies that the EOM must be defined in, or transformed to, the stability axes system (the axes system in which the aircraft's velocity vector lies on the x-axis). The velocity vector roll then involves only pure roll rate and bank angle, versus mixed rates and angles in the body axes system.

According to the QFT methodology, the second step of model development consists of reducing the partially linearized model of step one into a set of linear QFT models which, as a whole, accurately represent the nonlinear system. Because of the computational requirements of the QFT design process,

MIMO QFT has only been applied to 3x3 problems. Rather than venturing into new, higher-order QFT design methods, the nonlinear aircraft model is reduced to several 3x3 linear models. The reduction method used in this thesis involves a time-scale separation of the velocity vector roll. As shown in Figure 3, a velocity vector roll can be split into two primary regions, a transition region and a "free stream" region. In the "free stream" region the roll rate is nearly constant, as are all the other states of the system except the bank angle which may be obtained from the roll rate. The aircraft can therefore be modeled with the standard set of linear equations of motion, and the controls problem can then be treated as an optimal control problem of maximizing roll rate while minimizing excursions in AOA and sideslip with the available control authority. In contrast, the roll rate in the transition region changes dramatically, but in a relatively short amount of time. Because of the short time span of the transition region, the "fast" states of the system (pitch, roll and yaw rates) are dominant. If the pitch and yaw rates are kept to a minimal level, then changes in the corresponding "slower" states (AOA and sideslip) will be negligible and these states can be removed. Therefore, a three degree-of-freedom (DOF) system of the "fast" states can be used in the transition region, allowing the QFT design methodology to be used. For this reason, the scope of this thesis is limited to the initiation and termination phases of the velocity vector roll at moderate AOAs.
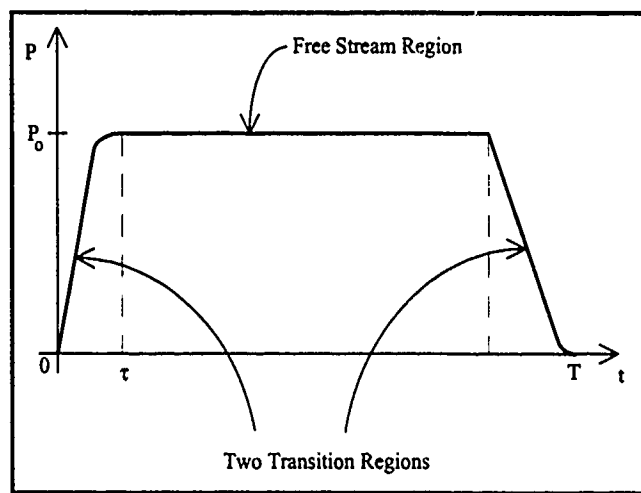
Figure 3. Time-Scale Separation of a Velocity Vector Roll

Because more than three control inputs are available in the HARV aircraft, a weighting matrix must be used to make the system square, that is, 3x3. Therefore, this second step of model development also requires the development of a weighting matrix and the formation of effective plants for the QFT design.

The second phase of this thesis is the design of the QFT compensator and prefilter. The design process involves the following steps:

1. Invert the plant matrices and ensure that the design is still tractable.

2. Define and model the desired design specifications.

3. Design the first loop compensator and prefilter.

4. Design the second and third loop compensators and prefilters using the standard or improved method, depending on the exact nature of the system.

5. Validate the design through a stability analysis and time domain tracking response.

These steps are explained in detail as they are used in the actual design.

The final phase of this thesis is the simulation of the flight control system. Closed-loop systems based on the 3x3 QFT model, and then on the nonlinear model, are modeled and simulated in MATLAB's dynamic simulation environment, Simulink. These simulations demonstrate the effectiveness of the flight control system in controlling the transition regions of a velocity vector roll.

1.6. Assumptions

A number of standard assumptions are generally made in this type of problem to simplify the system. Below is a list of all the assumptions that apply for this study.

- The aircraft mass is constant during command input.

- The aircraft is a rigid body.

- The earth is an inertial reference frame.

- The gravitational acceleration is constant.

- The atmosphere is fixed in relation to the earth and based on the NASA 1962 Standard Atmosphere.

- The aircraft thrust setting and velocity is constant.

10

1.7. Presentation

This thesis contains eight chapters. Chapter 2 presents the development of the partially linearized six DOF aircraft model appropriate to velocity vector design and analysis. Chapter 3 extends the aircraft model development to a three DOF system suitable for the QFT design technique, and presents a weighing matrix strategy. Chapter 4 discusses the QFT theory applicable to this study, Chapter 5 describes the actual QFT cascade compensator and prefilter designs, and Chapter 6 presents the design simulation results. Chapter 7 enhances the performance of the closed-loop system with a modified weighting matrix and compensator, and presents design simulation results for this modified system. Chapter 8 presents a summary of the highlights of the study, the conclusions drawn, and recommendations for future efforts.

1.8. Notation

Some of the standard notation used in this study is given below. This list is not all inclusive. Notation used for the QFT design process is generally standard QFT notation as it appears in the literature, e.g. [8], and its meaning is specified as it appears in this thesis.

- Scalar variables and scalar components of vectors and matrices are denoted by upper or lower case italic type.

- Vectors are denoted by lower and upper case boldface letters.

- Upper case vectors have s-plane transformed elements.

- Lower case vectors have time-domain element variables or are frequency plane elements of a matrix or vector.

- Matrices are denoted by upper case boldface letters.

- Matrices contain either time-domain or frequency-domain elements. $A(t)$ and $A(s)$ denote a matrix with time-domain and s-plane domain elements, respectively.

- When the independent variable is not given, the time-domain is usually assumed unless the frequency-domain is indicated by context.

- $\mathbf{adj}[A]$ denotes the adjoint matrix of A and $\mathbf{adj}_{ij}[A]$ denotes the ij element of $\mathbf{adj}[A]$.

- A^{-1} denotes the inverse of matrix A.

- A^T denotes the transpose of matrix or vector A.

- I_{nxn} denotes the nxn identitiy matrix.

2. The Aircraft

This chapter describes the baseline aircraft used in this study and the development of a partially linearized six DOF model of this aircraft, suitable for velocity vector roll analysis and design. The chapter concludes with an open loop simulation of the six DOF model, for model validation purposes.

2.1. Airframe

The aircraft to be used for this study is the NASA F-18 High Angle of Attack Research Vehicle (HARV). The HARV is a pre-production, single-seat F/A-18 aircraft, on loan to NASA from the US Navy. The HARV's a twin engines have been fitted with two-dimensional thrust vectoring nozzles to provide pitch and yaw moments at high AOA, low dynamic pressure F.C.s where the conventional aerodynamic control effectiveness is inadequate. The basic F-18 system, Fig. 4, has been extensively tested and was shown to be both robust and controllable in the high AOA regime, making the F-18 HARV an excellent platform for high AOA research [21].
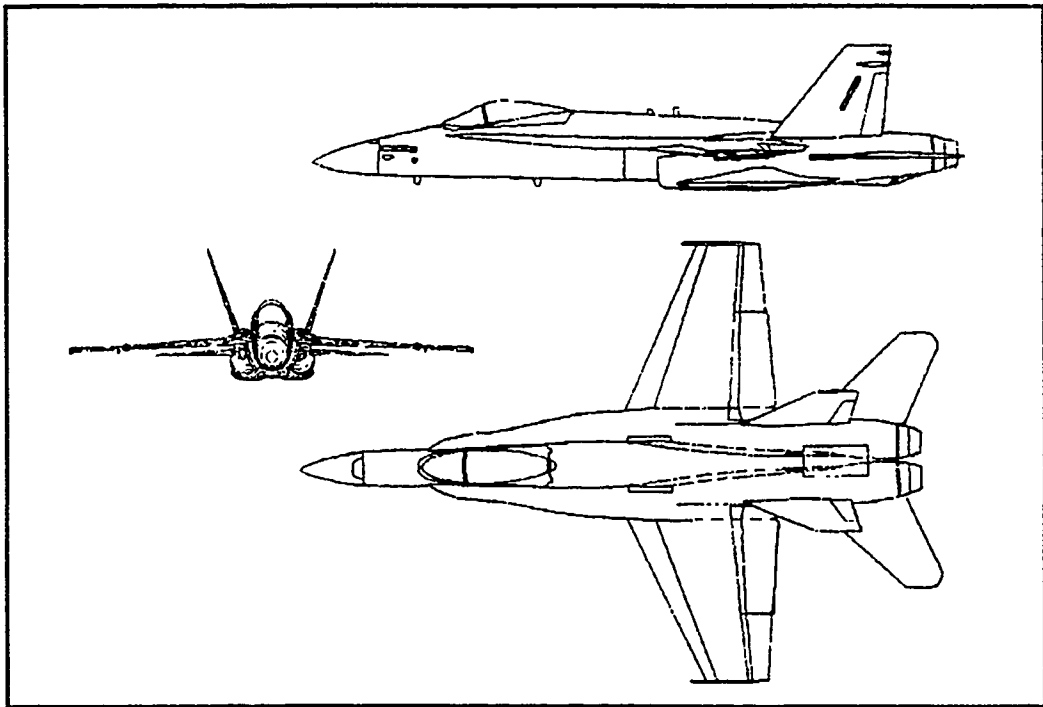
Figure 4. F-18 Aircraft

12

2.2. Nonlinear Model

A nonlinear model of the HARV aircraft is contained in the F-18 HARV Batch Simulation, provided by NASA. This model furnishes the nondimensional stability and control derivatives, and other pertinent aircraft data, to be used in the aircraft models developed in this work.

2.3. Six DOF Model Development

This section presents the development of a general partially linearized six degree of freedom (DOF) aircraft model, suitable for velocity vector roll design and analysis and tailored to the control inputs of the HARV aircraft.

2.3.1. General Model.
To properly account for the nonlinearities present in the system during a velocity vector roll at high AOAs, the system model must be derived from the nine nonlinear body-axes aircraft state equations of motion:

Force Equations

$$\dot{U} = VR - WQ + \tfrac{1}{m}\sum F_x \tag{1}$$

$$\dot{V} = WP - UR + \tfrac{1}{m}\sum F_y \tag{2}$$

$$\dot{W} = UQ - VP + \tfrac{1}{m}\sum F_z \tag{3}$$

Moment Equations

$$\dot{P} = \frac{I_{xz}}{D}(I_x - I_y + I_z)PQ + \frac{1}{D}(I_y I_z - I_z^2 - I_{xz}^2)QR + \frac{I_z}{D}\sum L + \frac{I_{xz}}{D}\sum N \tag{4}$$

$$\dot{Q} = \frac{I_z - I_x}{I_y}PR + \frac{I_{xz}}{I_y}(R^2 - P^2) + \frac{1}{I_y}\sum M \tag{5}$$

$$\dot{R} = \frac{1}{D}(I_x^2 - I_x I_y + I_{xz}^2)PQ + \frac{I_{xz}}{D}(I_y - I_x - I_z)QR + \frac{I_{xz}}{D}\sum L + \frac{I_x}{D}\sum N \tag{6}$$

Kinematic Equations

$$\dot{\theta} = Q\cos\phi - R\sin\phi \tag{7}$$

$$\dot{\phi} = P + Q\sin\phi\tan\theta + R\cos\phi\tan\theta \qquad (8)$$

$$\dot{\psi} = Q\frac{\sin\phi}{\cos\theta} + R\frac{\cos\phi}{\cos\theta} \qquad (9)$$

where the definition $D \equiv I_x I_z - I_{xz}^2$ is used. Both the force and moment state equations have aerodynamic and control input contributions which are accounted for with aerodynamic and control derivatives. Each derivative represents the change in that particular force or moment due to small aerodynamic or control surface perturbations. These derivatives can be estimated theoretically or measured in wind tunnel tests, and are symbolically represented in the following force and moment summation equations:

$$\sum L = \bar{q}Sb\left(\frac{b}{2U}C_{l_p}P + \frac{b}{2U}C_{l_r}R + C_{l_\beta}\beta + C_{l_{\delta_a}}\delta_a + C_{l_{\delta_r}}\delta_r\right) \qquad (10)$$

$$\sum M = \bar{q}Sc\left(C_{l_\alpha}\alpha + \frac{c}{2U}C_{m_q}Q + \frac{c}{2U}C_{m_\alpha}\dot{\alpha} + C_{m_{\delta_e}}\delta_e\right) \qquad (11)$$

$$\sum N = \bar{q}Sb\left(\frac{b}{2U}C_{n_p}P + \frac{b}{2U}C_{n_r}R + C_{n_\beta}\beta + C_{n_{\delta_a}}\delta_a + C_{n_{\delta_r}}\delta_r\right) \qquad (12)$$

$$\sum F_y = mg\sin\phi\cos\psi + \bar{q}S\left(\frac{b}{2U}C_{y_p}P + \frac{b}{2U}C_{y_r}R + C_{y_\beta}\beta + C_{y_{\delta_r}}\delta_r\right) \qquad (13)$$

$$\sum F_z = mg(1 - \cos\phi\cos\psi) + \bar{q}S\left(C_{z_\alpha}\alpha + \frac{c}{2U}C_{z_q}Q + \frac{c}{2U}C_{z_\alpha}\dot{\alpha} + C_{z_{\delta_e}}\delta_e\right) \qquad (14)$$

These force and moment equations summation can be inserted into the nonlinear force and moment state equations (1-6). Note that constant velocity and thrust have been assumed in this study, so the x-force summation equation and the thrust control inputs in Eqs. (11-14) are not required in this development.

Because QFT is a linear design technique, the state equations must be linearized for particular trimmed F.C.s. Linearization is typically based on the small perturbation theory, which assumes that only small excursions in the state variables occur about a given trim condition [10]. However, the velocity vector roll is a large amplitude maneuver consisting of a high roll rate and large excursion in Euler angles. Therefore, these state responses cannot be treated as small excursions, and the linearization technique must be modified. This modification is rather simple. All states in the system other than the roll rate and the Euler angles can still be represented as perturbation quantities (denoted by lower-case variables), and the

squares and products of these states can be neglected as is typically done in small disturbance theory linearization. The roll rate, P, and Euler angles, ϕ, θ, and ψ, cannot be considered small, however, so any second order terms involving them must remain. Additionally, the trigonometric terms in the kinematic equations will not undergo a Taylor approximation as is done in the small disturbance theory linearization, since the Euler angles are not considered small perturbations. The resulting equations are:

$$\dot{P} = \frac{\bar{q}Sb^2}{2D\bar{U}}\left(I_z C_{l_p} + I_{xz}C_{n_p}\right)P + \frac{I_{xz}}{D}(I_x - I_y + I_z)Pq + \frac{\bar{q}Sb^2}{2D\bar{U}}\left(I_z C_{l_r} + I_{xz}C_{n_r}\right)r$$
$$+ \frac{\bar{q}Sb}{D}\left(I_z C_{l_\beta} + I_{xz}C_{n_\beta}\right)\beta + \frac{\bar{q}Sb}{D}\left(I_z C_{l_{\delta_a}} + I_{xz}C_{n_{\delta_a}}\right)\delta_a + \frac{\bar{q}Sb}{D}\left(I_z C_{l_{\delta_r}} + I_{xz}C_{n_{\delta_r}}\right)\delta_r \tag{15}$$

$$\dot{\phi} = P + q\sin\phi\tan\theta + r\cos\phi\tan\theta \tag{16}$$

$$\dot{q} = \frac{I_z - I_x}{I_y}Pr + \frac{I_{xz}}{I_y}P^2 + \frac{\bar{q}Sc}{I_y}\left(C_{m_\alpha}\alpha + \frac{c}{2\bar{U}}C_{m_q}q + \frac{c}{2\bar{U}}C_{m_{\dot{\alpha}}}\dot{\alpha} + C_{m_{\delta_e}}\delta_e\right) \tag{17}$$

$$\dot{r} = \frac{1}{D}(I_x^2 - I_x I_y + I_{xz}^2)Pq + \frac{\bar{q}Sb^2}{2D\bar{U}}\left(I_{xz}C_{l_p} + I_x C_{n_p}\right)P + \frac{\bar{q}Sb^2}{2D\bar{U}}\left(I_{xz}C_{l_r} + I_x C_{n_r}\right)r$$
$$+ \frac{\bar{q}Sb}{D}\left(I_{xz}C_{l_\beta} + I_x C_{n_\beta}\right)\beta + \frac{\bar{q}Sb}{D}\left(I_{xz}C_{l_{\delta_a}} + I_x C_{n_{\delta_a}}\right)\delta_a + \frac{\bar{q}Sb}{D}\left(I_{xz}C_{l_{\delta_r}} + I_x C_{n_{\delta_r}}\right)\delta_r \tag{18}$$

$$\dot{w} = Uq - Pv + g(1 - \cos\phi\cos\psi) + \frac{\bar{q}S}{m}\left(C_{z_\alpha}\alpha + \frac{c}{2\bar{U}}C_{z_q}q + \frac{c}{2\bar{U}}C_{z_{\dot{\alpha}}}\dot{\alpha} + C_{z_{\delta_e}}\delta_e\right) \tag{19}$$

$$\dot{v} = Pw - Ur + g\sin\phi\cos\psi + \frac{\bar{q}S}{m}\left(\frac{b}{2\bar{U}}C_{y_p}P + \frac{b}{2\bar{U}}C_{y_r}R + C_{y_\beta}\beta + C_{y_{\delta_r}}\delta_r\right) \tag{20}$$

$$\dot{\theta} = q\cos\phi - r\sin\phi \tag{21}$$

$$\dot{\psi} = q\frac{\sin\phi}{\cos\theta} + r\frac{\cos\phi}{\cos\theta} \tag{22}$$

As can be seen from the equations. this linearization technique allows for high roll rates and large Euler angle excursions, but produces a set of equations which is only partially linearized; that is, the equations still contain some nonlinear terms (Pr, Pq, $P\alpha$, $P\beta$, and P^2). These terms are the nonlinearities that must be attacked with the QFT design technique.

Because q and r are to be kept small throughout the velocity vector roll, the assumption is made that $\theta \cong \psi \cong 0$. In addition, the AOA and sideslip angles may be approximated as:

$$\alpha = \arctan\left(\frac{w}{U}\right) \cong \frac{w}{U} \tag{23}$$

$$\beta = \arctan\left(\frac{v}{U}\right) \cong \frac{v}{U} \tag{24}$$

Thus, Eqs (16), (19), and (20) are reduced to:

$$\dot{\phi} = P \tag{25}$$

$$\dot{\alpha} = q - P\beta + \frac{g(1-\cos\phi)}{U} + \frac{\bar{q}S}{mU}\left(C_{z_\alpha}\alpha + \frac{c}{2U}C_{z_q}q + \frac{c}{2U}C_{z_{\dot\alpha}}\dot{\alpha} + C_{z_{\delta_e}}\delta_e\right) \tag{26}$$

$$\dot{\beta} = P\alpha - r + \frac{g\sin\phi}{U} + \frac{\bar{q}S}{mU}\left(\frac{b}{2U}C_{y_p}P + \frac{b}{2U}C_{y_r}R + C_{y_\beta}\beta + C_{y_{\delta_r}}\delta_r\right) \tag{27}$$

2.3.2. Aircraft Control Inputs. Equations (15), (25), (17), (18), (26), and (27) represent the complete six DOF dynamical system with three generalized control effectors, ailerons, elevators and a rudder. However, the control effectors for the actual F-18 HARV aircraft are grouped into twelve control effector groups:

- pitch and roll aileron $(\delta_{ap}, \delta_{ar})$
- pitch and roll elevator $(\delta_{ep}, \delta_{er})$
- pitch and yaw rudder $(\delta_{rp}, \delta_{ry})$
- pitch and roll leading edge flap $(\delta_{lefp}, \delta_{lefr})$
- pitch and roll trailing edge flap $(\delta_{tefp}, \delta_{tefr})$
- pitch and yaw thrust vectoring $(\delta_{TVp}, \delta_{TVy})$

To trim the HARV at thirty degrees AOA, the leading edge flaps are fully extended, as shown in Appendix A. Therefore, the leading edge flaps are not used as a control effector in this study. To further limit the complexity of the design, the trailing edge flap, pitch aileron, and pitch rudder groups are not used.

Therefore, the three general control effectors appearing in the six DOF equations are replaced with the true control effectors as follows:

$$\delta_e = \delta_{ep} + \delta_{TVp} \tag{28}$$

$$\delta_a = \delta_{ar} + \delta_{er} \tag{29}$$

$$\delta_r = \delta_{ry} + \delta_{TVy} \tag{30}$$

with each control effector group having its own stability derivative.

2.3.3. Transformation to Stability Axes. The stability derivative, moment of inertia, mass, dynamic pressure, wing area, and velocity terms appearing in the six DOF equations are readily obtained from the nonlinear F-18 HARV Batch Simulation for a particular trimmed F.C., as is described later. With the exception of the lift and drag stability derivatives and the velocity which are referenced to the stability axes, this simulation output is referenced to the body axes frame, and is therefore compatible with the terms in the six DOF equations above. However, it is more convenient to use the stability axes frame of reference to describe a velocity vector roll. Using fixed body axes, the velocity vector roll rate is described by:

$$\Omega = P\cos\alpha + R\sin\alpha \tag{31}$$

At zero degrees AOA, the body x-axes and the aircraft's velocity vector are aligned, and the velocity vector roll consists entirely of body axis roll rate P. However, as the AOA increases, the velocity vector roll includes an increasing body axis yaw rate component, R. At ninety degrees AOA, the velocity vector roll consists entirely of body axis yaw. Equation (31) is therefore rather difficult to command and measure with a linear control system. However, in the stability axes frame of reference, the stability x-axis is always aligned with the aircraft's velocity vector, and the ideal velocity vector roll then consists entirely of roll rate P with no yaw rate component. This simplifies the analysis, design, and simulation processes since the desired output is an actual state of the system and not a function of several states. Therefore a rotation equal to the AOA about the aircraft's y-axis is required to transform the terms of the six DOF

17

equations of motion into the stability axes frame of reference. This is accomplished by appropriately transforming each stability derivative and the moments and products of inertia. The stability derivative transformation yields:

$$C_{l_p}^s = C_{l_p}^b \cos^2 \alpha - \left(C_{l_r}^b + C_{n_p}^b\right)\sin\alpha\cos\alpha + C_{n_r}^b \sin^2 \alpha$$

$$C_{l_r}^s = C_{l_r}^b \cos^2 \alpha - \left(C_{n_r}^b - C_{l_p}^b\right)\sin\alpha\cos\alpha - C_{n_p}^b \sin^2 \alpha$$

$$C_{l_\beta}^s = C_{l_\beta}^b \cos\alpha - C_{n_\beta}^b \sin\alpha$$

$$C_{l_{\delta_a}}^s = C_{l_{\delta_a}}^b \cos\alpha + C_{n_{\delta_a}}^b \sin\alpha$$

$$C_{l_{\delta_e}}^s = C_{l_{\delta_e}}^b \cos\alpha + C_{n_{\delta_e}}^b \sin\alpha$$

$$C_{l_{\delta_r}}^s = C_{l_{\delta_r}}^b \cos\alpha + C_{n_{\delta_r}}^b \sin\alpha$$

$$C_{l_{\delta_{rv}}}^s = C_{l_{\delta_{rv}}}^b \cos\alpha + C_{n_{\delta_{rv}}}^b \sin\alpha \tag{32}$$

$$C_{n_p}^s = C_{n_p}^b \cos^2 \alpha - \left(C_{n_r}^b - C_{l_p}^b\right)\sin\alpha\cos\alpha - C_{l_r}^b \sin\alpha$$

$$C_{n_r}^s = C_{n_r}^b \cos^2 \alpha + \left(C_{l_r}^b + C_{n_p}^b\right)\sin\alpha\cos\alpha + C_{l_p}^b \sin\alpha$$

$$C_{n_\beta}^s = C_{n_\beta}^b \cos\alpha + C_{l_\beta}^b \sin\alpha$$

$$C_{n_{\delta_a}}^s = C_{n_{\delta_a}}^b \cos\alpha - C_{l_{\delta_a}}^b \sin\alpha$$

$$C_{n_{\delta_e}}^s = C_{n_{\delta_e}}^b \cos\alpha - C_{l_{\delta_e}}^b \sin\alpha$$

$$C_{n_{\delta_r}}^s = C_{n_{\delta_r}}^b \cos\alpha - C_{l_{\delta_r}}^b \sin\alpha$$

$$C_{n_{\delta_{rv}}}^s = C_{n_{\delta_{rv}}}^b \cos\alpha - C_{l_{\delta_{rv}}}^b \sin\alpha \tag{33}$$

$$C_{m_\alpha}^s = C_{m_\alpha}^b$$

$$C_{m_q}^s = C_{m_q}^b$$

$$C_{m_{\delta_q}}^s = C_{m_{\delta_q}}^b$$

$$C_{m_{\delta_{rv}}}^s = C_{m_{\delta_{rv}}}^b \tag{34}$$

$$C_{y_p}^s = C_{y_p}^b \cos\alpha - C_{y_r}^b \sin\alpha$$

$$C_{y_r}^s = C_{y_r}^b \cos\alpha + C_{y_p}^b \sin\alpha$$

$$C_{y_\beta}^s = C_{y_\beta}^b$$

$$C_{y_{\delta_a}}^s = C_{y_{\delta_a}}^b$$

$$C_{y_{\delta_e}}^s = C_{y_{\delta_e}}^b$$

$$C_{y_{\delta_r}}^s = C_{y_{\delta_r}}^b$$

$$C_{y_{\delta_{rv}}}^s = C_{y_{\delta_{rv}}}^b \tag{35}$$

$$C_{z_q}^s = -C_{L_q}^b$$

$$C_{z_\alpha}^s = -C_{L_\alpha}^b$$

18

$$C^{s}_{z_{l_{\varphi}}} = -C^{b}_{L_{l_{\varphi}}}$$
$$C^{s}_{z_{l_{m_{p}}}} = -C^{b}_{L_{l_{m_{p}}}} \tag{36}$$

where the b and s superscripts denotes body and stability axis derivatives, respectively, and the AOA is the trim AOA (30 degrees). Similarly, the inertia is transformed with the trim AOA [22]:

$$\begin{Bmatrix} I_{xx} \\ I_{zz} \\ I_{xz} \end{Bmatrix}_{stab} = \begin{bmatrix} \cos^2\alpha & \sin^2\alpha & -\sin2\alpha \\ \sin^2\alpha & \cos^2\alpha & \sin2\alpha \\ \frac{1}{2}\sin2\alpha & -\frac{1}{2}\sin2\alpha & \cos2\alpha \end{bmatrix} \begin{Bmatrix} I_{xx} \\ I_{zz} \\ I_{xz} \end{Bmatrix}_{body} \tag{37}$$

Note that all stability derivatives and moments of inertia from this point forward are in reference to the stability axes system, unless explicitly stated otherwise.

It is apparent that the six DOF equations of motion are quickly becoming very complex. Two steps are taken to alleviate this situation. First, the transformation of the stability derivatives and moments of inertia are performed before they are integrated into the equations of motion, and second, a set of consolidated stability derivatives which combine like terms in the equations of motion are defined. For example, in Eq. (15) the entire quantity by which the state P is multiplied is defined as the consolidated stability derivative $C_{m_{pr}}$. Based on this concept, the consolidated stability derivatives are defined as:

$$C_{l_p} \equiv \frac{\overline{q}Sb^2}{2D\overline{U}}(I_z C^s_{l_p} + I_{xz} C^s_{n_p})$$
$$C_{l_{pr}} \equiv \frac{I_{xz}}{D}(I_x - I_y + I_z)\frac{b}{c}$$
$$C_{l_r} \equiv \frac{\overline{q}Sb^2}{2D\overline{U}}(I_z C^s_{l_r} + I_{xz} C^s_{n_r})$$
$$C_{l_{\beta}} \equiv \frac{\overline{q}Sb}{D}(I_z C^s_{l_{\beta}} + I_{xz} C^s_{n_{\beta}})$$
$$C_{l_{\delta_a}} \equiv \frac{\overline{q}Sb}{D}(I_z C^s_{l_{\delta_a}} + I_{xz} C^s_{n_{\delta_a}})$$
$$C_{l_{\delta_r}} \equiv \frac{\overline{q}Sb}{D}(I_z C^s_{l_{\delta_r}} + I_{xz} C^s_{n_{\delta_r}})$$
$$C_{l_{\delta_{rn}}} \equiv \frac{\overline{q}Sb}{D}(I_z C^s_{l_{\delta_{rn}}} + I_{xz} C^s_{n_{\delta_{rn}}})$$
$$C_{l_{\delta_{rn_r}}} \equiv \frac{\overline{q}Sb}{D}(I_z C^s_{l_{\delta_{rn_r}}} + I_{xz} C^s_{n_{\delta_{rn_r}}}) \tag{38}$$

19

$$C_{m_e} \equiv \frac{\bar{q}Sc}{I_y}C_{m_e}^s$$

$$C_{m_e} \equiv \frac{\bar{q}Sc^2}{2I_y\bar{U}}C_{m_e}^s$$

$$C_{m_p} \equiv \frac{I_z - I_x}{I_y}$$

$$C_{m_{y^2}} \equiv \frac{I_{xz}}{I_y}$$

$$C_{m_a} \equiv \frac{\bar{q}Sc^2}{2I_y\bar{U}}C_{m_e}^s$$

$$C_{m_{\delta_e}} \equiv \frac{\bar{q}Sc}{I_y}C_{m_{\delta_e}}^s$$

$$C_{m_{\delta_{ry}}} \equiv \frac{\bar{q}Sc}{I_y}C_{m_{\delta_{ry}}}^s \tag{39}$$

$$C_{n_p} \equiv \frac{\bar{q}Sb^2}{2D\bar{U}}(I_x C_{n_p}^s + I_{xz}C_{l_p}^s)$$

$$C_{n_{pr}} \equiv \frac{I_x^2 - I_x I_y + I_{xz}^2}{D}$$

$$C_{n_r} \equiv \frac{\bar{q}Sb^2}{2D\bar{U}}(I_x C_{n_r}^s + I_{xz}C_{l_r}^s)$$

$$C_{n_\beta} \equiv \frac{\bar{q}Sb}{D}(I_x C_{n_\beta}^s + I_{xz}C_{l_\beta}^s)$$

$$C_{n_{\delta_e}} \equiv \frac{\bar{q}Sb}{D}(I_x C_{n_{\delta_e}}^s + I_{xz}C_{l_{\delta_e}}^s)$$

$$C_{n_{\delta_a}} \equiv \frac{\bar{q}Sb}{D}(I_x C_{n_{\delta_a}}^s + I_{xz}C_{l_{\delta_a}}^s)$$

$$C_{n_{\delta_{rr}}} \equiv \frac{\bar{q}Sb}{D}(I_x C_{n_{\delta_{rr}}}^s + I_{xz}C_{l_{\delta_{rr}}}^s)$$

$$C_{n_{\delta_{ry}}} \equiv \frac{\bar{q}Sb}{D}(I_x C_{n_{\delta_{ry}}}^s + I_{xz}C_{l_{\delta_{ry}}}^s) \tag{40}$$

$$C_{z_e} \equiv \frac{\bar{q}Sc}{2m\bar{U}^2}C_{z_e}^s$$

$$C_{z_e} \equiv \frac{\bar{q}S}{m\bar{U}}C_{z_e}^s$$

$$C_{z_a} \equiv \frac{\bar{q}Sc}{2m\bar{U}^2}C_{z_a}^s$$

$$C_{z_{\delta_e}} \equiv \frac{\bar{q}S}{m\bar{U}}C_{z_{\delta_e}}^s$$

$$C_{z_{\delta_{ry}}} \equiv \frac{\bar{q}S}{m\bar{U}}C_{z_{\delta_{ry}}}^s \tag{41}$$

$$C_{y_p} \equiv \frac{\bar{q}Sb}{2m\bar{U}^2}C_{y_p}^s$$

$$C_{y_r} \equiv \frac{\bar{q}Sb}{2m\bar{U}^2}C_{y_r}^s$$

$$C_{y_\beta} \equiv \frac{\bar{q}S}{m\bar{U}}C_{y_\beta}^s$$

$$C_{y_{\delta_{ar}}} \equiv \frac{\bar{q}S}{m\bar{U}}C_{y_{\delta_{ar}}}^s$$

$$C_{y_{\delta_{er}}} \equiv \frac{\bar{q}S}{m\bar{U}}C_{y_{\delta_{er}}}^s$$

$$C_{y_{\delta_{ry}}} \equiv \frac{\bar{q}S}{m\bar{U}}C_{y_{\delta_{ry}}}^s$$

$$C_{y_{\delta_{TVy}}} \equiv \frac{\bar{q}S}{m\bar{U}}C_{y_{\delta_{TVy}}}^s \tag{42}$$

The resulting non-dimensionalized six DOF stability-axes equations of motion, suitable for velocity vector roll analysis, is now written in a final form using the consolidated stability derivatives:

$$\dot{P} = C_{l_p}P + C_{l_{pq}}Pq + C_{l_r}r + C_{l_\beta}\beta + C_{l_{\delta_{ar}}}\delta_{ar} + C_{l_{\delta_{er}}}\delta_{er} + C_{l_{\delta_{ry}}}\delta_{ry} + C_{l_{\delta_{TVy}}}\delta_{TVy} \tag{43}$$

$$\dot{\phi} = P \tag{44}$$

$$\dot{q} = C_{m_{pr}}Pr - C_{m_{p2}}P^2 + C_{m_\alpha}\alpha + C_{m_q}q + C_{m_{\dot{\alpha}}}\dot{\alpha} + C_{m_{\delta_{ep}}}\delta_{ep} + C_{m_{\delta_{TVp}}}\delta_{TVp} \tag{45}$$

$$\dot{r} = C_{n_{pq}}Pq + C_{n_p}P + C_{n_r}r + C_{n_\beta}\beta + C_{n_{\delta_{ar}}}\delta_{ar} + C_{n_{\delta_{er}}}\delta_{er} + C_{n_{\delta_{ry}}}\delta_{ry} + C_{n_{\delta_{TVy}}}\delta_{TVy} \tag{46}$$

$$\dot{\alpha} = q - P\beta + \left(\frac{gb}{2\bar{U}^2}\right)(1 - \cos\phi) + C_{z_q}q + C_{z_{\dot{\alpha}}}\dot{\alpha} + C_{z_\alpha}\alpha + C_{z_{\delta_{ep}}}\delta_{ep} + C_{z_{\delta_{TVp}}}\delta_{TVp} \tag{47}$$

$$\dot{\beta} = P\alpha - r - \left(\frac{gb}{2\bar{U}^2}\right)\sin\phi + C_{y_p}P + C_{y_r}r + C_{y_\beta}\beta + C_{y_{\delta_{ar}}}\delta_{ar} + C_{y_{\delta_{er}}}\delta_{er} + C_{y_{\delta_{ry}}}\delta_{ry} + C_{y_{\delta_{TVy}}}\delta_{TVy} \tag{48}$$

2.4. Control Effector Sign Convention

The control effector group sign convention used in the HARV simulation is shown in Fig. 5,
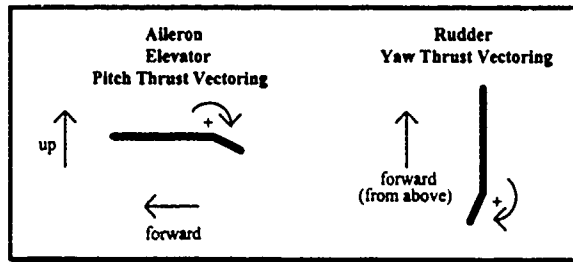
Figure 5. Control Effector Sign Convention

with the actuator deflection angle limits:

Ailerons: $+42° \Rightarrow -25°$ $(+0.73304 \Rightarrow -0.43633 \text{ rad})$

Elevators: $+10.5° \Rightarrow -24°$ $(+0.18326 \Rightarrow -0.41888 \text{ rad})$

Rudders: $\pm 30°$ $(\pm 0.52360 \text{ rad})$

Pitch Thrust Vectoring: $+16° \Rightarrow -20°$ $(+0.27925 \Rightarrow -0.34907 \text{ rad})$

Pitch Thrust Vectoring: $\pm 10°$ $(\pm 0.17453 \text{ rad})$

Actuator rate limits are not included in this work. The control effector groups defined in the state equations represent control surface pairs, with the sign convention shown in Table 1. Although each control actuator has the deflection limits presented above, the control effector groups are internally scaled such that a maximum control effector command for a differential control drives one control actuator to its maximum positive position, and the other control actuator to its maximum negative position. For instance, the maximum roll aileron command of 42 degrees drives the left aileron to the -25 degree position and the right aileron to the 42 degree position.

Table 1. Control Input Sign Convention

	Left Effector	Right Effector
Roll Aileron	+	-
Roll Elevator	+	-
Pitch Elevator	+	+
Pitch Thrust Vectoring	+	+
Yaw Thrust Vectoring	+	+
Yaw Rudder	+	+

2.5. Flight Conditions

In this study, the variation in the QFT plant parameters has two sources, the nonlinearities in the EOM and the change in aircraft characteristics over a range of F.C.s. While the use of QFT to account for the system nonlinearities is the primary focus of this study, the ability to design a single controller for a range of F.C.s is equally important. Having said this, it is important to note that the portion of the flight envelope in which high AOA flight and velocity vector rolls are feasible is very limited.

A range of F.C.s is typically defined by a range of speeds and altitudes. Regardless of the linear design technique used, specific points (specified by a single speed and a single altitude) within this range of F.C.s are selected as design points, and a linear model is extracted at each of these design points, as discussed in Chapter 1. The extracted linear model represents the trimmed aircraft at a particular speed and altitude; that is, the states of the aircraft are constant. Therefore, specifying a unique speed and altitude defines a unique AOA.

In this study, the design is limited to one AOA, viz., thirty degrees. As a result, only the range of altitudes or speeds may be specified, and the range of F.C.s becomes somewhat more limited. As can be seen in Fig. 1, the largest range of F.C.s in the high AOA region of the flight envelope occurs with changes in altitude. Therefore, variations in altitude, rather than in speed, define the range of F.C.s used in this study, allowing the robustness of QFT to be more fully exploited.

The altitudes chosen for this study are presented in Table 2, along with the aircraft's corresponding speed, thrust in the body x-axis, and throttle positions. This data is obtained from the F-18 HARV Batch Simulation. Flight conditions corresponding to altitudes equal to or greater than 25,000 feet cannot be attained due to a lack of engine power. The first three I.C.s, in the high AOA region of the flight envelope, are used in for the QFT design. The fourth F.C. is used only for model validation, as discussed in the next section.

Table 2. The Aircraft Flight Conditions

Flight Condition	1	2	3	4
Altitude (feet)	10,000	15,000	20,000	20,000
AOA (deg)	30	30	30	5
Speed (feet/sec)	218.609	236.485	256.8	553.012
Thrust, x-axis (lbf)	14757.4	14795.9	14835.4	3529.2
Right Throttle (%)	64.3	72.4	87.0	39.2
Left Throttle (%)	64.3	72.4	87.0	39.2

2.6. Six DOF Model Validation

The development of the final six DOF equations of motion involved a significant amount of manipulation, and therefore have a high probability of error. Before continuing with the design phase, it is

imperative that this six DOF system be validated. Not only does this save valuable time, but it also provides an opportunity to explore properties of the F-18 HARV which may compliment or detract from the design process to be undertaken. To perform this investigation, the six DOF system can be modeled in a simulation environment such as MATLAB's Simulink, and subjected to individual control inputs. A detailed study of the stability and control derivatives and of the aircraft's response to the control inputs should be sufficient to identify short-comings in the model development.

A top-level block diagram of the nonlinear six DOF system appears in Fig. 6. Since this is a nonlinear model (due to the Pr, Pq, $P\alpha$, $P\beta$, and P^2 terms), the differential state equations, Eqs. (43-48), must be implemented directly. Each state equation block in Fig. 6 contains continuous-time blocks
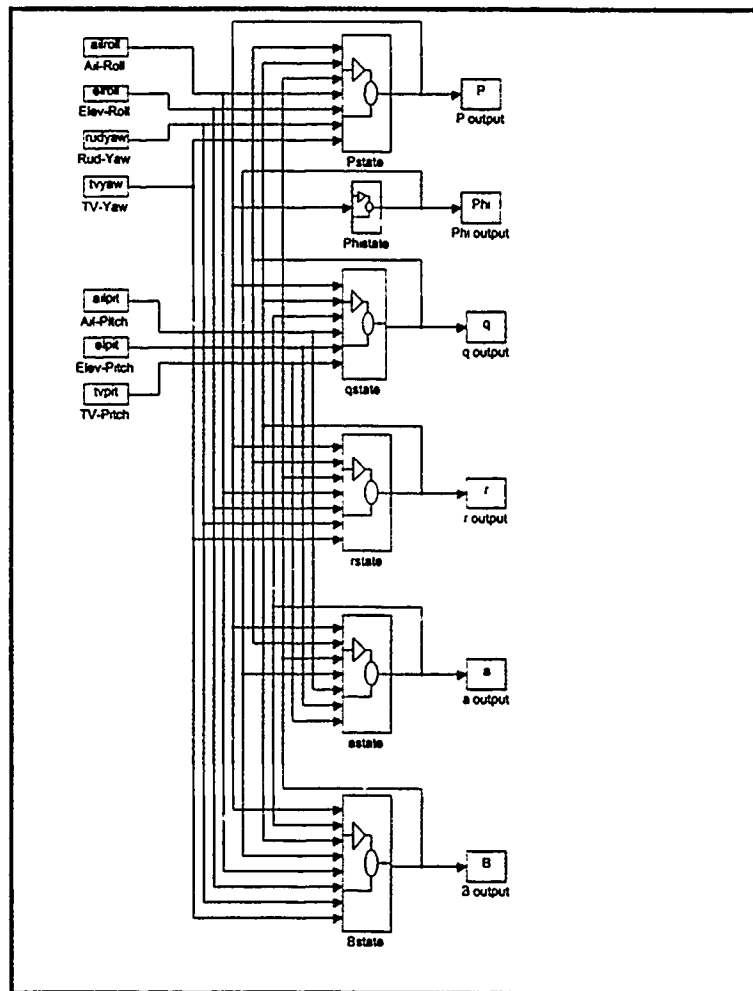
Figure 6. Six DOF Model, Top Level Block Diagram

representing the dynamics of that state and input blocks for the control inputs which affect that state. As an example, Fig. 7 shows the internal structure of the roll rate state block. Note that the control inputs (δ_{ar} = dar, etc.) have been implemented so that each input can be applied independently of or in combination with the others, allowing more freedom in the choice of validation simulations.

The stability derivatives shown in Fig. 7, and present in each of the state equation blocks, are the consolidated stability derivatives described earlier. These may be formed from the nondimensional stability derivatives and moments of inertia provided by the F-18 HARV Batch Simulation using Eqs. (32-42). Because the simulation's output is a Matrix$_x$ fsave file, this transformation is accomplished with the Matrix$_x$ script file, coef.m, listed in Appendix A. The transformed stability derivatives are then entered into MATLAB to be used in the validation simulation. The nondimensional and consolidated stability derivatives for each of the four F.C.s, as well as other pertinent aircraft data, are presented in Appendix A.

The outputs of the six DOF simulation model are the aircraft states, P, ϕ, q, r, α, and β, which are defined in the stability axes. To facilitate comparison with similar aircraft responses and with expected responses based on a knowledge of flight dynamics, the first aircraft model to be simulated should be
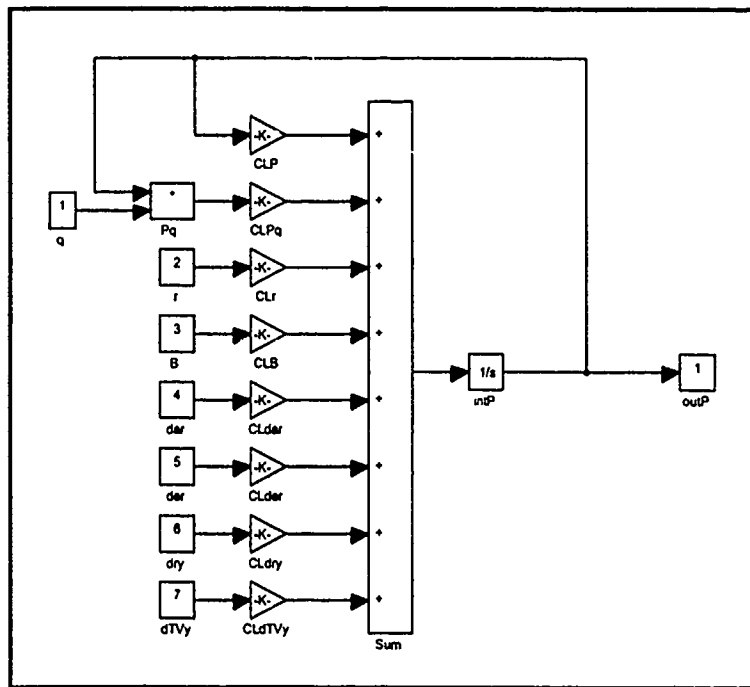
Figure 7. Six DOF Model, P State Block Diagram

trimmed at a relatively low AOA so that the stability and body axes are nearly aligned. Flight condition 4, in Table 2, is the trimmed condition used for this purpose.

With the consolidated stability derivatives representing F.C. 4 loaded into MATLAB, the simulation is subjected to maximum deflections in each of the individual control effector inputs. The aircraft state responses to each of these inputs are shown in Figs. 57-62 in Appendix B.

These plots show that the aircraft responds to all control inputs as expected, except for the perturbation in AOA, given a roll aileron command (Fig. 57). The pitch rate q is an increasingly positive quantity, so the AOA is also expected to increase. However, Fig. 57 shows that the AOA gradually decreases. An analysis of Eq. (47) provides an explanation for this phenomenon. While the AOA is directly tied to the pitch rate through the first term of the equation, high roll rates can actually cause the second term involving the sideslip angle to become dominant. Because of the adverse yaw effect, the sideslip angle due to an aileron roll command is positive, resulting in a *decreasing* AOA during high roll rates.

The consequences of this characteristic of high roll rates is rather significant. First, a decrease in AOA during a roll maneuver means that the aircraft is being unloaded during the maneuver. Second, proper control of the α and β states through a velocity vector roll is imperative! Equations (47) and (48) are closely coupled through the $P\alpha$ and $P\beta$ terms when the roll rate is relatively high, so the excursions in AOA and sideslip angle must be kept very small.

While the simulations of the six DOF aircraft model trimmed at a low AOA demonstrate the validity of the model, simulations of the aircraft models trimmed at thirty degrees AOA show the high AOA characteristics of the aircraft. Representative simulations for F.C. 1 of Table 2, Figs. 63-68, show that the basic response characteristics to the control inputs are similar, but much less in magnitude. This reduction in control effectiveness is due to the reduction in dynamic pressure and the changes in airflow at higher AOAs; the aerodynamic control surfaces are simply not as effective at high AOAs. In addition, the controls which primarily affect the roll channel at low AOAs affect both the stability axes roll and yaw

channels at higher AOAs. This coupling necessitates creative control blending techniques to produce the desired roll characteristics at high AOAs.

One suspicious response characteristic emerging from the initial thirty-degree AOA simulations is the lack of sideslip produced by yaw thrust vectoring, compared to that produced by the yaw rudder input. The speed of the aircraft trimmed at low AOAs results in a relatively high dynamic pressure (140 slug ft/sec²) so the effectiveness of the aerodynamic controls surfaces may be much greater than the effectiveness of thrust vectoring in these F.C.s. However, the speed of the aircraft trimmed at thirty degrees AOA results in a dynamic pressure of only 42 slug ft/sec² so the effectiveness of yaw thrust vectoring should be approaching, if not exceeding, that of the rudder. An analysis of the yaw thrust vectoring and rudder control derivatives shows that the rudder is again over three times as effective (at body axes yaw) as the thrust vectoring. This is not consistent with the literature [21] which indicates that yaw thrust vectoring is more effective than the rudder near this F.C. Through a discussion with NASA HARV program office [7], the cause of this inconsistency is easily explained. The nondimensional thrust vectoring control derivatives that the F-18 HARV Batch Simulation provides represent the *aerodynamic* effects caused by the movement of the thrust vectoring nozzle, not the moments caused by the vectored thrust. Therefore, the non-dimensional control derivatives representing the thrust vectoring effectiveness in pitch and yaw must be calculated from a knowledge of the system at the trim F.C.

While they do not include the negligible aerodynamic contributions described above, the following equations represent the force and moment effectiveness of the vectored thrust:

$$C_{n_{\delta_{TV}}} = \frac{-Tl_t \sin\gamma}{\bar{q}Sb\gamma} \qquad C_{y_{\delta_{TV}}} = \frac{T\sin\gamma}{\bar{q}S\gamma} \tag{49}$$

$$C_{m_{\delta_{TV}}} = \frac{-Tl_t \sin\gamma}{\bar{q}S\bar{c}\gamma} \qquad C_{z_{\delta_{TV}}} = \frac{T\sin\gamma}{\bar{q}S\gamma} \tag{50}$$

where

$$l_t = 19.73 \text{ ft}$$
$$S = 400 \text{ ft}^2$$

$$b = 37.4 \text{ ft}$$
$$\bar{c} = 11.523 \text{ ft} \tag{51}$$

and the other variables change with F.C. as shown in Table 3. The thrust used in these calculations is the thrust in the x-axis of the body axes system, and the resulting control derivatives are therefore also in the body axes system, as were the original.

These new control derivatives can be transformed to the stability axes system as described earlier, with the exception of the control derivative representing the change in z-force due to pitch thrust vectoring. The original control derivative obtained from the F-18 HARV Simulation represented a change in lift due to pitch thrust vectoring, and lift was already defined in the stability axes so no transformation was required. Now, however, this control derivative represents the change in body axes z-force, and must therefore be transformed to the stability axes system using:

$$C_{z_{\delta_{TV}}} = C^b_{z_{\delta_{TV}}} \cos\alpha \tag{52}$$

After this transformation, and the appropriate nondimensionalization with respect to time, these control derivatives are placed in the six DOF model. Simulation of this model, see e.g. Fig. 67, shows that the yaw thrust vectoring effectiveness is greater than the yaw rudder effectiveness, as expected, and therefore the six DOF model validation is complete.

Table 3. Thrust Vectoring Control Derivatives, Body Axes

Altitude (ft)	Thrust (lbf)	$\bar{q}$ (lb/ft^2)	$C_{n_{\delta_{TV}}}$	$C_{y_{\delta_{TV}}}$	$C_{m_{\delta_{TV}}}$	$C_{z_{\delta_{TV}}}$
10,000	14,757.0	42.000	-0.46340002	0.87841667	-1.5040494	0.87841667
15,000	14,795.9	41.900	-0.46571782	0.88281026	-1.5115722	0.88281026
20,000	14,835.4	41.856	-0.46745201	0.88609757	-1.5172008	0.88609757
25,000	14,124.4	41.800	-0.44564519	0.84476077	-1.4464228	0.84476077

This chapter describes the development of a three DOF QFT plant model from the partially

linearized six DOF model. Included in this development is an approach to representing the system

nonlinearities with linear QFT models, the incorporation of actuator dynamics into these models, and an

approach to a weighting matrix strategy. The chapter concludes with an open-loop simulation of the QFT

model, ensuring its validity.

3.1. Three DOF QFT Plant

As previously mentioned, minimizing the pitch and yaw rates in the transitional region allows the

corresponding "slower" states (AOA and sideslip) to become negligibly small, and allows these slower

states to be removed from the six DOF model. The resulting three DOF system of the "fast" states of the

aircraft in the transition region, based on the assumption that $\alpha \cong \beta \cong 0$ and $\phi \cong 0$ or π, is:

$$\dot{P} = C_{l_P} P + C_{l_{Pq}} Pq + C_{l_r} r + C_{l_{\delta_{ar}}} \delta_{ar} + C_{l_{\delta_{er}}} \delta_{er} + C_{l_{\delta_{ry}}} \delta_{ry} + C_{l_{\delta_{TVy}}} \delta_{TVy} \tag{53}$$

$$\dot{q} = C_{m_{Pr}} Pr - C_{m_{P^2}} P^2 + C_{m_q} q + C_{m_{\delta_{ep}}} \delta_{ep} + C_{m_{\delta_{TVp}}} \delta_{TVp} \tag{54}$$

$$\dot{r} = C_{n_{Pq}} Pq + C_{n_P} P + C_{n_r} r + C_{n_{\delta_{ar}}} \delta_{ar} + C_{n_{\delta_{er}}} \delta_{er} + C_{n_{\delta_{ry}}} \delta_{ry} + C_{n_{\delta_{TVy}}} \delta_{TVy} \tag{55}$$

with the initial or final conditions (as indicated in Figure 3):

$$
\begin{array}{cc}
\textit{Initiate Roll} & \textit{Arrest Roll} \\
P(0) = 0, P(\tau) = P_0 & \text{or} \quad P(0) = P_0, P(\tau) = 0
\end{array}
\tag{56}
$$

$$q(0) = 0, q(\tau) = q_0 \quad \text{or} \quad q(0) = q_f, q(\tau) = 0 \tag{57}$$

$$r(0) = 0, r(\tau) = r_0 \quad \text{or} \quad r(0) = r_f, r(\tau) = 0 \tag{58}$$

The two transition regions are treated independently so that the final conditions of states q and r from roll

initiation may be slightly different from the initial conditions of these states in the roll arresting transition

region. This provides more flexibility to the optimal control solution in the free stream region by allowing

it to end with different conditions than it started with. This may be desirable, or necessary, depending on

the characteristics of the roll arresting transition region. Regardless, these states must still be relatively close to zero for the transitional region model to be valid.

The three DOF equations of motion presented above are nonlinear because of the roll rate terms. One approach to removing this nonlinearity is to introduce a roll rate parameter P_{param} which ranges from zero up to the maximum desired roll rate P_0. The roll rate parameter then becomes a bounded structured uncertainty in the three DOF linear QFT model:

$$\dot{x}(t) = A\,x(t) + B\,u(t)$$
$$y(t) = C\,x(t) + D\,u(t)$$
(59)

where

$x(t)$ is the state vector (3x1):

$$x(t) = \begin{bmatrix} P(t) \\ q(t) \\ r(t) \end{bmatrix} \begin{matrix} \text{roll rate (rad / sec)} \\ \text{pitch rate (rad / sec)} \\ \text{yaw rate (rad / sec)} \end{matrix}$$
(60)

$u(t)$ is the input or forcing function vector (6x1):

$$u(t) = \begin{bmatrix} \delta_{ar}(t) \\ \delta_{er}(t) \\ \delta_{ep}(t) \\ \delta_{TVp}(t) \\ \delta_{TVy}(t) \\ \delta_{ry}(t) \end{bmatrix} \begin{matrix} \text{differential (roll) ailerons (rad)} \\ \text{differential (roll) elevators (rad)} \\ \text{pitch elevators (rad)} \\ \text{pitch thrust vectoring (rad)} \\ \text{yaw thrust vectoring (rad)} \\ \text{yaw rudder (rad)} \end{matrix}$$
(61)

$y(t)$ is the output vector (3x1)

$$y(t) = \begin{bmatrix} P(t) \\ q(t) \\ r(t) \end{bmatrix} \begin{matrix} \text{roll rate (rad / sec)} \\ \text{pitch rate (rad / sec)} \\ \text{yaw rate (rad / sec)} \end{matrix}$$
(62)

A is the plant dynamics matrix of constant coefficients (3x3)

$$A = \begin{bmatrix} C_{l_p} & C_{l_{p_1}} P_{param} & C_{l_r} \\ -C_{m_{\dot{r}}} P_{param} & C_{m_q} & C_{m_{r}} P_{param} \\ C_{n_p} & C_{n_{p_1}} P_{param} & C_{n_r} \end{bmatrix} \tag{63}$$

B is the input or forcing function matrix of constant coefficients (3x6)

$$B = \begin{bmatrix} C_{l_{\delta_a}} & C_{l_{\delta_s}} & 0 & 0 & C_{l_{\delta_{ry}}} & C_{l_{\delta_{rz}}} \\ 0 & 0 & C_{m_{\delta_e}} & C_{m_{\delta_{ry}}} & 0 & 0 \\ C_{n_{\delta_a}} & C_{n_{\delta_s}} & 0 & 0 & C_{n_{\delta_{ry}}} & C_{n_{\delta_{rz}}} \end{bmatrix} \tag{64}$$

C is the output matrix of constant coefficients (3x3), and is equal to the identity matrix

$$C = I_{3x3} \tag{65}$$

D is the input or forcing function feedforward matrix of constant coefficients (3x6)

$$D = 0_{3x6} \tag{66}$$

Based on a projected maximum roll rate of 24 deg/sec, reasonable dimensional values for the roll rate parameter appearing in A are 0, 8, 16 and 24 deg/sec yielding four plant cases for each F.C. Note that this roll rate parameter must also be nondimensionalized to rad/sec before being used in the equations. However, for ease of understanding, the dimensional values of 0, 8, 16, and 24 are used in this document. The twelve plant cases used in this study are listed at the end of Appendix A.

The QFT plant matrix $P_L(s)$ of system transfer functions, to be loaded (hence the subscript L) into the QFT design package is derived from Eq. (59) using Laplace transform notation. Assuming zero initial conditions, with D = 0:

$$sX(s) = A X(s) + B U(s) \tag{67}$$

$$(sI - A)X(s) = B U(s) \tag{68}$$

$$X(s) = (sI - A)^{-1} B U(s) \tag{69}$$

$$Y(s) = C(sI - A)^{-1} B U(s) \tag{70}$$

31

$$Y(s) = P_L(s)U(s) \qquad (71)$$

The plant matrix is then:

$$P_L(s) = C(sI - A)^{-1}B \qquad (72)$$

and dimensionally, P_L for the HARV is:

$$P_{L3x6}(s) = C_{3x3}\left[(sI - A)^{-1}\right]_{3x3} B_{3x6}$$

The individual elements of P_L are all functions of the Laplace variable s and relate each control input in the state equations to each system output. $P_L(s)$ is symbolically represented as:

$$P_L(s) = \begin{bmatrix} \dfrac{P(s)}{\delta_{ar}(s)} & \dfrac{P(s)}{\delta_{er}(s)} & \dfrac{P(s)}{\delta_{ep}(s)} & \dfrac{P(s)}{\delta_{TVp}(s)} & \dfrac{P(s)}{\delta_{TVy}(s)} & \dfrac{P(s)}{\delta_{ry}(s)} \\ \dfrac{q(s)}{\delta_{ar}(s)} & \dfrac{q(s)}{\delta_{er}(s)} & \dfrac{q(s)}{\delta_{ep}(s)} & \dfrac{q(s)}{\delta_{TVp}(s)} & \dfrac{q(s)}{\delta_{TVy}(s)} & \dfrac{q(s)}{\delta_{ry}(s)} \\ \dfrac{r(s)}{\delta_{ar}(s)} & \dfrac{r(s)}{\delta_{er}(s)} & \dfrac{r(s)}{\delta_{ep}(s)} & \dfrac{r(s)}{\delta_{TVp}(s)} & \dfrac{r(s)}{\delta_{TVy}(s)} & \dfrac{r(s)}{\delta_{ry}(s)} \end{bmatrix} \qquad (73)$$

3.2. Actuator Dynamics

Although the plant matrix $P_L(s)$ accurately models the aircraft state dynamics, it does not account for actuator dynamics inherent in each control effector of the aircraft. These actuator dynamics can have a significant impact on the stability of an aircraft, and therefore cannot be ignored. The actuator dynamics are approximated by second and fourth-order transfer functions [1], as shown in Table 4, and placed into an $l x l$ actuator matrix $T_{ACT}(s)$:

$$T_{ACT}(s) = \begin{bmatrix} T_a & 0 & 0 & 0 & 0 & 0 \\ 0 & T_e & 0 & 0 & 0 & 0 \\ 0 & 0 & T_e & 0 & 0 & 0 \\ 0 & 0 & 0 & T_{TV} & 0 & 0 \\ 0 & 0 & 0 & 0 & T_{TV} & 0 \\ 0 & 0 & 0 & 0 & 0 & T_r \end{bmatrix} \qquad (74)$$

32

Table 4. HARV control effector actuator dynamics

Effector	Transfer Function
Aileron	$T_a(s) = \dfrac{5625}{s^2 + 885s + 5625}$
Elevator	$T_e(s) = \dfrac{2137.718\left(s^2 + 112744s + 6872.41\right)}{s^4 + 154.102s^3 + 16121.7834s^2 + 495588.89s + 14691275.7264}$
Thrust Vector	$T_{TV}(s) = \dfrac{400}{s^2 + 26s + 400}$
Rudder	$T_r(s) = \dfrac{5184}{s^2 + 99.36s + 5184}$

The system mxl plant matrix $P(s)$ which includes the actuator dynamics can now be defined as:

$$P(s)_{mxl} = P_L(s)_{mxl} \cdot T_{ACT}(s)_{lxl} \tag{75}$$

3.3. Effective Plant $P_e(s)$

Although a linear plant $P(s)$ has been identified, this system still cannot be used directly in the QFT

design process. The QFT design methodology requires a square mxm plant. In other words, the system

must have the same number of inputs as outputs. QFT requires a square plant because the QFT design

equations require the inversion of $P(s)$, the system plant. For systems with more inputs than outputs, like

the HARV model developed here , an *effective* system must be formed by means of a weighting matrix. A

weighting matrix takes m desired input commands and appropriately "splits" them into the l actual

command inputs of the plant. For the HARV, the lxm weighting matrix $W(s)$ must transform three

command inputs (since there are three states) into the six HARV control inputs used in the design.

Recall that the six DOF equations of motion, as originally stated, contained three control inputs,

which are redefined as the six actual control inputs in Eqs. (28) to (30). The three original control inputs

are ideal for use in the weighting matrix since they represent the primary controls which produce moments

about the three general axes of interest. Therefore, the weighting matrix $W(s)$ relates these three control

inputs to the actual six control inputs of the plant, as shown in Figure 8. This is represented symbolically

as:

33
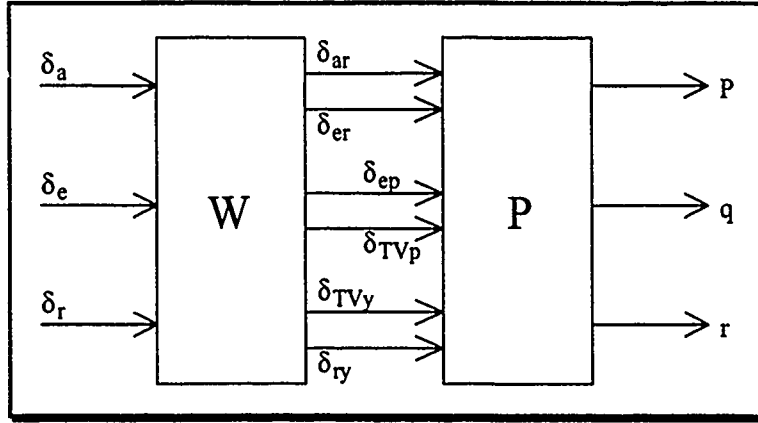
Figure 8. Effective plant (P_e), Block Diagram

$$\mathbf{P}_{e_{3x3}}(s) = \mathbf{P}_{3x6}(s) \cdot \mathbf{W}_{6x3}(s) \tag{76}$$

The *effective* plant is now square, with the generalized three-axis rate command inputs and the three-axes output states P, q, and r.

3.4. Weighting Matrix W(s)

The formation of an effective plant matrix with a weighting matrix is a simple concept. However, the choice of the weighting matrix is not a trivial matter; the proper choice of a weighting matrix is very critical to the success of the overall design. A successful weighting matrix design can make the compensator design a much simpler task by reducing the cross-coupling effects of the control inputs. The opposite is also true, however. A poor choice of the weighting matrix can actually r ike the system impossible to control. Unfortunately there is no easy method of designing the weighting matrix. Previously designed weighting matrices generally offer a good starting point, but no weighting matrices oriented towards velocity vector rolls at high AOAs have been found in the literature. Therefore the weighting matrix must be based on insight into this particular controls problem, the nature of the plant, and the MIMO QFT design methodology.

A first attempt at a successful weighting matrix design is to borrow the general flight control concept of an aileron-rudder interconnect and use it to account for the cross-coupling effects found at high AOAs. For instance, a roll command would not only command roll, but also yaw to remove the adverse

34

yaw produced by the aileron deflections. Looking first at the system with three generalized control

effectors, as in Eq's. (15), (25), (17), (18), (26), and (27), the weighting matrix is designed to weight the

cross-coupled control inputs based on the ratio of the appropriate control derivatives. Each of these control

derivatives indicates the effectiveness of that control effector in producing a particular force or moment.

For example, given a δ_a command, the three corresponding weighting matrix outputs (denoted with a "hat")

can be defined as:

$$\hat{\delta}_a = \delta_a$$

$$\hat{\delta}_r = \frac{C_{n_{\delta_a}}}{C_{n_{\delta_r}}} \delta_a$$

$$\hat{\delta}_e = 0 \tag{77}$$

Here, the aileron commands not only the differential ailerons, but also the rudder based on the ratio $\mathfrak{c}^{\mathfrak{f}}$

ailerons' (adverse) yaw effectiveness to the rudders' yaw effectiveness. Similarly, a yaw command

generates an aileron command based on the ratio of the rudder and aileron roll effectiveness derivatives. A

pitch command produces no aileron or rudder commands since the longitudinal channel is still ideally

uncoupled from the lateral channels. The resulting weighting matrix scheme, for the three general control

inputs, is therefore defined as:

$$\left\{ \begin{matrix} \hat{\delta}_a \\ \hat{\delta}_e \\ \hat{\delta}_r \end{matrix} \right\} = \left[\begin{array}{c|c|c} 1 & 0 & \dfrac{C_{l_{\delta_r}}}{C_{l_{\delta_a}}} \\ \hline 0 & 1 & 0 \\ \hline \dfrac{C_{n_{\delta_a}}}{C_{n_{\delta_r}}} & 0 & 1 \end{array} \right] \left\{ \begin{matrix} \delta_a \\ \delta_e \\ \delta_r \end{matrix} \right\} \tag{78}$$

However, as noted earlier, the weighting matrix for this design must have three control inputs and six

control outputs. Therefore a second weighting matrix is defined to direct the three weighted control

outputs of the first weighting matrix into the actual control groups available on the aircraft. This direct

connection must contain scale factors to account for dissimilar maximum control deflections within the control effectors in each group. For instance, a maximum aileron command should command the roll ailerons to forty-two degrees, but the roll elevators only to thirty degrees. Scaling is achieved by multiplying the input command by the ratio of the maximum actuator limits to the maximum allowed input command. This arrangement is described by the equation:

$$
\begin{Bmatrix} \delta_{ar} \\ \delta_{er} \\ \delta_{ep} \\ \delta_{TVp} \\ \delta_{TVy} \\ \delta_{ry} \end{Bmatrix} =
\begin{bmatrix}
\dfrac{\delta_{ar}^{max}}{\hat{\delta}_a^{max}} & 0 & 0 \\
\dfrac{\delta_{er}^{max}}{\hat{\delta}_a^{max}} & 0 & 0 \\
0 & \dfrac{\delta_{ep}^{max}}{\hat{\delta}_e^{max}} & 0 \\
0 & \dfrac{\delta_{TVp}^{max}}{\hat{\delta}_e^{max}} & 0 \\
0 & 0 & \dfrac{\delta_{TVy}^{max}}{\hat{\delta}_r^{max}} \\
0 & 0 & \dfrac{\delta_{ry}^{max}}{\hat{\delta}_r^{max}}
\end{bmatrix}
\begin{Bmatrix} \hat{\delta}_a \\ \hat{\delta}_e \\ \hat{\delta}_r \end{Bmatrix}
\tag{79}
$$

Because the control derivatives in Eq. (77) are not directly available, these two weighting matrices must be combined to form the single weighting matrix:

$$
\mathbf{W} = \begin{bmatrix}
\dfrac{\delta_{ar}^{max}}{\delta_{a}^{max}} & 0 & \left(\dfrac{C_{l_{s_{TV_y}}}+C_{l_{s_{r_y}}}}{C_{l_{s_{er}}}}\right)\left(\dfrac{\delta_{ar}^{max}}{\delta_{r}^{max}}\right) \\
\dfrac{\delta_{er}^{max}}{\delta_{a}^{max}} & 0 & \left(\dfrac{C_{l_{s_{TV_y}}}+C_{l_{s_{r_y}}}}{C_{l_{s_{er}}}}\right)\left(\dfrac{\delta_{er}^{max}}{\delta_{r}^{max}}\right) \\
0 & \dfrac{\delta_{ep}^{max}}{\delta_{e}^{max}} & 0 \\
0 & \dfrac{\delta_{TVp}^{max}}{\delta_{e}^{max}} & 0 \\
\left(\dfrac{C_{n_{s_{er}}}+C_{n_{s_{ar}}}}{C_{n_{s_{TV_y}}}}\right)\left(\dfrac{\delta_{TV_y}^{max}}{\delta_{a}^{max}}\right) & 0 & \dfrac{\delta_{TV_y}^{max}}{\delta_{r}^{max}} \\
\left(\dfrac{C_{n_{s_{ar}}}+C_{n_{s_{er}}}}{C_{n_{s_{r_y}}}}\right)\left(\dfrac{\delta_{r_y}^{max}}{\delta_{a}^{max}}\right) & 0 & \dfrac{\delta_{r_y}^{max}}{\delta_{r}^{max}}
\end{bmatrix}
\tag{80}
$$

The control derivatives in this matrix change with F.C., and must be obtained from the F-18 HARV Batch Simulation and transformed as described earlier. The other required control effector group command limits for the F-18 HARV are:

$$
\delta_{ar}^{max} = \pm 42^\circ, \quad \delta_{er}^{max} = \pm 24^\circ, \quad \delta_{r_y}^{max} = \pm 30^\circ, \quad \delta_{TV_y}^{max} = \pm 10^\circ
$$

$$
\delta_{ep}^{max} = \pm 24^\circ, \quad \delta_{TVp}^{max} = \pm 20^\circ
$$

$$
\delta_{a}^{max} = \pm 3 \text{ inches} \quad, \quad \delta_{e}^{max} = \pm 5 \text{ inches} \quad, \quad \delta_{r}^{max} = \pm 1 \text{ unit}
\tag{81}
$$

While this weighting matrix is based on sound principles, it has two primary limitations. First, it will only work if the control derivatives in the numerator and denominator of each fraction are such that the resulting control surface command is within the allowable limits, given a maximum general control input. If not, the general control input will command more control authority than is available. For instance, if the thrust vectoring and the rudder are as ineffective in the yaw channel at thirty degrees AOA as the simulation indicates, this weighting matrix will try to command more thrust vectoring and rudder than is available to compensate for a maximum roll command. A possible solution is to scale the denominators of the cross-coupling elements up so that the resulting commands are within the limits. Some, but not all,

decoupling will then still be possible. Given the transformed control derivatives from the simulation and the thrust vectoring control derivatives in Table 3, the denominator of the W(6,1) element must be increased by a factor of ten to prevent the rudder from saturating.

Second, since this weighting matrix contains control derivatives which vary with F.C., and the plant cases vary with F.C., the weighting matrix must be re-evaluated each time the F.C. is changed. In a sense, this violates the whole purpose of the QFT design, which is to design a single compensator control system which takes into account plant variation so that gain scheduling of compensators is not required, or is greatly reduced. By introducing a weighting matrix which changes with F.C., a control system element which must be gain scheduled is actually being added to the system. It is hoped that the actual variation in the weighting matrix elements over the limited flight envelope will be small enough that a constant weighting matrix can be used in place of the scheduled matrix. The weighting matrices for the three F.C.s considered in this thesis appear in Table 5.

Table 5. Scheduled Weighting Matrices

	10,000 ft			15,000 ft			20,000 ft		
W	0.2443	0	0.7247	0.2443	0	0.7425	0.2443	0	0.7593
	0.1396	0	0.3045	0.1396	0	0.3123	0.1396	0	0.3199
	0	0.0838	0	0	0.0838	0	0	0.0838	0
	0	0.0698	0	0	0.0698	0	0	0.0698	0
	−0.0399	0	0.1745	−0.0391	0	0.1745	−0.0384	0	0.1745
	−0.1194	0	0.5236	−0.1182	0	0.5236	−0.1168	0	0.5236

It is obvious from these matrices that the variations in the weighting matrix elements between F.C.s are indeed minimal. Therefore a single constant weighting matrix is sufficient for the entire range of F.C.s, *eliminating the need for weighting matrix scheduling.* For simplicity, each of the constant weighting matrix elements is taken as the mean value of the same elements in each of the three scheduled matrices. The resulting constant weighting matrix used in the QFT design is:

$$W = \begin{bmatrix} 0.2443 & 0 & 0.742167 \\ 0.1396 & 0 & 0.31223 \\ 0 & 0.0838 & 0 \\ 0 & 0.0698 & 0 \\ -0.03913 & \iota & \hat{\ }.1745 \\ -0.11813 & 0 & 0.5236 \end{bmatrix} \tag{82}$$

3.5. QFT Model Validation

Before using the weighting matrix and plant models in the QFT design process, each is validated

through simulation. To validate the weighting matrix design, the constant weighting matrix, Eq. (82), is

inserted in front of the six DOF model control inputs, yielding the system in Fig. 69, Appendix B. The six

state responses to each of the three available control inputs (roll, pitch, or yaw) are shown in Figs. 70-72,

Appendix B. Comparison of Fig. 70 and Fig. 63 shows that the introduction of the weighting matrix nearly

doubles the roll rate while almost halving the adverse yaw rate, given a roll command. Similarly, the yaw

rate response to a yaw command is nearly double for the system employing the weighting matrix.

However, the roll rate responses to the yaw command show somewhat unexpected results. Incorporation of

the weighting matrix yields a large positive roll rate rather than the mild negative roll rate experienced

without the weighting matrix. Unfortunately, a negative yaw command is required to maintain a near-zero

yaw rate in the roll simulation, and the resulting roll rate will therefore be reduced slightly.

The validation of the QFT plant models may be accomplished with or without the incorporation of

the weighting matrix, since six DOF simulations for both cases are available. For purposes of this study,

the former is selected. However, if the results are significantly different than those obtained in the six DOF

simulation, an examination of the bare QFT plants is required.

The weighting matrix is incorporated into the QFT model by performing the matrix multiplication:

$$B'_{3x3} = B_{3x6} \cdot W_{6x3} \tag{83}$$

The newly obtained control matrix is then placed in a Simulink state-space block, along with the A, C, and

D system matrices defined in Eqs. (63), (65), and (66) and presented in Appendix A. The resulting system

is depicted in Fig. 73, Appendix B.

The three output state responses (P, q, and r) to the three available control inputs are shown in Figs. 74-77 for F.C. 1 and *Pparam* values of 0, 8, 16, and 24 deg/sec (note, the nondimensional values of rad/sec are used for *Pparam* in the actual simulation). These results compare favorably with the state responses of the six DOF system to the same input, Fig. 70. As expected, the pitch rate increases as the value of *Pparam* is increased. Starting at a constant zero value for a *Pparam* value of zero, the amount of pitch rate due to a roll command directly reflects the amount of coupling present in the system, due the nonlinearities in the six DOF system. To show the effect of the F.C. on the state responses, simulations are performed for F.C.s 2 and 3. The results of these simulations, Figs. 78 and 79, show that the change in altitude has very little effect on the state response to a roll command. It is expected then, that the variation in the QFT model parameters is rather small.

This chapter presents the QFT theory as it applies to this work. The discussion includes the formation of the effective plant, the definition and modeling of performance and stability specifications, the formation of plant templates, the definition and formation of the bounds used in the QFT design, and the design of the cascade compensator and the prefilter. As each subject is introduced, the concept is applied to this particular problem, up to the actual compensator and prefilter design process. It is assumed that the reader is familiar with basic continuous system multiple-input single-output (MISO) and multiple-input multiple-output (MIMO) QFT design methods; for a more complete discussion of these topics, reference Chapter 21 of the D'Azzo and Houpis textbook [8] and the Flight Dynamics Laboratory technical report [17]. The QFT design in this study is performed using the MIMO/QFT CAD Program developed by Richard Sating. For ease of understanding, the notation used in this chapter corresponds to the notation used in the software documentation [25].

4.1. Effective Plants

The QFT design methodology begins with the formation of a set of N effective plant matrices, $\mathbf{P}_{e_i}(s)$ where $i = 1, 2, ..., N$, which define the characteristics of the plant over the range of plant parameter uncertainty [see Eqs. (72), (75), and (76) in Chapter 2]. The formation of the effective plants is automated within the CAD package, which reads the system matrices from input files, and allows for manual definition of the weighting matrix and actuator models. The system matrices for the $N = 12$ plant cases (four linearized plants at each of the three F.C.s) used in this study are presented at the end of Appendix A. The actuator models and the constant weighting matrix are defined in Chapter 2, Table 4 and Eq. (82). With this information, the CAD package generates the twelve effective plants listed in Appendix C. The frequency response of these plants appears in the form of a Bode plot, Fig. 80, Appendix C.

41

4.2. QFT Compensation

The goal of the QFT methodology is to design the compensator $G(s)$ and the prefilter $F(s)$, shown in the MIMO QFT system block diagram of Fig. 9, which allow the closed-loop system to meet required performance specifications based on a particular input. In this study, both the compensator and the prefilter are diagonal; this limitation is imposed by the MIMO QFT CAD Program. The control ratio matrix relating the closed-loop system outputs $Y(s)$ to inputs $R(s)$ can be formed from the block diagram.

$$E(s) = F(s)R(s) - Y(s) \tag{84}$$

$$Y(s) = P_e(s)G(s)E(s) \tag{85}$$

Substituting Eq. (84) into Eq. (85) and rearranging yields:

$$\frac{Y(s)}{R(s)} = \left[I + P_e(s)G(s)\right]^{-1} P_e(s)G(s)F(s) \tag{86}$$

$$T(s) = \left[I + P_e(s)G(s)\right]^{-1} P_e(s)G(s)F(s) \tag{87}$$

$$T(s) = \begin{bmatrix} \dfrac{P(s)}{P_{cmd}(s)} & \dfrac{P(s)}{q_{cmd}(s)} & \dfrac{P(s)}{r_{cmd}(s)} \\[2mm] \dfrac{q(s)}{P_{cmd}(s)} & \dfrac{q(s)}{q_{cmd}(s)} & \dfrac{q(s)}{r_{cmd}(s)} \\[2mm] \dfrac{r(s)}{P_{cmd}(s)} & \dfrac{r(s)}{q_{cmd}(s)} & \dfrac{r(s)}{r_{cmd}(s)} \end{bmatrix} = \begin{bmatrix} t_{11}(s) & t_{12}(s) & t_{13}(s) \\[2mm] t_{21}(s) & t_{22}(s) & t_{23}(s) \\[2mm] t_{31}(s) & t_{32}(s) & t_{33}(s) \end{bmatrix} \tag{88}$$
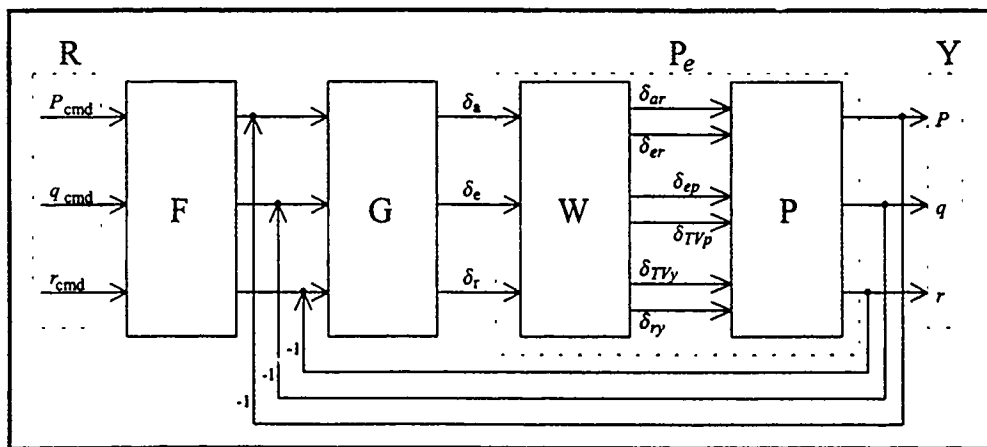
Figure 9. MIMO QFT Control Structure, Block Diagram

42

4.3. Response Models

The performance specifications define the bounds for the elements of the control ratio matrix given by Eq. (88). The ideal control ratio matrix has principal diagonal elements (t_{11}, t_{22}, and t_{33}) which meet the individual desired response characteristics and off-diagonal elements which are desired to be equal to zero. However, the uncertainty of the plant prohibits a single response characteristic for each of the principal diagonal elements to be met for all plant cases, and the coupled nature of the system does not allow the off-diagonal (cross-coupling) elements of the control matrix to be zero. Therefore, an appropriate set of response characteristics which bound the elements of the control ratio matrix is identified.

For the principal diagonal elements of the control matrix, an upper (fast) and lower (slow) response bound is specified, and all plant cases must fall within these bounds to meet the performance specifications. Typically, these bounds can be determined from the source of performance specifications for military aircraft, MIL-STD-1797A [19]; however, this military specification does not apply to high AOA maneuvering [11]. Therefore, current literature is used to determine an appropriate response characteristic.

In this study, the principal diagonal elements of the control matrix represent the roll, pitch, and yaw angular rates, defined in the stability axes. Therefore the control ratio element of primary interest for a velocity vector roll is the roll rate element, $t_{11}(s)$. The bounds for this element can be derived from a paper published by the NASA HARV Program Office [21] which discusses high AOA flight control system development. In this paper, the authors use a maximum roll rate of 35 deg/sec at 30 degrees AOA, Mach 0.25 as the upper design limit criteria. In the simulations presented by the authors, however, a maximum roll rate of approximately 24 deg/sec is actually achieved in the first second, with a commanded roll doublet at 35 degrees AOA. Based on this response, a desired maximum roll rate between 20 and 30 deg/sec at 30 degrees AOA is respectable for a one-second time period of the transition region of the velocity vector roll. The exact nature of this response can be defined with physical insight into the problem. The roll rate response of a typical fighter aircraft is overdamped, so the roll rate for this problem is bounded by a slightly underdamped response, $\zeta = 0.9$, and an overdamped response with settling times of 1 second. Two transfer functions which represent these specifications are:

$$T_{R_v}(s) = b_{ii} = \frac{36}{s^2 + 8.4s + 36} \tag{89}$$

$$T_{R_L}(s) = a_{ii} = \frac{507}{s^3 + 25s^2 + 198.25s + 507} \tag{90}$$

The time and frequency response characteristics of these specifications are shown in Fig. 10. Note that Eq. (90), the lower bound, has a higher order denominator than Eq. (89), the upper bound, to ensure that the difference between these bounds continues to increase with increasing frequency.

The response characteristics of the other two principal diagonal elements are not of primary concern in this study. Obviously, they must still be reasonable, since the flight control system will utilize these two channels to control the aircraft. Therefore, for simplicity, the same bounds used for $t_{11}(s)$ are used for $t_{22}(s)$ and $t_{33}(s)$.

Because the cross-coupling effects are not desired, only an upper bound defining the maximum allowable cross-coupling response is required. In flight control systems, the allowable cross-coupling is typically five percent of the desired response. For a 20 deg/sec roll rate, maximum cross-coupling responses of 1 deg/sec are permitted. Given this pitch and yaw rate cross-coupling and a 1 second transition region of the velocity vector roll, the maximum perturbation in sideslip and AOA is less than 1 deg, which fits well with the assumptions made in forming the QFT models. The upper bound on the off-diagonal elements can therefore be represented by the five percent constant:

$$T_{D_v}(s) = b_{ij}\big|_{i \neq j} = 0.05 = -26 \text{ dB} \tag{91}$$

The time and frequency response characteristics of the cross-coupling specifications are shown in Fig. 10.

4.4. Stability Specifications

In addition to meeting the desired performance specifications, the QFT compensator must provide an acceptable stability margin. The stability margin can be specified in terms of a phase margin γ, a gain margin g_m, or the corresponding M_L contour on the Nichols chart. If any one of the three stability requirements are specified, the remaining two can be calculated. Typically, the phase margin angle is specified for flight control systems:
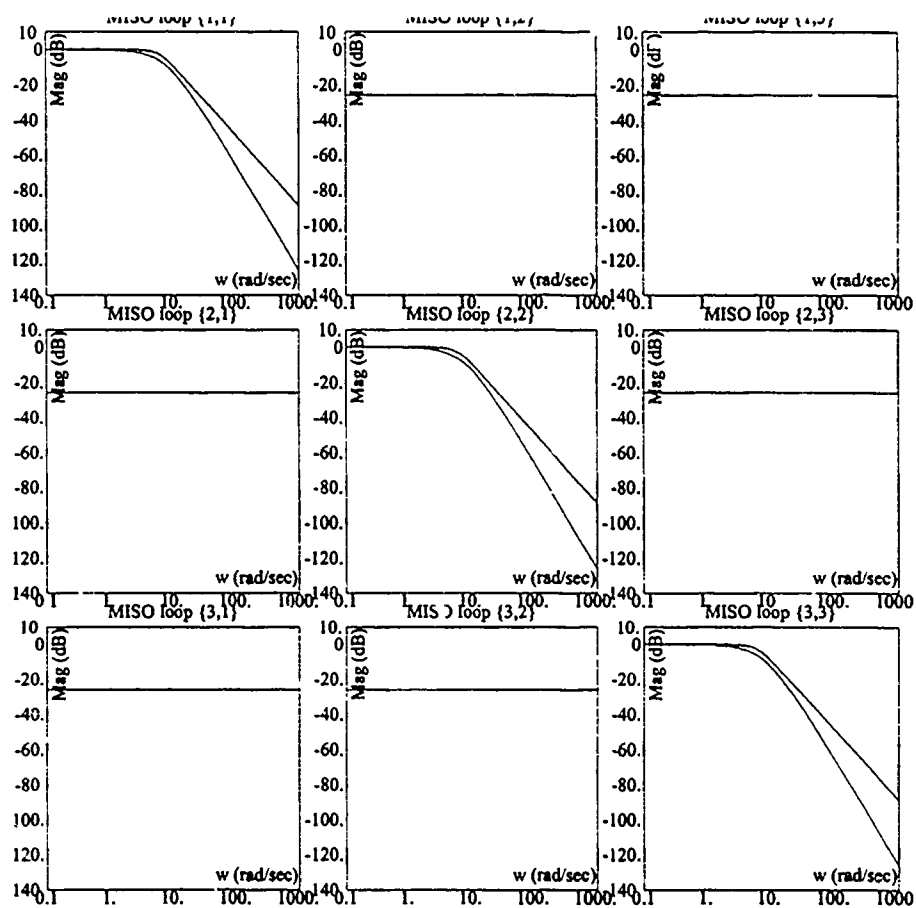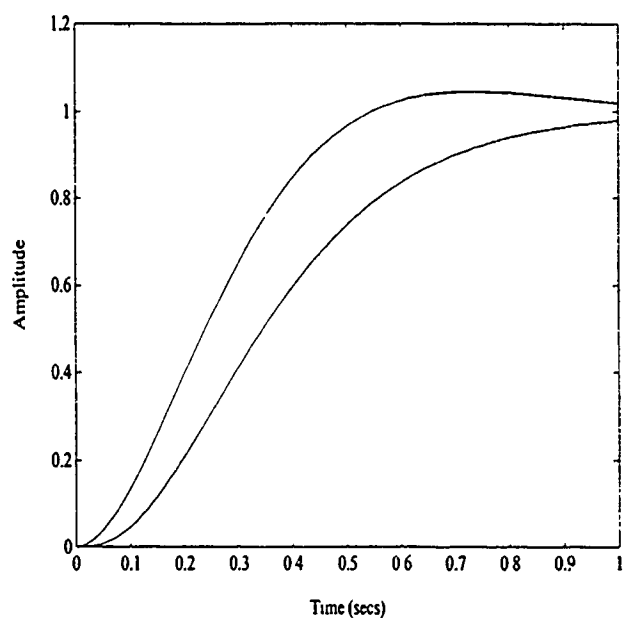
Figure 10. Time and Frequency Response of Principal Diagonal Tracking Bounds

45

$$\gamma = 45° \tag{92}$$

The corresponding 3.01 dB M_L contour is the stability specification used directly for the QFT design technique, placing an upper limit on the magnitude of the closed-loop frequency response.

4.5. Design Equations - MISO Equivalent Method

The MIMO design technique is not applied directly to the MIMO system in the form of Eq. (87). Instead, the problem is decomposed into a set of m^2 equivalent MISO system problems to which QFT is then applied. This decomposition transforms the difficult MIMO design problem into a set of m straightforward MISO design problems. The simplicity gained by use of this transformation is one of the major strengths of the QFT design process. The method of decomposing the MIMO plant into a set of MISO equivalent plants is given below without proof; for more information see [17].

The first step in the process is to form the **Q** matrix; this is performed in the QFT CAD package. The mathematical basis of this operation involves the polynomial inverse of the effective plant matrix:

$$\mathbf{P}_e^{-1} = \left\{ p_{ij}^* \right\} = \left\{ 1 / q_{ij} \right\} \tag{93}$$

and the inversion of the elements of $\mathbf{P}_e^{-1}$:

$$\mathbf{Q} = \left\{ q_{ij} \right\} = \left\{ 1 / p_{ij}^* \right\} \tag{94}$$

The **Q** matrices for this study and a Bode plot of their frequency response are presented in Appendix D.

Two conditions must be met for the application of QFT to a MIMO system and its MISO equivalent form. These conditions result directly from the MISO equivalent derivation. First, $\mathbf{P}_e^{-1}$ must exist. This condition is obvious from Eq. (93) and serves to ensure controllability of $\mathbf{P}_e$. Second, *diagonal dominance* must exist in order to apply the QFT Method 1 design technique. This condition results from a disturbance response analysis of the MISO equivalent form. For the 3x3 case, diagonal dominance exists if:

$$\left| p_{11}^* p_{22}^* p_{33}^* \right| \geq \left| p_{11}^* p_{23}^* p_{32}^* \right| + \left| p_{12}^* p_{21}^* p_{33}^* \right| + \left| p_{12}^* p_{23}^* p_{31}^* \right| + \left| p_{13}^* p_{22}^* p_{31}^* \right| + \left| p_{13}^* p_{21}^* p_{32}^* \right|$$
$$\text{as } \omega \Rightarrow \infty \tag{95}$$

46

If diagonal dominance does not exist, it may be possible to achieve it by reordering the designation of the plant inputs or the plant outputs, or by changing the values in the weighting matrix. If not, the Method 2 QFT design technique may be applied to the problem. In the CAD package, the diagonal dominance condition is checked by plotting the normalized difference between the two sides of the diagonal dominance inequality described by Eq. (95) versus frequency for each plant case, as shown in Fig. 11. In this representation, positive values indicate the degree by which the diagonal dominance condition is satisfied, and negative values indicate the degree by which the diagonal dominance condition is not satisfied. For this study, the diagonal dominance condition is satisfied as the frequency approaches infinity, as shown in Fig. 11.

The role of the **Q** matrix elements in the array of MISO equivalent plants is illustrated in Fig. 12. The MISO loops are decoupled except through the disturbance inputs. Each MISO loop has one command input and one disturbance input. The disturbance input is a function of the other controlled outputs. By the principle of superposition, the MISO loop transmission consists of both a tracking and a disturbance component. However, when using a diagonal prefilter, only the diagonal MISO loops have a transfer function component due to tracking:
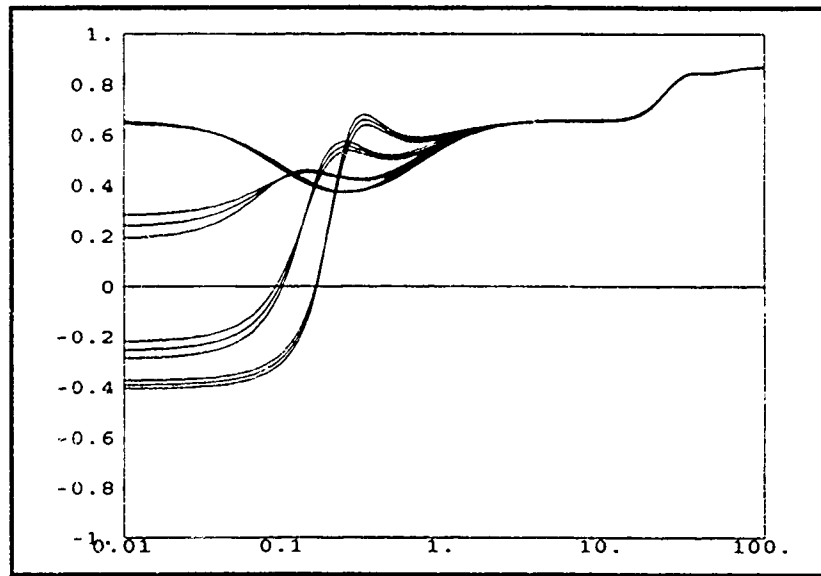
Figure 11. Diagonal Dominance Condition

47
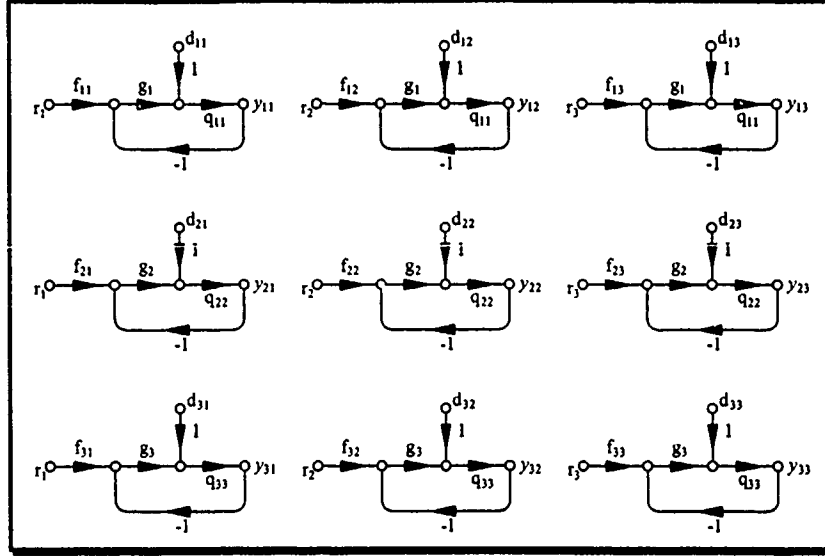
Figure 12. MISO Equivalents for 3x3 Effective Plant

$$t_{ij} = t_{r_i} + t_{d_{ii}} \tag{96}$$

while the off-diagonal loops, with $f_{ij} = 0$ and $i \neq j$, have a transfer function component due to disturbance only:

$$t_{ij} = t_{d_{ij}} \text{ where } i \neq j. \tag{97}$$

The expressions for tracking and disturbance transfer function components can be derived from the signal flow graph of the (i,j) MISO loop and are given, respectively, by:

$$\left(t_{r_i}\right)_l = f_{ij}\left[\frac{g_i(q_{ii})_l}{1+g_i(q_{ii})_l}\right] = f_{ij}\left[\frac{(L_i)_l}{1+(L_i)_l}\right] \tag{98}$$

$$\left(t_{d_i}\right)_l = \frac{(d_{ij})_l(q_{ii})_l}{1+g_i(q_{ii})_l} = \frac{(d_{ij})_l(q_{ii})_l}{1+(L_i)_l} \tag{99}$$

where l is the index which specifies one of the N linear plants and where:

$$L_i = g_i q_{ii} \tag{100}$$

is defined as the loop transmission transfer function.

48

The disturbance input, a function of all other controlled outputs, is represented by the equation:

$$d_{ij} = -\sum_{k \neq i} \frac{t_{kj}}{q_{ik}} \tag{101}$$

The MISO loops, each representing a closed loop control ratio element of Eq. (88), are required to satisfy the performance and stability design specifications (defined in the previous two sections) placed on the closed loop system.

The diagonal MISO loop responses must lie within an upper and lower bound; this is expressed as:

$$a_{ii} \leq |t_{ii}|_l \leq b_{ii} \quad \text{for } l = 1, 2, \ldots, J \tag{102}$$

The off-diagonal MISO loop responses must lie below an upper bound; this is expressed as:

$$|t_{ij}|_l \leq b_{ii} \quad \text{for } l = 1, 2, \ldots, J \tag{103}$$

For each row of MISO loops the stability margin is defined by:

$$\left| \frac{(L_i)_l}{1 + (L_i)_l} \right| \leq M_L \quad \text{for } l = 1, 2, \ldots J \tag{104}$$

In order to design a compensator g_i for the MISO loops, the specifications are translated into bounds on the Nichols chart which must r ɤ ʌiolated by the MISO open loop transmission $g_i q_{ii}$. In order for these bounds to take into accoun ɤ ʌ cases, a set of templates, each outlining the range of structured plant uncertainty at a particular frequency, are used to generate the bounds. Template and bound formation is discussed in the following sections.

4.6. Templates

A plant template outlines the range of uncertainty in the frequency domain transmission of a plant transfer function for a specific frequency. A template for a particular frequency is formed by plotting all plant transfer functions q_{ii} for that frequency on the Nichols chart, and connecting the points outlining the structured uncertainty region. The 0.16 rad/sec template for the roll rate channel is shown in Fig. 13.

49
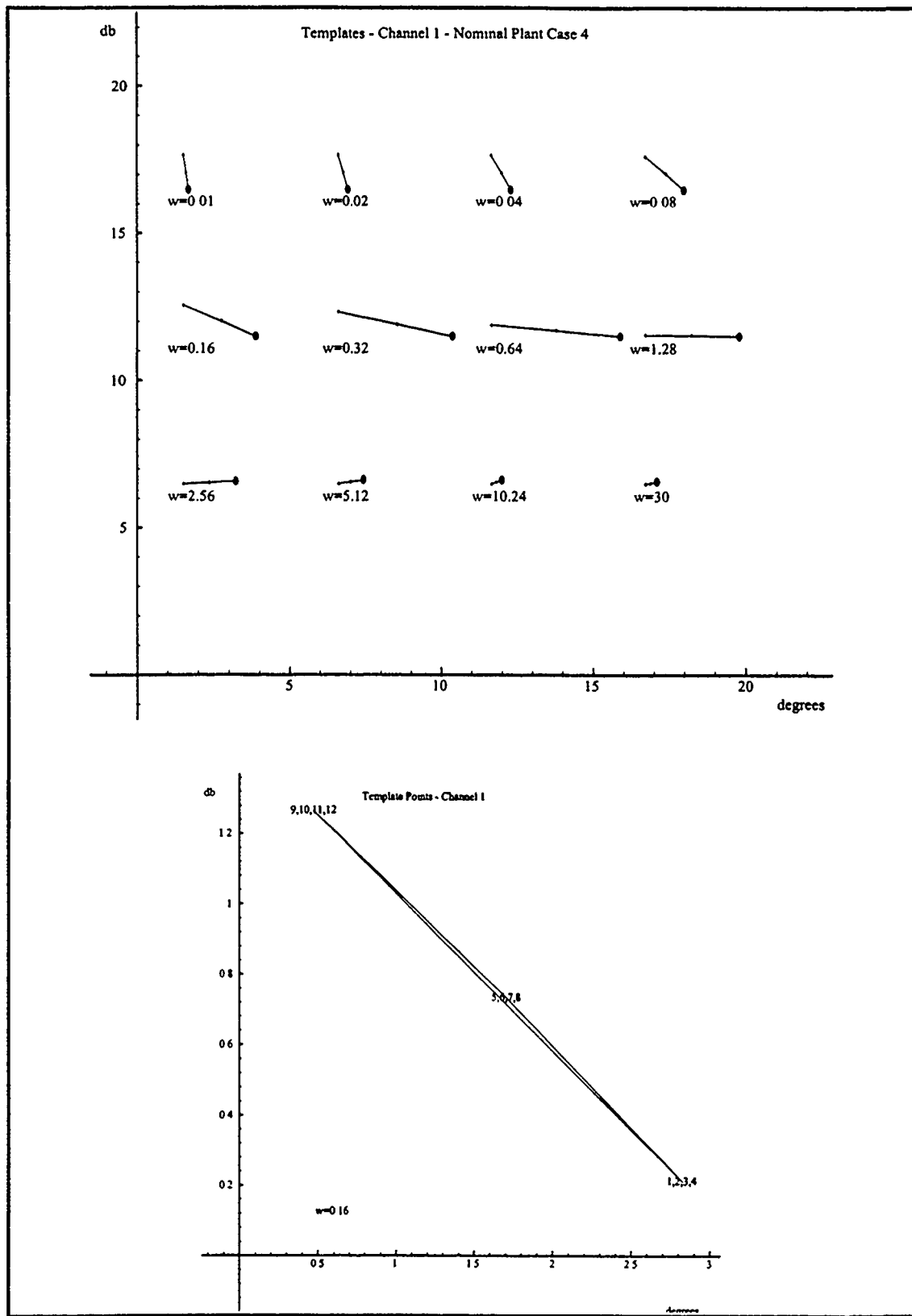
Figure 13. Roll Rate Channel Templates

An interesting plant characteristic is ascertained from plant groupings in this template. The first four plant cases represent the plant variation due to the a change in the roll rate parameter at one altitude, 10,000 feet. Similarly, the next two sets of four plant cases represent the plant variation due to the same nonlinearity, but at the altitudes of 15,000 and 20,000 feet. Consequently, the template shows that the greatest amount of plant variation is due to changes in altitude rather than nonlinearities present in the velocity vector roll.

The generation of templates for all frequencies of interest gives a clear picture of the frequency dependent nature of the plant uncertainty. So what are the frequencies of interest? This question is answered by referring back to the performance specifications. Since the response of the closed-loop system for all plant cases is to fall within the upper and lower tracking bounds in Fig. 10, these bounds are used to identify the frequency range of interest. In control system design, a response lower that -12 dB is typically considered negligible. Therefore, from Fig. 10, the high frequency cut-off point can be identified as the frequency at which the upper tracking bound crosses the -12 dB line:

$$\omega_h \cong 10 \ \text{rad/sec.} \qquad (105)$$

The low frequency cut-off point is identified as the frequency at which the upper and lower bounds are nearly identical. This frequency is identified from Fig. 10 as:

$$\omega_l \cong 0.1 \ \text{rad/sec} \qquad (106)$$

Since these frequencies are based on the desired performance specifications (which are rather arbitrarily chosen by the designer), they do not take into account the plant characteristics. Therefore, to allow the design to take into account the slower dynamics of the aircraft in the high AOA region of the flight envelope, the low frequency cut-off is lowered to 0.01 rad/sec (approximately one decade below the corner frequency of the first dynamics appearing in the effective plant Bode plots, Fig. 80, Appendix C). Additionally, the high frequency cut-off is raised to 30 rad/sec, not to account for plant dynamics, but to aid in the design process using this particular CAD package. The open-loop transmission $L_i(j\omega)$ of the system is plotted on the Nichols chart in the compensator design process, and the frequency values chosen

for plant template evaluation are identified on this plot. Flight performance specifications require that the open-loop transmission has a phase margin frequency ω_ϕ less than 30 rad/sec. That is, the open-loop transmission must be 0 dB or less at frequencies greater than 30 rad/sec. Thus, specifying a template at 30 rad/sec results in the plotting of a labeled 30 rad/sec point on the open-loop transmission plot. This point provides a quick go/no-go condition for the ω_ϕ frequency requirement during the design process.

The templates frequencies are typically chosen to be one octave apart, starting from the lowest frequency value, to provide sufficient resolution over the frequency range of interest. Therefore the template frequencies used in this study are:

$$\omega = 0.01,\ 0.02,\ 0.04,\ 0.08,\ 0.16,\ 0.32,\ 0.64,\ 1.28,\ 2.56,\ 5.12,\ 10.24,\ 30 \quad \text{rad/sec} \qquad (107)$$

and the corresponding templates for the roll-rate channel of this study are presented in Fig. 13. The templates for the other two channels are very similar, and are therefore not shown.

From the templates, a nominal plant must be chosen. The nominal plant P_0 is used to synthesize the nominal loop transmission L_0 and the performance bounds, which are displayed on the Nichols in the compensator design steps. This guarantees that if the nominal loop transmission meets or exceeds all stability and performance bounds, all plant cases and all points within the uncert :nty region will also meet of exceed these bounds. The nominal plant is typically chosen to be the plant in the lower left corner of the template with the fewest number of (preferably none) unstable poles. In this study, none of the plants have unstable poles, and plants 1, 2, 3 and 4 are all in the bottom portion of the template at low frequencies. Plant 4 is chosen since it has the greatest number of dynamic elements to be compensated. With this nominal plant the stability, cross-coupling disturbance, and tracking bounds are formed and plotted on the Nichols chart as described in the following sections.

4.7. Bounds on Nichols Chart

4.7.1. Stability Bounds. The stability bounds constrain the maximum closed loop transmission based on the open loop transfer function to have a bounded magnitude, as described in Eq. (104). This

specification is met by requiring that the open-loop MISO transfer function, for all J plants, does not

violate the M_L contour on the Nichols chart. This is assured by plotting a bound on the Nichols chart

which the nominal open loop plant transmission $L_{io} = g_i q_{iio}$ must not violate. Keeping the nominal open

loop plant transmission outside this bound ensures that no other plant in the template penetrates the M_L

contour for that particular frequency. Because the shape of the template plotted at each frequency is

unique, the stability bound for each frequency is also unique. Figure 14 shows the stability bounds for the

roll channel in this study.

4.7.2. Cross-Coupling Disturbance Bounds. The responses of the off-diagonal MISO loops result

from coupling and are considered undesirable components which are added to the commanded diagonal

MISO loop response. Performance specifications require that the magnitude of the transmission t_{ij} for these

off-diagonal MISO loops remain below the bounds b_{ij} where $i \neq j$, as shown in Eq. (101) and (103).

Keeping the open-loop transmission above the cross-coupling disturbance bound on the Nichols chart at

each frequencies ensures that this condition is met. The cross-coupling disturbance bounds generated for

the roll channel of this study appear in Fig. 15. These bounds are verified by hand calculations, using the

pertinent equations presented in [24].
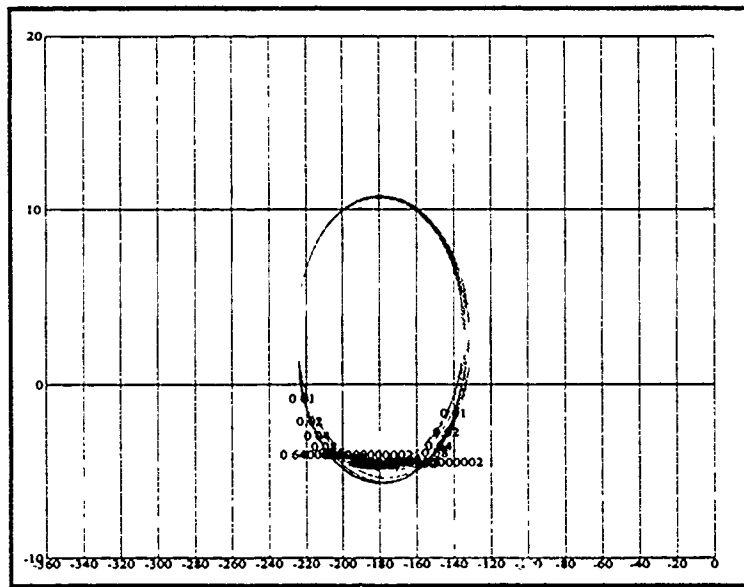
Figure 14. Roll Rate Channel Stability Bounds
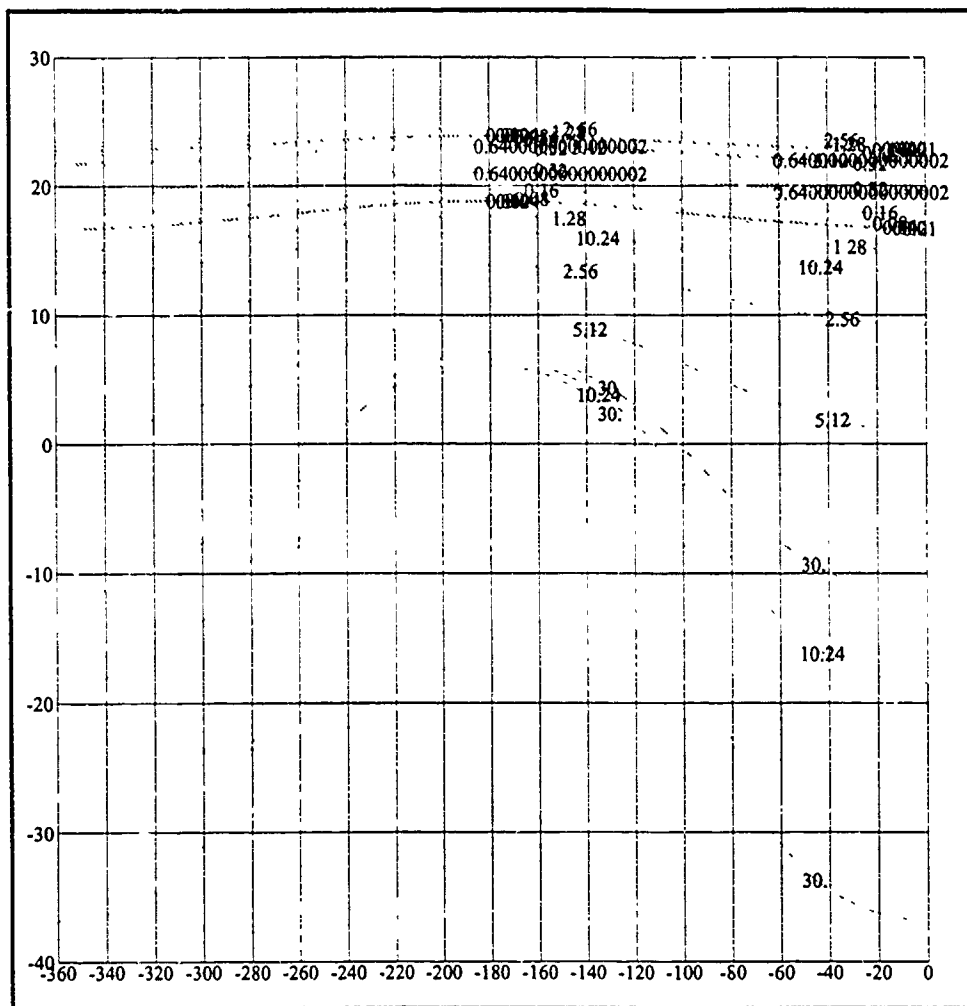
Figure 15. Roll Rate Channel Cross-Coupling Disturbance Bounds

4.7.3. Tracking Bounds. Tracking bounds are used to ensure that the variation in closed-loop

frequency domain transmission t_{ii} does not exceed the variation δ_R permitted by the performance tolerances

a_{ii} and b_{ii}, where:

$$\delta_R = 20 \log\left(\frac{b_{ii}}{a_{ii}}\right) = 20 \log(b_{ii}) - 20 \log(a_{ii}) \tag{108}$$

Since the closed-loop transmission consists of two parts, as described in Eq. (96), and the tracking bounds

are used only for the tracking portion of the transmission, the tracking bounds must be slightly more

restrictive than if no cross-coupling disturbance is present. These more restrictive tracking bounds are

54

called allocated tracking bounds in the CAD package. A more detailed explanation, and a method of formulating these bounds, can be found in [24]. Figure 16 shows the allocated tracking bounds for the roll-rate channel in this study.

4.7.4. Composite Bounds. To reduce the number of bounds plotted on the Nichols chart while designing the compensator, the CAD package allows the formation of composite bounds. A composite bound is simply the most restrictive portion of each of the three bounds for a given frequency. Only this composite bound is plotted, reducing the clutter on the screen. The composite bounds are used in the design process, and may therefore be seen in the design chapter.
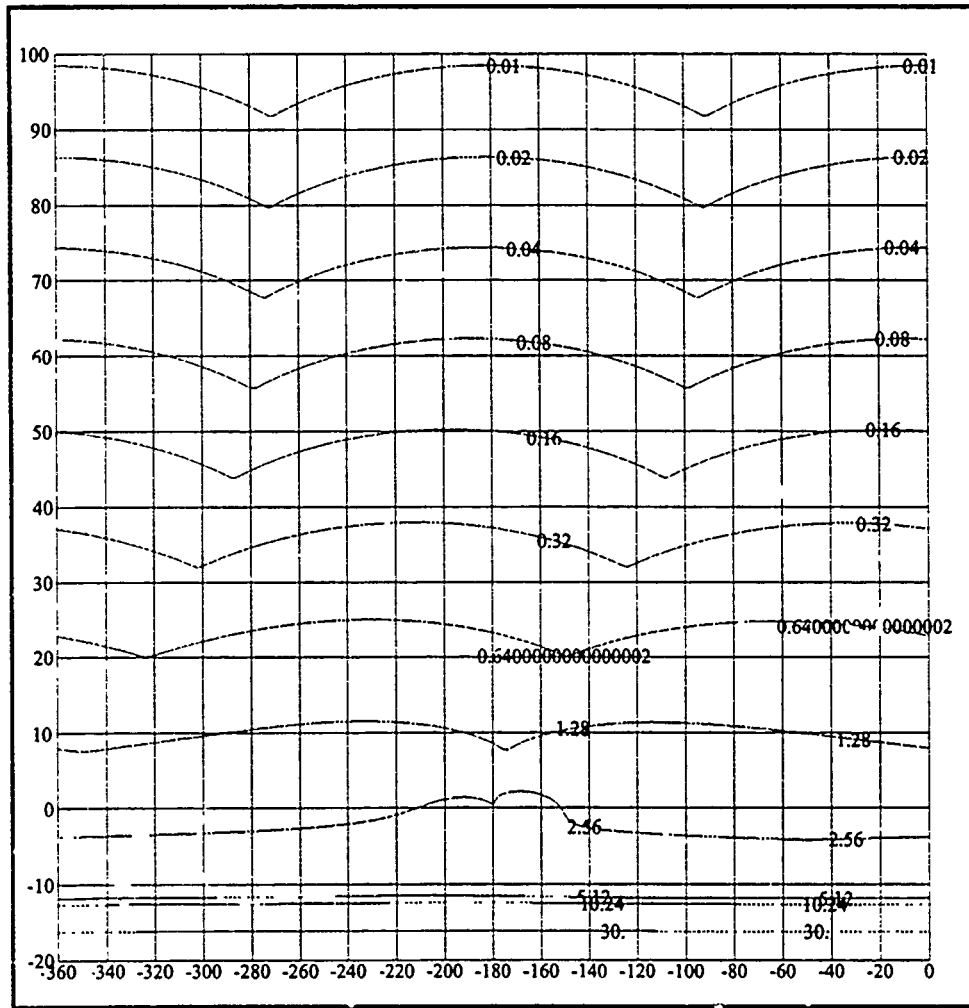
Figure 16. Roll Rate Channel Allocated Tracking Bounds

4.8. Loop Shaping

The interactive design of each compensator element, g_i, is performed graphically by plotting the nominal open-loop transmission $L_{io} = g_i q_{iio}$ on the Nichols chart, along with the aforementioned composite bounds. At the onset of the design, g_i is a unity gain element and the open-loop transmission is therefore equivalent to the expression $L_{io} = q_{iio}$. Starting with this open-loop transmission ensures that one obtains a minimum order compensator element. The interactive design of the compensator element g_i then involves "building up" the compensator element transfer function from its unity value by inserting poles and zeros and by adjusting the gain of the element until a desirable loop shape is obtained on the Nichols chart.

In general, the less bandwidth used to do a particular control job, the more optimal it is. For the QFT problem, this translates to synthesizing L_{io} such that it exactly meets every composite boundary at the respective bound frequency, and remains just outside the phase margin angle boundary on the Nichols chart. The tradeoff for optimality is complexity of compensation; more poles and zeros are required to closely meet the optimum loop transmission. For implementation, especially in a digital system, it is necessary to keep the magnitude of the poles and zeros to a minimum. While digital implementation requirements are not specifically addressed in this study, this guideline are followed to maintain the reasonableness of the design. A successful compensator is achieved when the open-loop transmission meets all composite bounds and the 20 rad/sec phase margin frequency requirement.

4.9. Prefilter Synthesis

A compensator satisfying all bounds on the Nichols chart guarantees that the *range of variation* in the closed loop transmission t_{ii} is acceptable for the corresponding MISO loop, that is:

$$\Delta t_{ii} \leq \delta_{R_i} \tag{109}$$

However, the compensator design does not guarantee that this transmission lies entirely within desired tracking bounds a_{ii} and b_{ii}. Therefore, a prefilter is interactively designed in the CAD package for each MISO loop such that the tracking bounds are satisfied for all plant cases, as explained in detail in [24]. This prefilter synthesis completes the design phase for each MISO loop.

56

This chapter presents the MIMO QFT compensator and prefilter design technique, as applied to this study. The design process is explained in detail for the channel of primary interest, the roll rate channel. Interesting highlights of the pitch and yaw rate channel designs are then presented. The chapter concludes with a summary of the compensator and prefilter designs for all three channels.

5.1. Design Overview

The closed-loop MIMO system resulting from the MISO equivalent system designs is robust, and relatively simple to achieve. Using the Method 1 QFT design technique, each of the MISO equivalent loops is designed independently of the others; the order of design is not important, and no iteration between the loops is required. However, there is generally correlation between the MISO equivalent loops which may, in some cases, be used to further optimize the loop transmissions. The disturbance inputs in the design equations for each MISO loop utilize the *worst case* cross-coupling disturbances that can be produced by the other loops, resulting in some inherent overdesign. After the compensator and prefilter for a particular loop have been designed, however, the cross-coupling effects of that loop are known, and this information may be used to reduce the overdesign in the other channels. This is the essence of a QFT Method 2 (or Improved Method) design. Obviously, the first MISO loop design is performed using the original (Method 1) design technique, since no knowledge of the other loops yet exists. The Method 2 design technique is then applied to the remaining loops.

In a Method 2 design, the order in which the MISO loops are designed is no longer irrelevant. Typically, the loop with the least uncertainty, and therefore the smallest bandwidth requirement, is chosen as the first design loop. The reason for this choice can be seen in the development of the Method 2 design technique presented in [17]. Any loop designed with Method 2 will have a bandwidth equal to or greater than the previously designed loops. Choosing the loop with the lowest bandwidth then supports the bandwidth minimization optimality criterion stated in the previous chapter. In this study, the bandwidth can most easily be obtained from the Bode plot of the **Q** matrix, Fig. 81, Appendix D. Bandwidth is

typically defined as the half-power point, the frequency at which the magnitude is 3 dB down from (70.0% of) the $\omega = 0$ value. This frequency, for the three channels in this study, is approximately 0.6, 0.2, and 0.12 rad/sec respectively, so the third (yaw rate) channel would typically be designed first. Additionally, the most restrictive disturbance bounds for the primary channel of interest in this study, the first (roll rate) channel, are due to the cross-coupling effects of the third channel. Therefore, a Method 2 design based on the yaw rate channel should potentially yield the best results.

In this study, however, the Method 2 design technique does not produce any significant performance improvements for two reasons. First, the roll rate tracking bounds of Fig. 16 are much more dominant at low frequencies than the roll rate cross-coupling disturbance bounds of Fig. 15 (the bounds for the yaw channel are very similar). Second, the phase margin frequency of all three channels is very high. Initial design steps for the yaw channel show that the low frequency allocated tracking bounds make the 30 rad/sec phase margin frequency requirement discussed in the previous chapter very difficult to meet. An initial Method 1 design for the yaw channel has a phase margin frequency of approximately 27 rad/sec. Because the phase margin frequencies of the succeeding channels to be designed using Method 2 will be greater than this, the 30 rad/sec requirement is very difficult to meet. A preliminary design of the second (pitch rate) channel shows the same dilemma, the allocated tracking bounds require a phase margin frequency within only a few degrees of the 30 rad/sec requirement. Therefore, the Method 2 design technique is not suitable to this study. Additional justification for this statement is provided in the following detailed design sections.

Because the Method 2 design technique is not applicable, and because the diagonal dominance condition is satisfied for this system, the Method 1 design technique is employed in this study. The QFT compensator and prefilter designs for the channel of primary interest, the roll rate channel, are performed first, followed by the designs for pitch and the yaw rate channels.

5.2. Roll Rate Channel Design

Plant case #4 is selected as the nominal plant for the roll rate channel design as discussed in Chapter 4. The nominal plant transfer function associated with this loop, from Appendix D, can be represented in pole-zero format:

$$q_{11_o} = \frac{382.638\,(-15.5951 \pm j41.2)(-21.797 \pm j32.8031)(-55.805 \pm j83.9308)}{(-0.5778)(-13.8037 \pm j18.5569)(-15.947 \pm j39.4318)(-48.7136 \pm j53.6489)(-57.6412 \pm j84.2113)} \tag{110}$$

where the negative signs denote left-half plane roots and the first term in the numerator is the gain.

5.2.1. Compensator Design. The initial open-loop transmission ($L_{i_o} = q_{11_o}$ since $g_1 = 1$) along with the composite bounds, is shown in Fig. 17. For stability, the nominal loop transmission must pass around the right side of the stability contour, and to meet the performance specifications, the nominal loop transmission must lie above the composite bounds at each corresponding frequency.

Before designing the compensator, several of its characteristics can be identified. First, the bandwidth of the open-loop transmission must be small enough that the aircraft body-bending modes are not excited by commanded or disturbance inputs. Therefore, a high-frequency roll-off rate of at least -60 dB/sec is designed into the open-loop transmission. This roll-off rate is achieved by ensuring that the transfer function for the open-loop transmission has an excess of at least three poles over the number of zeros. Since the plant itself has three excess poles, the compensator for this channel must have at least an equal number of poles and zeros, although more poles are allowed. Second, to allow closed-loop tracking of a step input, the open-loop transmission must contain a pure integrator (pole at the origin). Because the plant itself does not contain a pure integrator, this is the first element to be included in the compensator, g_1. Finally, the gain of g_1 must be increased to raise the open-loop transmission above the low-frequency allocated tracking bounds.

With these basic characteristics of the compensator identified, the design process begins. Knowledge of the plant transfer function, the graphical display of the CAD package, and automatic gain adjustment in the CAD package, make the selection and adjustment of compensator poles and zeros a
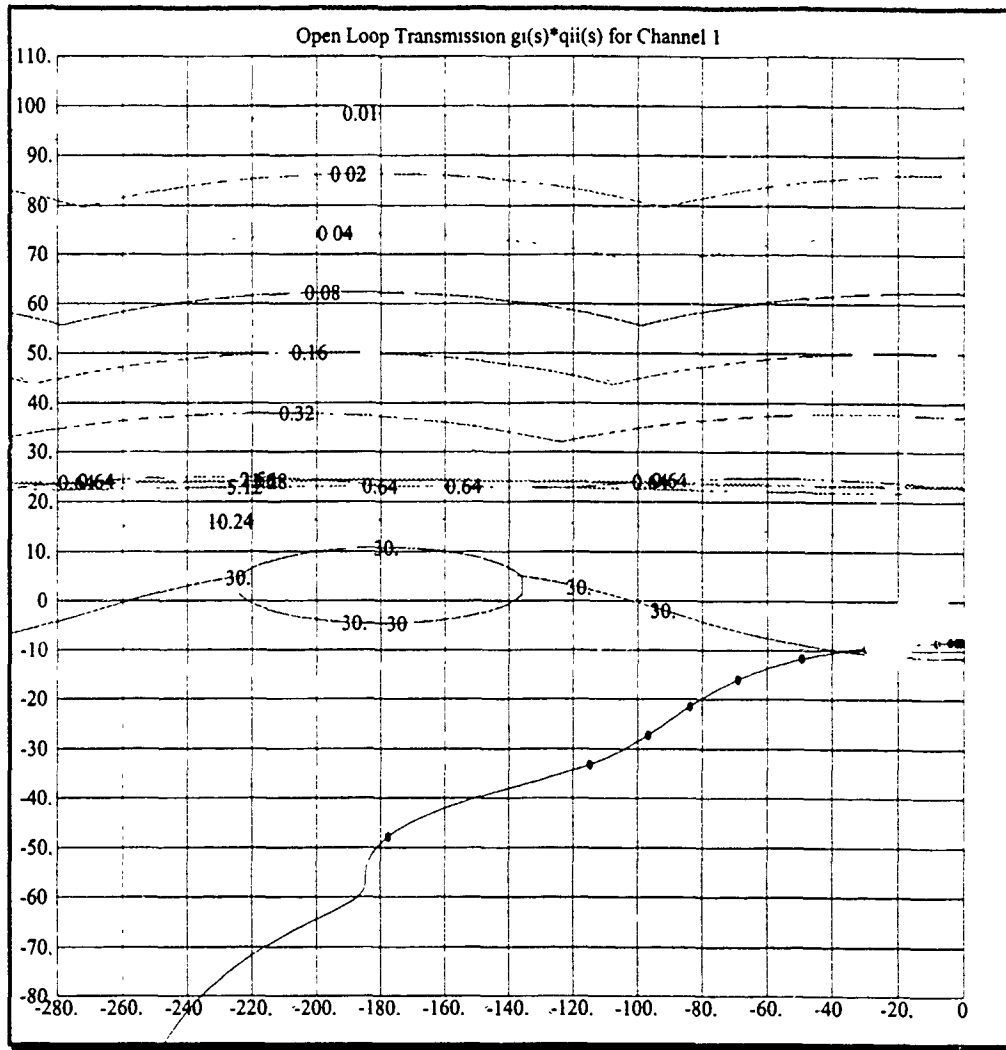
Figure 17. Roll Rate Channel, Initial Loop Transmission and Bounds

relatively straightforward task, provided that the bounds can be met. In the case of this channel, however,

these bounds are not easily met. The compensator transfer function, in pole-zero format,

$$g_1 = \frac{900(-35)(-10.25 \pm j17.7535)(-5)}{(0)(-60)(-50)(-20)} \tag{111}$$

yields the open-loop transmission shown in Fig. 18. The allocated tracking bound of 0.01 rad/sec makes

the 30 rad/sec ω_ϕ requirement just attainable. However, this requirement is met only at the expense of

violating the $\omega = 10.24$ rad/sec cross-coupling disturbance bound from the yaw channel (the dotted curve).

The tradeoff is then between the allowable cross-coupling in the yaw rate channel and the 30 rad/sec ω_ϕ

60

requirement. In flight control system design, the latter is a more fast design rule than the former. Additionally, the disturbance bound is a mere reflection of the rather arbitrary cross-coupling disturbance specifications set at the beginning of the QFT design. As can be seen in Fig. 18, the disturbance bound violation is less than 5 dB, and does not result in a significant degradation of the closed-loop response, as shown later. Therefore, with the 30 rad/sec ω_ϕ requirement having greatest priority, the compensator of Eq. (111) is chosen as the final design for the roll rate channel, despite the cross-coupling disturbance bound violation. Figure 19 shows that the open-loop transmissions for all twelve plant cases meet the desired stability specification of $\gamma = 45°$. Again, note the grouping of the plants by the three F.C.s.
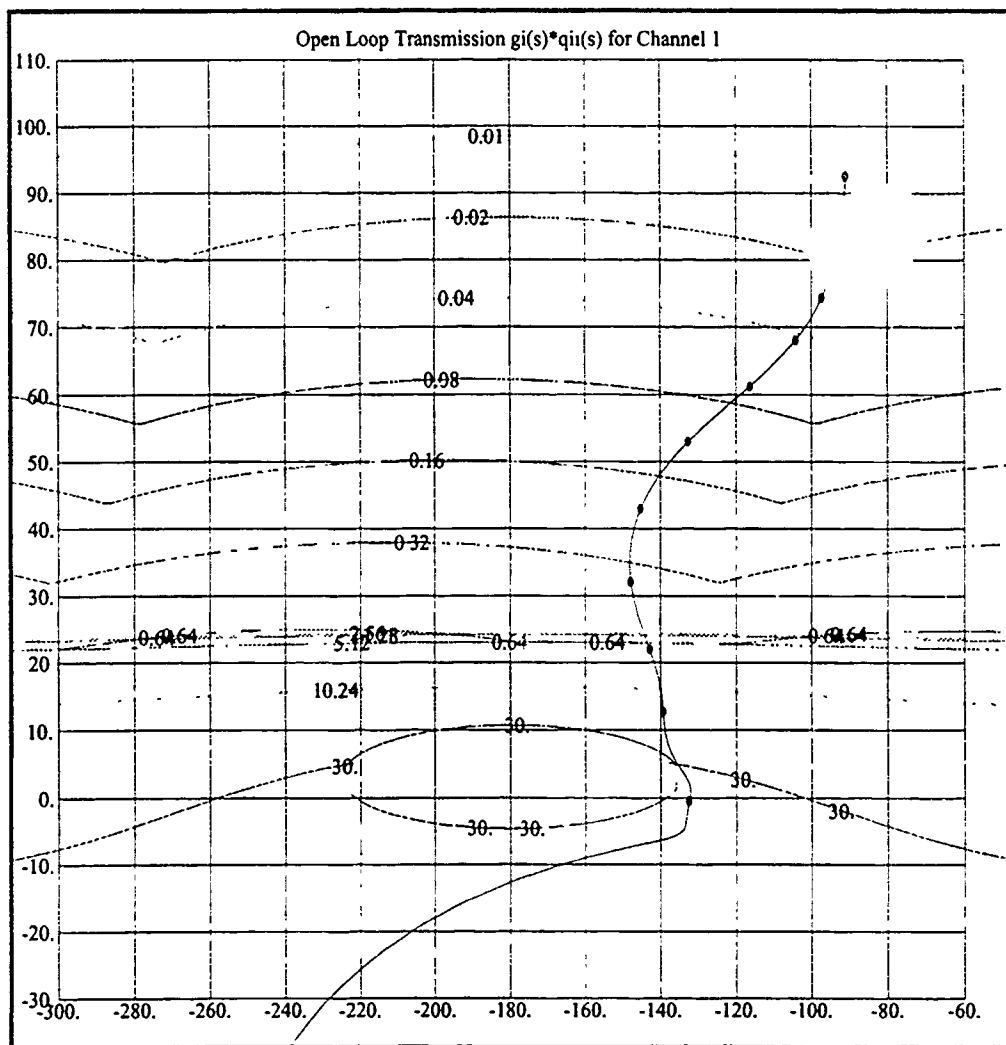
Figure 18. Roll Rate Channel, Compensator Design
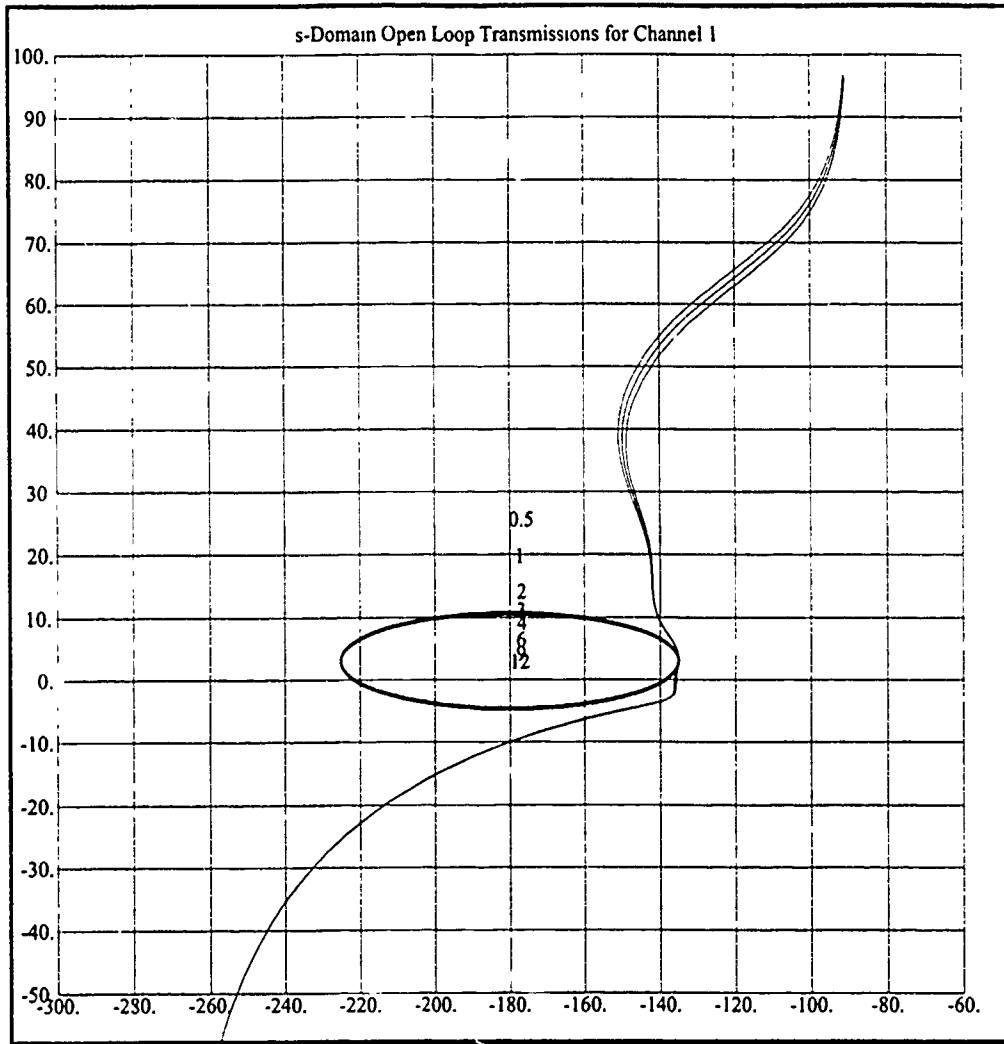
Figure 19. Roll Rate Channel, Stability Validation

5.2.2. Prefilter Design. Like the compensator design, the prefilter design is rather straightforward using the CAD package. The object of the design process is to design the prefilter transfer function which causes the nominal open-loop transmission due to tracking, t_{r_1}, to fall within a set of bounds representing the tracking specifications. Simple selection of appropriate poles and zeros, with the automatic gain adjustment provided by the CAD package, produces a prefilter to meet the bounds:

$$f_1 = \frac{23.04}{(-3.744 \pm j3.00374)} \tag{112}$$

as shown in Fig.20.

62
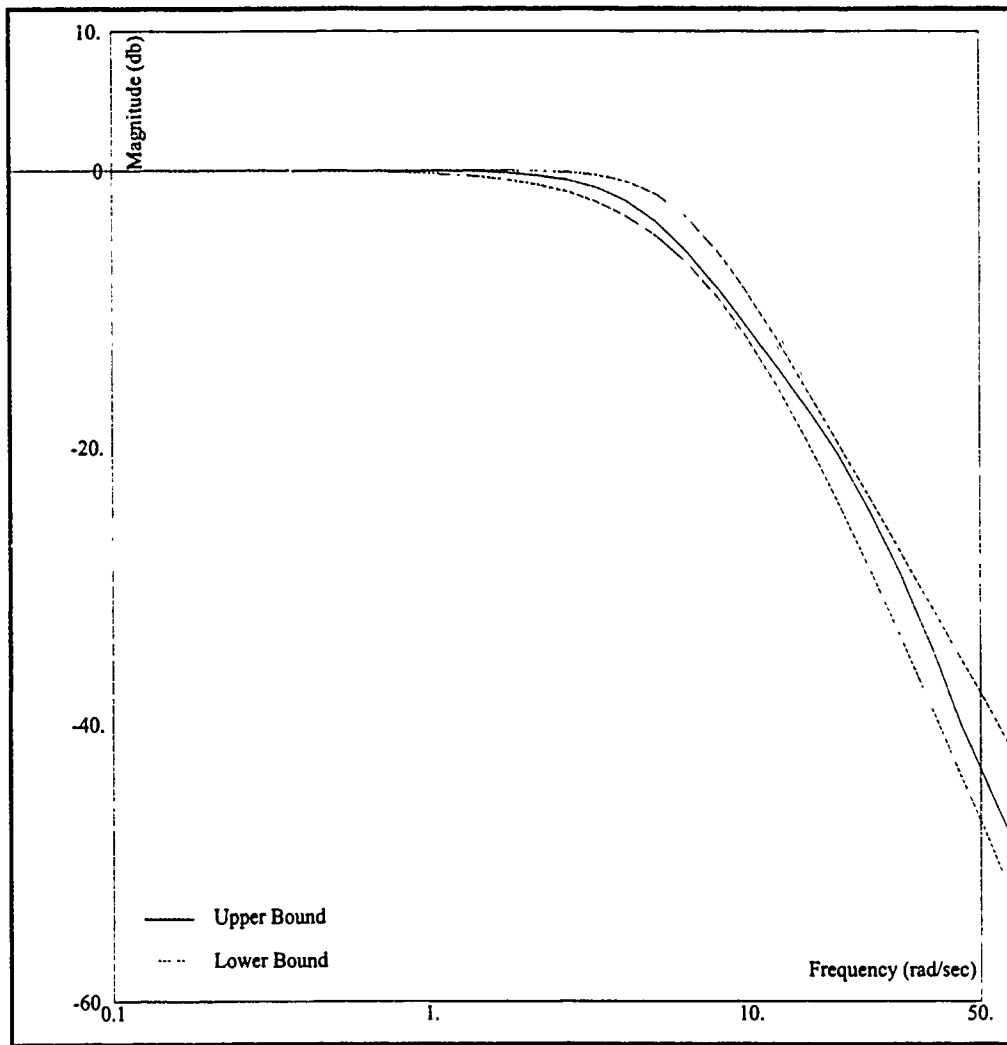
Figure 20. Roll Rate Channel, Prefilter Design

The successful design of the compensator and prefilter completes the roll rate channel design. The performance validation of this channel, along with the other two channels, is presented in the validation section of this chapter.

5.3. Pitch and Yaw Rate Channel Designs

The compensator and prefilter designs for the pitch and yaw rate channels are relatively similar to the roll rate channel design. However, several differences are worth noting, and are therefore presented in this section.

63

Plant case #4 is again chosen as the nominal plant for both the pitch and yaw rate channels, as it was for the roll-rate channel. The plant transfer functions for these two channels in pole-zero format are:

$$q_{22_4} = \frac{-204.4086\,(-14.7658 \pm j21.9937)(-17.1538 \pm j86.6395)}{(-0.1485)(-13 \pm j15.1987)(-14.924 \pm j33.1999)(-62.127 \pm j85.0196)} \tag{113}$$

$$q_{33_4} = \frac{-853.0411\,(-15.5951 \pm j41.2003)(-21.797 \pm j32.8030)(-55.805 \pm j83.9308)}{(-0.1181)(-13.1446 \pm j15.9248)(-15.7355 \pm j42.0323)(-49.6517 \pm j52.1523)(-55.2737 \pm j83.7978)} \tag{114}$$

5.3.1. Compensator Designs. The composite bounds for the pitch channel, shown in Fig. 21, are very similar to those in the roll rate channel design. However, the initial open-loop transmission does not start with a zero degree phase angle, as does the roll rate channel open-loop transmission, due to the negative gain. Therefore, to achieve the initial -90 degree phase angle required for perfect tracking, the compensators for the pitch and yaw rate channels must have a negative gain and a pole at the origin. Introducing a negative gain shifts the start of the open-loop transmission back over to the zero degree phase angle line (where the roll channel open-loop transmission starts), and the pole at the origin (pure integrator) shhifts open-loop transmission to the -90 degree phase angle line, ensuring perfect tracking. Again, the number of poles must equal or exceed the number of zeros in the compensators for both the pitch and yaw channels, so that the open-loop transmissions have a high-frequency roll-off of at least -60 dB/dec.

Using the CAD package, the following compensators for the pitch and yaw rate channels are realized:

$$g_2 = \frac{-1225\,(-5.5)(-17.1 \pm j22.8)(-32)}{(0)(-57 \pm j18.735)(-65)} \tag{115}$$

$$g_3 = \frac{-300\,(-6)(-14.35 \pm j14.6399)}{(0)(-50)(-50)} \tag{116}$$

Figure 21. Pitch Rate Channel, Initial Open-Loop Transmission and Bounds

The open-loop transmissions for these final compensator designs, as well as the stability validation plots for all plant cases, appear in Figs. 22 - 25. It should be noted that no performance bounds are violated to meet the $\omega_\phi = 30$ rad/sec phase margin frequency requirement.
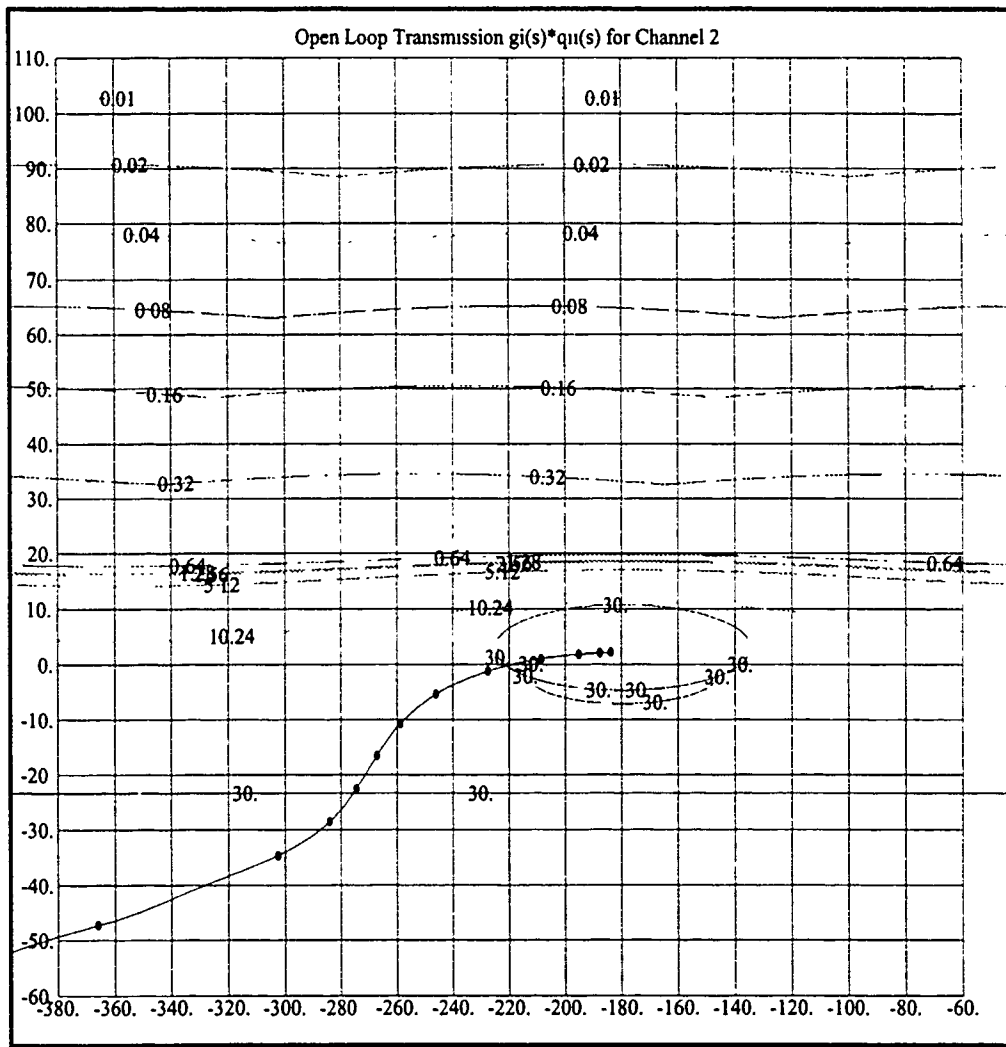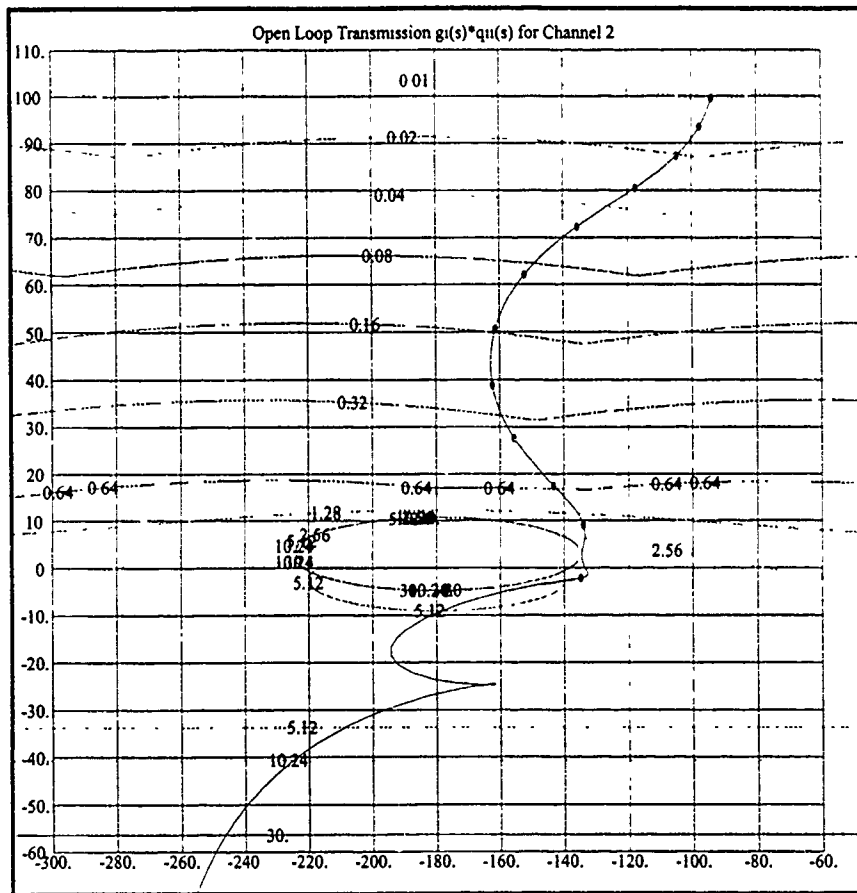
Figure 22. Pitch Rate Channel, Final Compensator Design
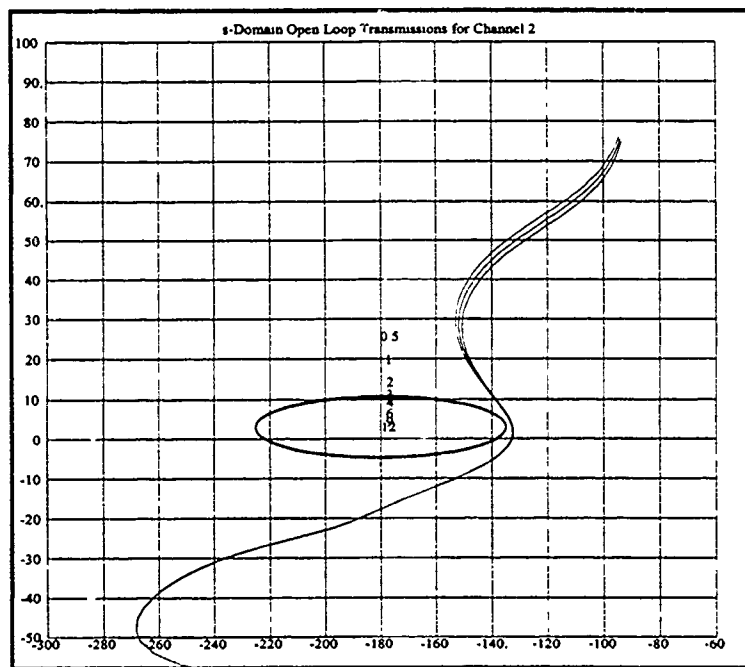
Figure 23. Pitch Rate Channel, Stability Validation

66

Figure 24. Yaw Rate Channel, Final Compensator Design

Figure 25. Yaw Rate Channel, Stability Validation
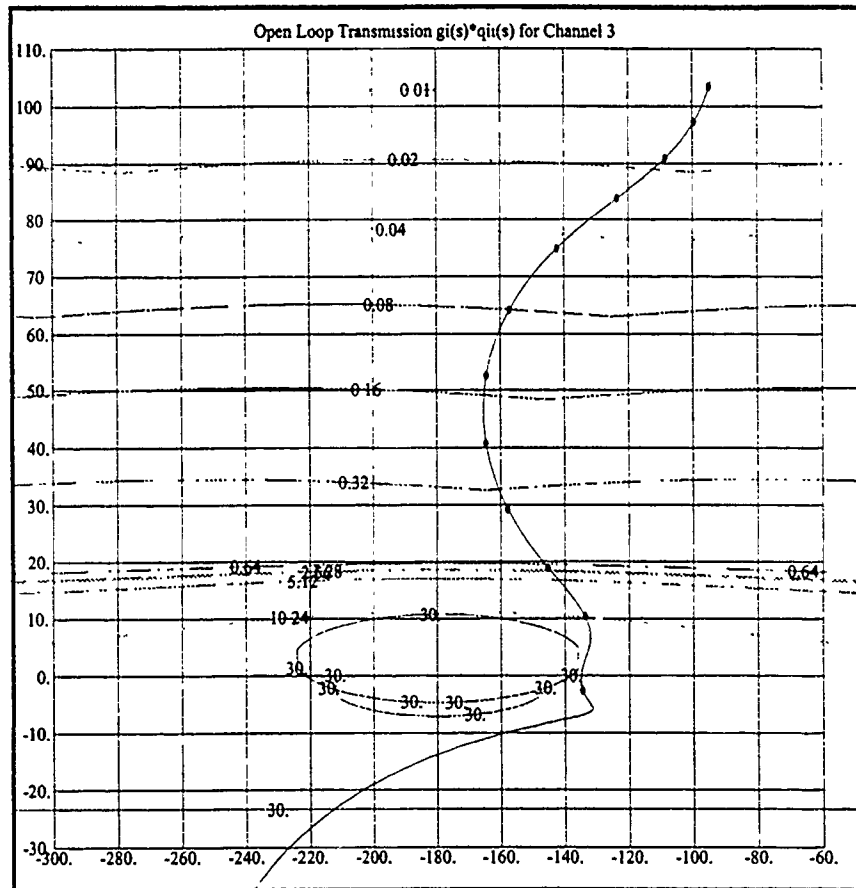
5.3.2. Prefilter Designs. The prefilter designs for the pitch and yaw rate channels are identical to each other, and very similar to the roll rate channel prefilter design.

$$f_2 = f_3 = \frac{25}{(-4 \pm j3)} \tag{117}$$

The prefilter design plots are nearly identical to the roll rate channel prefilter design plot shown in Fig. 19 and are therefore not included in this presentation.

5.4. Performance Validation

If all bounds are met in the design process, the compensator and the prefilter should yield a system which meets all stability and performance bounds. Figures 19, 22, and 24, demonstrate that the compensated system meets the stability specifications. The CAD package also provides a means to test the tracking response of the closed loop system. A visual inspection of the Bode plots of the transfer function matrix $\mathbf{T} = \{t_{ij}\}$ for all plant cases, and of the performance bounds a_{ii} and b_{ij}, allows easy identification of performance violations, as shown in Fig. 26.

The consequences of violating the -26 dB cross-coupling disturbance bound in the roll rate channel design is evident in the $\{1,3\}$ element of the tracking validation matrix. A close-up view of this element, Fig. 27, shows that the actual violation is approximately 4 dB, which is very close to the violation seen on the Nichols chart during the compensator design (Fig. 18). This violation translates to a maximum yaw rate output, due to cross-coupling, of approximately 1.5 deg/sec, given a 20 deg/sec roll rate command. The *maximum* sideslip angle that can develop in the one second transition region of the velocity vector roll is 1.5 deg, which is not large enough to invalidate the near-zero assumption used in the QFT model development. Therefore, the cross-coupling disturbance bound violation is deemed acceptable. All other performance bound violations appearing in Fig. 26 occur at frequencies well above the bandwidth frequency of approximately 10 rad/sec, and are therefore also deemed negligible.
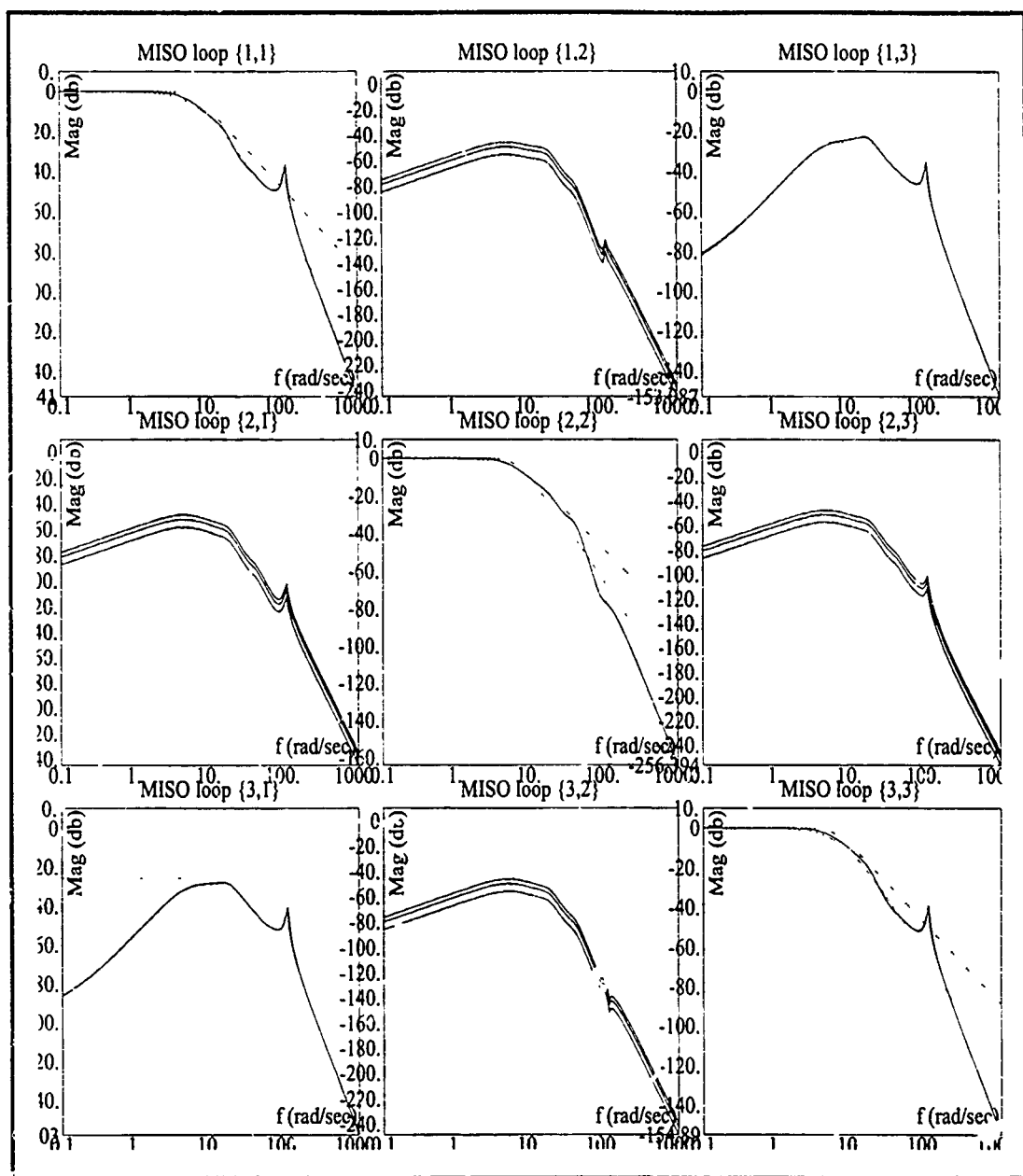
Figure 26. Tracking Validation for MIMO System

69
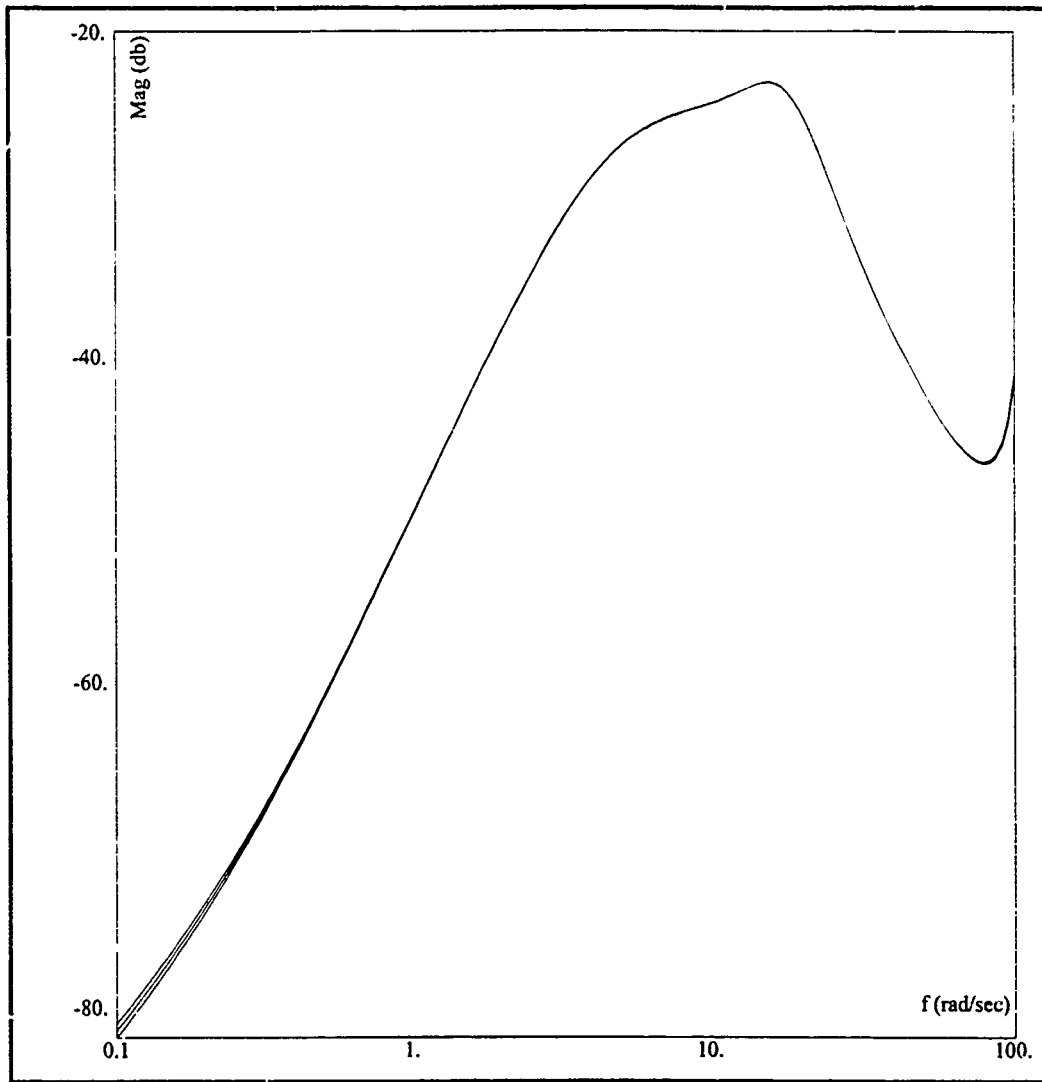
Figure 27. Tracking Validation, {1,3} Element Close-Up

5.5. Design Summary

The compensator and prefilter designs for the three channel MIMO system are summarized in Table

6. The QFT designs are shown to provide a stable closed-loop system meeting the desired phase margin

angle of forty-five degrees, the phase margin frequency requirement of 30 rad/sec, and acceptable tracking

performance requirements. The MIMO compensator and prefilter,

$$\mathbf{G}(s) = \begin{bmatrix} g_1(s) & 0 & 0 \\ 0 & g_2(s) & 0 \\ 0 & 0 & g_3(s) \end{bmatrix} \qquad (118)$$

70

$$F(s) = \begin{bmatrix} f_1(s) & 0 & 0 \\ 0 & f_2(s) & 0 \\ 0 & 0 & f_3(s) \end{bmatrix} \tag{119}$$

are therefore ready for simulation of the velocity vector roll maneuver.

Table 6. Design Summary, Compensator and Prefilter Transfer Functions

g_1	g_2	g_3
$\dfrac{900\,(-5)(-10.25\pm j17.7535)(-35)}{(0)(-20)(-50)(-60)}$	$\dfrac{-1225\,(-5.5)(-17.1\pm j22.8)(-32)}{(0)(-57\pm j18.735)(-65)}$	$\dfrac{-300\,(-6)(-14.35\pm j14.6399)}{(0)(-50)(-50)}$
f_1	f_2	f_3
$\dfrac{23.04}{(-3.744\pm j3.00374)}$	$\dfrac{25}{(-4\pm j3)}$	$\dfrac{25}{(-4\pm j3)}$

This chapter describes the various simulations used to validate the QFT compensator designed in the previous chapter. All simulation steps, including model development, input definition, and output analysis, are presented as the simulation complexity increases from basic linear simulations to complex nonlinear six DOF simulations. All simulations are performed in MATLAB's Simulink program running on a Sun SparcStation 2. The Simulink block diagrams, based on the three DOF linear model developed in Chapter 3 and the six DOF partially linearized model presented in Chapter 2, are presented for each simulation, and the simulation output plots are presented in this chapter and in Appendix E.

6.1. Three DOF Simulation

The first, and most basic, method of validating the QFT design is to form a closed-loop system around the linear three DOF open-loop model presented in Chapter 3 and shown in Fig. 73, Appendix B. Because this model, fitted with the proper **A** and **B** matrices, exactly matches the plants entered into the QFT CAD package, these closed-loop simulations only show that the QFT design methodology has been successfully applied to the plants loaded into the CAD package. These simulations *do not* validate the applicability of the three DOF models and of the QFT design to the *nonlinear* plant performing a velocity vector roll maneuver; this nonlinear design validation is performed using the six DOF model in the upcoming sections of this chapter.

To form the closed-loop system, the compensator, prefilter, weighting matrix, and actuator dynamics are incorporated into the open-loop three DOF model. Because the actuator models must be placed between the weighting matrix and the plant control inputs, the weighting matrix of the three DOF open-loop simulation cannot be "rolled into" the **B** matrix of the state-space model as done in the open-loop model development in Chapter 3. Instead, the weighting matrix must be placed as a separate entity in the forward path, ahead of the actuator models and after the compensator and prefilter blocks. A feedback loop is placed around the compensator, weighting matrix, actuator models, and plant model, producing the closed-loop three DOF system shown in Figs. 28-30.
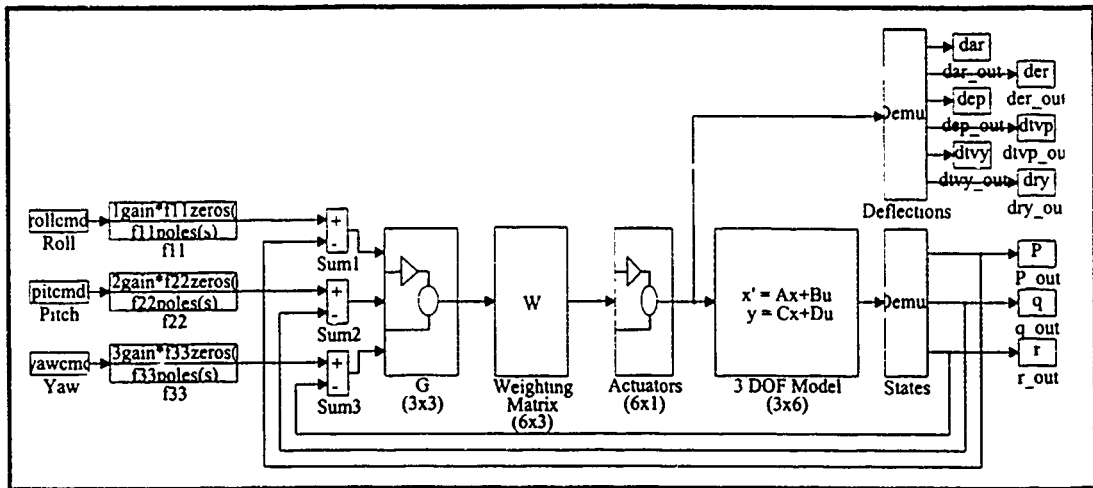
Figure 28. Three DOF Closed-Loop System, Top-Level Block Diagram
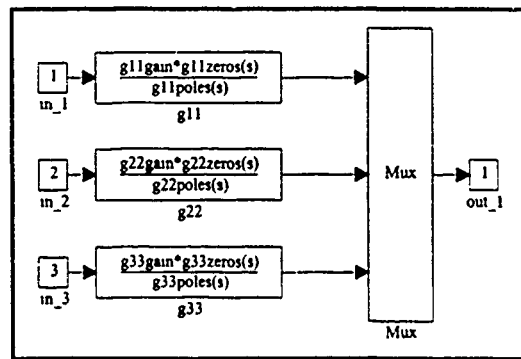
Figure 29. Compensator (G) Block Diagram
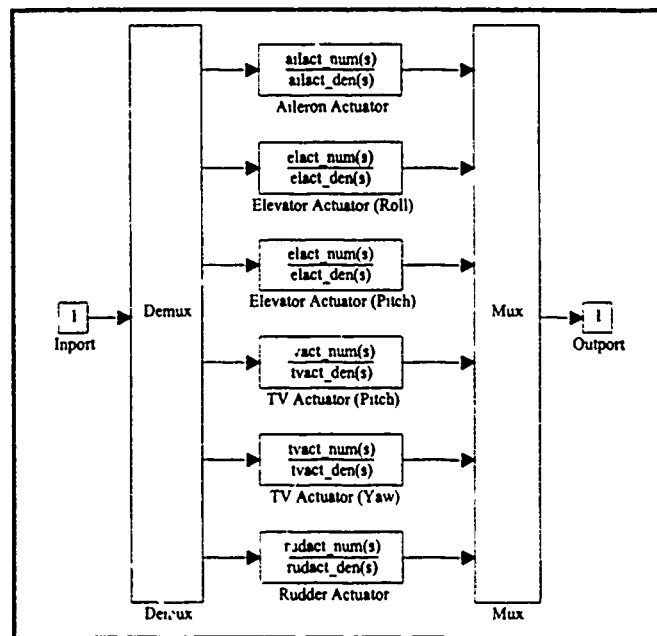
Figure 30. Actuator Dynamics Block Diagram

An exhaustive time-domain validation of the QFT design requires that simulations be performed on all twelve linear plant cases used in the design process. However, six simulations covering the entire range of variation in the nonlinear parameter (*Pparam* = 0, 8, 16, 24 deg/sec) at an altitude of 10,000 feet, and the entire range of altitudes (10, 15, 20 kft) for the maximum value of the nonlinear parameter (Pparam = 24 deg/sec), are sufficient to demonstrate the applicability of the QFT design to a velocity vector roll using the three DOF closed-loop system. These simulations are identical to those used to validate the open-loop three DOF model in Appendix B.

The velocity vector roll maneuver is simulated by commanding a 20 deg/sec (0.349 rad/sec) step roll rate and a constant zero pitch and yaw rate, to each of the closed-loop models described in the previous paragraph. The desired response to these inputs is a 20 deg/sec roll rate and near-zero pitch and yaw rates throughout the one-second transition region of the velocity vector roll. The simulated aircraft response to these inputs, as well as the simulated control effector group commands, is presented in Fig's. 82 -93, Appendix E. These plots show that the 20 deg/sec roll rate can be achieved in the required one-second time period, while regulating the pitch and yaw rates within the maximum allowable 1 deg/sec rate design specification. As expected, the cross-coupling effect in the pitch rate channel increases as the value of *Pparam* increases, yet the pitch rate remains within the design specifications for all plant cases. Similarly, the cross-coupling in the yaw rate channel stays well below the maximum allowable rate for all plant cases.

Interestingly, the changes in *Pparam* and the resulting changes in pitch rate response have no noticeable effect on the response in the roll and yaw rate channels, even though the equations for these two channels include the modeled nonlinearity *Pparam*q*. This implies that this nonlinearity is non- dominant in these state equations. The F.C. grouping of the open-loop transmission plots in the design chapter provide an early indication of this phenomenon.

One of the limitations of linear design techniques is the inability to account for, or design to, the nonlinearities caused by control surface saturation. While the aircraft state responses described above are impressive, the control effector group commands required to achieve these rates are not reasonable. The maximum permitted control effector group commands are presented in Eq. (81), Chapter 3. For all plant

74

cases, the yaw thrust vectoring and the yaw rudder control effector group commands that these simulations use to maintain the low yaw rate exceed their respective limits by approximately fifty percent. To properly account for the limits on control effector group limits, saturation blocks are added to the closed-loop system. The addition of saturation blocks is postponed, however, until the more realistic six DOF simulations are introduced.

The over-taxing of only the yaw control effectors does point out one characteristic of the aircraft and the weighting matrix and compensator designs; that is, the initiation of the velocity vector roll causes the yaw control effectors to saturate before the roll control effectors. This characteristic implies that the maximum velocity vector roll rate is limited by the cross-coupling characteristics of the aircraft, which the control system cannot overcome. Looking at the yaw rate response, it is tempting to conclude that the yaw rate cross-coupling design specifications should be relaxed slightly such that the yaw rate would be allowed to drift closer to the -1 rad/sec design limit. In this way, the yaw control effector commands would be reduced, and perhaps not exceed the saturation limits. This is not a reasonable solution, however, because the cross-coupling disturbance bounds are frequency dependent. For the frequencies in this particular simulation the yaw rate only drifts to slightly more than -0.4 deg/sec. However, based on the cross-coupling disturbance bounds in the roll channel design Nichols charts, this yaw rate approaches, and actually slightly exceeds, the maximum allowable negative excursion of -1 deg/sec for higher frequency inputs. Therefore, the saturation of the yaw control effectors is simply a characteristic of the aircraft which must be accepted.

One final point of interest is the small oscillations that appear in the roll aileron control effector group commands. Surprisingly, these oscillations are not visibly present in any other control effector group commands or in the roll rate response. However, some very slight oscillations are present in the yaw rate response to the maneuver. Since the roll and yaw channels are highly coupled, the oscillations in the yaw channel are likely the source or the result of the oscillations in the roll aileron control effector group commands. A more thorough investigation of this phenomenon is performed in Chapter 7.

Barring the control effector command characteristics, the three DOF simulations demonstrate that the QFT compensated system meets the desired performance requirements. The next simulation step is to incorporate the QFT design into the partially linearized six DOF model.

6.2. Six DOF Simulation, No Control Effector Limits

The three DOF simulations in the previous chapter demonstrate that the QFT design methodology is successfully applied to the linear plants entered into the CAD package. The six DOF simulations presented in this section extend the design validation by incorporating the true roll rate induced nonlinearities into the plant model. Therefore these simulations validate the primary focus of this study: treating the nonlinearities introduced by the velocity vector roll maneuver as structured uncertainty in the QFT design methodology.

The closed-loop six DOF system is based on the open-loop six DOF model, Fig. 6 in Chapter 2, and includes the QFT prefilter and a feedback path encompassing the compensator, weighting matrix, actuator models, and six DOF plant model, as shown in Fig. 31. All system components, with the exception of the six DOF plant model, are identical to those in the three DOF closed-loop system.

Recall that the development of the three DOF linear plant from the six DOF nonlinear plant in Chapter 3 is based on the following assumptions:
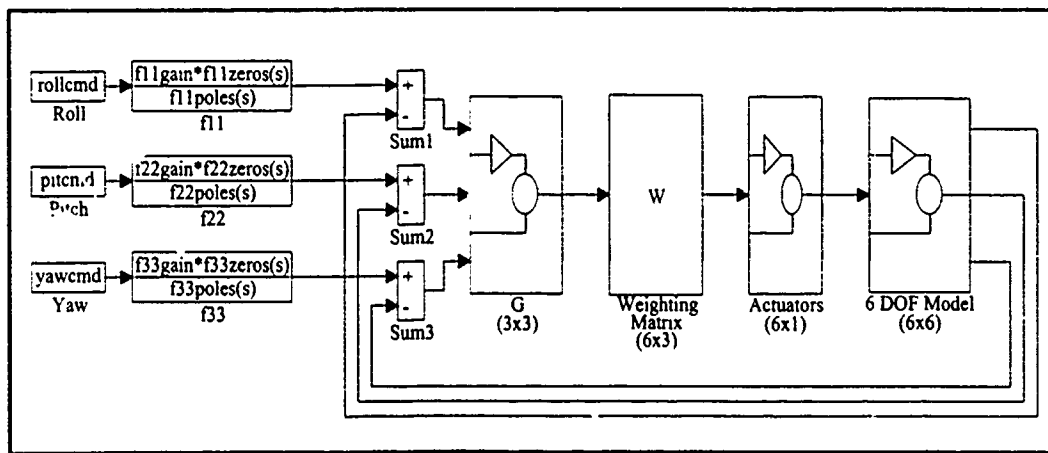
Figure 31. Six DOF Closed-Loop System, Block Diagram

- the regulation of the fast pitch and yaw states to a near zero value produces negligibly small sideslip and yaw angles, therefore $\alpha \cong \beta \cong 0$

- $\phi \cong 0$ or π

Therefore, proper validation of this development requires that the six DOF simulations support these assumptions in both the velocity vector roll initiation and arrest transition regions. Because the nonlinearities due to the velocity vector roll maneuver are now included in the six DOF plant model, only three velocity vector roll simulations, corresponding to the three F.C.s, in each transition region of the velocity vector roll are required to validate the design.

6.2.1. Initiating the Velocity Vector Roll. This transition region is the most straightforward to simulate with the six DOF closed-loop system. The aircraft is assumed to be trimmed at thirty degrees AOA, and thus all model states are equal to zero. The inputs required to initiate a 20 deg/sec velocity vector roll are a 20 deg/sec (0.349 rad/sec) step velocity vector roll rate command (P), and a constant zero pitch and yaw rate command.

The state responses to the velocity vector roll command are presented in Figs. 94 - 99, Appendix E, along with the control effector group commands for each F.C. These plots show that the state responses and control effector group commands are virtually identical for all three F.C.s. Therefore, the discussion in this chapter focuses on the 10,000 foot altitude F.C., but is equally applicable to the other two.

The roll and yaw rates experienced in the six DOF simulations are virtually identical to those in the three DOF simulations of the previous section, confirming that the nonlinearities, due to the Pq term, in the roll and yaw rate channels of the EOM, Eqs. (53) and (55), are indeed negligible in the transition region of the velocity vector roll at high AOA. This finding is, of course, based on the requirement that the pitch rate is regulated to a small value by the control system throughout the transition region of the velocity vector roll. This requirement is upheld with the QFT compensated system; the magnitude of the pitch rate falls within the range of pitch rates experienced in the linear three DOF simulations as the nonlinear parameter *Pparam* varies from 0 to 24 deg/sec. Note that the pitch rate increases more slowly in the six DOF simulations than in the three DOF simulations since the nonlinearity increases gradually with the roll rate.

The most important assumption in the three DOF model development is that the AOA and sideslip angle remain close to zero ($\alpha \cong \beta \cong 0$). This assumption not only guarantees that the terms containing α and β in the three rate equations are non-dominant, but also provides the necessary conditions for a successful velocity vector roll. Any significant departure in AOA or sideslip angle means that a true velocity vector roll has not been performed. Regulating the pitch and yaw rates to near-zero values helps ensure that this terminal condition is met. Indeed, the state response plots indicate that the small α and β assumption is justified for the velocity vector roll initiation maneuver.

The final assumption, $\phi \cong 0$ or π radians, cannot be validated as easily. The simulation plots show that over the 1 second period of the simulation, nearly 15 degrees of bank angle develop; this can hardly be considered neglible. Does this mean that the development is invalid? To answer this question, one must look at the six DOF EOM presented in Eqs. (43) to (48), Chapter 2. The basis for the bank angle assumption lies in the trigonometric contributions of the bank angle to the AOA and sideslip state equations. A zero bank angle causes the trigonometric terms in both equations to be zero, removing any dependence of these states on the bank angle; this ensures that states are driven primarily by the pitch and yaw rates which are regulated by the control system. As the bank angle departs from zero, the trigonometric terms increase, along with the potential of bank angle dominance. Because the AOA and sideslip excursions in the simulations do remain negligibly small, the violation of the bank angle assumption is justified, *in this transitions region of the velocity vector roll maneuver.* However, using the design outside the short time period of the transition region, or when the bank angle does not begin with a zero value, may result in larger excursions. This situation is discussed in the following section.

6.2.2. Arresting the Velocity Vector Roll. The second transition region, arresting the velocity vector roll, is far more difficult to simulate than the first transition region, initiating the velocity vector roll. One cannot adopt the simplistic "run of the mill" approach of assuming an initially quiescent plant, because each dynamic element in the system has associated with it an initial condition (IC) that is compatible with a

78

steady angular rate velocity vector roll. To illustrate this fact, and to determine the IC requirements, consider the following development.

Arresting a velocity vector roll implies that the aircraft is already rolling about its velocity vector with some roll rate P. In an ideal velocity vector roll, the other states in the six DOF EOM are all zero, except for the bank angle which increases linearly at the rate of the velocity vector roll. The initial conditions attributed to the six DOF model used in the previous section are therefore:

$$
\begin{aligned}
P_0 &= 0.34907 \text{ rad/sec} \quad (20 \text{ deg/sec}) \\
\phi_0 &= 0 \text{ rad} \\
q_0 &= 0 \text{ rad/sec} \\
\alpha_0 &= 0 \text{ rad} \\
r_0 &= 0 \text{ rad/sec} \\
\beta_0 &= 0 \text{ rad}
\end{aligned}
\tag{120}
$$

where the bank angle is given an IC of zero to remove its side-effects from the six DOF model.

Before simulating the velocity vector roll arrest maneuver, the ICs are tested on the closed-loop system to ensure that they properly define the state of the aircraft. The simplest way to isolate the effects of the ICs on the aircraft is to command the system to maintain the states defined by the ICs. For the ICs in Eq. (120), the command is a 20 deg/sec roll rate and zero pitch and yaw rates. Properly defined ICs should yield a system response to the commanded inputs in which all states of the system simply maintain their ICs. The simulated response, however, is far from the ideal response, as shown in Figs. 32 and 33. Almost immediately the roll rate drops below zero from its 20 deg/sec IC, and the yaw rate rises to nearly 10 deg/sec, well outside the design specifications. In addition, the oscillations which appear rather benignly in the velocity vector roll initiation simulations now appear in alarming proportions in the roll and yaw rate states, and in the roll channel control effector groups. Again, because the actuators are treated as linear devices with no saturation, the control effector group commands violate their limits, but this time by orders of magnitude. Obviously, the ICs have not been properly defined for this simulation.
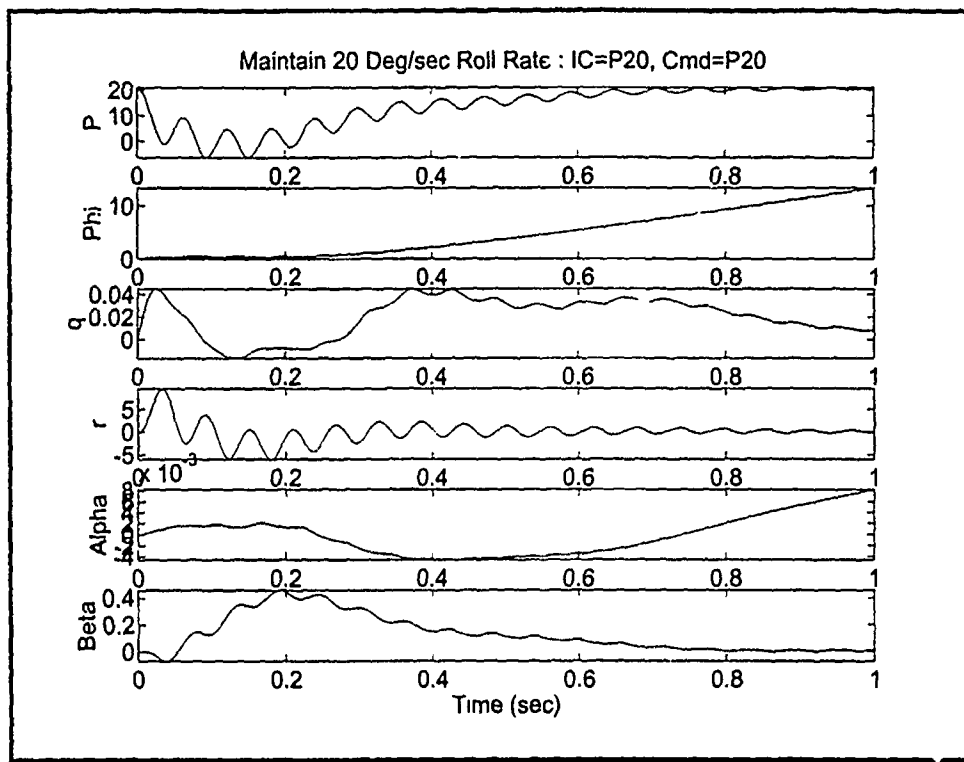
Figure 32. Maintaining Roll Rate, Other ICs = 0
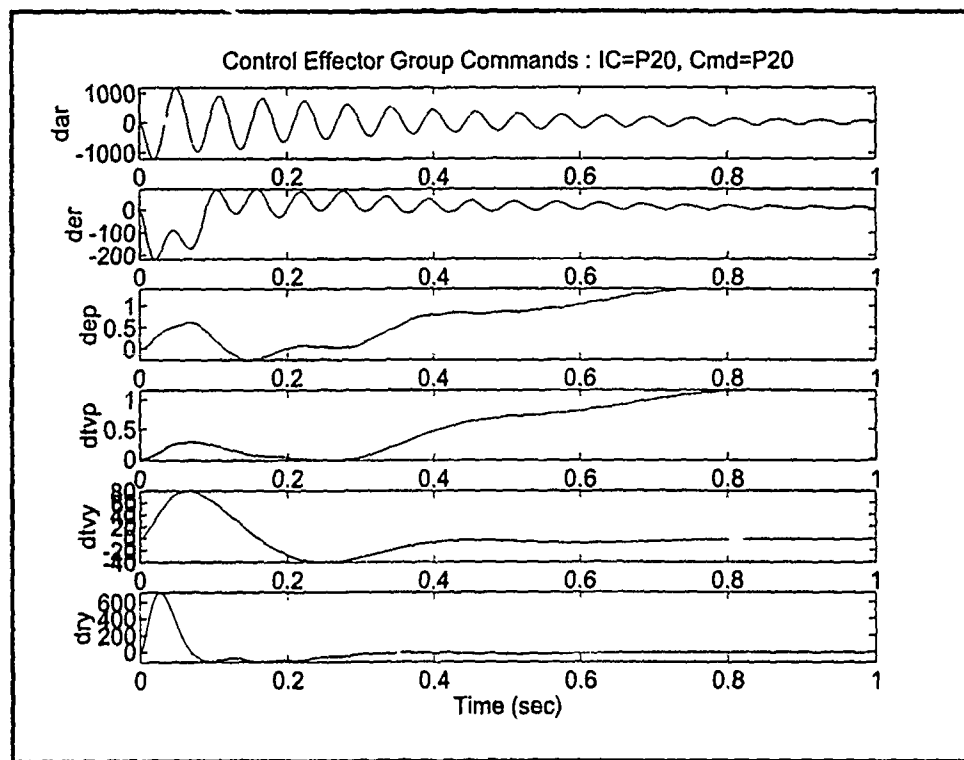
Figure 33. Control Effector Group Commands for Maintaining Roll Rate, Other ICs = 0

It appears that some dynamics in the system are not being properly accounted for by the ICs. From the six DOF EOM, the only dynamics in the system appear to be in the six states. However, an inspection of the system block diagram, Figs 28 - 30, reveals the other dynamic elements of the system which have not been accounted for: the prefilter, compensator, and actuators. To properly describe the aircraft's dynamics at any point in time, all states of each dynamic element in the system must be appropriately defined. For instance, the previous simulation does not account for the control effector group commands required to maintain the 20 deg/sec roll rate used as an initial condition. Because the actuators do not respond instantaneously, the time required to get the actuators to the correct position is sufficient to bring the roll rate back to a zero value, and to set up severe oscillations in the system! Appropriately defined ICs must therefore satisfy the input, output and state conditions of the aircraft, that is, the *trim condition* for the current augmented state of the aircraft. For instance, if the trim condition models a constant roll rate, the actuator dynamics (as well as all other dynamic) states must represent the actuator positions required to maintain the roll.

For this six DOF system, the trim condition requires the identification of 39 states, which are quantitatively identified in Table 7. Obviously, the determination of the appropriate ICs for all 39 states, especially the internal states of the actuators, is a computationally intensive task. MATLAB's Simulink includes a function called trim which may be used to evaluate these ICs. An alternate method, perhaps more realistic to this design, is to use the final state conditions from the velocity vector roll initiation

Table 7. States in Six DOF Model

Source	Number of States	State Names
Six DOF Model	6	$P, \phi, q, \alpha, r, \beta$
Aileron Actuator	2	Roll Aileron
Elevator Actuator	8	Roll, Pitch Elevator
TV Actuator	4	Pitch, Yaw TV
Rudder Actuator	2	Yaw Rudder
Compensator	11	g_1, g_2, g_3
Prefilter	6	f_1, f_2, f_3

simulation as the ICs for the velocity vector roll arrest simulation. This is equivalent to commanding a 20 to 0 deg/sec roll rate doublet, but allows the modification of the states between simulations.

This new IC concept is tested by simulating the continuation of the velocity vector roll, as done for the previous IC concept. Applying the velocity vector roll initiation final conditions to the model, and commanding a 20 deg/sec roll rate, yields the aircraft response in Figs. 34 and 35. This response is far more realistic than the previous results, with no discontinuities between the final state responses of the velocity vector roll initiation simulations and the initial state responses of this simulation. These ICs are therefore considered acceptable for simulating a velocity vector roll arrest.

To simulate the velocity vector roll arrest, the final state values of the velocity vector roll initiation are again used as ICs. However, to explore the effects of the bank angle on the system, the bank angle IC is changed to 170 degrees. While changing just one IC violates the trim condition, the impact on the system is rather insignificant since the bank angle only affects the "slow" AOA equation through the trigonometric contribution. The commanded input for the velocity vector roll arrest is a 0 rad/sec command in all three closed-loop system inputs.

The closed-loop system response to the velocity vector roll arrest command is shown in Figs. 36 and 37. The roll rate tracks the zero input within the one-second transition period, and the pitch and yaw rates stay well below the maximum 1 deg/sec allowed by the specifications, thereby validating the QFT compensator design. In fact, the pitch and yaw rate responses look very much... the inverse of the velocity vector roll initiation responses, with a slight offset due to the initial conditions, as expected. Most importantly, the AOA and sideslip angles remain relatively small, validating the $\alpha \cong \beta \cong 0$ assumption.

It is interesting to note, however, that the worst of these two angles, the AOA, continues to steadily increase, even as the other states of the system appear to flatten out to some steady-state value. This clearly identifies the dominance of the bank angle term in the AOA state equation, and identifies one of the limitations of this three-axis rate-commanded control system. The AOA state equations is a differential equation. Therefore, a dominant *constant* bank angle term produces a linearly increasing (first-order) AOA response, and a dominant *increasing* bank angle term produces a second-order AOA response.
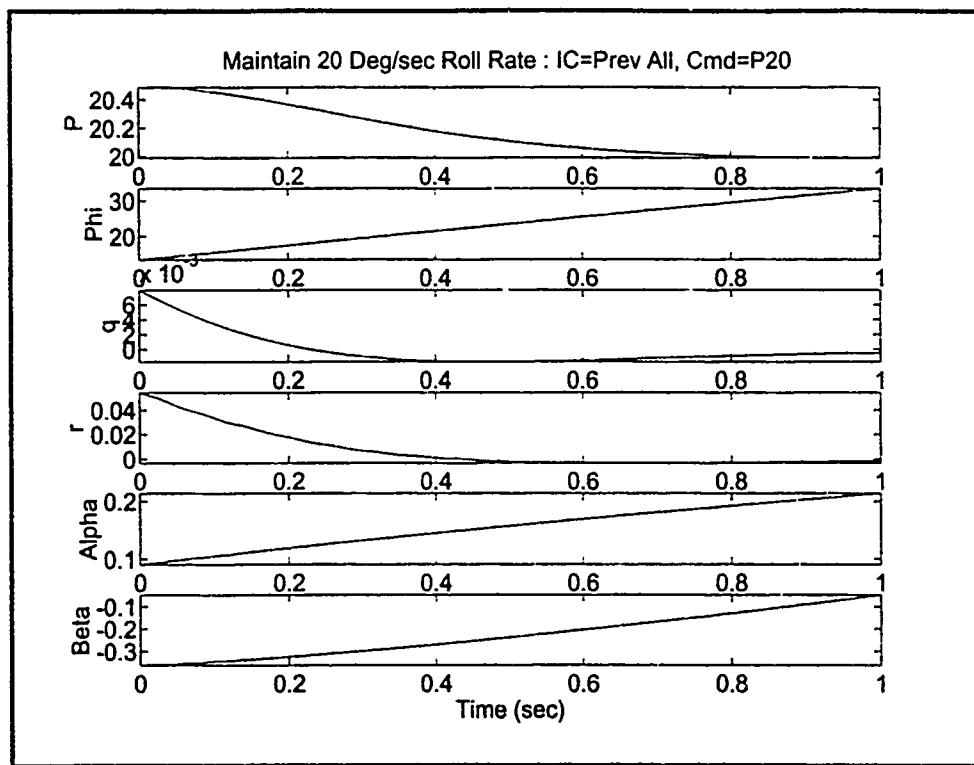
Figure 34. Maintaining Roll Rate, ICs = Final States
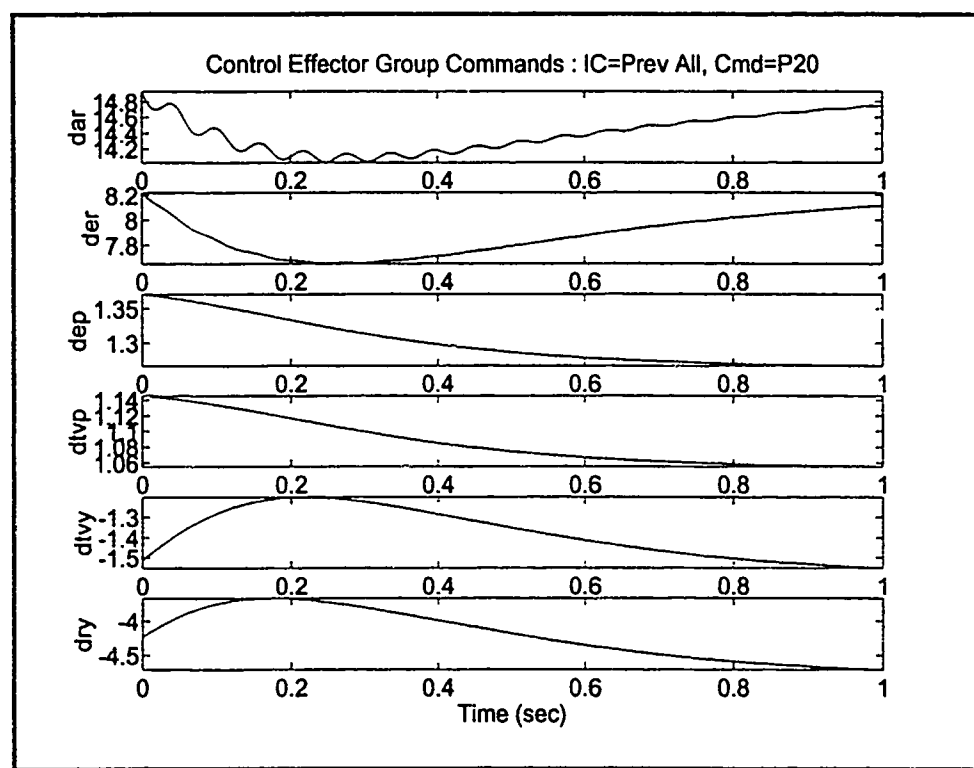
Figure 35. Control Effector Group Commands for Maintaining Roll Rate, ICs = Final States

83
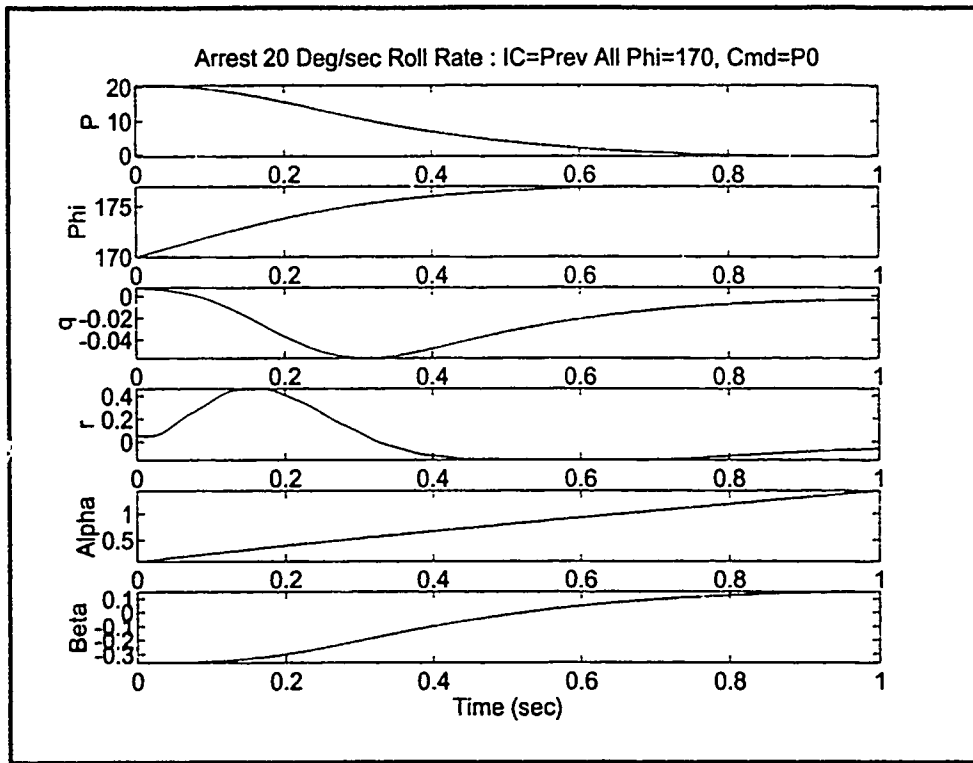
Figure 36. Arresting a Velocity Vector Roll, 10kft
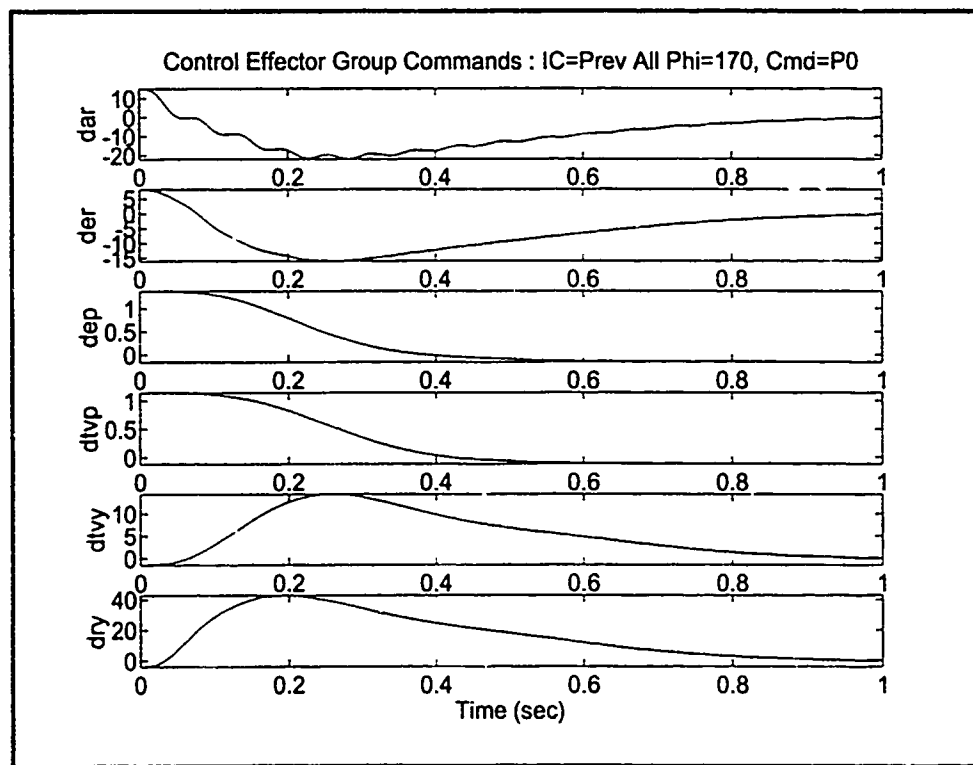
Figure 37. Control Effector Group Commands, Velocity Vector Roll Arrest, 10kft

In this simulation, the bank angle increases only slightly, so the AOA appears to increase linearly. This increase is, however, independent of the pitch rate regulation when the bank angle term is dominant. In other words, the assumption that the AOA remains small when the pitch rate is kept near zero is not valid when the bank angle term of the AOA state equation is dominant. And when is the bank angle dominant? Looking at the velocity vector roll initiation state response plot, Fig. 94, Appendix E, it appears the bank angle becomes dominant at a rather low bank angle, perhaps two or three degrees. Therefore, even in the velocity vector roll initiation transition region, the AOA seems to be driven primarily by the bank angle. The fact that the AOA stayed relatively close to zero therefore has little to do with the regulation of the pitch rate state. Instead the magnitude of the bank angle term (which is primarily a function of airspeed), the ICs, and the relatively short time period for each simulation are the primary contributors to the low AOA responses.

This AOA dependence on the bank angle and the ICs has several rather significant implications with respect to the use of the three-axis rate-commanded control system designed in this study. First, this velocity vector roll control system should only be applied when the AOA is very close to the desired final value of the AOA. Second, this velocity vector control system should only be used for short periods of time (less than two seconds). If used for longer periods of time, the lack of AOA control results in a significant departure from the desired final AOA. Finally, the control systems ICs used for the arrest of a velocity vector roll can, and should, be tailored such that the desired final conditions (presumably all aircraft dynamic states equal to zero) are attained at the end of the maneuver. This "tailoring" must be performed by the optimal controller used in the "free-stream' region of the velocity vector roll. Foresight into these limitations of the control system lead to the time-scale separation concept introduced at the onset of this study.

As in the previous simulations, oscillations are present in the roll aileron control effector command. These oscillations are again relatively small, and are considered acceptable. However, they do indicate the potential for catastrophic oscillations as experienced in the first IC simulation, and are therefore studied in further detail in Chapter 7.

6.3. Six DOF Simulation, Limited Control Effectors

In the previous sections, the linear control system design has been shown to produce a closed-loop system meeting all pre-defined stability and performance specifications, even using a nonlinear six-DOF aircraft model. However, as previously mentioned, one limitation of linear design techniques is the inability to account for the saturation limits of control effectors. In this section, the control effector saturation limits for the HARV are integrated into the six DOF nonlinear model, and simulations of a velocity vector roll initiation and arrest are performed to determine the impact of the saturation limits on the closed-loop system performance. Because the velocity vector roll is a large amplitude maneuver requiring large excursions in the control effectors, the saturation limits are expected to have a significant detrimental effect on the closed-loop system performance. And, since the linear control system design technique does not incorporate the control effector limits into the compensator and prefilter designs, the performance of the limited system does not meet the desired specifications.

The need for limited control effector excursions is apparent in the previous simulations. For instance, the commanded yaw rudder in Fig. 37 is slightly more than 40 degrees, but the limits on the yaw rudder are only ±30 degrees. In Fig. 33, the roll aileron commands are over 1000 degrees (nearly three revolutions)! Obviously, these control effector commands are unrealistic, and the resulting state responses for these simulations are invalid. Therefore, the effects of control effector saturation are added to the six DOF simulation. Control effector saturation is modeled in the closed-loop system with saturation blocks, as shown in Figs. 38 and 39. The limits placed on the saturation blocks are defined in Eq. (81), Chapter 3, and represent positional (magnitude) limits; control effector rate limits are not included in this study. All other blocks in the closed-loop system remain the same.

The simulations performed with the limited six DOF closed-loop system are the velocity vector roll initiation and arrest. The initiation simulation is performed first, using the same input commands as in the previous initiation simulations. The arresting simulation follows, using the final states of the initiation simulation as ICs, and using the same input commands as in the previous arresting simulations.
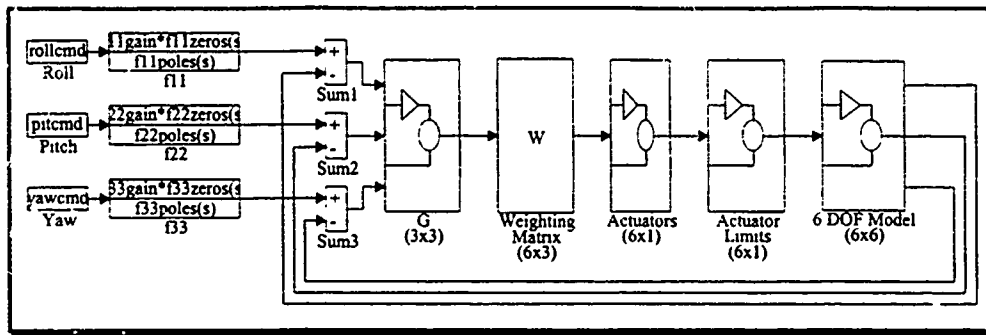
Figure 38. Six DOF Closed-Loop System with Limited Control Effector Groups
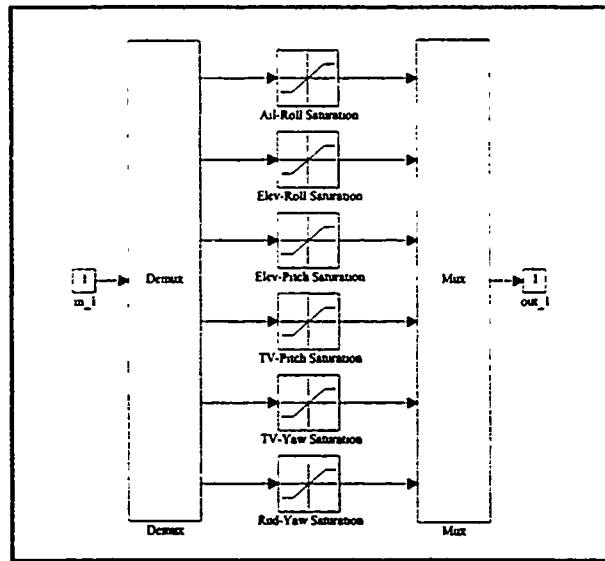
Figure 39. Control Effector Group Saturation, Block Diagram

The response of the limited six DOF closed-loop system to the velocity vector roll initiation

commands is shown in Figs. 40 and 41. A comparison with the response of the closed-loop system without

control effector limits, Figs. 94 and 99, Appendix E, leads to the conclusions presented in this section.

The control effector limits have very little effect on the roll rate, and the corresponding bank angle,

achieved during the one-second transition region. This is expected, since the roll control effectors did not

reach their maximum values in the previous simulations.

The most dramatic effect of the control effector limits is in the yaw rate response. In the control

effector limited system, the yaw rate slightly exceeds the 1 deg/sec design specification in the negative

direction, and doubles the specification in the positive direction. The control effector group commands

show the cause of this violation. The yaw control effectors saturate in a relatively short amount of time,

and therefore limit the ability of the control system to counter the cross-coupling in that channel. Another result of this yaw control limiting also appears in the pitch rate channel, where the response is more sluggish than in previous simulations, but still well within the maximum allowable departure limit of 1 deg/sec.

More important than the pitch and yaw rates, however, are the AOA and sideslip angle channels. As discussed in the previous sections, these angles must be kept near zero for a velocity vector roll to be considered successful. Figure 40 shows that these angles are near zero throughout the entire period. In fact, these angles are actually smaller than those in the unlimited control effector simulations. The smaller and differently responding AOA indicates that the AOA state equation is actually dominated by the $P\beta$ term at near-zero bank angles, in contrast to the bank angle domination experienced at high bank angles. In fact, it appears that the bank angle does not become dominant in the AOA state equation until the bank angle is at approximately 10 degrees, contrary to the previous conclusion that bank angle domination occurs when the bank angle reaches 2 or 3 degrees. The sideslip angle term domination in the AOA state equation indicates that at low bank angles, the sideslip ICs must be near-zero, and must be kept small until the bank angle term begins to dominate. Since this condition is met in this simulation, where the sideslip is initially zero, the compensator and prefilter are deemed acceptable for the velocity vector roll initiation transition region.

The response to the velocity vector roll arrest commands, appears in Figs. 42 and 43. Again, as in the initiation region, the roll rate, bank angle, and pitch rate states are relatively unaffected by the control effector limits, since the roll control effector commands do not reach their limits. The yaw rate channel, however, is significantly different than yaw rate response of the unlimited model to the velocity vector roll arrest commands, Fig. 36, due to the saturation of the yaw control effectors. The yaw rate does remain within the 1 deg/sec specifications for the majority of the period, with only two slight violations. Despite these violations, however, the sideslip angle remains sufficiently close to zero, and the integrity of the velocity vector roll is not compromised.
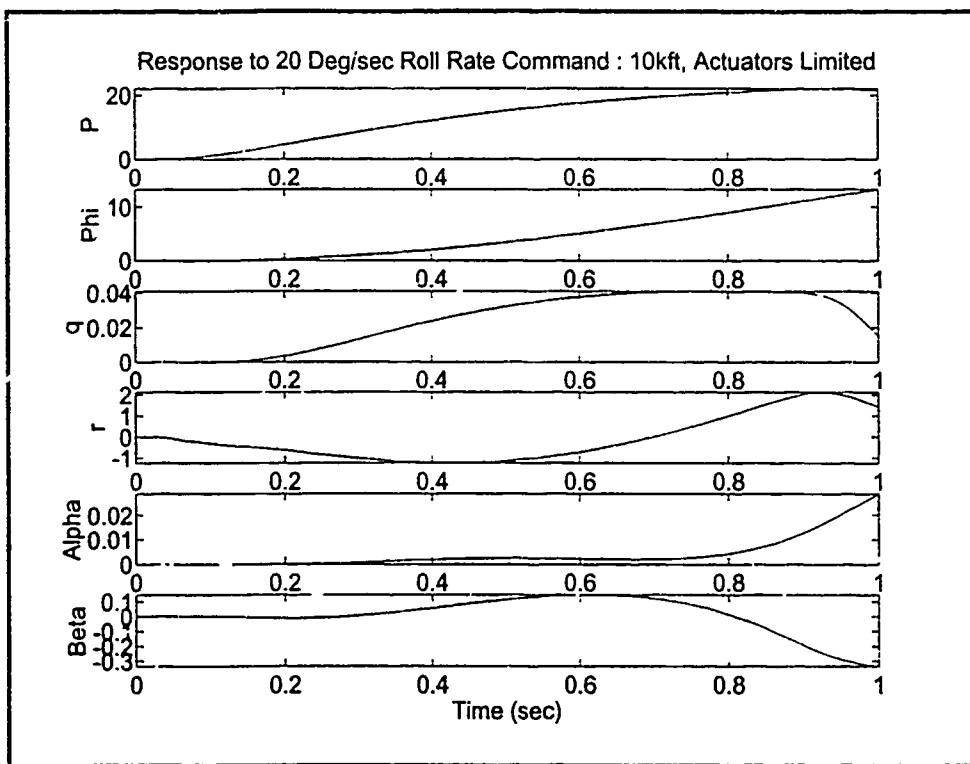
Figure 40. Response to Roll Command, Limited Closed-Loop System, 10kft
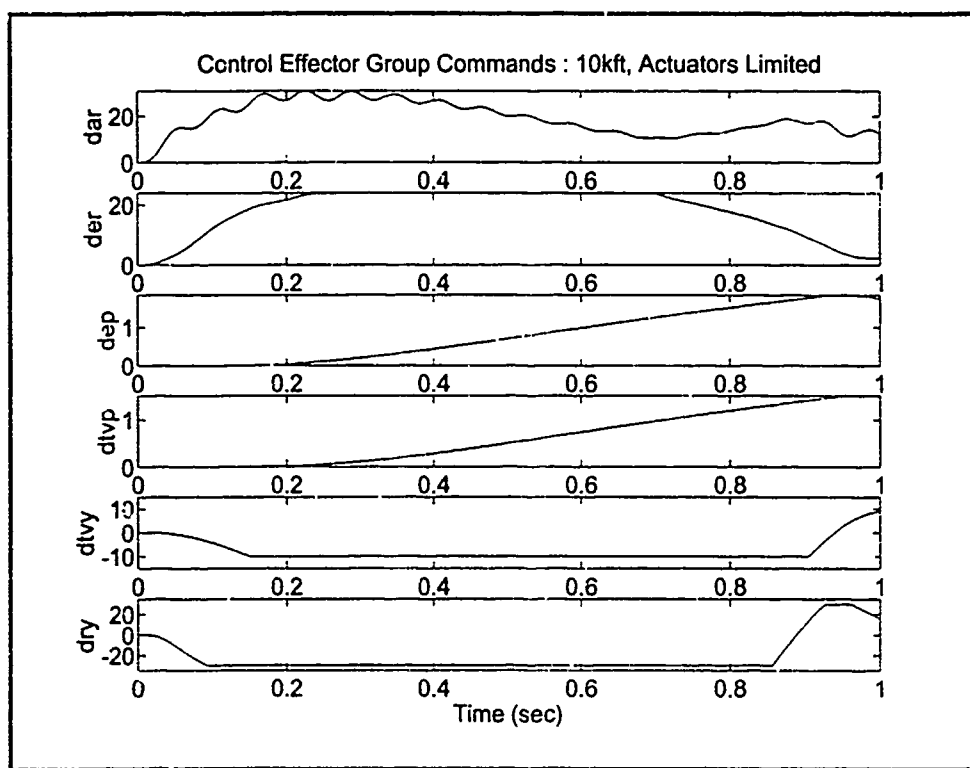
Figure 41. Limited Control Effector Group Commands, Roll Initiation
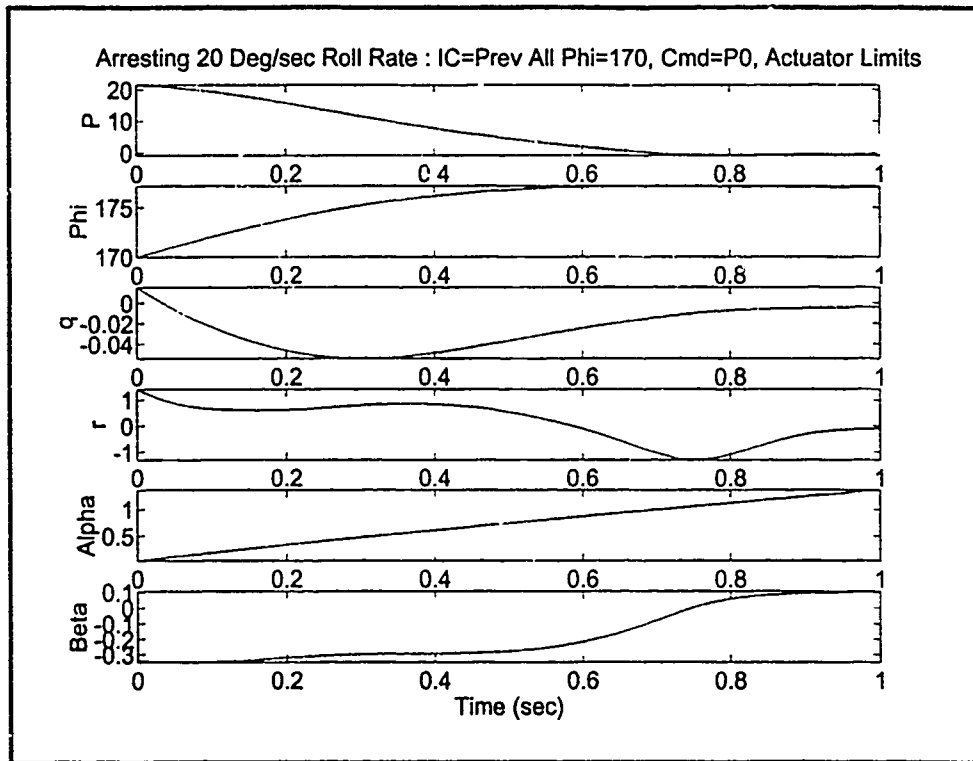
Figure 42. Arresting a Velocity Vector Roll, Limited Closed Loop System, 10kft
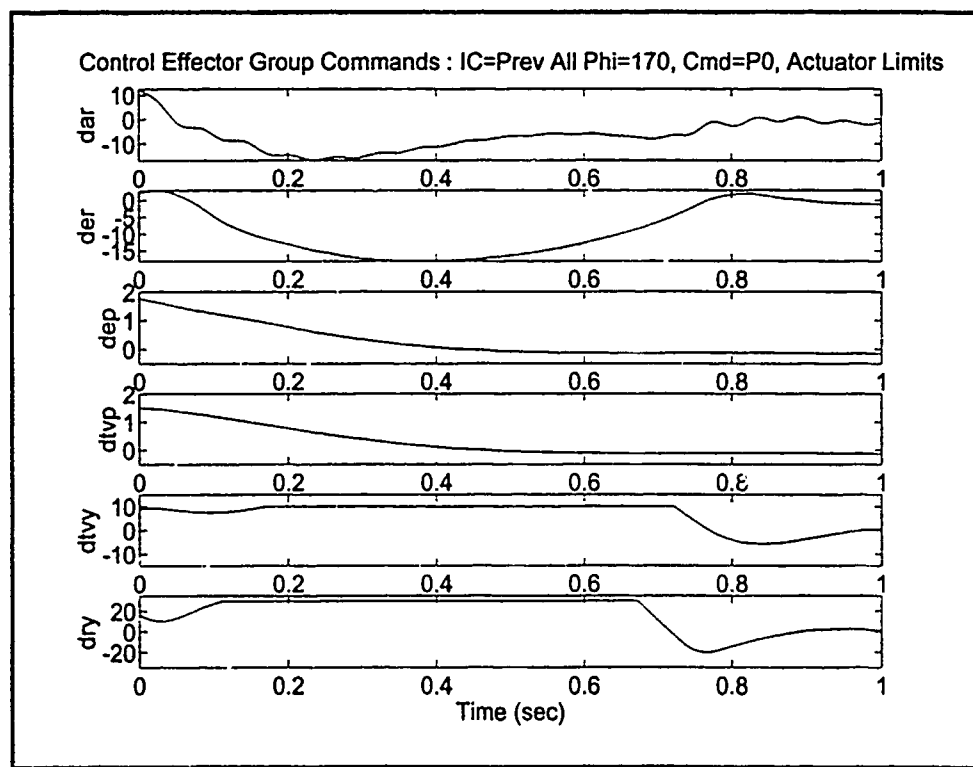
Figure 43. Limited Control Effector Group Commands, Velocity Vector Roll Arrest, 10kft

The AOA response to the velocity vector roll arrest command is nearly identical to that obtained in the arrest simulations for the unlimited control effector model because the bank angle term in the AOA state equation is dominant when the bank angle is near 180 degrees. With a near-zero IC, the AOA reaches a final value of approximately 1.5 degrees, but is still increasing. Therefore, one desired quality of a future control system designed for the "free-stream" region of the velocity vector roll is that it drives the AOA to some slightly negative value. From the control effector command plots, it appears that this quality could be rather readily achieved, since the pitch control commands are well within their limits, leaving plenty of pitch control authority.

Based on the simulation results presented in this chapter, the QFT designed compensator and prefilter are deemed to be acceptable for the initiation and the arrest of the velocity vector roll maneuver of the HARV aircraft even with limited control effectors. Attention can now be turned to the oscillations present in the aileron control effector commands; this is the focus of Chapter 7.

The purpose of this chapter is to identify and eliminate the source of oscillations in the roll aileron control effector commands of the of the previous chapter. A potential flaw in the weighting matrix is identified and corrected, and the three-axis rate-commanded QFT control system is redesigned to account for these changes. Velocity vector roll initiation and arrest simulations are then performed with the re-designed system to demonstrate its improved performance.

7.1. Weighting Matrix

All simulations in the previous chapter reveal small oscillations in the roll aileron control effector commands. Because these oscillation do not appear in the AOA, bank angle, and sideslip angle state responses, they are not a cause for alarm. However, they are a source of unnecessary wear on the actuators, and are therefore undesirable. The cause of these oscillations is not immediately apparent from the design. It is noted that very slight oscillations do appear in the yaw rate responses of some of the velocity vector roll simulations. Because the roll and yaw channels of the aircraft are highly coupled at high AOA, the oscillations in the yaw rate channel are likely the source of the result of the oscillations in the roll aileron control effector commands.

The weighting matrix design, Eq. (80), Chapter 3, is the most obvious place to start the investigation. Recall that the weighting matrix is based on the aileron-rudder interconnect concept. Therefore, the weighting matrix should include off-diagonal terms to command the yaw control effector groups when a command is issued to the roll control effector groups. These off-diagonal terms are the {5,1} and {6,1} elements of the weighting matrix. However, the implementation of the weighting matrix also includes off-diagonal terms in the {1,3} and {2,3} elements of W; these elements correspond to a rudder-aileron interconnect which has been inadvertently added to the design. This rudder-aileron interconnect is undesirable for two reasons. First, this interconnect could conceivably allow small oscillations in the yaw channel be fed back into the roll aileron command signals. This is exactly the situation encountered in the simulations. Second, the reverse interconnect closes a loop around the roll and

yaw command inputs which could, under the right circumstances, introduce unstable oscillations between the two channels, leading to a loss of control. While this is not observed in the simulations, small changes in the aircraft or actuator dynamics could lead to this condition.

The apparent remedy to the situation is to zero out the $W\{1,3\}$ and $W\{2,3\}$ elements. The resulting weighting matrix is:

$$W = \begin{bmatrix} 0.2443 & 0 & 0 \\ 0.1396 & 0 & 0 \\ 0 & 0.0838 & 0 \\ 0 & 0.0698 & 0 \\ -0.03913 & 0 & 0.1745 \\ -0.11813 & 0 & 0.5236 \end{bmatrix} \tag{121}$$

Velocity vector roll simulations with this new weighting matrix incorporated in the closed-loop systems of the previous chapter, show that the oscillations in the roll aileron control effector commands are significantly reduced. Even though these simulations indicate that the rudder-aileron interconnect is the likely source of the oscillations, the modified closed-loop system is not valid. Recall that the QFT design starts with the definition of the effective plants. As shown in Eq. (76), the effective plant contains the weighting matrix. A change in the weighting matrix then requires the re-design of the entire QFT compensator and prefilter; simply changing the weighting matrix in the closed-loop system does not yield a closed-loop system which meets the design specifications.

7.2. QFT Compensator and Prefilter

The QFT design process presented in this chapter is identical to that presented in Chapter 5. No changes are made to the stability and performance specifications, the loaded plants, and the actuator models; only the weighting matrix is modified as described in the previous section. The Q matrices formed with the new weighting matrix are not presented in this thesis, but are available in a supplementary document from the thesis advisor. The Bode plot of the Q matrices appears in Fig. 44, and shows that the change in the weighting matrix produced very little change in the frequency response of the system, although the bandwidth of the roll rate channel does appear to be slightly higher.

93
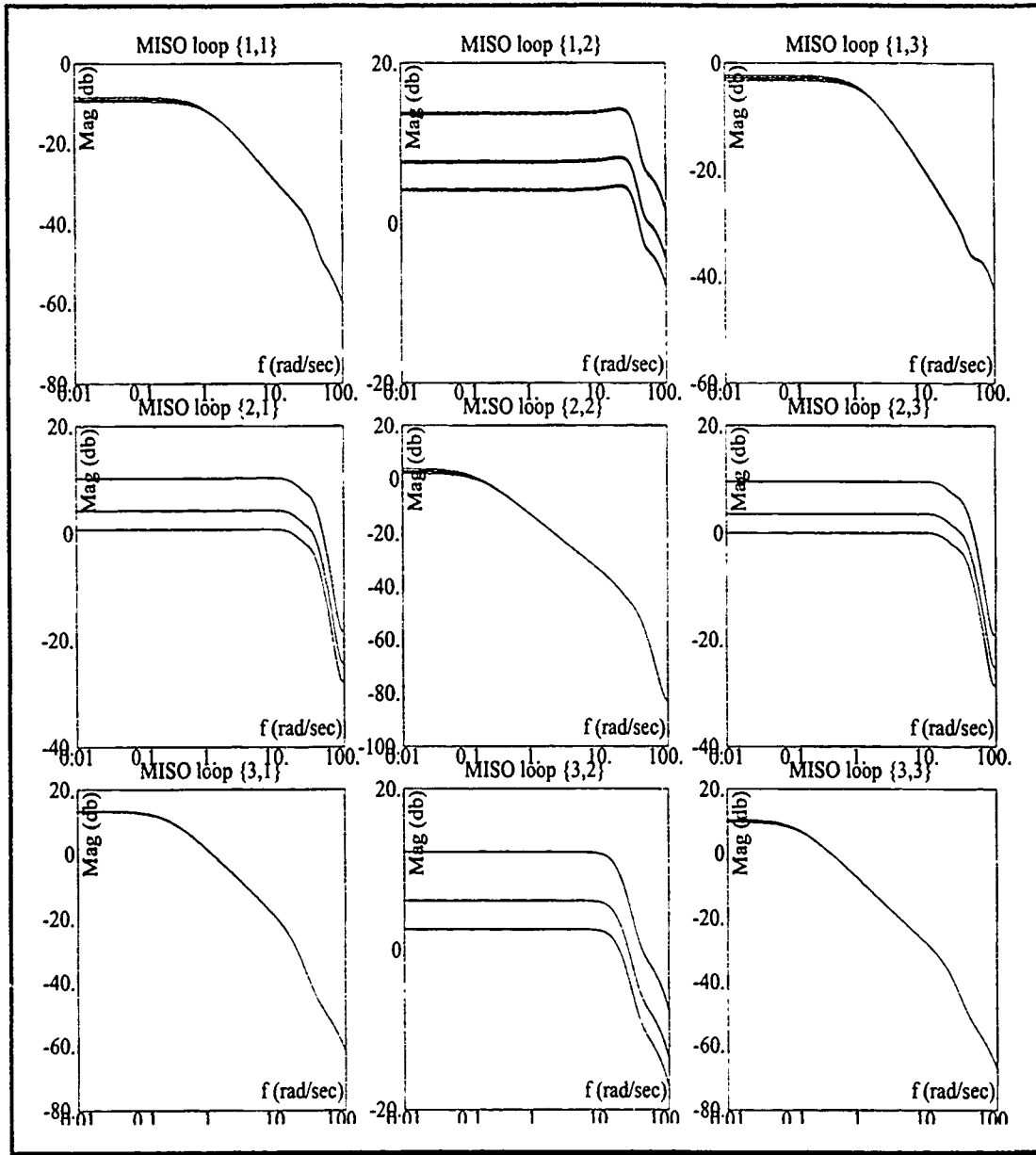
Figure 44. Q Matrix Frequency Response, Re-designed System

Because the Method 1 design technique is used, the diagonal dominance condition, described in Eq. (95), must again be satisfied. Figure 45 shows that the diagonal dominance condition is satisfied (all plant cases are positive) as the frequency approaches infinity. The Method 1 design technique is therefore applied to this system.
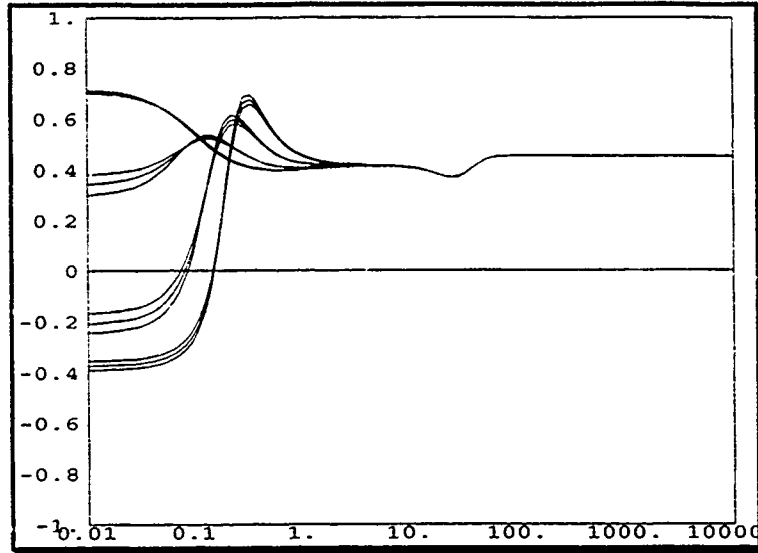
Figure 45. Diagonal Dominance Condition, Re-designed System

The new channel 1 nominal plant (plant case 4) transfer function in pole-zero format is:

$$q_{11_s} = \frac{1240.8763(-15.62475 \pm j41.9236)(-21.8558 \pm j32.8318)(-55.2305 \pm j83.7803)}{(-1.0213)(-14.924 \pm j33.2)(-20.4535 \pm j30.9478)(-44.25 \pm j60.5552)(-62.127 \pm j85.0196)} \quad (122)$$

This transfer function is similar to the one used in the previous roll rate channel design, Eq. (110), but the gain is now significantly higher (nearly four times the previous value) and the poles and zeros are slightly farther away from the origin. These differences are reflected in the $\mathbf{Q}$ matrix Bode plot as discussed earlier.

Using the same design technique as in Chapter 5, the following roll rate channel compensator is realized:

$$g_1 = \frac{205.128(-13)(-24 \pm j18)}{(0)(-50)(-60)} \quad (123)$$

The corresponding Nichols plot of the nominal loop transmission, with the associated bounds appears in Fig. 46. One benefit of the new weighting matrix is immediately apparent from this figure. The increased phase margin frequency of the bare plant permits the compensated system to meet the yaw rate cross-coupling disturbance bounds, which were violated in the previous design, while still meeting the 30 rad/sec ω_{ϕ} requirement. Therefore, no stability or performance bounds are violated with the newly designed weighting matrix.

95

The Bode plot used in the prefilter design shows that the same roll rate channel prefilter designed in Chapter 5 may be used for this new system. This Bode plot is visually identical to that shown in Fig. 20, and is therefore not included in this section. Additionally, the pitch rate channel compensator and prefilter designs from the previous design are found to be acceptable for this new system, so a re-design is not necessary for this channel.

Figure 46. Roll Rate Channel, Bounds and Compensated System
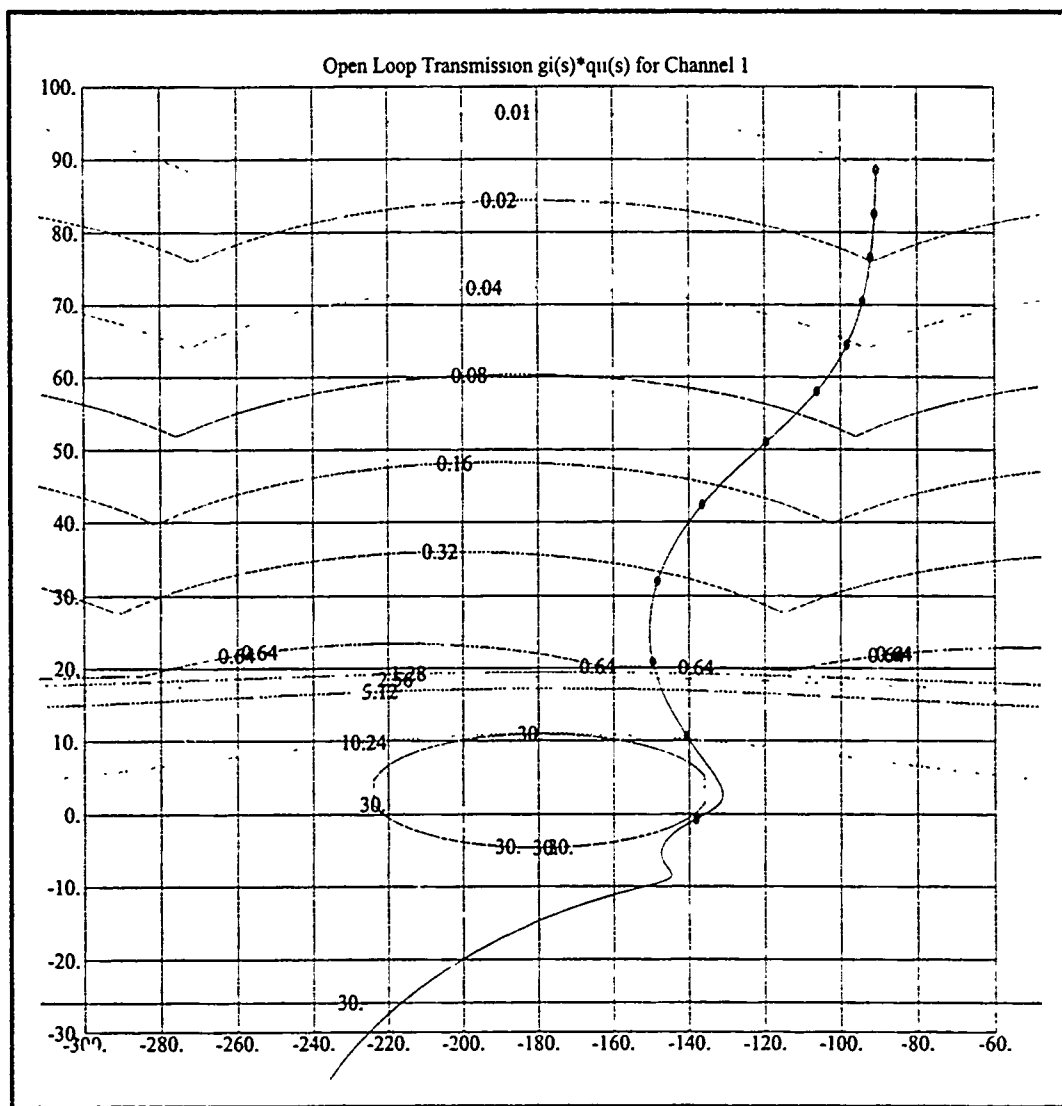
The yaw rate channel does have to be re-designed, however. The yaw rate channel nominal plant (plant case 4) transfer function has changed to:

$$q_{33_*} = \frac{-518.8974(-15.6247 \pm j41.9236)(-21.8559 \pm j32.8318)(-55.2305 \pm j83.7803)}{(-0.1181)(-13.1446 \pm j15.9248)(-15.7355 \pm j42.0323)(-49.6517 \pm j52.1523)(-55.2737 \pm j83.7978)} \qquad (124)$$

While this is only slightly different than the respective nominal plant transfer function in the previous design, the changes are substantial enough to require a modified compensator. The following compensator, obtained using the CAD package, satisfies all bounds as shown in Fig. 47.

$$g_3 = \frac{-500(-6)(-14 \pm j14.2829)}{(0)(-50)(-50)} \qquad (125)$$

Figure 47. Yaw Rate Channel, Bounds and Compensated System
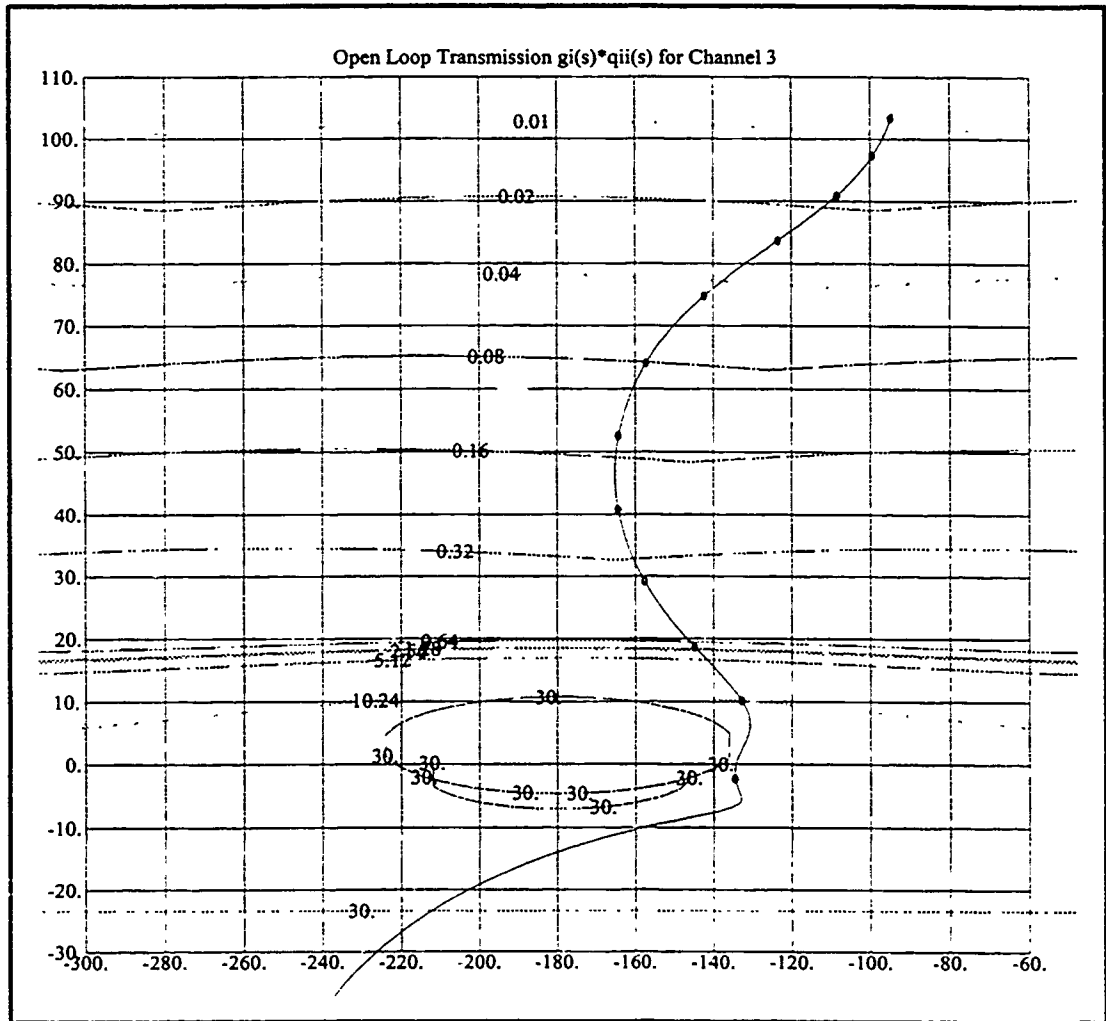
The prefilter from the previous design is satisfactory, so the re-design of the three-axis rate-commanded QFT control system is complete, provided that the system satisfies all performance bounds. The tracking validation results from the CAD package, Fig. 48, show that all performance bounds are met with this new compensator and prefilter, so the control system is ready for simulation.
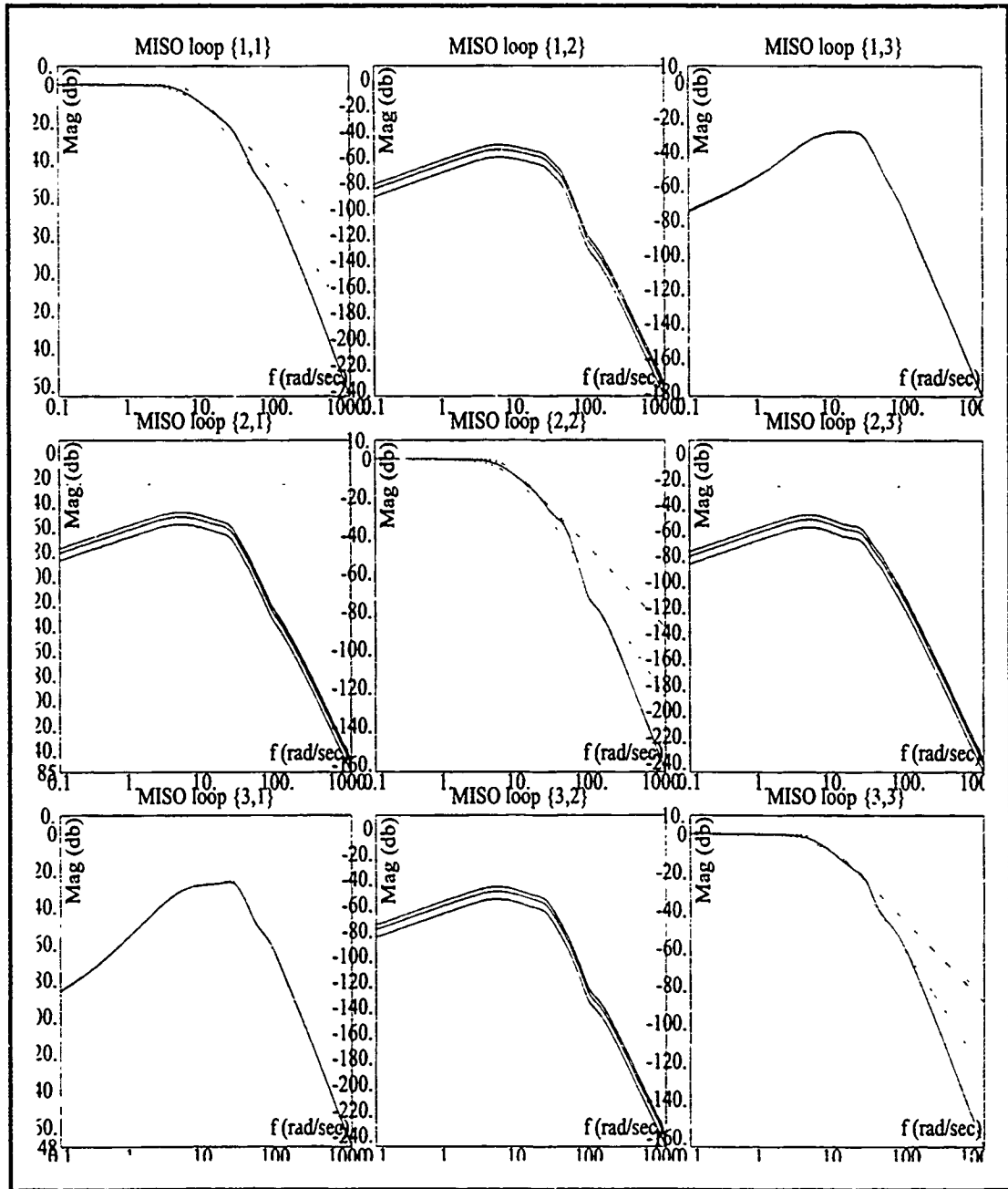
Figure 48. Tracking Validation for Re-designed System

7.3. Closed-Loop Simulations

The effects of the re-designed weighting matrix and compensator on the closed-loop system performance can most easily be seen in simulations of the six DOF system containing no control effector group limits, since the true (not limited) control effector group commands are used within the simulation. The most realistic responses, however, are obtained through simulations with the control effector group limited six DOF model. Therefore, velocity vector roll initiation and arrest simulations are performed with each of these models, and these simulations are then compared to those obtained with the previous design. The closed-loop systems used for these simulations are exactly the same as those used in the Chapter 6 simulations, but the re-designed weighting matrix (W) and compensator (G) replace those from the previous design. The commanded inputs and the method of setting the ICs for the velocity vector roll arrest are also identical to those presented in Chapter 6.

7.3.1. Six DOF Simulation, No Control Effector Limits. The response of the six DOF closed-loop system with no control effector limits to a velocity vector roll command is shown in Figs. 49 and 50. The benefit of the re-designed system is immediately apparent; the roll aileron control effector commands and the yaw rate response contain none of the unwanted oscillations which are present in the previous simulations. As anticipated from the design phase, the performance specifications are also easily met. In fact, the response of the re-designed system is nearly identical to that of the previous system. The primary difference between the two, other than the lack of oscillations, is a slight increase in the magnitude of the yaw rate response, and a corresponding increase in the size of the yaw control effector group commands. While this increase does not come close to violating the performance requirement, it is likely to have a negative impact on the performance of the system when the control effector limits are enforced. From this velocity vector roll initiation simulation, however, the re-design is shown to be successful, removing all the unwanted control effector oscillations.
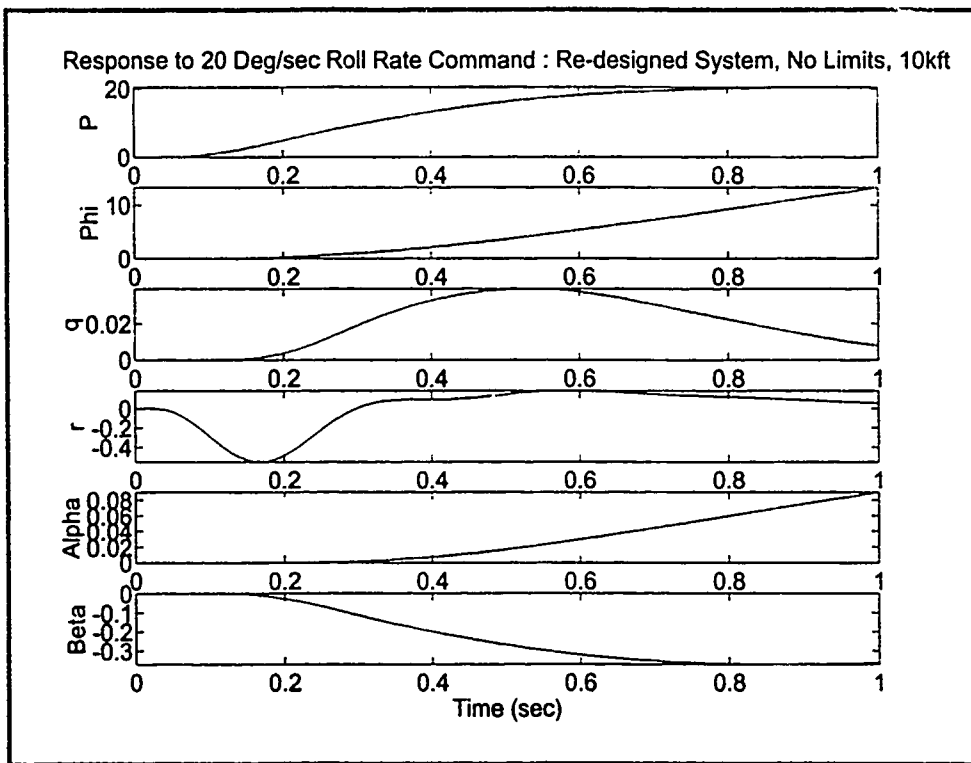
Figure 49. Response to Roll Command, Re-designed System, 10kft
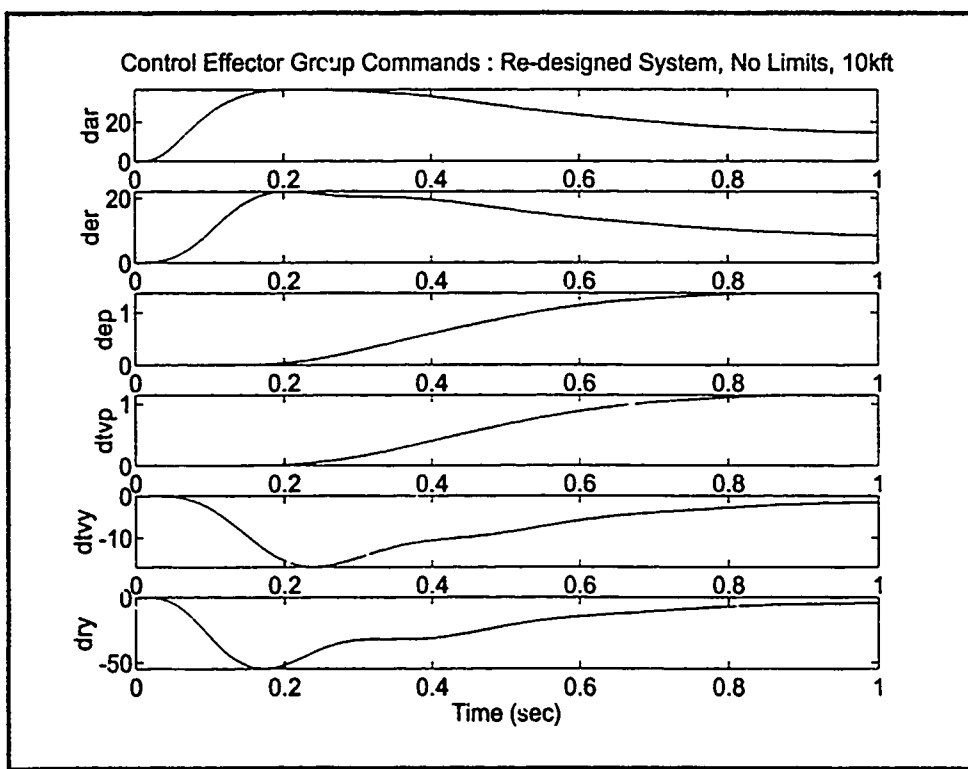
Figure 50. Control Effector Group Commands, Re-designed System Roll Initiation

100

The system response to the velocity vector roll arrest command, using the final conditions of the roll initiation simulation as ICs, is shown in Figs. 51 and 52. This simulation also demonstrates that the re-designed weighting matrix and compensator eliminate all oscillations in the state responses and the control effector commands. As in the roll initiation simulations, the yaw control effector commands and the yaw rate response are slightly larger than in the Chapter 6 simulations, but the yaw rate response still remains well within the specification limits. The overall aircraft response to the maneuver is virtually identical to the response of the previous design, and the re-designed weighting matrix and compensator is again shown to be acceptable and beneficial to the performance of the closed-loop system.

7.3.2. Six DOF Simulation, Limited Control Effectors. The response of the control effector limited six DOF system to the velocity vector roll initiation command is shown in Figs. 53 and 54. The control effector limits have the same effect on the response of this system as they do on the previous system, Figs. 40 and 41; the yaw rate exceeds the 1 deg/sec design specification. Also, as predicted, the yaw rate of the re-designed system exceeds the specification to a greater degree than the previous system, nearly doubling the allowable 1 deg/sec yaw rate.

Not predicted, however, are the *benefits* of this increased violation. The final value of the sideslip angle is slightly smaller due to the increased yaw rate response. As a result, the AOA, which has been shown in this study to be dominated by the sideslip angle at small bank angles, actually decreases during the velocity vector roll initiation, rather than increasing as in the roll initiation of the previous system. The consequence of this phenomenon is not immediately apparent, until one considers the response characteristics of the AOA throughout the remainder of the velocity vector roll maneuver; the AOA increases significantly as the bank angle increases. Therefore, any slight decrease in the AOA during the initiation transition region helps in controlling the maneuver after the initiation of the transition region.

This impact of this benefit on the velocity vector roll arrest simulation is seen in Fig. 55 and 56. Although completely dominated by the bank angle, the AOA response is slightly smaller in magnitude than in the previous design's velocity vector roll simulations, and the final sideslip angle is much closer to zero.
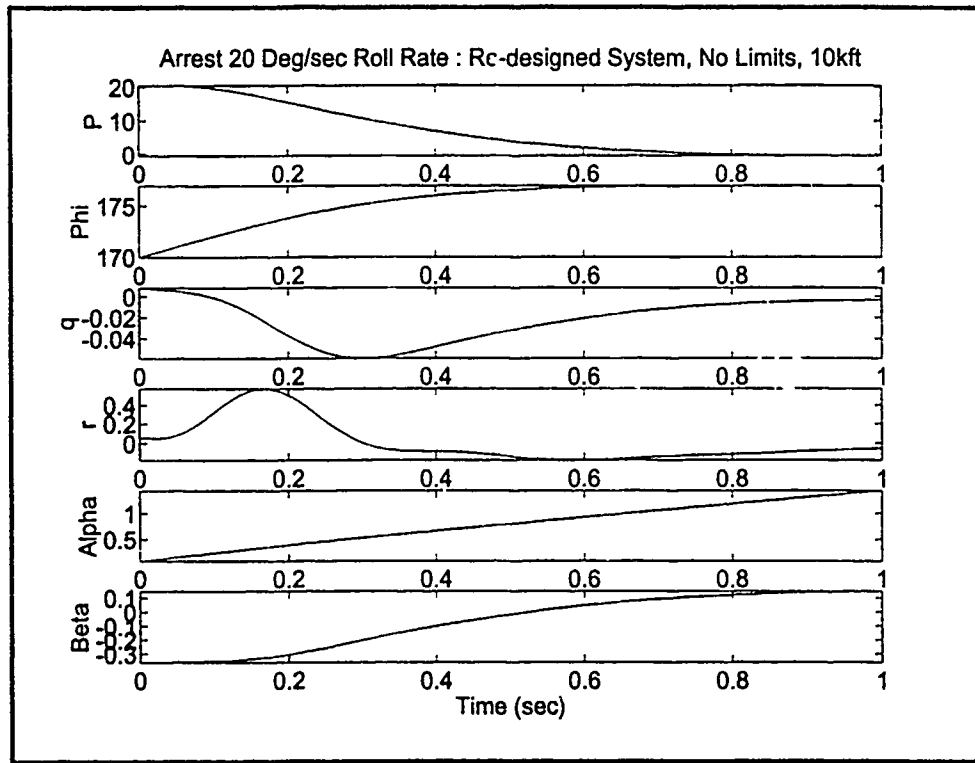
Figure 51. Arresting a Velocity Vector Roll, Re-designed System, 10kft
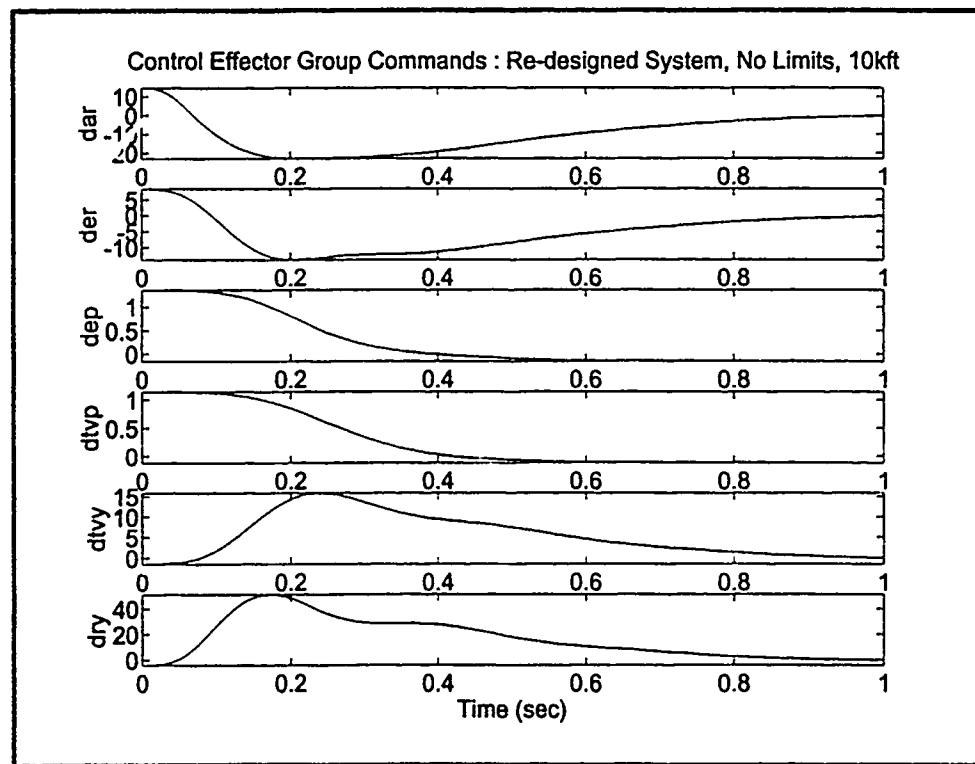
Figure 52. Control Effector Group Commands, Re-designed System Velocity Vector Roll Arrest
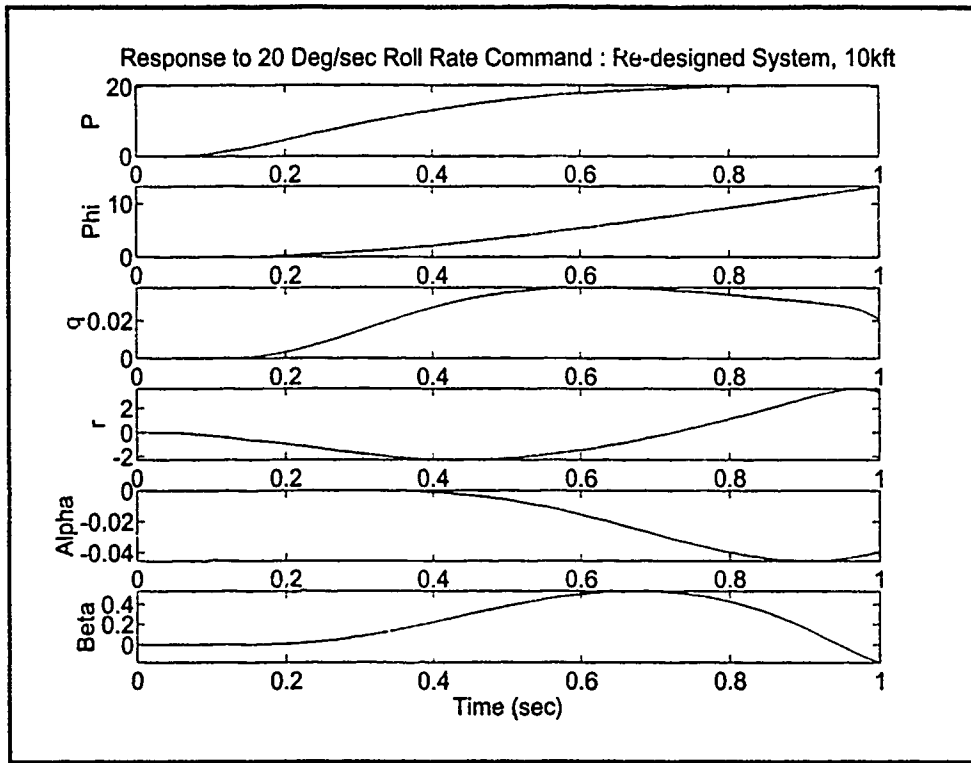
Figure 53. Response to Roll Command, Re-designed Limited System
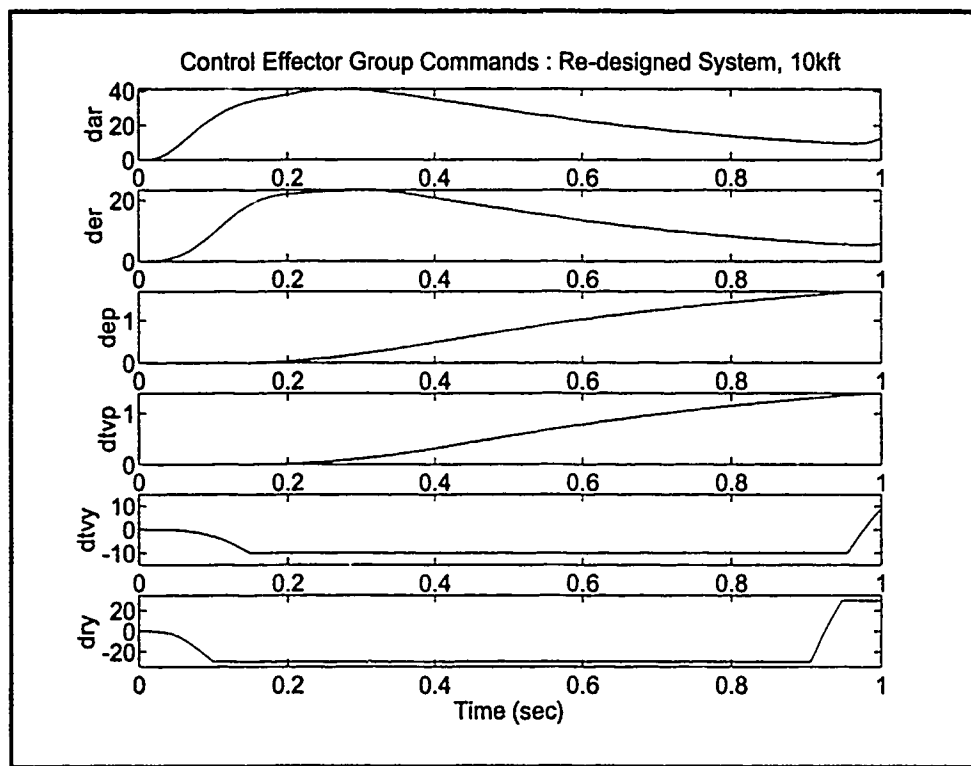
Figure 54. Limited Control Effector Group Commands, Re-designed System Roll Initiation

103
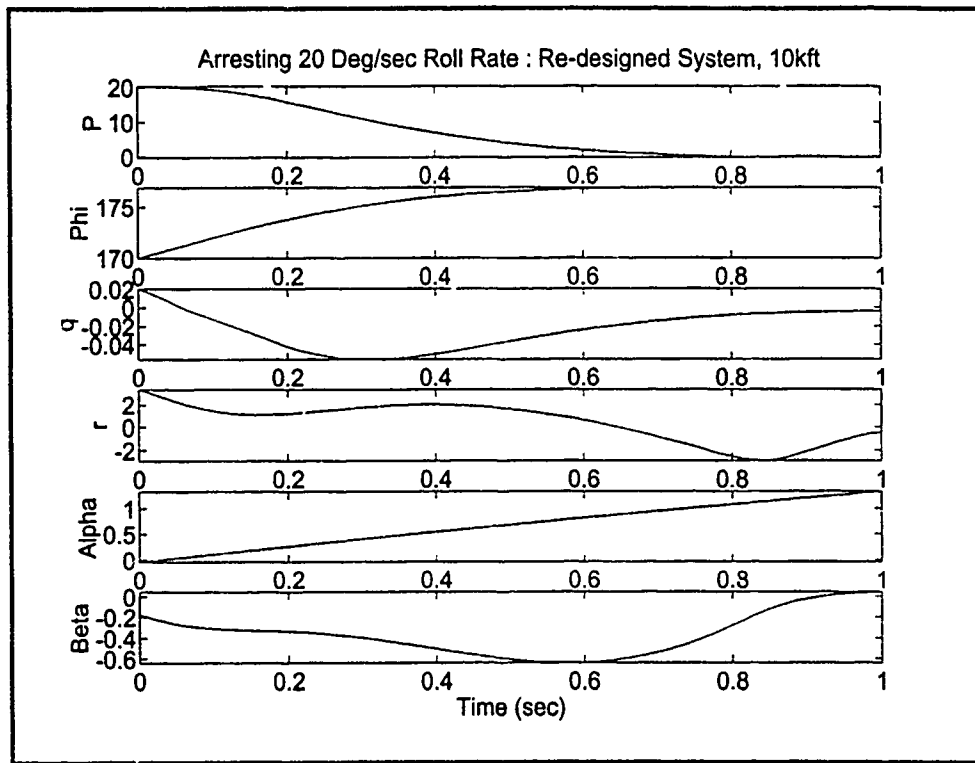
Figure 55. Arresting a Velocity Vector Roll, Re-designed Limited System
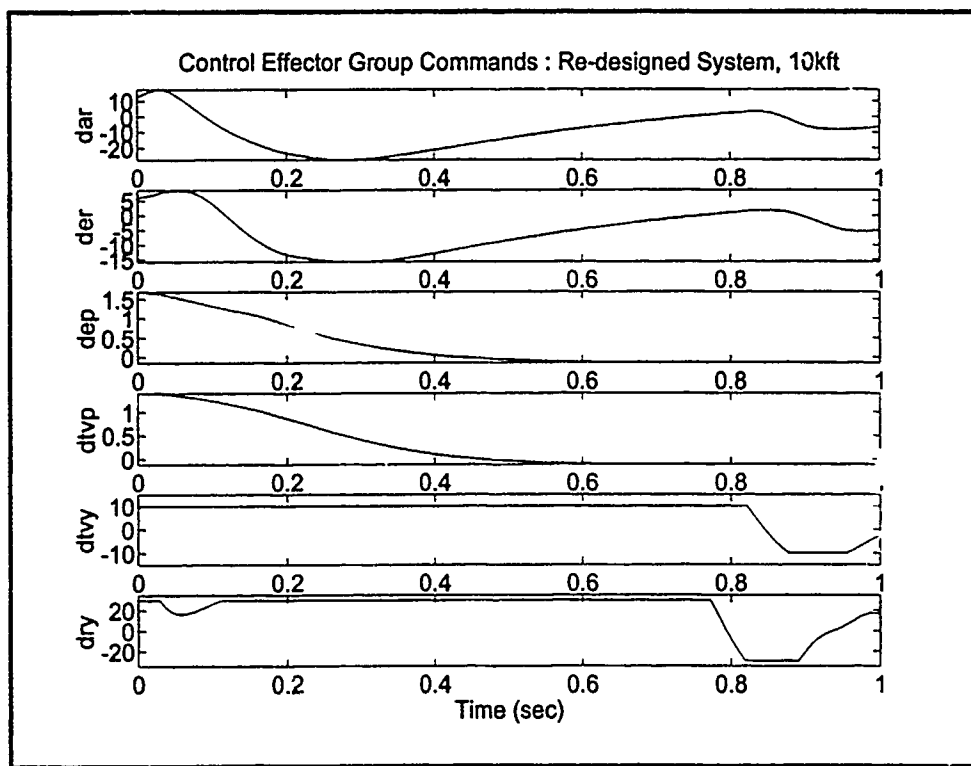
Figure 56. Limited Control Effector Group Commands, Re-designed System Roll Arrest

104

Based on the final conditions of the AOA and sideslip angle, the re-designed system is better suited to the velocity vector roll maneuver. Moreover, the re-designing of the weighting matrix and compensator has completely eliminated the oscillations in the state responses and control effector commands. These two criteria indicate that the re-design is successful.

8. Conclusions and Recommendations

8.1. Summary

This thesis develops an innovative approach to the design of a flight control system for performing the velocity vector roll maneuver at high angles of attack. A six DOF aircraft model is developed from the fundamental nine-state EOM using a modified linearization technique. This technique is based on the time-scale separation of the velocity vector roll's states, and accounts for nonlinearities due to the "high" stability axis roll rate and the bank angle achieved during the velocity vector roll maneuver.

The system nonlinearities, and changes in system parameters due to changes in flight condition, are then jointly treated as structured uncertainty in the development of a three DOF model for use in the QFT design process. The QFT robust control design technique is therefore used to jointly address nonlinearity and structured uncertainty. A weighting matrix, based on the fundamentals of the aileron-rudder interconnect, transforms this three DOF model to a square (*mxm*) plant. The MIMO QFT CAD package is then used to design a three-axes rate-commanded control system to meet previously defined stability and performance specifications.

Closed-loop control system models based on the three and six DOF models are formed in MATLAB's Simulink environment, and velocity vector roll initiation and arrest simulations are performed to demonstrate the accuracy of the models and the performance of the closed-loop control system. With all performance specification met, the six DOF model is enhanced to include control effector limiting (saturation), and the simulations are again performed. Despite slight violations in the yaw rate design specification, these simulations demonstrate the successful initiation and arrest of a realistic velocity vector roll, with negligible excursions in AOA and sideslip angle.

The presence of small oscillations in the roll aileron control effector commands, however, leads to the enhancement of the control system design. The weighting matrix is modified/simplified to remove cyclic interactions between the roll and yaw controls, and the QFT controller is modified to account for the changes in the weighting matrix. Velocity vector roll initiation and arrest simulations of the resulting six DOF closed-loop system are then employed to demonstrate the removal of the oscillations and the

106

improvement in velocity vector roll performance. This improvement in the system performance illustrates the dual purpose of the weighting matrix $\mathbf{W} = \{w_{ij}\}$, i.e., to obtain a $m \times m$ effective plant matrix and to provide an opportunity to optimize the system's performance by "fine tuning" the w_{ij} elements.

8.2. Conclusions

This thesis has shown the effective application of QFT to a unique controls problem, the initiation and arrest of the velocity vector roll maneuver at high angles of attack. Through simulation, several key characteristics of the velocity vector roll have been identified. In particular, the stability axis roll rate, and subsequently the bank angle, achieved in the velocity vector roll maneuver is shown to be driven primarily by the differential aileron and elevator control inputs, as expected. However, the rudder and thrust vectoring yaw control inputs have been shown to contribute very little to the development of the desired roll rate. This is expected at low angles of attack, but not immediately obvious for high angles of attack where the velocity vector roll maneuver includes a fair amount of body axis yaw. Simulation also revealed the dependence of the AOA state on the nonlinear $P\beta$ term at small bank angles. This enforces the requirement for strict control over the sideslip angle in the transition region of the velocity vector roll. For bank angles greater than ten degrees, the trigonometric force term is shown to dominate the AOA state response. It is this term which limits the application of the three-axis rate-commanded control system developed in this thesis to the transition region of the large-amplitude velocity vector roll maneuver.

Most importantly, this thesis demonstrates that the QFT robust control design technique can be used to jointly address system nonlinearity and structured uncertainty in the design of a control system for a large-amplitude maneuver such as the velocity vector roll with excellent results. The closed-loop control system is shown to effectively initiate and arrest the velocity vector roll maneuver, with truly negligible excursions in the AOA and sideslip angle.

8.3. Recommendations

In this thesis, the QFT design technique is successfully employed to attack the nonlinearities associated with the thirty-degree angle of attack (AOA) velocity vector roll maneuver over the operating

range of the aircraft at this AOA. Specifically, this thesis produced a flight control system capable of controlling the transition regions of the maneuver-- initiating and arresting the velocity vector roll.

While this control system has been shown to produce superb results in these transition regions of the maneuver, it has been shown (not in this thesis) to be unacceptable in the so called "free-stream" or steady-state region of the velocity vector roll. In this region, the roll rate is maintained at the constant value achieved in the initiation region as the aircraft rolls through the desired bank angle. The most logical extension of this thesis would therefore be the design of the compensator for the "free-stream" region of the velocity vector roll maneuver. This design could be accomplished using optimal control techniques, or perhaps through an innovative inner- or outer-loop modification to the present design.

A second course of study based on this thesis is the extension of the present design to include a range of AOAs above 30 degrees. This would require the formation of additional linear models from NASA's HARV Simulation, and the re-application of QFT to the problem.

A third course of study, most likely following the previous two, is the design of a control system to perform the velocity vector roll maneuver in the presence of aerodynamic or mass asymmetries (such as an asymmetric weapons load). The NASA HARV Simulation provides the capability to model these effects, so sufficient data should be available to construct an appropriate model.

A final course of study, is the design of a digital control system equivalent to the present design, and the incorporation of this design into NASA's HARV Simulation. This is not a trivial procedure, according to the HARV Program Office, and would require the use of the Ada programming language, but should be easily achievable in the time allotted to a Master's thesis. This study would familiarize the student with the procedures required to code a flight control algorithm, and also introduce the student to the real-time programming aspects of the Ada language.

This appendix presents the F-18 HARV data obtained from NASA's F-18 HARV Batch Simulation. This data includes the aircraft weight, moments/products of inertia, and nondimensional stability and control derivatives for each trimmed F.C. The artificial stability derivatives calculated from the nondimensional stability derivatives are also presented for each F.C. This appendix concludes with a listing of the system (**A, B**) matrices for each of the twelve plant cases.

A.1. F-18 HARV General Information

All simulations are based on a single aircraft configuration, called 60% Fuel Batch. This section lists the elements of this configuration, and general properties of the aircraft, which are not a function of F.C.

- Wing Span - 37.4 ft

- Wing Area (S) - 400 ft^2

- Mean Aerodynamic Chord (MAC) - 11.52 ft

- Empty Weight - 29,615 lbs

- Fuel Weight (60% full) - 6,149 lbs

- Take-Off Weight - 35,764.60 lbs

- Moments/Products of Inertia (body axes), no fuel - $I_{xx} = 21500.0$ slug ft^2
  $I_{yy} = 170105.2$ slug ft^2
  $I_{zz} = 184471.0$ slug ft^2
  $I_{xz} = -1774.7$ slug ft^2

- Moments/Products of Inertia (body axes), with fuel - $I_{xx} = 22632.600$ slug ft^2
  $I_{yy} = 174246.297$ slug ft^2
  $I_{zz} = 189336.406$ slug ft^2
  $I_{xz} = -2131.800$ slug ft^2

- Center of Gravity (CG) Parameters -   CG Percent Chord = 23.3 %
  CG Buttline = 0.0 in
  CG Waterline = 105.388 in
  CG Fuselage Station = 456.249 in

A.2. F-18 HARV Batch Simulation Nondimensional Derivatives, Baseline, 20,000 ft.

Trimmed at 5 degrees AOA, 20,000 feet altitude, the nondimensional derivatives (in body axes), as output from the F-18 Batch Simulation, are:

```
ACOF        6      9     0(1P6E12.5)
              CL          CM          CN          CDrag        CLift        CY
  Q      0.00000E+00 -3.71272E+00  0.00000E+00  5.20518E-03  2.40643E+00  0.00000E+00
  ALP   -7.10861E-11 -3.11500E-01  3.43670E-11  6.18516E-01  4.94306E+00 -6.03242E-12
  V      1.27650E-14 -1.34003E-04  8.41471E-15  2.03717E-05  3.50386E-04 -5.42413E-14
  THA    0.00000E+00 -1.12700E-04  0.00000E+00  4.26894E-07  2.32230E-04  0.00000E+00
  H     -1.20563E-16  1.25263E-07  1.30104E-18  4.28408E-08  2.98023E-08 -8.32667E-17
  P     -4.06333E-01 -5.36539E-05 -5.85787E-02  0.00000E+00  1.26245E-04  2.15190E-02
  R      1.37166E-01  0.00000E+00 -1.82833E-01  0.00000E+00  0.00000E+00  2.16500E-01
  BTA   -1.01383E-01  0.00000E+00  1.25369E-01  0.00000E+00  0.00000E+00 -1.13102E+00
  PHI    0.00000E+00 -4.10885E-06  0.00000E+00  0.00000E+00  8.53788E-06  0.00000E+00


BCOF        6     12     0(1P6E12.5)
              CL          CM          CN          CDrag        CLift        CY
  PITAIL  0.00000E+00 -1.84000E-01  1.15667E-10 -7.00960E-04  4.67127E-01 -2.00939E-10
  PITEL   0.00000E+00 -1.18726E+00  3.85556E-11  1.15982E-01  9.52633E-01 -6.69800E-11
  PITRUD  0.00000E+00  0.00000E+00 -1.92778E-11  0.00000E+00  0.00000E+00  3.34898E-11
  PITLEF  1.01774E-12 -1.27762E-01 -3.54012E-11 -6.28605E-02 -1.12713E-01  5.62960E-11
  PITTEF -2.03549E-12  1.38977E-01  5.21495E-12  1.11556E-01  9.71530E-01 -1.08125E-11
  PITVEC  6.70909E-16 -7.05745E-02 -1.81786E-06  1.68749E-02  4.53596E-02  3.15803E-06
  ROLAIL  6.24927E-02  0.00000E+00 -2.21591E-03  0.00000E+00  0.00000E+00 -2.23350E-02
  ROLEL   5.07091E-02  0.00000E+00  1.05630E-02  0.00000E+00  0.00000E+00 -4.19262E-02
  YAWRUD  1.75819E-02  0.00000E+00 -7.87271E-02  0.00000E+00  0.00000E+00  2.47648E-01
  ROLLEF  0.00000E+00  0.00000E+00  0.00000E+00  0.00000E+00  0.00000E+00  0.00000E+00
  ROLTEF  6.07203E-02  0.00000E+00  0.00000E+00  0.00000E+00  0.00000E+00  0.00000E+00
  YAWVEC  2.31685E-12  0.00000E+00 -6.20600E-03  0.00000E+00  0.00000E+00  1.07812E-02


XZERO      11      1     0(1P6E12.5)
      Q           ALP           V           THA           H            P
 0.00000E+00  8.72665E-02  5.53012E+02  8.72665E-02  2.00000E+04  0.00000E+00
      R           BTA          PHI          PSI           Y
 0.00000E+00  1.85970E-10  0.00000E+00  0.00000E+00  0.00000E+00


UZERO      12      1     0(1P6E12.5)
    PITAIL       PITEL        PITRUD        PITLEF        PITTEF       PITVEC
 0.00000E+00  3.75194E-01  0.00000E+00  6.63998E+00  7.00000E+00  0.00000E+00
    ROLAIL       ROLEL        YAWRUD        ROLLEF        ROLTEF       YAWVEC
 0.00000E+00  0.00000E+00  8.98123E-09  0.00000E+00  0.00000E+00  0.00000E+00
```

The following engine data can also be extracted from the Batch Simulation:

- Cockpit Throttle Positions - Left = 39.2, Right = 39.2

- Thrust (in body axes) - x = 3529.2 lbs, y = 0.0 lbs, z = 0.0 lbs

From this data, the artificial stability derivatives, as defined in Eqs. (38) to (42), can be calculated using the coef.m script file (listed in section A.7.):

```
CYDTVY  =   1.119172448262450030E-01;
CYDRY   =   3.12788148676786601E-02;
CYDER   =  -5.295426766664163971E-03;
CYDAR   =  -2.82098918654543089E-03;
CYB     =  -1.428518106000699042E-01;
CYR     =   9.291480304326270573E-04;
CYP     =   1.09672683398896138E-05;
CZDTVP  =   1.114913655556130081E-01;
CZDEP   =  -1.20320904040579060E-01;
CZDAP   =  -5.899978579554409655E-02;
CZA     =  -6.24325892475722233E-01;
CZQ     =  -3.16575007501449651E-03;
CNDTVY  =  -7.208432159840005514E+00;
CNDRY   =  -1.43616956742789847E+00;
CNDER   =  -4.77809549704238612E-01;
CNDAR   =  -8.23752335045641604E-01;
CNB     =   3.16897639924039964E+00;
CNR     =  -1.43471934732934181E-01;
CNP     =   1.126781273248304002E-01;
CNPQ    =  -7.86130642208682451E-01;
CMDTVP  =  -7.78805531720038324E+00;
CMDEP   =  -6.09441174369732330E+00;
CMDAP   =  -9.44503950979825424E-01;
CMPP    =  -9.51143618349126752E-02;
CMPR    =   9.37930013834121779E-01;
CMQ     =  -1.985025460879914816E-01;
CMA     =  -1.59898359092508491E+00;
CLDTVY  =   4.79222221794896874E-02;
CLDRY   =   2.25545361510145348E+00;
CLDER   =   6.480739474960235395E+00;
CLDAR   =   7.98827233307507889E+00;
CLB     =  -1.55558538023918231E+01;
CLR     =   5.72017749256467534E-01;
CLPQ    =  -1.46051082571169583E-01;
CLP     =  -1.74169506105079064E+00;
CALP    =   9.96194694832095329E-01;
CBAR    =   1.15199999999999996E+01;
UBAR    =   5.53013999999999944E+02;
ALPHA   =   6.72664999999999969E-02;
```

111

A.3. F-18 HARV Batch Simulation Nondimensional Derivatives, 10,000 ft.

Trimmed at 30 degrees AOA, 10,000 feet altitude, the nondimensional derivatives (in body axes), as output from the F-18 Batch Simulation, are:

```
ACOF          6    9    0(1P6E12.5)
            CL            CM            CN          CDrag        CLift         CY
Q      0.00000E+00  -5.07495E+00   0.00000E+00   0.00000E+00   3.48158E+00   0.00000E+00
ALP    1.15422E-09  -2.12670E-01  -5.88752E-10   3.24937E+00   2.24708E+00  -3.93562E-10
V     -1.74347E-13  -7.21766E-05  -5.36515E-14   1.41591E-04   1.82152E-04   5.41067E-13
THA    0.00000E+00  -1.14109E-03   0.00000E+00   0.00000E+00   1.99103E-03   0.00000E+00
H     -1.49186E-16   4.37722E-07   2.77556E-17   1.49012E-07  -6.55651E-07   3.33067E-16
P     -4.55000E-01  -9.10769E-05   2.84673E-02   0.00000E+00   1.59697E-04   7.42491E-03
R      3.21637E-01   0.00000E+00  -2.52124E-01   0.00000E+00   0.00000E+00  -3.04499E-01
BTA   -8.02402E-02   0.00000E+00   1.22902E-02   0.00000E+00   0.00000E+00  -7.95848E-01
PHI    0.00000E+00  -1.73959E-05   0.00000E+00   0.00000E+00   3.07364E-05   0.00000E+00


BCOF          6   12    0(1P6E12.5)
               CL            CM            CN          CDrag        CLift         CY
PITAIL   -1.72190E-10  -6.79479E-02   2.75504E-09   0.00000E+00   1.66584E-01  -6.19884E-09
PITEL     7.97951E-11  -7.92848E-01  -1.27673E-09   5.80181E-01   5.79326E-01   2.87263E-09
PITRUD   -2.51984E-11   5.33617E-08   4.03177E-10   0.00000E+00   0.00000E+00  -9.07149E-10
PITLEF    2.88305E-10  -4.25398E-02   6.34661E-10  -1.80194E-01   2.05452E-01  -9.09670E-10
PITTEF    5.02948E-10   6.37031E-02  -1.74676E-09   2.63756E-01   3.74769E-01   3.62860E-09
PITVEC    1.04994E-11  -1.04696E-01  -1.67991E-10   5.89797E-02   7.00857E-02   3.77980E-10
ROLAIL    2.73366E-02   5.33617E-08  -8.48735E-03   0.00000E+00   0.00000E+00   4.07787E-02
ROLEL     3.71075E-02   1.06723E-07  -1.03387E-02   0.00000E+00   0.00000E+00   4.21615E-02
YAWRUD    1.88148E-03   0.00000E+00  -3.79409E-02   0.00000E+00   0.00000E+00   1.01513E-01
ROLLEF    0.00000E+00   0.00000E+00   0.00000E+00   0.00000E+00   0.00000E+00   0.00000E+00
ROLTEF    4.82789E-02   5.33617E-08   0.00000E+00   0.00000E+00   0.00000E+00   0.00000E+00
YAWVEC    7.26265E-04   0.00000E+00  -1.16202E-02   0.00000E+00   0.00000E+00   2.61455E-02


XZERO        11    1    0(1P6E12.5)
        Q            ALP             V            THA            H             P
0.00000E+00   5.23599E-01   2.18609E+02   5.23599E-01   1.00000E+04   0.00000E+00
        R            BTA            PHI            PSI            Y
0.00000E+00   1.17521E-09   0.00000E+00   0.00000E+00   0.00000E+00


UZERO        12    1    0(1P6E12.5)
     PITAIL         PITEL         PITRUD         PITLEF         PITTEF         PITVEC
0.00000E+00  -5.02130E+00   0.00000E+00   3.30000E+01   0.00000E+00   0.00000E+00
     ROLAIL         ROLEL         YAWRUD         ROLLEF         ROLTEF         YAWVEC
0.00000E+00   0.00000E+00  -1.77888E-07   0.00000E+00   0.00000E+00   0.00000E+00
```

The following engine data can also be extracted from the Batch Simulation:

- Cockpit Throttle Positions - Left = 64.3, Right = 64.3

- Thrust (in body axes) - x = 14757.4 lbs, y = 0.0 lbs, z = 0.0 lbs

From this data, the artificial stability derivatives, as defined in Eqs. (38) to (42), can be calculated using the coef.m script file (listed in section A.7.):

```
CYDTVY =   6.07323504920353266E-02;
CYDRY  =   7.01844956505434051E-03;
CYDER  =   2.91497996647757966E-03;
CYDAR  =   2.81937534383262670E-03;
CYB    =  -5.50236821830639086E-02;
CYR    =  -1.53763068401784899E-03;
CYP    =   9.38457290429957716E-04;
CZDTVP =   5.25957515434202355E-02;
CZDEP  =  -4.00536907856596791E-02;
CZDAP  =  -1.15173564208033690E-02;
CZA    =  -1.55359585950984674E-01;
CZQ    =  -6.34235205542993744E-03;
CNDTVY =  -1.41606909428348504E+00;
CNDRY  =  -1.41754003974047776E-01;
CNDER  =  -5.57081131379304040E-01;
CNDAR  =  -4.13036419923716702E-01;
CNB    =   5.27025869224455823E-01;
CNR    =  -2.60164532435097628E-01;
CNP    =   3.89255881241448110E-01;
CNPQ   =  -4.17016401506588308E-01;
CMDTVP =  -1.67065042890981963E+00;
CMDEP  =  -3.80670460478496397E-01;
CMDAP  =  -7.54743764019671221E-02;
CMPP   =  -4.20386456347477622E-01;
CMPR   =   4.571658205C5391451E-01;
CMQ    =  -1.485284702227803383E-01;
CMA    =  -2.36227103845834036E-01;
CLDTVY =  -6.26816425598615390E-01;
CLDRY  =  -7.75106600801798475E-03;
CLDER  =   8.72972801702200707E-01;
CLDAR  =   6.41896658951537580E-01;
CLB    =  -1.30196038910815171E+00;
CLR    =   4.06908064564558858E-01;
CLPQ   =  -6.45516574609137028E-01;
CLP    =  -8.82656869723266513E-01;
CALP   =   8.66025291583566226E-01;
CBAR   =   1.15199999999999996E+01;
UBAR   =   2.18609000000000009E+02;
ALPHA  =   5.23599000000000037E-01;
```

113

A.4. F-18 HARV Batch Simulation Nondimensional Derivatives, 15,000 ft.

Trimmed at 30 degrees AOA, 15,000 feet altitude, the nondimensional derivatives (in body axes), as output from the F-18 Batch Simulation, are:

```
ACOF         6      9     0(1P6E12.5)
            CL          CM          CN         CDrag       CLift         CY
Q      0.00000E+00 -5.06097E+00  0.00000E+00  0.00000E+00  3.40663E+00  0.00000E+00
ALP   -4.20491E-10 -2.14963E-01  9.60210E-11  3.23240E+00  2.22478E+00  9.30845E-10
V      7.60607E-14 -6.60131E-05 -4.08562E-14  1.43826E-04  1.63794E-04 -1.53925E-13
THA    0.00000E+00 -9.35965E-04  0.00000E+00  0.00000E+00  1.56755E-03  0.00000E+00
H      6.59195E-17  3.56697E-07  1.73472E-17  1.19209E-07 -5.36442E-07 -2.91434E-16
P     -4.55000E-01 -9.44755E-05  2.82338E-02  0.00000E+00  1.72755E-04  3.32254E-03
R      3.19054E-01  0.00000E+00 -2.56602E-01  0.00000E+00  0.00000E+00 -3.00859E-01
BTA   -8.28843E-02  0.00000E+00  1.21966E-02  0.00000E+00  0.00000E+00 -7.88583E-01
PHI    0.00000E+00 -1.54749E-05  0.00000E+00  0.00000E+00  2.39061E-05  0.00000E+00


BCOF         6     12     0(1P6E12.5)
             CL          CM          CN         CDrag       CLift         CY
PITAIL   3.37922E-11 -6.80724E-02 -5.40674E-10  0.00000E+00  1.67424E-01  1.21652E-09
PITEL    6.75843E-11 -7.98659E-01 -1.08135E-09  5.79169E-01  5.72697E-01  2.43303E-09
PITRUD   5.91363E-11  5.33617E-08 -9.46181E-10  0.00000E+00  0.00000E+00  2.12891E-09
PITLEF  -1.13537E-10 -3.87360E-02 -3.02435E-10 -1.79138E-01  2.04957E-01  4.65040E-10
PITTEF  -1.21885E-10  6.62973E-02 -6.21136E-10  2.56121E-01  3.74253E-01  1.52065E-09
PITVEC  -1.05601E-11 -9.06547E-02  1.68961E-10  5.13754E-0'  6.11227E-02 -3.80162E-10
ROLAIL   2.69037E-02  0.00000E+00 -8.47069E-03  0.00000E+00  0.00000E+00  3.94373E-02
ROLEL    3.64862E-02 -5.33617E-08 -1.03963E-02  0.00000E+00  0.00000E+00  3.99876E-02
YAWRUD   1.88945E-03  5.33617E-08 -3.76628E-02  0.00000E+00  0.00000E+00  1.01319E-01
ROLLEF   0.00000E+00  0.00000E+00  0.00000E+00  0.00000E+00  0.00000E+00  0.00000E+00
ROLTEF   4.77594E-02  0.00000E+00  0.00000E+00  0.00000E+00  0.00000E+00  0.00000E+00
YAWVEC   6.21646E-04  0.00000E+00 -9.94633E-03  0.00000E+00  0.00000E+00  2.23792E-02


XZERO        11      1     0(1P6E12.5)
       Q           ALP          V          THA           H           P
 0.00000E+00  5.23599E-01  2.36465E+02  5.23599E-01  1.50000E+04  0.00000E+00
       R           BTA          PHI         PSI           Y
 0.00000E+00 -5.06074E-10  0.00000E+00  0.00000E+00  0.00000E+00


UZERO        12      1     0(1P6E12.5)
    PITAIL       PITEL       PITRUD       PITLEF       PITTEF       PITVEC
 0.00000E+00 -5.00296E+00  0.00000E+00  3.30000E+01  6.30319E-06  0.00000E+00
    ROLAIL       ROLEL       YAWRUD       ROLLEF       ROLTEF       YAWVEC
 0.00000E+00  0.00000E+00 -1.31265E-07  0.00000E+00  0.00000E+00  0.00000E+00
```

The following engine data can also be extracted from the Batch Simulation:

- Cockpit Throttle Positions - Left = 72.4, Right = 72.4

- Thrust (in body axes) - x = 14795.9 lbs, y = 0.0 lbs, z = 0.0 lbs

From this data, the artificial stability derivatives, as defined in Eqs. (38) to (42), can be calculated using the coef.m script file (listed in section A.7.):

```
CYDTVY  =   5.62893535363834657E-02;
CYDRY   =   6.46025682908673606E-03;
CYDER   =   2.54967149279788355E-03;
CYDAR   =   2.51458350996103730E-03;
CYB     =  -5.02812770660163028E-02;
CYR     =  -1.30530668481651816E-03;
CYP     =   7.72963122386306377E-04;
CZDTVP  =   4.87480038093969434E-02;
CZDEP   =  -3.65160503483797361E-02;
CZDAP   =  -1.06752143166929953E-02;
CZA     =  -1.41855428776592629E-01;
CZQ     =  -5.29057335148337346E-03;
CNDTVY  =  -1.41826673391359392E+00;
CNDRY   =  -1.40690802118758979E-01;
CNDER   =  -5.47160656642931120E-01;
CNDAR   =  -4.05893637928946560E-01;
CNB     =   5.36251727364312036E-01;
CNR     =  -2.43489795403019987E-01;
CNP     =   3.60744643563561673E-01;
CNPQ    =  -4.17016401506588308E-01;
CMDTVP  =  -1.67504824526445262E+00;
CMDEP   =  -8.85033712921329485E-01;
CMDAP   =  -7.54344080758695690E-02;
CMPP    =  -4.20386456347477622E-01;
CMPR    =   4.57165820505391451E-01;
CMQ     =  -1.36600117052837783E-01;
CMA     =  -2.38211179027229047E-01;
CLDTVY  =  -6.31048958702400076E-01;
CLDRY   =  -7.15697473992911622E-03;
CLDER   =   8.56012853795270368E-01;
CLDAR   =   6.30079020518260258E-01;
CLB     =  -1.33173714977577773E+00;
CLR     =   3.79247861782185947E-01;
CLPQ    =  -6.45516574609137028E-01;
CLP     =  -8.15887876688384250E-01;
CALP    =   8.66025291583566226E-01;
CBAR    =   1.15199999999999996E+01;
UBAR    =   2.36485000000000014E+02;
ALPHA   =   5.23599000000000037E-01;
```

A.5. F-18 HARV Batch Simulation Nondimensional Derivatives, 20,000 ft.

Trimmed at 30 degrees AOA, 20,000 feet altitude, the nondimensional derivatives (in body axes), as output from the F-18 Batch Simulation, are:

```
ACOF        6     9    0(1P6E12.5)
             CL          CM          CN         CDrag        CLift         CY
Q       0.00000E+00 -5.04509E+00  0.00000E+00  0.00000E+00  3.32137E+00  0.00000E+00
ALP     1.50425E-09 -2.18009E-01 -5.85953E-10  3.21220E+00  2.20005E+00 -1.56396E-09
V      -2.51910E-13 -6.12410E-05  1.01212E-14  1.46121E-04  1.49667E-04  6.50813E-13
THA     0.00000E+00 -7.62326E-04  0.00000E+00  0.00000E+00  1.22262E-03  0.00000E+00
H      -2.63678E-16  2.76603E-07  1.73472E-18  1.19209E-07 -4.17233E-07  6.10623E-16
P      -4.55000E-01 -9.08667E-05  2.79639E-02  0.00000E+00  1.40697E-04 -1.40942E-03
R       3.16091E-01  0.00000E+00 -2.61805E-01  0.00000E+00  0.00000E+00 -2.96541E-01
BTA    -8.59409E-02  0.00000E+00  1.20974E-02  0.00000E+00  0.00000E+00 -7.80454E-01
PHI     0.00000E+00 -1.36606E-05  0.00000E+00  0.00000E+00  2.39061E-05  0.00000E+00


BCOF        6    12    0(1P6E12.5)
             CL          CM          CN         CDrag        CLift         CY
PITAIL -1.36602E-10 -6.83410E-02  2.18564E-09  0.00000E+00  1.68698E-01 -4.91768E-09
PITEL   3.41502E-11 -8.07822E-01 -5.46409E-10  5.77036E-01  5.67342E-01  1.22942E-09
PITRUD  9.81830E-11  0.00000E+00 -1.57093E-09  0.00000E+00  0.00000E+00  3.53459E-09
PITLEF  3.75575E-10 -3.44516E-02  3.22622E-10 -1.77917E-01  2.04346E-01 -5.76549E-11
PITTEF  4.97325E-10  6.97972E-02 -1.65775E-10  2.47293E-01  3.73047E-01  0.00000E+00
PITVEC  0.00000E+00 -9.07701E-02  0.00000E+00  5.15769E-02  6.15385E-02  0.00000E+00
ROLAIL  2.64623E-02  0.00000E+00 -8.50624E-03  0.00000E+00  0.00000E+00  3.81613E-02
ROLEL   3.58307E-02  0.00000E+00 -1.04212E-02  0.00000E+00  0.00000E+00  3.74159E-02
YAWRUD  1.90066E-03  0.00000E+00 -3.74120E-02  0.00000E+00  0.00000E+00  1.01232E-01
ROLLEF  0.00000E+00  0.00000E+00  0.00000E+00  0.00000E+00  0.00000E+00  0.00000E+00
ROLTEF  4.72042E-02  0.00000E+00  0.00000E+00  0.00000E+00  0.00000E+00  0.00000E+00
YAWVEC  5.50954E-04  0.00000E+00 -8.81526E-03  0.00000E+00  0.00000E+00  1.98343E-02


XZERO      11     1    0(1P6E12.5)
        Q          ALP           V          THA           H            P
   0.00000E+00  5.23599E-01  2.56800E+02  5.23599E-01  2.00000E+04  0.00000E+00
        R          BTA          PHI          PSI           Y
   0.00000E+00  1.63791E-09  0.00000E+00  0.00000E+00  0.00000E+00


UZERO      12     1    0(1P6E12.5)
      PITAIL       PITEL        PITRUD       PITLEF       PITTEF       PITVEC
   0.00000E+00 -5.01436E+00  0.00000E+00  3.30000E+01  6.30319E-06  0.00000E+00
      ROLAIL       ROLEL        YAWRUD       ROLLEF       ROLTEF       YAWVEC
   0.00000E+00  0.00000E+00  1.83643E-08  0.00000E+00  0.00000E+00  0.00000E+00
```

The following engine data can also be extracted from the Batch Simulation:

- Cockpit Throttle Positions - Left = 87.0, Right = 87.0

- Thrust (in body axes) - x = 14835.4 lbs, y = 0.0 lbs, z = 0.0 lbs

From this data, the artificial stability derivatives, as defined in Eqs. (38) to (42), can be calculated using the coef.m script file (listed in section A.7.):

```
CYDTVY   =   5.19705693029802809E-02;
CYDRY    =   5.93736496950251179E-03;
CYDER    =   2.19448251503881215E-03;
CYDAR    =   2.238201021521161608E-03;
CYB      =  -4.57744610390796725E-02;
CYR      =  -1.09983602696355344E-03;
CYP      =   6.28040194070461264E-04;
CZDTVP   =   4.50078274343774370E-02;
CZDEP    =  -3.32752145223594725E-02;
CZDAP    =  -9.89431795899651037E-03;
CZA      =  -1.29035283321024985E-01;
CZQ      =  -4.36938839968372197E-03;
CNDTVY   =  -1.42090693238723520E+00;
CNDRY    =  -1.39931739907884517E-01;
CNDER    =  -5.37362629128103175E-01;
CNDAR    =  -3.99310273294799345E-01;
CNB      =   5.47856597658433531E-01;
CNR      =  -2.27787006386213520E-01;
CNP      =   3.33720585358794453E-01;
CNPQ     =  -4.17016401506588308E-01;
CMDTVP   =  -1.67938378549336464E+00;
CMDEP    =  -8.94175076588127782E-01;
CMDAP    =  -7.56463910479155538E-02;
CMPP     =  -4.20386456347477622E-01;
CMPR     =   4.57165820505391451E-01;
CMQ      =  -1.25257363524697934E-01;
CMA      =  -2.41313326787214427E-01;
CLDTVY   =  -6.34422020472934722E-01;
CLDRY    =  -6.53432305109070272E-03;
CLDER    =   8.39389853231515937E-01;
CLDAR    =   6.18798723580269661E-01;
CLB      =  -1.36833774347255410E+00;
CLR      =   3.53140735752541457E-01;
CLPQ     =  -6.45516574609137028E-01;
CLP      =  -7.52518470968063458E-01;
CALP     =   8.66025291583566226E-01;
CBAR     =   1.15199999999999996E+01;
UBAR     =   2.56800000000000011E+02;
ALPHA    =   5.23599000000000037E-01;
```

A.6. System Matrices

This section lists the system matrices for the twelve F.C.s. The elements of these system matrices are described in Eqs. (63) and (64), and are obtained from the artificial stability and control derivatives in this appendix. The **C** and **D** matrices are not listed here since they are simply the identity matrix and the zero matrix, respectivley, and do not change.

Table 8. A Matrices for 12 Plant Cases

Nonlinearity	Altitude		
	10,000 feet	15,000 feet	20,000 feet
$P_{param} = 0$ deg/sec	$\begin{bmatrix} -0.8827 & 0 & 0.4096 \\ 0 & -0.1485 & 0 \\ 0.3893 & 0 & -0.2602 \end{bmatrix}$	$\begin{bmatrix} -0.8159 & 0 & 0.3792 \\ 0 & -0.1366 & 0 \\ 0.3607 & u & -0.2435 \end{bmatrix}$	$\begin{bmatrix} -0.7525 & 0 & 0.3531 \\ 0 & -0.1253 & 0 \\ 0.3337 & 0 & -0.2278 \end{bmatrix}$
$P_{param} = 8$ deg/sec	$\begin{bmatrix} -0.8827 & -0.0901 & 0.4096 \\ 0.0587 & -0.1485 & 0.0638 \\ 0.3893 & -0.0582 & -0.2602 \end{bmatrix}$	$\begin{bmatrix} -0.8159 & -0.0901 & 0.3792 \\ 0.0587 & -0.1366 & 0.0638 \\ 0.3607 & -0.0582 & -0.2435 \end{bmatrix}$	$\begin{bmatrix} -0.7525 & -0.0901 & 0.3531 \\ 0.0587 & -0.1253 & 0.0638 \\ 0.3337 & -0.0582 & -0.2278 \end{bmatrix}$
$P_{param} = 16$ deg/sec	$\begin{bmatrix} -0.8827 & -0.1803 & 0.4096 \\ 0.1174 & -0.1485 & 0.1277 \\ 0.3893 & -0.1165 & -0.2602 \end{bmatrix}$	$\begin{bmatrix} -0.8159 & -0.1803 & 0.3792 \\ 0.1174 & -0.1366 & 0.1277 \\ 0.3607 & -0.1165 & -0.2435 \end{bmatrix}$	$\begin{bmatrix} -0.7525 & -0.1803 & 0.3531 \\ 0.1174 & -0.1253 & 0.1277 \\ 0.3337 & -0.1165 & -0.2278 \end{bmatrix}$
$P_{param} = 24$ deg/sec	$\begin{bmatrix} -0.8827 & -0.2704 & 0.4096 \\ 0.1761 & -0.1485 & 0.1915 \\ 0.3893 & -0.1747 & -0.2602 \end{bmatrix}$	$\begin{bmatrix} -0.8159 & -0.2704 & 0.3792 \\ 0.1761 & -0.1366 & 0.1915 \\ 0.3607 & -0.1747 & -0.2435 \end{bmatrix}$	$\begin{bmatrix} -0.7525 & -0.2704 & 0.3531 \\ 0.1761 & -0.1253 & 0.1915 \\ 0.3337 & -0.1747 & -0.2278 \end{bmatrix}$

Table 9. B Matrices for Flight Conditions

Altitude (feet)	B
10,000	$\begin{bmatrix} 0.6419 & 0.8730 & 0 & 0 & -0.6268 & -0.0078 \\ 0 & 0 & -0.8807 & -1.6707 & 0 & 0 \\ -0.4130 & -0.5571 & 0 & 0 & -1.4161 & -0.1418 \end{bmatrix}$
15,000	$\begin{bmatrix} 0.6301 & 0.8560 & 0 & 0 & -0.6310 & -0.0072 \\ 0 & 0 & -0.8850 & -1.6750 & 0 & 0 \\ -0.4059 & -0.5472 & 0 & 0 & -1.4183 & -0.1407 \end{bmatrix}$
20,000	$\begin{bmatrix} 0.6188 & 0.8394 & 0 & 0 & -0.6344 & -0.0065 \\ 0 & 0 & -0.8942 & -1.6794 & 0 & 0 \\ -0.3993 & -0.5374 & 0 & 0 & -1.4209 & -0.1399 \end{bmatrix}$

A.7. Plant Generation Script File

This Matrix$_x$ script file, coef.m, generates the linear models from the HARV Simulation output.

Not all portions of this file are applicable to all aspects of this thesis.

```
//------------------------------------------------------------------
//  Set up initial values
//
alpha = xzero(2);
qbar = 0.5*2.377e-3*(1-(0.703e-5)*(xzero(5)))**4.14*(xzero(3))**2;
ubar = xzero(3);
mass = 1111.5961;
cbar = 11.52;
b = 37.4;
s = 400;
Ixxo = 22632.6;
Iyyo = 174246.297;
Izzo = 189336.406;
Ixzo = -2131.8;

calp = cos(alpha);
salp = sin(alpha);

IF     xzero(5) = 10000, bCndtvy = -0.46340002; bCydtvy = 0.87841667;...
                         bCmdtvp = -1.50404937; bCzdtvp = 0.87841667;...
ELSEIF xzero(5) = 15000, bCndtvy = -0.46571782; bCydtvy = 0.88281025;..
                         bCmdtvp = -1.51157220; bCzdtvp = 0.98281026;...
ELSEIF xzero(5) = 20000, bCndtvy = -0.46745201; bCydtvy = 0.88609757;...
                         bCmdtvp = -1.51720083; bCzdtvp = 0.88609757;...
ELSEIF xzero(5) = 25000, bCndtvy = -0.44564519; bCydtvy = 0.84476077;...
                         bCmdtvp = -1.44642280; bCzdtvp = 0.84476077;...
END

//------------------------------------------------------------------
//  Transform to new axis system
//
dClp = acof(1,6)*calp**2-(acof(1,7)+acof(3,6))*salp*calp+acof(3,7)*salp**2;
dClr = acof(1,7)*calp**2-(acof(3,7)-acof(1,6))*salp*calp-acof(3,6)*salp**2;
dClb = acof(1,8)*calp-acof(3,8)*salp;
dCldar = bcof(1,7)*calp+bcof(3,7)*salp;
dClder = bcof(1,8)*calp+bcof(3,8)*salp;
dCldry = bcof(1,9)*calp+bcof(3,9)*salp;
dCldtvy = bcof(1,12)*calp+bCndtvy*salp;

dCma = acof(2,2);
dCmq = acof(2,1);
dCmdap = bcof(2,1);
dCmdep = bcof(2,2);
dCmdtvp = bCmdtvp;

dCnp = acof(3,6)*calp**2-(acof(3,7)-acof(1,6))*salp*calp-acof(1,7)*salp**2;
dCnr = acof(3,7)*calp**2+(acof(1,7)+acof(3,6))*salp*calp+acof(1,6)*salp**2;
dCnb = acof(3,8)*calp+acof(1,8)*salp;
dCndar = bcof(3,7)*calp-bcof(1,7)*salp;
dCnder = bcof(3,8)*calp-bcof(1,8)*salp;
dCndry = bcof(3,9)*calp-bcof(1,9)*salp;
dCndtvy = bCndtvy*calp-bcof(1,12)*salp;

dCzq = -acof(5,1);
dCza = -acof(5,2);
dCzdap = -bcof(5,1);
dCzdep = -bcof(5,2);
dCzdtvp = bCzdtvp*calp;
```

```
dCyp = acof(6,6)*calp-acof(6,7)*salp;
dCyr = acof(6,7)*calp+acof(6,6)*salp;
dCyb = acof(6,8);
dCydar = bcof(6,7);
dCyder = bcof(6,8);
dCydry = bcof(6,9);
dCydtvy = bCydtvy;


Ixx = Ixxo*calp**2-Ixzo*2*calp*salp+Izzo*salp**2;
Iyy = Iyyo;
Izz = Izzo*calp**2+Ixzo*2*calp*salp+Ixxo*salp**2;
Ixz = (Ixxo-Izzo)*salp*calp+Ixzo*(calp**2-salp**2);
//-----------------------------------------------------------------
//  Completely non-dimensionalize the transformed derivatives
//
d = Ixx*Izz-Ixz**2;
n1 = (qbar*s*b**2)/(2*d*ubar);
n2 = (qbar*s*cbar**2)/(2*Iyy*ubar);
n3 = (qbar*s*cbar)/(2*mass*ubar**2);
n4 = (qbar*s*b)/(2*mass*ubar**2);

Clp = n1*(Izz*dClp+Ixz*dCnp);
Clpq = (Ixz/D)*(Ixx-Iyy+Izz);
Clr = n1*(Izz*dClr+Ixz*dCnr);
Clb = (qbar*s*b)/d*(Izz*dClb+Ixz*dCnb);
Cldar = (qbar*s*b)/d*(Izz*dCldar+Ixz*dCndar);
Clder = (qbar*s*b)/d*(Izz*dClder+Ixz*dCnder);
Cldry = (qbar*s*b)/d*(Izz*dCldry+Ixz*dCndry);
Cldtvy = (qbar*s*b)/d*(Izz*dCldtvy+Ixz*dCndtvy);

Cma = (qbar*s*cbar)/Iyy*dCma;
Cmq = n2*dCmq;
Cmpr = (Izz-Ixx)/Iyy;
Cmpp = Ixz/Iyy;
Cmdap = (qbar*s*cbar)/Iyy*dCmdap;
Cmdep = (qbar*s*cbar)/Iyy*dCmdep;
Cmdtvp = (qbar*s*cbar)/Iyy*dCmdtvp;

Cnpq = (Ixx**2-Ixx*Iyy+Ixz**2)/d;
Cnp = n1*(Ixz*dClp+Ixx*dCnp);
Cnr = n1*(Ixz*dClr+Ixx*dCnr);
Cnb = (qbar*s*b)/d*(Ixz*dClb+Ixx*dCnb);
Cndar = (qbar*s*b)/d*(Ixz*dCldar+Ixx*dCndar);
Cnder = (qbar*s*b)/d*(Ixz*dClder+Ixx*dCnder);
Cndry = (qbar*s*b)/d*(Ixz*dCldry+Ixx*dCndry);
Cndtvy = (qbar*s*b)/d*(Ixz*dCldtvy+Ixx*dCndtvy);

Czq = n3*dCzq;
Cza = (qbar*s)/(mass*ubar)*dCza;
Czdap = (qbar*s)/(mass*ubar)*dCzdap;
Czdep = (qbar*s)/(mass*ubar)*dCzdep;
Czdtvp = (qbar*s)/(mass*ubar)*dCzdtvp;

Cyp = n4*dCyp;
Cyr = n4*dCyr;
Cyb = (qbar*s)/(mass*ubar)*dCyb;
Cydar = (qbar*s)/(mass*ubar)*dCydar;
Cyder = (qbar*s)/(mass*ubar)*dCyder;
Cydry = (qbar*s)/(mass*ubar)*dCydry;
Cydtvy = (qbar*s)/(mass*ubar)*dCydtvy;
//-----------------------------------------------------------------
//  Define A Matrix of Plant
//      x = [P q r]'
//
```

```
Pparam = pi/180*[0,8,16,24];      // Average Roll Rate Variation, rad/sec
//
a1 = [ Clp              Clpq*Pparam(1)      Clr;
       -Cmpp*Pparam(1)      Cmq          Cmpr*Pparam(1);
        Cnp             Cnpq*Pparam(1)      Cnr         ];
a2 = [ Clp              Clpq*Pparam(2)      Clr;
       -Cmpp*Pparam(2)      Cmq          Cmpr*Pparam(2);
        Cnp             Cnpq*Pparam(2)      Cnr         ];
a3 = [ Clp              Clpq*Pparam(3)      Clr;
       -Cmpp*Pparam(3)      Cmq          Cmpr*Pparam(3);
        Cnp             Cnpq*Pparam(3)      Cnr         ];
a4 = [ Clp              Clpq*Pparam(4)      Clr;
       -Cmpp*Pparam(4)      Cmq          Cmpr*Pparam(4);
        Cnp             Cnpq*Pparam(4)      Cnr         ];
//------------------------------------------------------------------------
//  Define Original B Matrix (Before incorporation of Weighting Matrix)
//  Assumptions:  Rudder only used for yaw (no pitch) and ailerons not
//                used for pitch.
//
//      u_orig = [dar der dep dtvp dtvy dry]
//
Borig = [ Cldar Clder   0       0   Cldtvy Cldry;
            0     0    Cmdep  Cmdtvp  0      0   ;
          Cndar Cnder   0       0   Cndtvy Cndry];
//------------------------------------------------------------------------
// Define Weighting Matrices.  W0 is "straight through" approach
//                             W1 is "aileron-rudder interconnect" approach
//
// Assumptions:  +/- Max surface deflections are equal
//
darmax = 42*pi/180;
dermax = 24*pi/180;
drymax = 30*pi/180;
dtvymax = 10*pi/180;
depmax = 24*pi/180;
dtvpmax = 20*pi/180;
dahatmax = 3.0;         // Max lateral stick (inches)
dehatmax = 5.0;         // Max longitudinal stick (inches)
drhatmax = 1.0;         // Full left or right

W0 = [ darmax/dahatmax  0                   0;
       dermax/dahatmax  0                   0;
       0                depmax/dehatmax     0;
       0                dtvpmax/dehatmax    0;
       0                0                   dtvymax/drhatmax;
       0                0                   drymax/drhatmax  ];

W1 = [ darmax/dahatmax  0   -(Cldtvy+Cldry)/Cldar*darmax/drhatmax;
       dermax/dahatmax  0   -(Cldtvy+Cldry)/Clder*dermax/drhatmax;
       0  depmax/dehatmax   0;
       0  dtvpmax/dehatmax  0;
       -(Cndar+Cnder)/Cndtvy*dtvymax/dahatmax     0  dtvymax/drhatmax;
       -(Cndar+Cnder)/(10*Cndry)*drymax/dahatmax          0  drymax/drhatmax  ];
//------------------------------------------------------------------------
//  Define New B Matrices (Incorporation of Weighting Matries), B = Borig*W
//      u = [da de dr]
B0 = Borig * W0;
B1 = Borig * W1;


//-------------------------- ---------------------------------------------
//  Define C and D Matrices for MIMO QFT Package
//
C = eye(3);
D = 0*ones(3,6);
Dw = 0*ones(3);
```

121

B.1. Six DOF Bare Aircraft Open-Loop Simulations

This section contains the simulations validating the six DOF model developed in Chapter 2 (Fig. 6). State responses to each of the six control inputs are obtained first for a low AOA F.C. (20,000 feet, 5 degrees AOA) and then for a high AOA F.C. (10,000 feet, 30 degrees AOA). Note, actuator response characteristics are not included in these simulation.
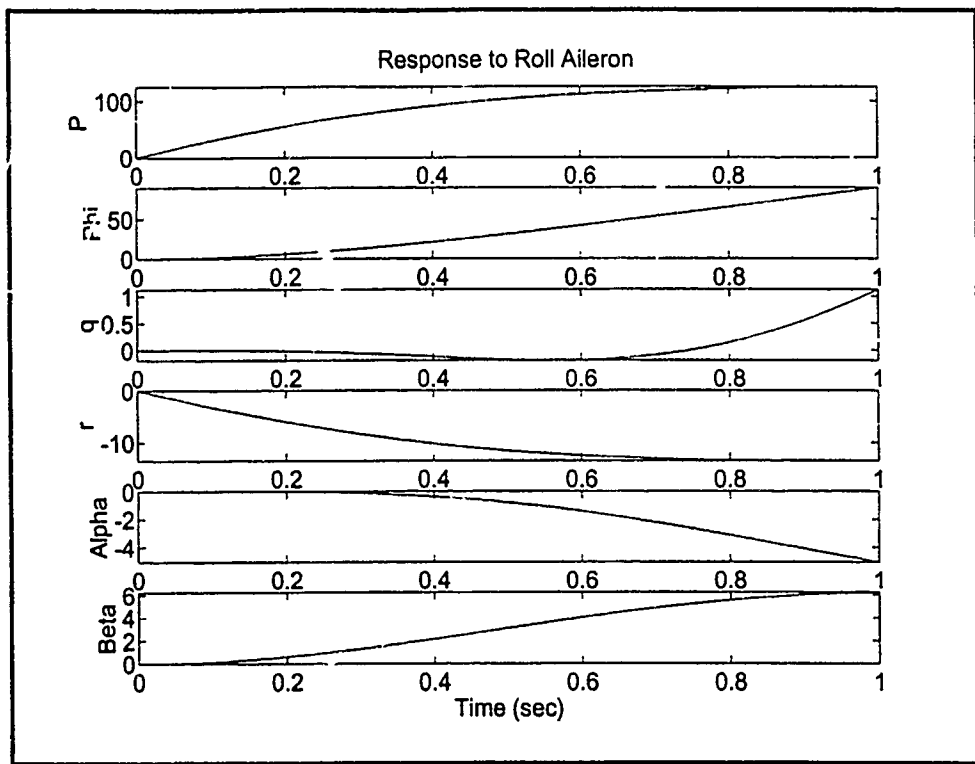
Figure 57. Response to Aileron Roll Command, 6 DOF Model, 20kft, Low AOA
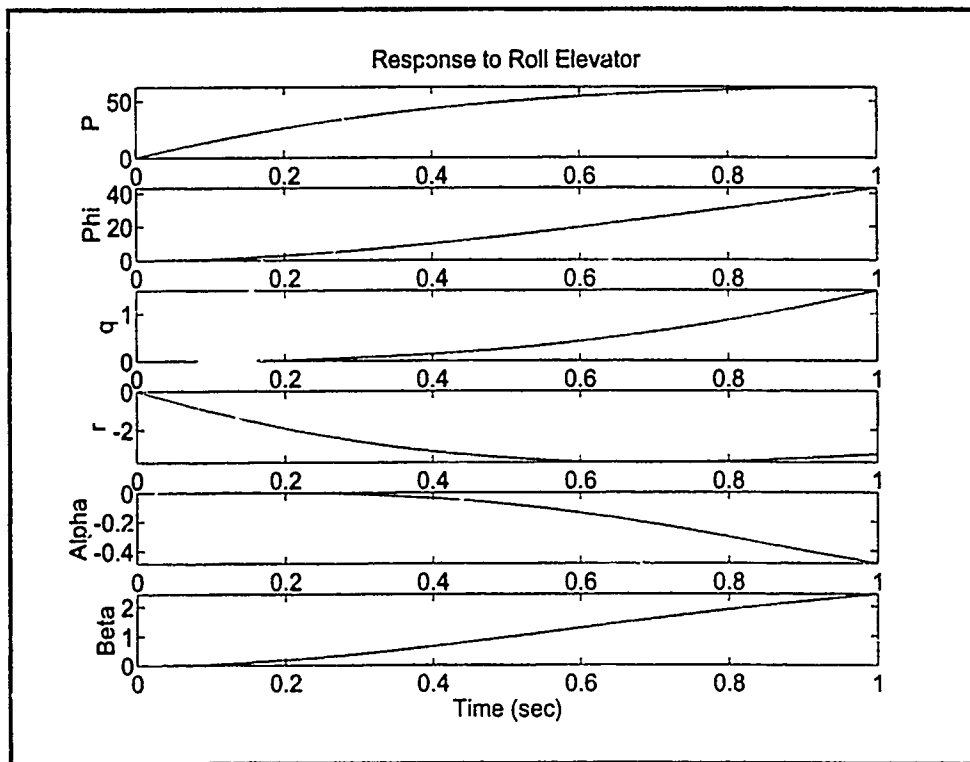
Figure 58. Response to Elevator Roll Command, 6 DOF Model, 20kft, Low AOA

123
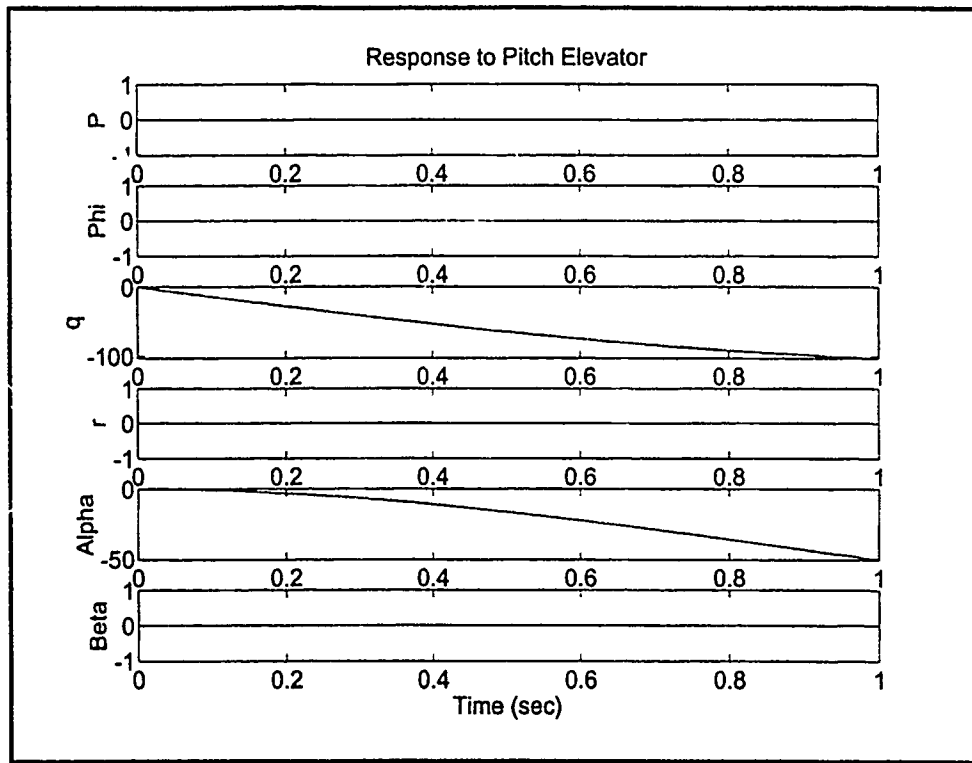
Figure 59. Response to Elevator Pitch Command, 6 DOF Model, 20 kft, Low AOA
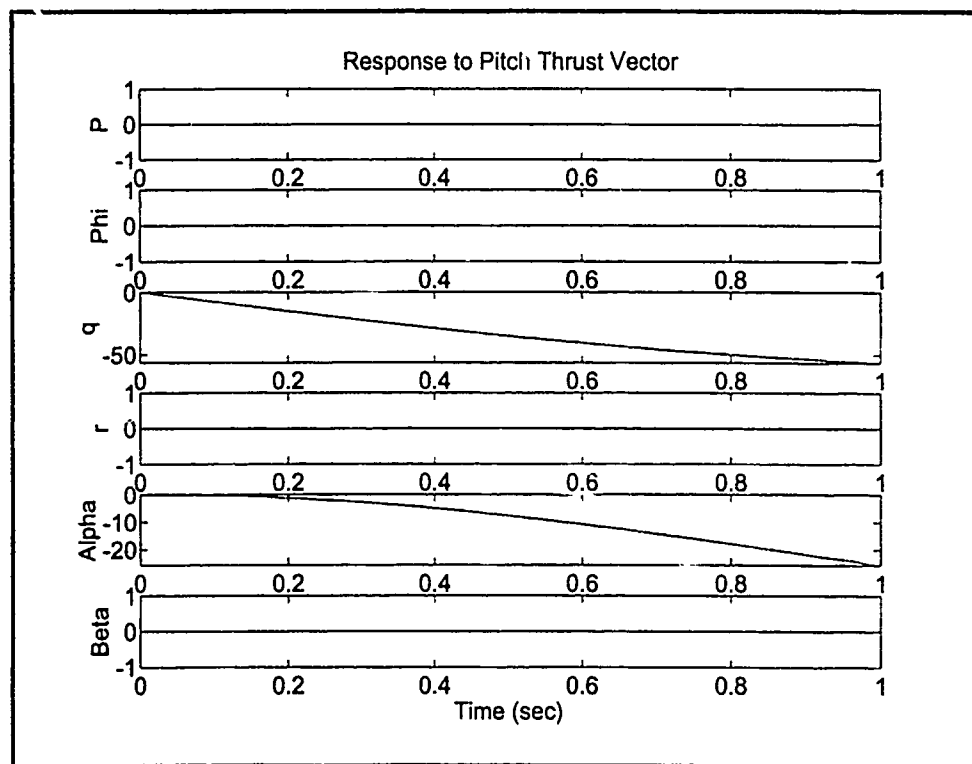
Figure 60. Response to Thrust Vectored Pitch Command, 6 DOF Model, 20 kft, Low AOA

124
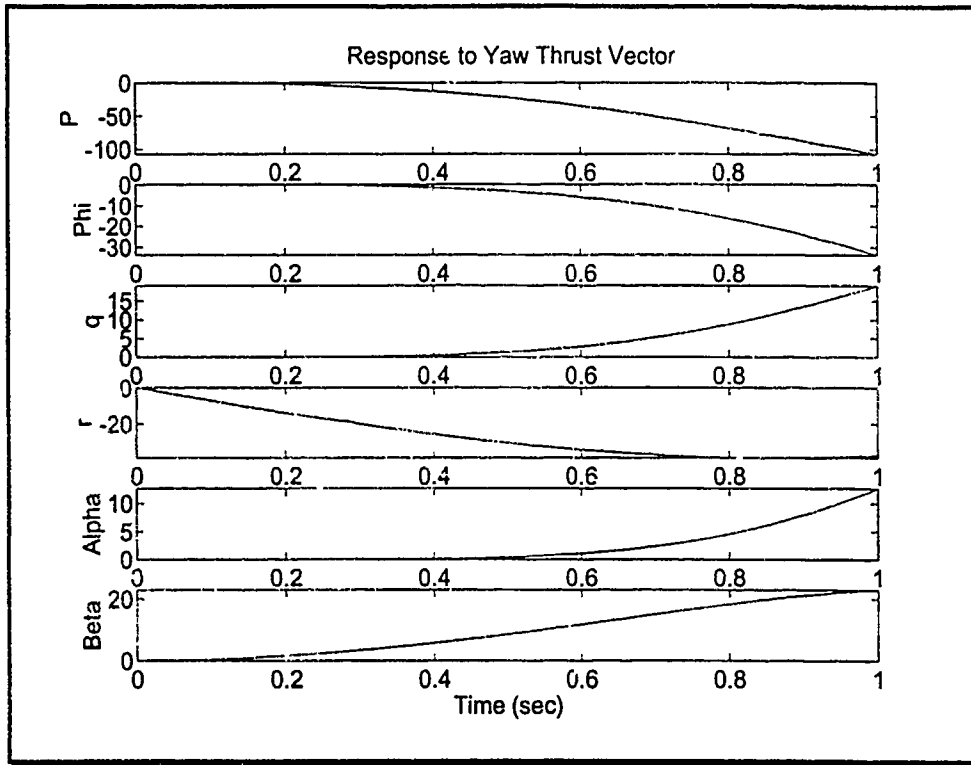
Figure 61. Response to Thrust Vectored Yaw Command, 6 DOF Model, 20 kft, Low AOA
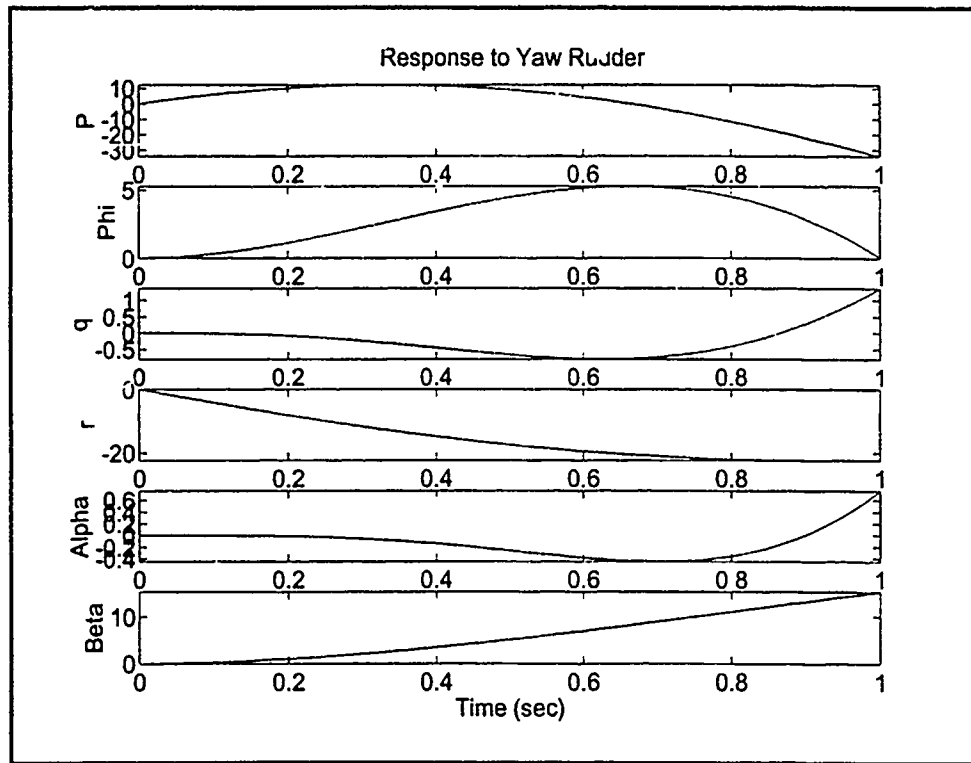
Figure 62. Response to Rudder Yaw Command, 6 DOF Model, 20 kft, Low AOA
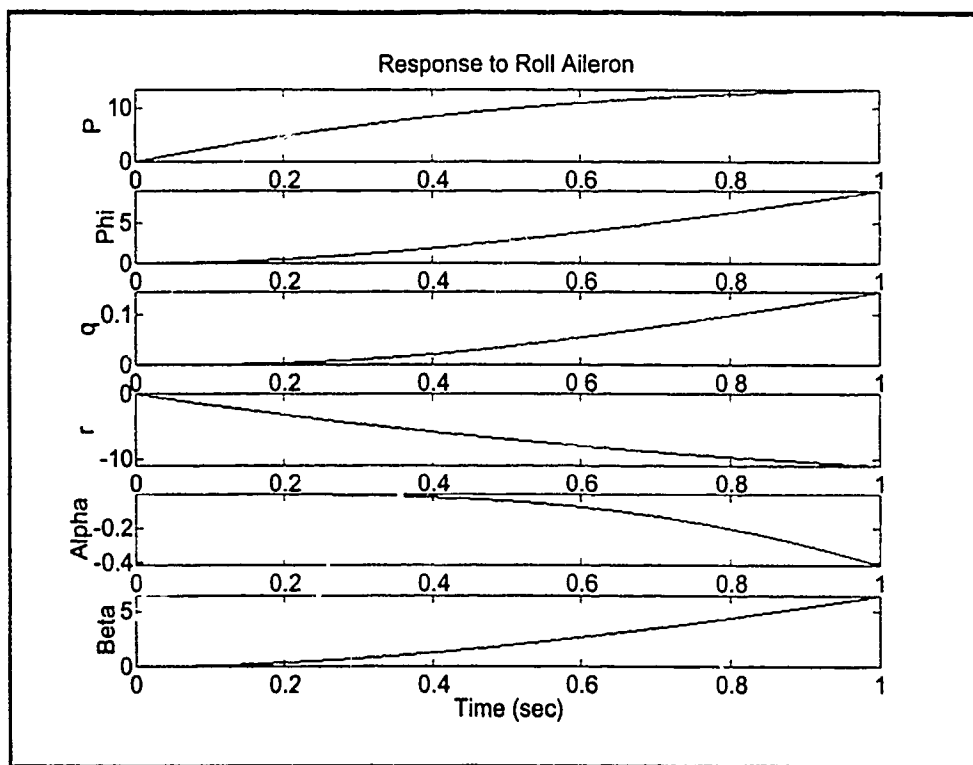
Figure 63. Response to Aileron Roll Command, 6 DOF Model, 10kft
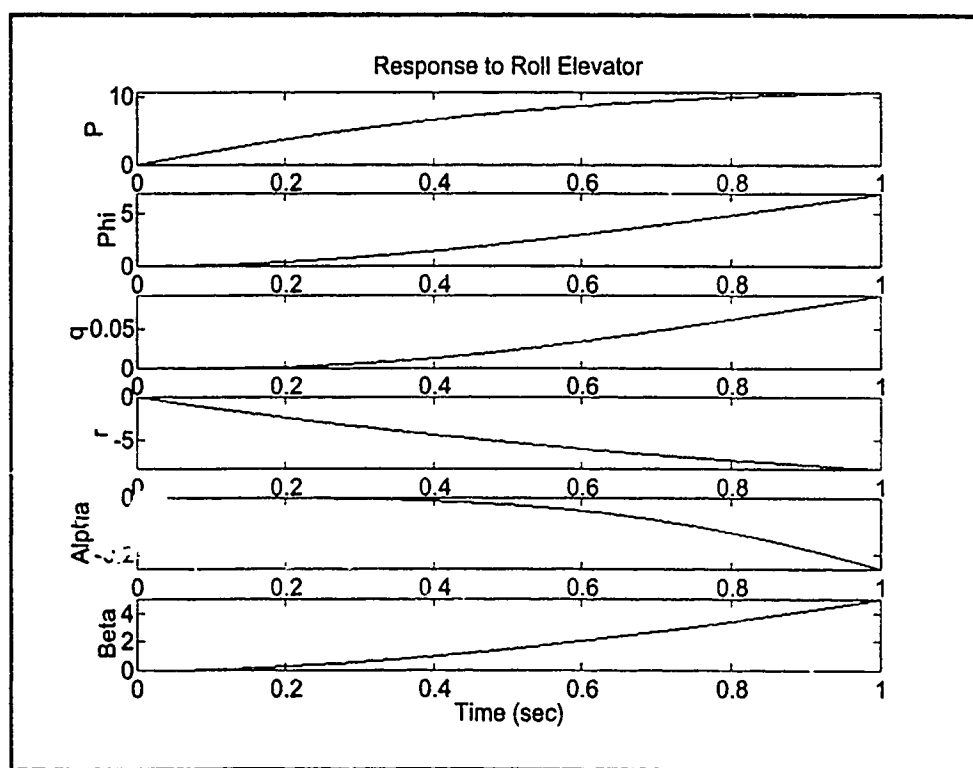
Figure 64. Response to Elevator Roll Command 6 DOF Model, 10kft

126
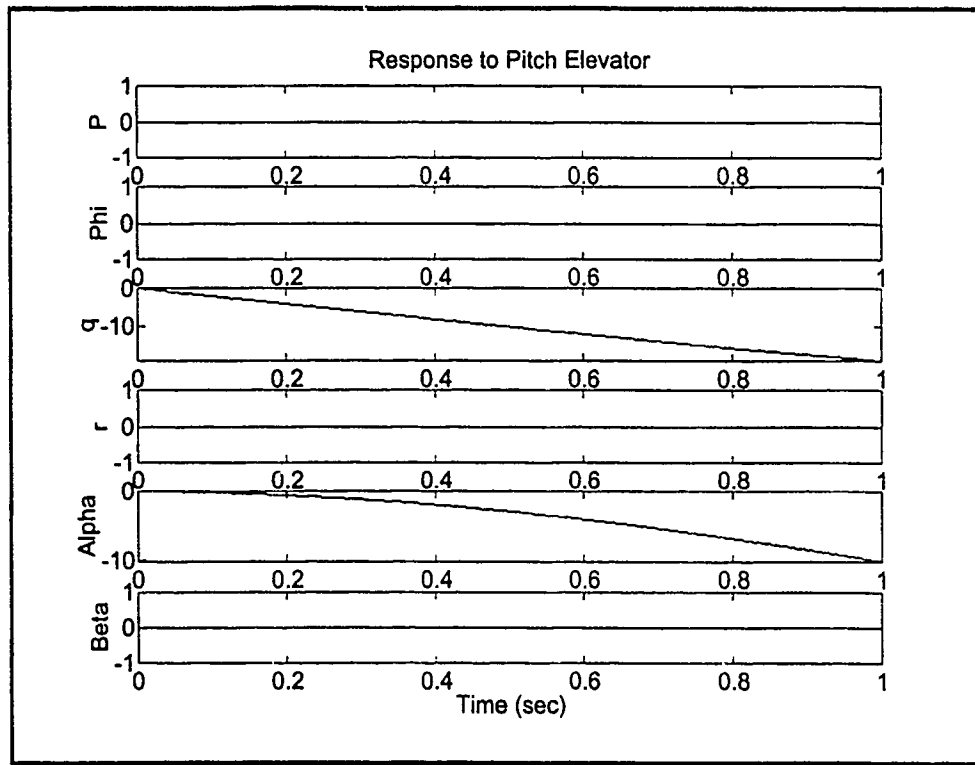
Figure 65. Response to Elevator Pitch Command, 6 DOF Model, 10kft
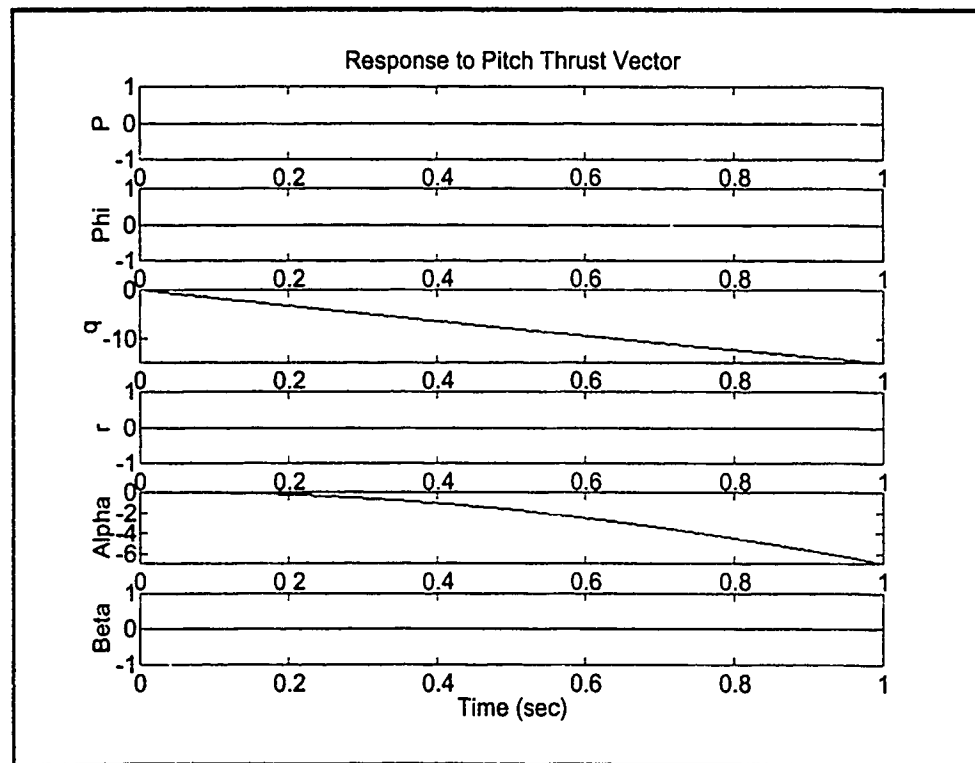
Figure 66. Response to Thrust Vectored Pitch Command, 6 DOF Model, 10kft

127
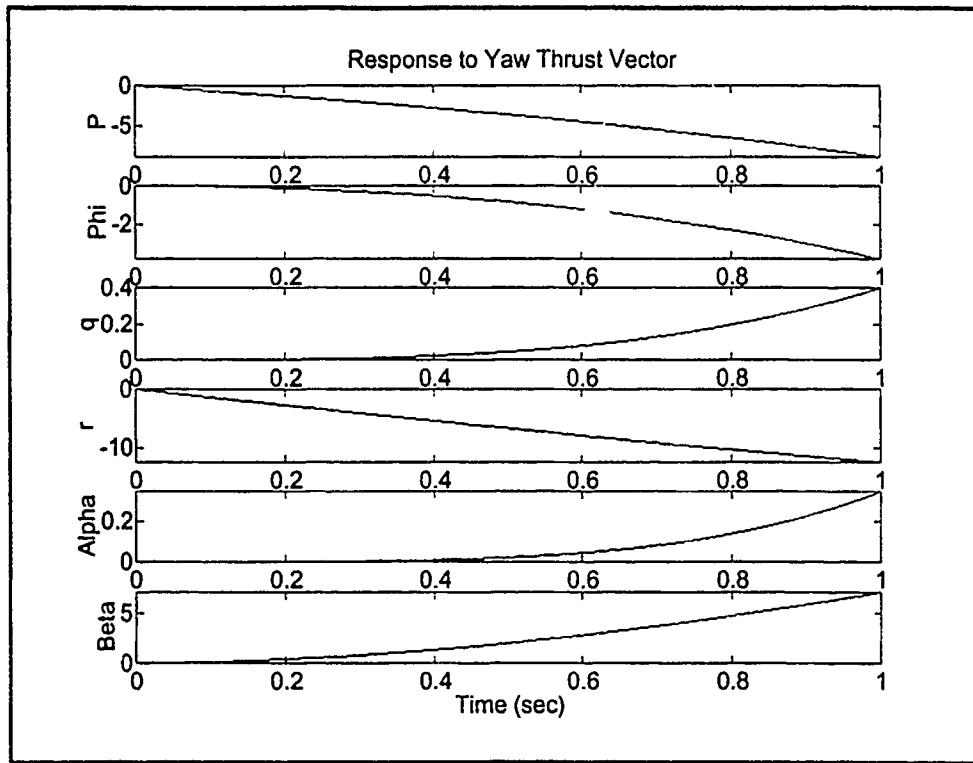
Figure 67. Response to Thrust Vectored Yaw Command, 6 DOF Model, 10kft
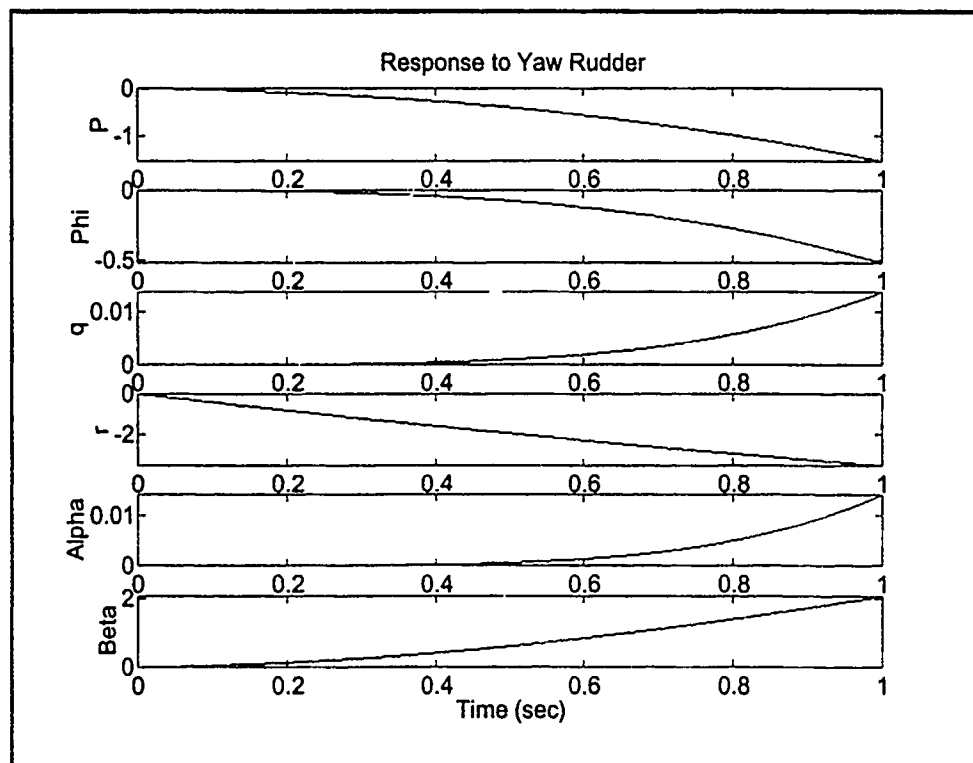
Figure 68. Response to Rudder Yaw Command, 6 DOF Model, 10kft

B.2. Six DOF Aircraft with Weighting Matrix Open-Loop Simulations

This section contains the simulations validating the weighting matrix. The weighting matrix is placed in front of the six DOF model control inputs (Fig. 69), and responses are obtained for all three control inputs (roll, pitch, and yaw) at 10,000 feet, thirty degrees AOA. Note, the actuator response characteristics are not included in these simulations.
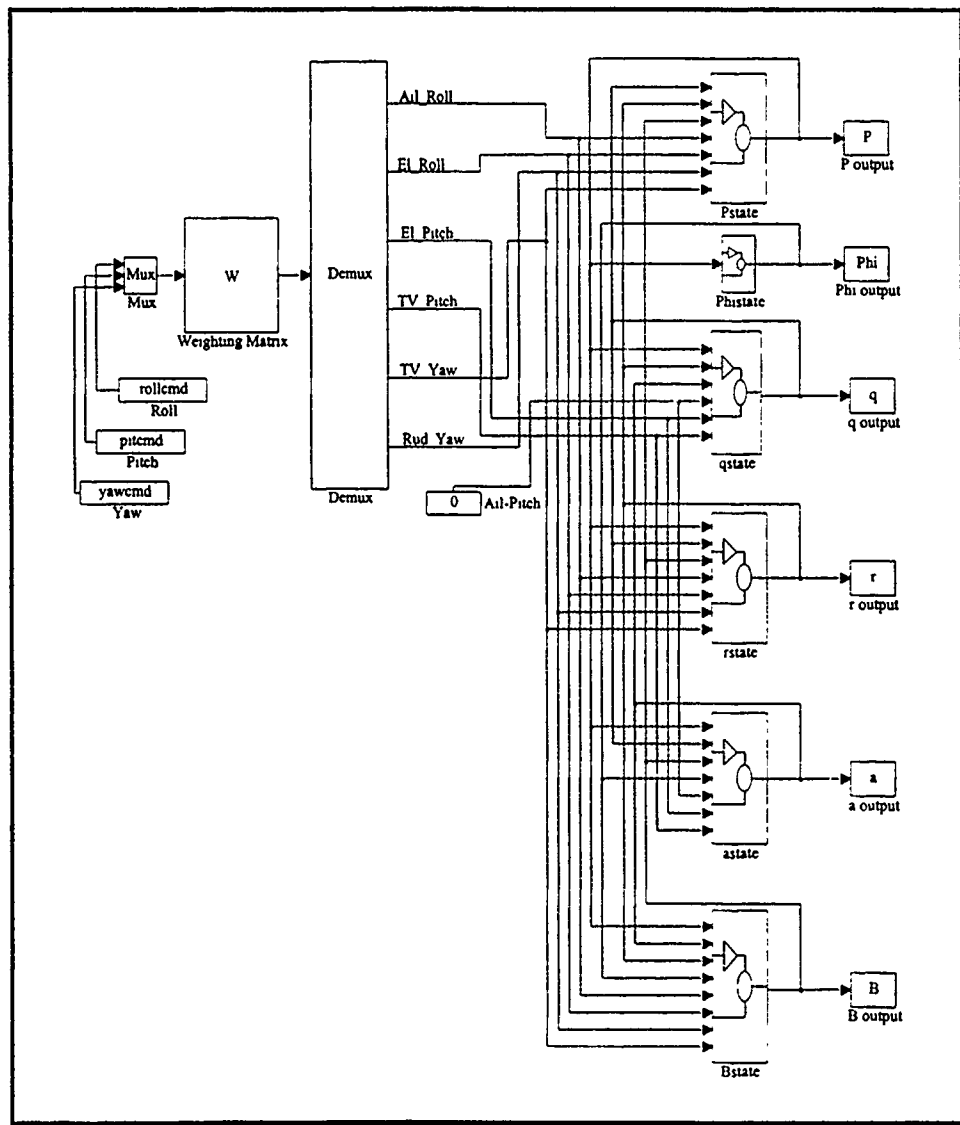
Figure 69. 6 DOF Model with Weighting Matrix
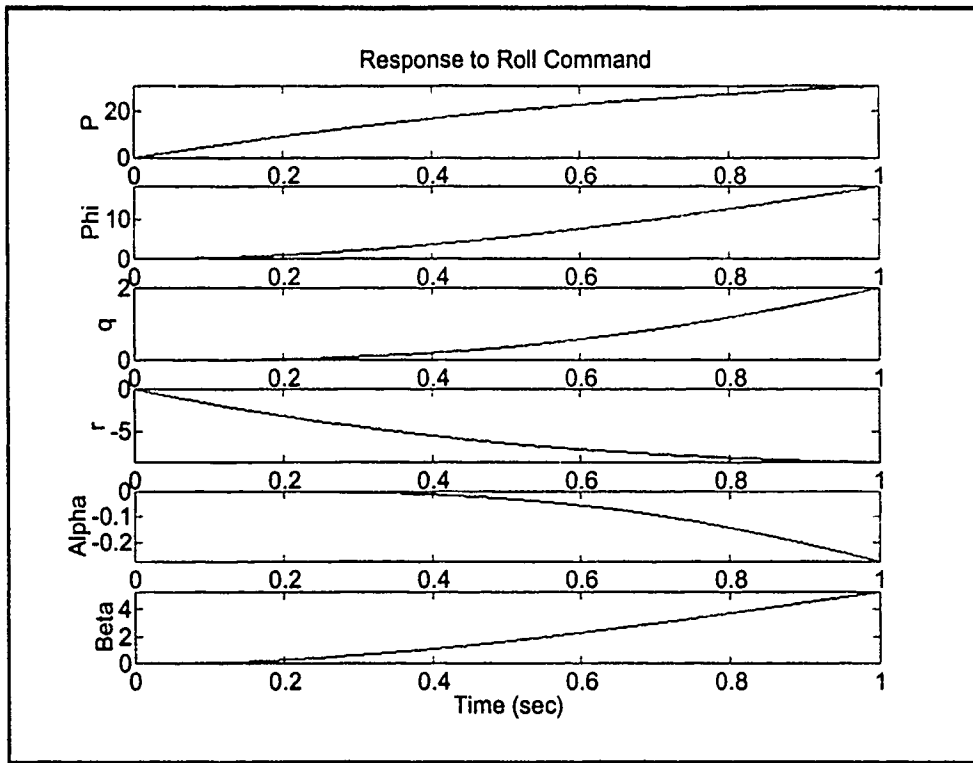
Figure 70. Response to Roll Command, 6 DOF Weighted Model, 10kft
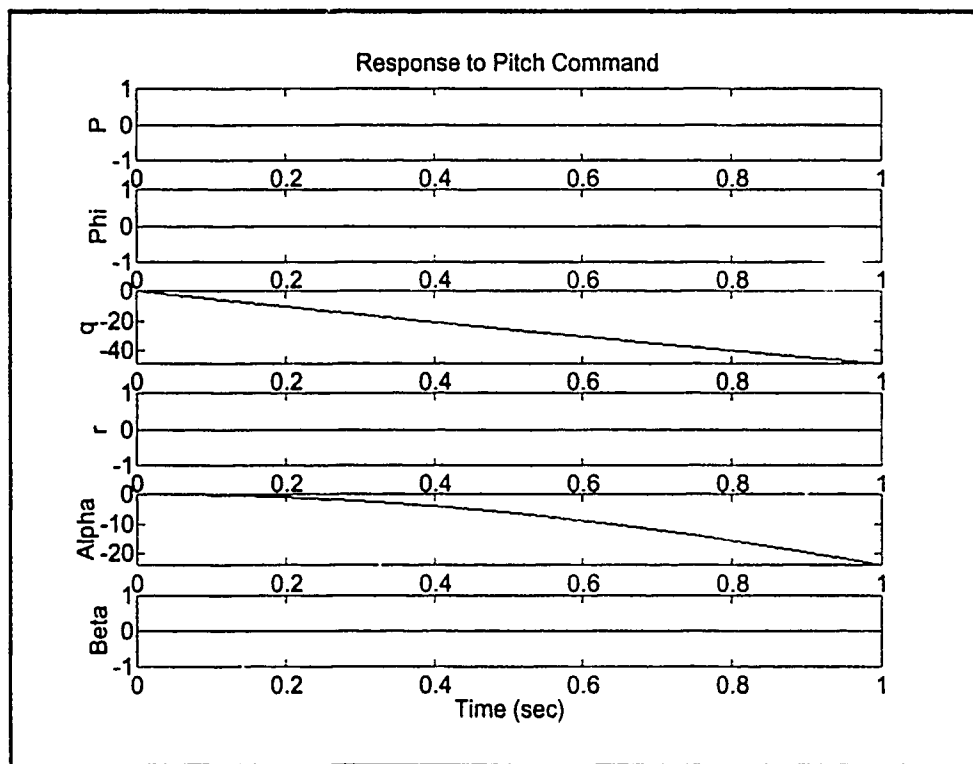
Figure 71. Response to Pitch Command, 6 DOF Weighted Model, 10kft
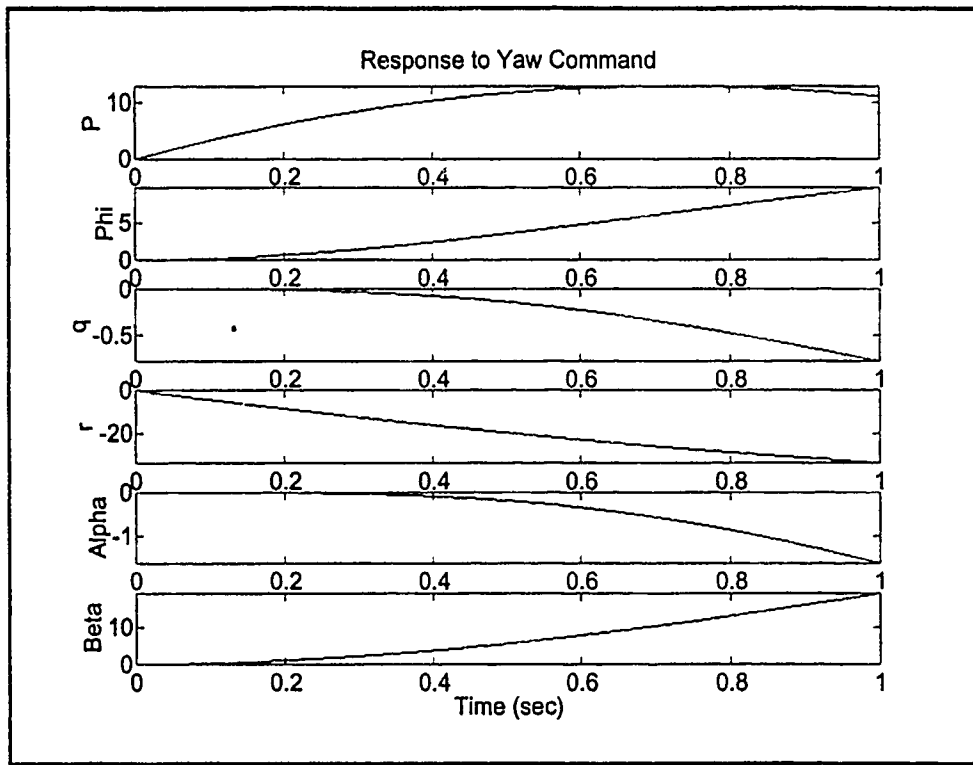
Figure 72. Response to Yaw Command, 6 DOF Weighted Model, 1υkft

B.3. Weighted QFT Models, Open-Loop Simulations

This section contains the simulations validating the QFT models. The weighting matrix has been incorporated into the QFT model by performing the matrix multiplication $\mathbf{B'} = \mathbf{B*W}$. The $\mathbf{B'}$ matrix is then used in the state-space block of the Simulink simulation in place of $\mathbf{B}$ (Fig. 73). Representative responses to each of the three command inputs (roll, pitch, yaw) are given for all four QFT models (Pparam = 0, 8, 16, 24) at 10,000 feet altitude. In addition, responses to a roll command with Pparam = 24 at 15,000 and 20,000 feet are included for further comparis   to the six DOF simulation results.
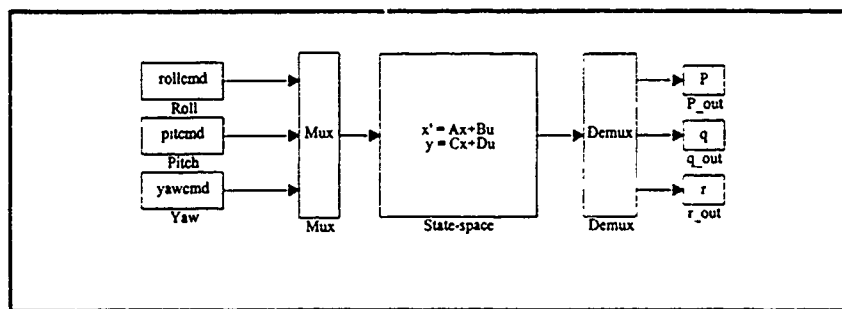
Figure 73. 3x3 QFT Linear Simulation Model

131
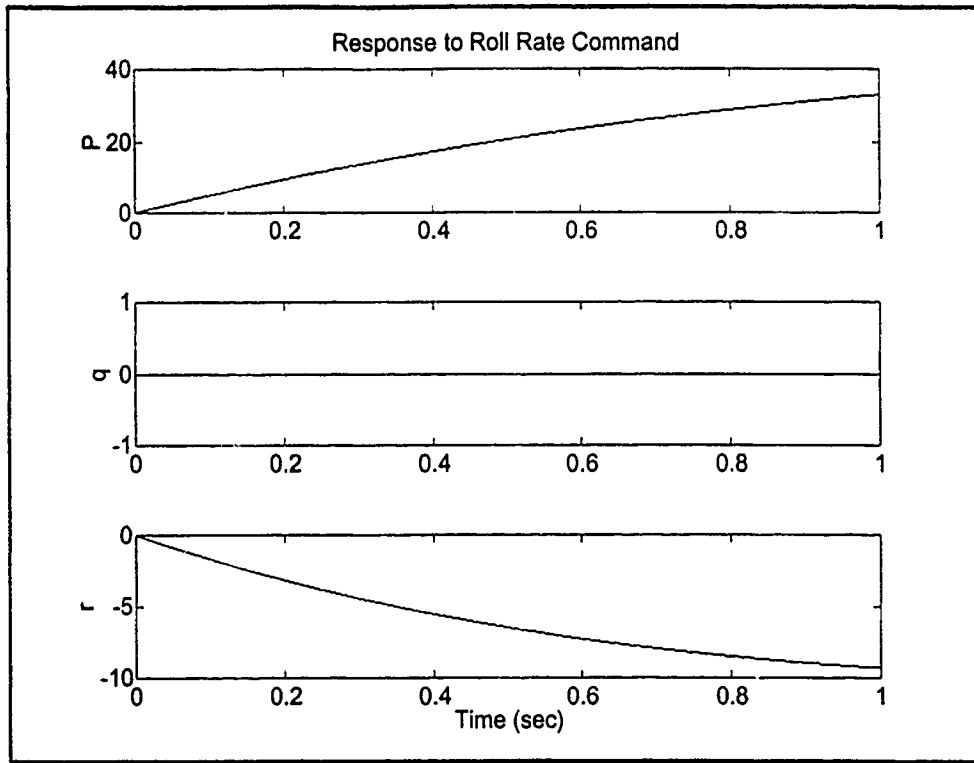
Figure 74. Response to Roll Command, Weighted QFT Model, Pparam=0, 10kft
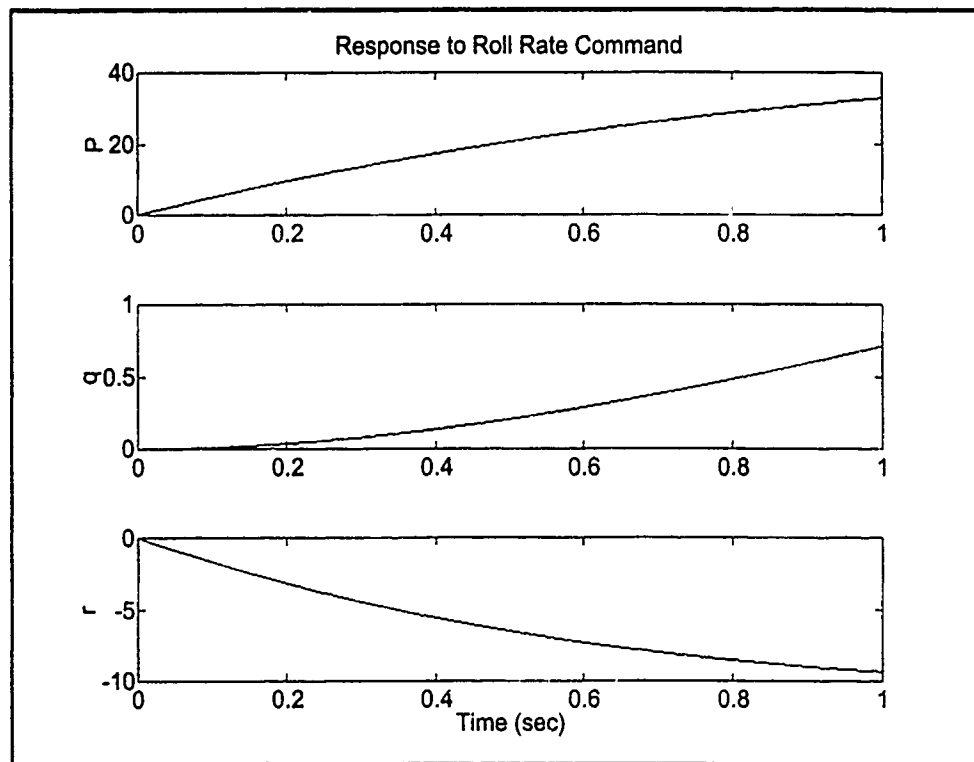
Figure 75. Response to Roll Command, Weighted QFT Model, Pparam=8, 10kft

132
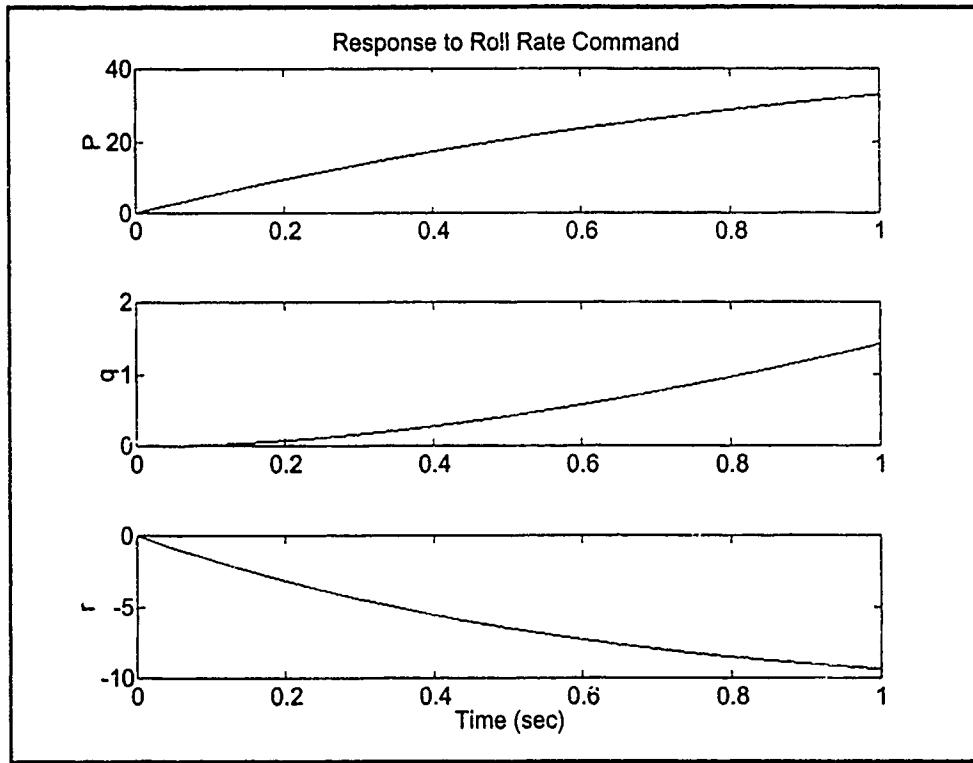
Figure 76. Response to Roll Command, Weighted QFT Model, Pparam=16, 10kft
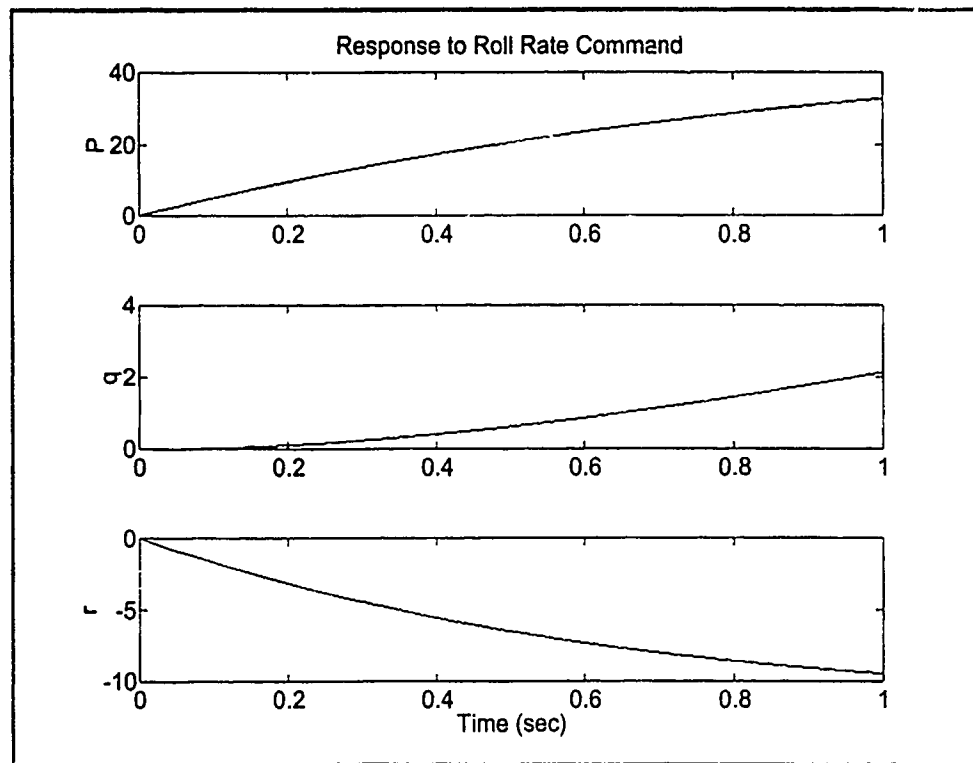
Figure 77. Response to Roll Command, Weighted QFT Model, Pparam=24, 10kft

133
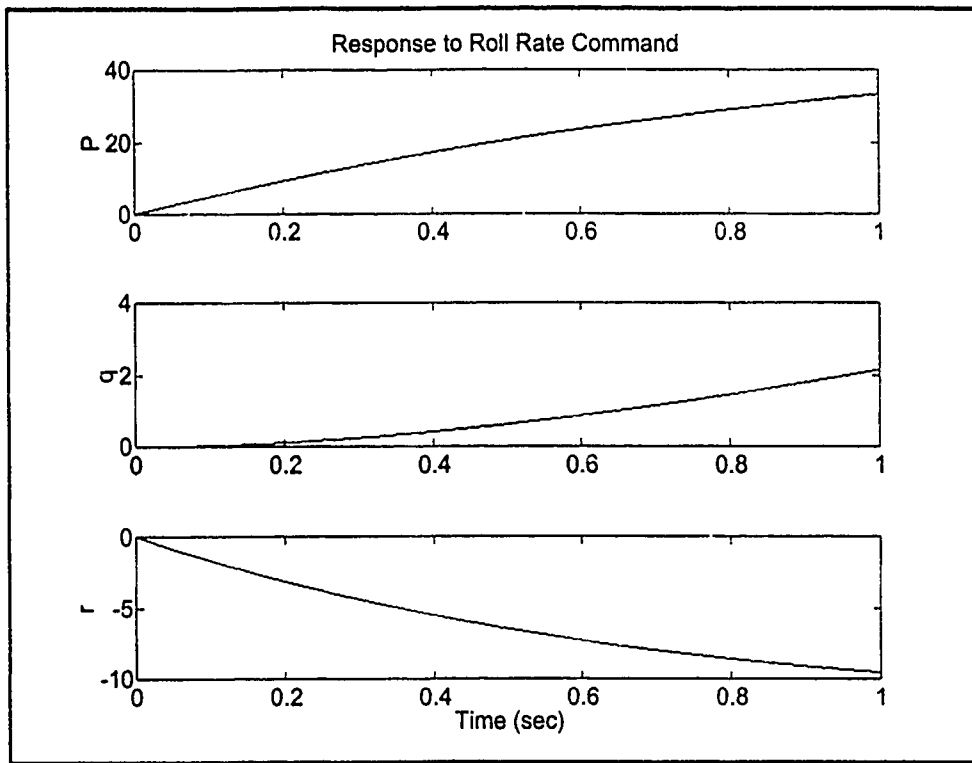
Figure 78. Response to Roll Command, Weighted QFT Model, Pparam=24, 15kft
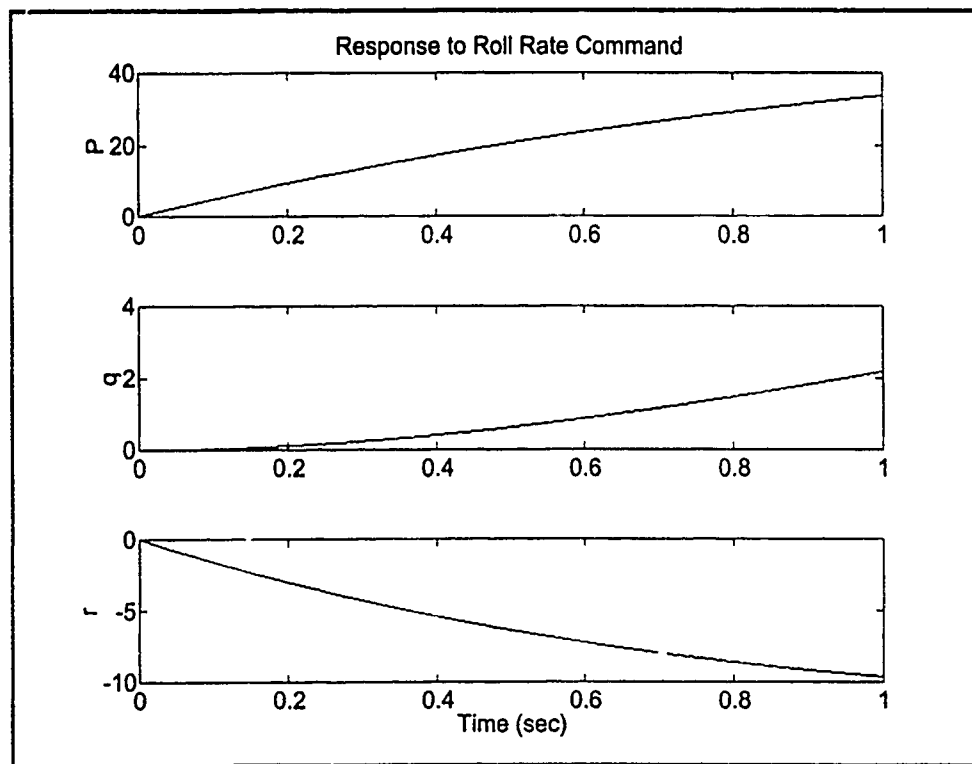
Figure 79. Response to Roll Command, Weighted QFT Model, Pparam=24, 20kft

Appendix C: Effective Plant Transfer Functions

This chapter presents the effective plant transfer functions for each of the twelve plant cases. The

twelve cases are defined in the MIMO QFT CAD Package as:

```
                    Current List of Plant Models

        Plant     Comments                   Parameter      Value
        -----     --------                   ---------      ----------
        #1                                   h              10000
                                             P              0

        #2                                   h              10000
                                             P              8

        #3                                   h              10000
                                             P              16

        #4                                   h              10000
                                             P              24

        #5                                   h              15000
                                             P              0

        #6                                   h              15000
                                             P              8

        #7                                   h              15000
                                             P              16

        #8                                   h              15000
                                             P              24

        #9                                   h              20000
                                             P              0

        #10                                  h              20000
                                             P              8

        #11                                  h              20000
                                             P              16

        #12                                  h              20000
                                             P              24
```

C.1. Effective Plants

Choice> 3 Effective Plant Pe s-Domain Transfer Functions

Plant Case: 1 Element: (1, 1)
```
        Roots of Numerator              Roots of Denominator
        -------------------             --------------------
        -0.1180659113                   -0.06617260399
        -13.1445853 + 15.92479066 I     -1.076648798
        -13.1445853 - 15.92479066 I     -13. + 15.19868415 I
        -15.73553132 + 42.03227768 I    -13. - 15.19868415 I
        -15.73553132 - 42.03227768 I    -14.924 + 33.19991301 I
        -49.65172678 + 52.15231675 I    -14.924 - 33.19991301 I
        -49.65172678 - 52.15231675 I    -44.25 + 60.55524337 I
        -55.27372311 + 83.79775981 I    -44.25 - 60.55524337 I
        -55.27372311 - 83.79775981 I    -49.68 + 52.11427444 I
                                        -49.68 - 52.11427444 I
                                        -62.127 + 85.0195617 I
                                        -62.127 - 85.0195617 I
        Factored form gain multiplier: 1157.161246
```

Plant Case: 1 Element: (1, 2)
```
        Roots of Numerator              Roots of Denominator
        -------------------             --------------------
        Factored form gain multiplier: 0
```

Plant Case: 1 Element: (1, 3)
```
        Roots of Numerator              Roots of Denominator
        -------------------             --------------------
        0.250583541                     -0.06617260399
        -12.76209141 + 13.81487535 I    -1.076648798
        -12.76209141 - 13.81487535 I    -13. + 15.19868415 I
        -15.27589594 + 39.8708367 I     -13. - 15.19868415 I
        -15.27589594 - 39.8708367 I     -14.924 + 33.19991301 I
        -49.72241744 + 52.05562842 I    -14.924 - 33.19991301 I
        -49.72241744 - 52.05562842 I    -44.25 + 60.55524337 I
        -56.7089719 + 84.15858497 I     -44.25 - 60.55524337 I
        -56.7089719 - 84.15858497 I     -49.68 + 52.11427444 I
                                        -49.68 - 52.11427444 I
                                        -62.127 + 85.0195617 I
                                        -62.127 - 85.0195617 I
        Factored form gain multiplier: 3197.602531
```

Plant Case: 1 Element: (2, 1)
```
        Roots of Numerator              Roots of Denominator
        -------------------             --------------------
        Factored form gain multiplier: 0
```

Plant Case: 1 Element: (2, 2)
```
        Roots of Numerator              Roots of Denominator
        -------------------             --------------------
        -14.76581091 + 21.99367018 I    -0.1485284702
        -14.76581091 - 21.99367018 I    -13. + 15.19868415 I
        -17.15376289 + 86.63948955 I    -13. - 15.19868415 I
        -17.15376289 - 86.63948955 I    -14.924 + 33.19991301 I
                                        -14.924 - 33.19991301 I
                                        -62.127 + 85.0195617 I
                                        -62.127 - 85.0195617 I
        Factored form gain multiplier: -204.4085555
```

Plant Case: 1 Element: (2, 3)
```
        Roots of Numerator              Roots of Denominator
        -------------------             --------------------
        Factored form gain multiplier: 0
```

Plant Case: 1 Element: (3, 1)
```
        Roots of Numerator              Roots of Denominator
        -------------------             --------------------
        0.2226635869                    -0.06617260399
        -12.40529826 + 11.65364509 I    -1.076648798
        -12.40529826 - 11.65364509 I    -13. + 15.19868415 I
        -15.00543659 + 42.44927428 I    -13. - 15.19868415 I
        -15.00543659 - 42.44927428 I    -14.924 + 33.19991301 I
        -50.55177141 + 50.69631972 I    -14.924 - 33.19991301 I
        -50.55177141 - 50.69631972 I    -44.25 + 60.55524337 I
        -54.36332547 + 83.74883311 I    -44.25 - 60.55524337 I
        -54.36332547 - 83.74883311 I    -49.68 + 52.11427444 I
```

```
                                             -49.68 - 52.11427444 I
                                             -62.127 + 85.0195617 I
                                             -6^.127 - 85.0195617 I
              Factored form gain multiplier: -624.8642066

Plant Case: 1  Element: (3, 2)
              Roots of Numerator              Roots of Denominator
              -------------------             --------------------
              Factored form gain multiplier: 0

Plant Case: 1  Element: (3, 3)
              Roots of Numerator              Roots of Denominator
              -------------------             --------------------
              -0.57779199                     -0.06617260399
              -13.80372315 + 18.55693714 I    -1.076648798
              -13.80372315 - 18.55693714 I    -13. + 15.19868415 I
              -15.94702152 + 39.43184289 I    -13. - 15.19868415 I
              -15.94702152 - 39.43184289 I    -14.924 + 33.19991301 I
              -48.71359453 + 53.64893544 I    -14.924 - 33.19991301 I
              -48.71359453 - 53.64893544 I    -44.25 + 60.55524337 I
              -57.64123437 + 84.21130541 I    -44.25 - 60.55524337 I
              -57.64123437 - 84.21130541 I    -49.68 + 52.11427444 I
                                              -49.68 - 52.11427444 I
                                              -62.127 + 85.0195617 I
                                              -62.127 - 85.0195617 I
              Factored form gain multiplier: -2579.738509

Plant Case: 2  Element: (1, 1)
              Roots of Numerator              Roots of Denominator
              -------------------             --------------------
              -0.1333221792 + 0.07425268253 I -0.1080975896 + 0.07658317 I
              -0.1333221792 - 0.07425268253 I -0.1080975896 - 0.07658317 I
              -13.14455974 + 15.92480228 I    -1.075154693
              -13.14455974 - 15.92480228 I    -13. + 15.19868415 I
              -15.73553272 + 42.03227784 I    -13. - 15.19868415 I
              -15.73553272 - 42.03227784 I    -14.924 + 33.19991301 I
              -49.65172585 + 52.15231623 I    -14.924 - 33.19991301 I
              -49.65172585 - 52.15231623 I    -44.25 + 60.55524337 I
              -55.27372321 + 83.79776009 I    -44.25 - 60.55524337 I
              -55.27372321 - 83.79776009 I    -49.68 + 52.11427444 I
                                              -49.68 - 52.11427444 I
                                              -62.127 + 85.0195617 I
                                              -62.127 - 85.0195617 I
              Factored form gain multiplier: 1157.161246

Plant Case: 2  Element: (1, 2)
              Roots of Numerator              Roots of Denominator
              -------------------             --------------------
              -0.5230351441                   -0.1080975896 + 0.07658317 I
              -14.76581091 + 21.99367018 I    -0.1080975896 - 0.07658317 I
              -14.76581091 - 21.99367018 I    -1.075154693
              -17.15376289 + 86.63948955 I    -13. + 15.19868415 I
              -17.15376289 - 86.63948955 I    -13. - 15.19868415 I
              -1.690230139e13                 -14.924 + 33.19991301 I
                                              -14.924 - 33.19991301 I
                                              -62.127 + 85.0195617 I
                                              -62.127 - 85.0195617 I

                                          -12
              Factored form gain multiplier: 1.09000372 10

Plant Case: 2  Element: (1, 3)
              Roots of Numerator              Roots of Denominator
              -------------------             --------------------
              0.2213005055                    -0.1080975896 + 0.07658317 I
              -0.1191011217                   -0.1080975896 - 0.07658317 I
              -12.76216403 + 13.81485561 I    -1.075154693
              -12.76216403 - 13.81485561 I    -13. + 15.19868415 I
              -15.27589417 + 39.87083626 I    -13. - 15.19868415 I
              -15.27589417 - 39.87083626 I    -14.924 + 33.19991301 I
              -49.72241888 + 52.05562921 I    -14.924 - 33.19991301 I
              -49.72241888 - 52.05562921 I    -44.25 + 60.55524337 I
              -56.70897176 + 84.15858459 I    -44.25 - 60.55524337 I
              -56.70897176 - 84.15858459 I    -49.68 + 52.11427444 I
                                              -49.69 - 52.11427444 I
                                              -62.127 + 85.0195617 I
                                              -62.127 - 85.0195617 I
              Factored form gain multiplier: 3197.602531
```

Plant Case: 2 Element: {2, 1}
```
        Roots of Numerator               Roots of Denominator
        -------------------               --------------------
        -0.3354757393                    -0.1080975896 + 0.07658317 I
        -14.24297905 + 20.50922195 I     -0.1080975896 - 0.07658317 I
        -14.24297905 - 20.50922195 I     -1.075154693
        -16.83484837 + 41.10016652 I     -13. + 15.19868415 I
        -16.83484837 - 41.10016652 I     -13. - 15.19868415 I
        -48.22212047 + 54.32054519 I     -14.924 + 33.19991301 I
        -48.22212047 - 54.32054519 I     -14.924 - 33.19991301 I
        -56.74455107 + 83.92480943 I     -44.25 + 60.55524337 I
        -56.74455107 - 83.92480943 I     -44.25 - 60.55524337 I
        -2.717886681e12                  -49.68 + 52.11427444 I
                                         -49.68 - 52.11427444 I
                                         -62.127 + 85.0195617 I
                                         -62.127 - 85.0195617 I
```
Factored form gain multiplier: $1.0315126 \ 10^{-11}$

Plant Case: 2 Element: {2, 2}
```
        Roots of Numerator               Roots of Denominator
        -------------------               --------------------
        -0.06617260399                   -0.1080975896 + 0.07658317 I
        -1.076648798                     -0.1080975896 - 0.07658317 I
        -14.76581091 + 21.99367018 I     -1.075154693
        -14.76581091 - 21.99367018 I     -13. + 15.19868415 I
        -17.15376289 + 86.63948955 I     -13. - 15.19868415 I
        -17.15376289 - 86.63948955 I     -14.924 + 33.19991301 I
                                         -14.924 - 33.19991301 I
                                         -62.127 + 85.0195617 I
                                         -62.127 - 85.0195617 I
```
Factored form gain multiplier: -204.4085555

Plant Case: 2 Element: {2, 3}
```
        Roots of Numerator               Roots of Denominator
        -------------------               --------------------
        37.97965347                      -0.1080975896 + 0.07658317 I
        -2.538773868                     -0.1080975896 - 0.07658317 I
        -12.66342271 + 39.983698 I       -1.075154693
        -12.66342271 - 39.983698 I       -13. + 15.19868415 I
        -36.51975006                     -13. - 15.19868415 I
        -52.4476482 + 84.09578587 I      -14.924 + 33.19991301 I
        -52.4476482 - 84.09578587 I      -14.924 - 33.19991301 I
        -54.02567326 + 42.30252203 I     -44.25 + 60.55524337 I
        -54.02567326 - 42.80252203 I     -44.25 - 60.55524337 I
        -1.260164292e12                  -49.68 + 52.11427444 I
                                         -49.68 - 52.11427444 I
                                         -62.127 + 85.0195617 I
                                         -62.127 - 85.0195617 I
```
Factored form gain multiplier: $1.8266564 \ 10^{-11}$

Plant Case: 2 Element: {3, 1}
```
        Roots of Numerator               Roots of Denominator
        -------------------               --------------------
        0.1779069697                     -0.1080975896 + 0.07658317 I
        -0.1035524666                    -0.1080975896 - 0.07658317 I
        -12.40540876 + 11.65363828 I     -1.075154693
        -12.40540876 - 11.65363828 I     -13. + 15.19868415 I
        -15.00543422 + 42.44927371 I     -13. - 15.19868415 I
        -15.00543422 - 42.44927371 I     -14.924 + 33.19991301 I
        -50.55177317 + 50.69632077 I     -14.924 - 33.19991301 I
        -50.55177317 - 50.69632077 I     -44.25 + 60.55524337 I
        -54.36332527 + 83.7488326 I      -44.25 - 60.55524337 I
        -54.36332527 - 83.7488326 I      -49.68 + 52.11427444 I
                                         -49.68 - 52.11427444 I
                                         -62.127 + 85.0195617 I
                                         -62.127 - 85.0195617 I
```
Factored form gain multiplier: -624.8642066

Plant Case: 2 Element: {3, 2}
```
        Roots of Numerator               Roots of Denominator
        -------------------               --------------------
        -1.485201811                     -0.1080975896 + 0.07658317 I
        -14.76581091 + 21.99367018 I     -0.1080975896 - 0.07658317 I
```

138

```
       -14.76581091 - 21.99367018 I      -1.075154693
       -17.15376289 + 86.63948955 I      -13. + 15.19868415 I
       -17.15376289 - 86.63948955 I      -13. - 15.19868415 I
       -9.829231029e12                   -14.924 + 33.19991301 I
                                         -14.924 - 33.19991301 I
                                         -62.127 + 85.0195617 I
                                         -62.127 - 85.0195617 I

                                            -12
       Factored form gain multiplier: 1.210876964 10

Plant Case: 2  Element: {3, 3}
       Roots of Numerator                Roots of Denominator
       ------------------                --------------------
       -0.1681583335                     -0.1080975896 + 0.07658317 I
       -0.5582181348                     -0.1080975896 - 0 07658317 I
       -13.80369432 + 18.55695501 I      -1.075154693
       -13.80369432 - 18.55695501 I      -13. + 15.19868415 I
       -15.94702363 + 39.43184308 I      -13. - 15.19868415 I
       -15.94702363 - 39.43184308 I      -14.924 + 33.19991301 I
       -48.71359314 + 53.64893471 I      -14.924 - 33.19991301 I
       -48.71359314 - 53.64893471 I      -44.25 + 60.55524337 I
       -57.64123449 + 84.21130579 I      -44.25 - 60.55524337 I
       -57.64123449 - 84.21130579 I      -49.68 + 52.11427444 I
                                         -49.68 - 52.11427444 I
                                         -62.127 + 85.0195617 I
                                         -62.127 - 85.0195617 I
       Factored form gain multiplier: -2579.738509

Plant Case: 3  Element: {1, 1}
       Roots of Numerator                Roots of Denominator
       ------------------                --------------------
       -0.1333971474 + 0.1508305649 I    -0.1102810409 + 0.1693450017 I
       -0.1333971474 - 0.1508305649 I     0.1102810409 - 0.1693450017 I
       -13.14448306 + 15.92483713 I      -1.07078779
       -13.14448306 - 15.92483713 I      -13. + 15.19868415 I
       -15.7355369 + 42.0322783 I        -13. - 15.19868415 I
       -15.7355369 - 42.0322783 I        -14.924 + 33.19991301 I
       -49.65172307 + 52.15231468 I      -14.924 - 33.19991301 I
       -49.65172307 - 52.15231468 I      -44.25 + 60.55524337 I
       -55.27372352 + 83.79776093 I      -44.25 - 60.55524337 I
       -55.27372352 - 83.79776093 I      -49.68 + 52.11427444 I
                                         -49.68 - 52.11427444 I
                                         -62.127 + 85.0195617 I
                                         -62.127 - 85.0195617 I
       Factored form gain multiplier: 1157.161246

Plant Case: 3  Element: {1, 2}
       Roots of Numerator                Roots of Denominator
       ------------------                --------------------
       4.245414924e14                    -0.1102810409 + 0.1693450017 I
       -0.5230351441                     -0.1102810409 - 0.1693450017 I
       -14.76581091 + 21.99367018 I      -1.07078779
       -14.76581091 - 21.99367018 I      -13. + 15.19868415 I
       -17.15376289 + 86.63948955 I      -13. - 15.19868415 I
       -17.15376289 - 86.63948955 I      -14.924 + 33.19991301 I
                                         -14.924 - 33.19991301 I
                                         -62.127 + 85.0195617 I
                                         -62.127 - 85.0195617 I

                                            -14
       Factored form gain multiplier: -8.679279517 10

Plant Case: 3  Element: {1, 3}
       Roots of Numerator                Roots of Denominator
       ------------------                --------------------
       0.05131616753 + 0.05994986898 I   -0.1102810409 + 0.1693450017 I
       0.05131616753 - 0.05994986898 I   -0.1102810409 - 0.1693450017 I
       -12.76238192 + 13.81479643 I      -1.07078779
       -12.76238192 - 13.81479643 I      -13. + 15.19868415 I
       -15.27588884 + 39.87083494 I      -13. - 15.19868415 I
       -15.27588884 - 39.87083494 I      -14.924 + 33.19991301 I
       -49.72242321 + 52.05563157 I      -14.924 - 33.19991301 I
       -49.72242321 - 52.05563157 I      -44.25 + 60.55524337 I
       -56.70897135 + 84.15858347 I      -44.25 - 60.55524337 I
       -56.70897135 - 84.15858347 I      -49.68 + 52.11427444 I
                                         -49.68 - 52.11427444 I
                                         -62.127 + 85.0195617 I
```

139

-62.127 - 85.0195617 I
            Factored form gain multiplier: 3197.602531

Plant Case: 3 Element: (2, 1)
            Roots of Numerator   Roots of Denominator
            ------------------   --------------------
            6.151289702e12   -0.1102810409 + 0.1693450017 I
            -0.3354757393   -0.1102810409 - 0.1693450017 I
            -14.24297905 + 20.50922195 I   -1.07078779
            -14.24297905 - 20.50922195 I   -13. + 15.19868415 I
            -16.83484837 + 41.10016652 I   -13. - 15.19868415 I
            -16.83484837 - 41.10016652 I   -14.924 + 33.19991301 I
            -48.22212047 + 54.32054519 I   -14.924 - 33.19991301 I
            -48.22212047 - 54.32054519 I   -44.25 + 60.55524337 I
            -56.74455107 + 83.92480943 I   -44.25 - 60.55524337 I
            -56.74455107 - 83.92480943 I   -49.68 + 52.11427444 I
                                               -49.68 - 52.11427444 I
                                               -62.127 + 85.0195617 I
                                               -62.127 - 85.0195617 I
                                                     -12
            Factored form gain multiplier: -9.11527336 10

Plant Case: 3 Element: (2, 2)
            Roots of Numerator   Roots of Denominator
            ------------------   --------------------
            -0.06617260399   -0.1102810409 + 0.1693450017 I
            -1.076648798   -0.1102810409 - 0.1693450017 I
            -14.76581091 + 21.99367018 I   -1.07078779
            -14.76581091 - 21.99367018 I   -13. + 15.19868415 I
            -17.15376289 + 86.63948955 I   -13. - 15.19868415 I
            -17.15376289 - 86.63948955 I   -14.924 + 33.19991301 I
                                               -14.924 - 33.19991301 I
                                               -62.127 + 85.0195617 I
                                               -62.127 - 85.0195617 I
            Factored form gain multiplier: -204.4085555

Plant Case: 3 Element: (2, 3)
            Roots of Numerator   Roots of Denominator
            ------------------   --------------------
            2.315106326e12   -0.1102810409 + 0.1693450017 I
            37.97965347   -0.1102810409 - 0.1693450017 I
            -2.538773868   -1.07078779
            -12.66342271 + 39.983698 I   -13. + 15.19868415 I
            -12.66342271 - 39.983698 I   -13. - 15.19868415 I
            -36.51975006   -14.924 + 33.19991301 I
            -52.4476482 + 84.09578587 I   -14.924 - 33.19991301 I
            -52.4476482 - 84.09578587 I   -44.25 + 60.55524337 I
            -54.02567326 + 42.80252203 I   -44.25 - 60.55524337 I
            -54.02567326 - 42.80252203 I   -49.68 + 52.11427444 I
                                               -49.68 - 52.11427444 I
                                               -62.127 + 85.0195617 I
                                               -62.127 - 85.0195617 I
                                                     -11
            Factored form gain multiplier: -1.988580086 10

Plant Case: 3 Element: (3, 1)
            Roots of Numerator   Roots of Denominator
            ------------------   --------------------
            0.03750631916 + 0.155294993 I   -0.1102810409 + 0.1693450017 I
            0.03750631916 - 0.155294993 I   -0.1102810409 - 0.1693450017 I
            -12.40574026 + 11.65361791 I   -1.07078779
            -12.40574026 - 11.65361791 I   -13. + 15.19868415 I
            -15.0054271 + 42.44927198 I   -13. - 15.19868415 I
            -15.0054271 - 42.44927198 I   -14.924 + 33.19991301 I
            -50.55177845 + 50.69632392 I   -14.924 - 33.19991301 I
            -50.55177845 - 50.69632392 I   -44.25 + 60.55524337 I
            -54.36332468 + 83.74883107 I   -44.25 - 60.55524337 I
            -54.36332468 - 83.74883107 I   -49.68 + 52.11427444 I
                                               -49.68 - 52.11427444 I
                                               -62.127 + 85.0195617 I
                                               -62.127 - 85.0195617 I
            Factored form gain multiplier: -624.8642066

140

Plant Case: 3 Element: (3, 2)

Roots of Numerator	Roots of Denominator
-1.485201811	-0.1102810409 + 0.1693450017 I
-14.76581091 + 21.99367018 I	-0.1102810409 - 0.1693450017 I
-14.76581091 - 21.99367018 I	-1.07078779
-17.15376289 + 86.63948955 I	-13. + 15.19868415 I
-17.15376289 - 86.63948955 I	-13. - 15.19868415 I
-2.427762003e13	-14.924 + 33.19991301 I
	-14.924 - 33.19991301 I
	-62.127 + 85.0195617 I
	-62.127 - 85.0195617 I

Factored form gain multiplier: 9.804906259 10^{-13}

Plant Case: 3 Element: (3, 3)

Roots of Numerator	Roots of Denominator
-0.2451779596	-0.1102810409 + 0.1693450017 I
-0.4813665423	-0.1102810409 - 0.1693450017 I
-13.80360782 + 18.55700864 I	-1.07078779
-13.80360782 - 18.55700864 I	-13. + 15.19868415 I
-15.94702994 + 39.43184365 I	-13. - 15.19868415 I
-15.94702994 - 39.43184365 I	-14.924 + 33.19991301 I
-48.71358895 + 53.64893255 I	-14.924 - 33.19991301 I
-48.71358895 - 53.64893255 I	-44.25 + 60.55524337 I
-57.64123484 + 84.21130695 I	-44.25 - 60.55524337 I
-57.64123484 - 84.21130695 I	-49.68 + 52.11427444 I
	-49.68 - 52.11427444 I
	-62.127 + 85.0195617 I
	-62.127 - 85.0195617 I

Factored form gain multiplier: -2579.738509

Plant Case: 4 Element: (1, 1)

Roots of Numerator	Roots of Denominator
-0.133522104 + 0.226886148 I	-0.1137334365 + 0.2590698828 I
-0.133522104 - 0.226886148 I	-0.1137334365 - 0.2590698828 I
-13.14435526 + 15.92489521 I	-1.063882999
-13.14435526 - 15.92489521 I	-13. + 15.19868415 I
-15.73554388 + 42.03227907 I	-13. - 15.19868415 I
-15.73554388 - 42.03227907 I	-14.924 + 33.19991301 I
-49.65171843 + 52.15231208 I	-14.924 - 33.19991301 I
-49.65171843 - 52.15231208 I	-44.25 + 60.55524337 I
-55.27372402 + 83.79776234 I	-44.25 - 60.55524337 I
-55.27372402 - 83.79776234 I	-49.68 + 52.11427444 I
	-49.68 - 52.11427444 I
	-62.127 + 85.0195617 I
	-62.127 - 85.0195617 I

Factored form gain multiplier: 1157.161246

Plant Case: 4 Element: (1, 2)

Roots of Numerator	Roots of Denominator
8.878894811e13	-0.1137334365 + 0.2590698828 I
-0.5230351441	-0.1137334365 - 0.2590698828 I
-14.76581091 + 21.99367018 I	-1.063882999
-14.76581091 - 21.99367018 I	-13. + 15.19868415 I
-17.15376289 + 86.63948955 I	-13. - 15.19868415 I
-17.15376289 - 86.63948955 I	-14.924 + 33.19991301 I
	-14.924 - 33.19991301 I
	-62.127 + 85.0195617 I
	-62.127 - 85.0195617 I

Factored form gain multiplier: -6.224954272 10^{-13}

Plant Case: 4 Element: (1, 3)

Roots of Numerator	Roots of Denominator
0.05167697995 + 0.2405466283 I	-0.1137334365 + 0.2590698828 I
0.05167697995 - 0.2405466283 I	-0.1137334365 - 0.2590698828 I
-12.76274509 + 13.81469789 I	-1.063882999
-12.76274509 - 13.81469789 I	-13. + 15.19868415 I
-15.27587997 + 39.87083275 I	-13. - 15.19868415 I
-15.27587997 - 39.87083275 I	-14.924 + 33.19991301 I

141

```
            -49.72243041 + 52.05563551 I        -14.924 - 33.19991301 I
            -49.72243041 - 52.05563551 I        -44.25 + 60.55524337 I
            -56.70897067 + 84.1585816 I         -44.25 - 60.55524337 I
            -56.70897067 - 84.1585816 I         -49.68 + 52.11427444 I
                                                -49.68 - 52.11427444 I
                                                -62.127 + 85.0195617 I
                                                -62.127 - 85.0195617 I
            Factored form gain multiplier: 3197.602531

Plant Case: 4  Element: (2, 1)
            Roots of Numerator                  Roots of Denominator
            -------------------                 --------------------
            1.751624825e13                      -0.1137334365 + 0.2590698828 I
            -0.3354757393                       -0.1137334365 - 0.2590698828 I
            -14.24297905 + 20.50922195 I        -1.063882999
            -14.24297905 - 20.50922195 I        -13. + 15.19868415 I
            -16.83484837 + 41.10016652 I        -13. - 15.19868415 I
            -16.83484837 - 41.10016652 I        -14.924 + 33.19991301 I
            -48.22212047 + 54.32054519 I        -14.924 - 33.19991301 I
            -48.22212047 - 54.32054519 I        -44.25 + 60.55524337 I
            -56.74455107 + 83.92480943 I        -44.25 - 60.55524337 I
            -56.74455107 - 83.92480943 I        -49.68 + 52.11427444 I
                                                -49.68 - 52.11427444 I
                                                -62.127 + 85.0195617 I
                                                -62.127 - 85.0195617 I

                                        -12
            Factored form gain multiplier: -4.801600749 10

Plant Case: 4  Element: (2, 2)
            Roots of Numerator                  Roots of Denominator
            -------------------                 --------------------
            -0.06617260399                      -0.1137334365 + 0.2590698828 I
            -1.076648798                        -0.1137334365 - 0.2590698828 I
            -14.76581091 + 21.99367018 I        -1.063882999
            -14.76581091 - 21.99367018 I        -13. + 15.19868415 I
            -17.15376289 + 86.63948955 I        -13. - 15.19868415 I
            -17.15376289 - 86.63948955 I        -14.924 + 33.19991301 I
                                                -14.924 - 33.19991301 I
                                                -62.127 + 85.0195617 I
                                                -62.127 - 85.0195617 I
            Factored form gain multiplier: -204.4085555

Plant Case: 4  Element: (2, 3)
            Roots of Numerator                  Roots of Denominator
            -------------------                 --------------------
            1.381470153e12                      -0.1137334365 + 0.2590698828 I
            37.97965347                         -0.1137334365 - 0.2590698828 I
            -2.538773868                        -1.063882999
            -12.66342271 + 39.983698 I          -13. + 15.19868415 I
            -12.66342271 - 39.983698 I          -13. - 15.19868415 I
            -36.51975006                        -14.924 + 33.19991301 I
            -52.4476482 + 84.09578587 I         -14.924 - 33.19991301 I
            -52.4476482 - 84.09578587 I         -44.25 + 60.55524337 I
            -54.02567326 + 42.80252203 I        -44.25 - 60.55524337 I
            -54.02567326 - 42.80252203 I        -49.68 + 52.11427444 I
                                                -49.68 - 52.11427444 I
                                                -62.127 + 85.0195617 I
                                                -62.127 - 85.0195617 I

                                        -11
            Factored form gain multiplier: -4.998777203 10

Plant Case: 4  Element: (3, 1)
            Roots of Numerator                  Roots of Denominator
            -------------------                 --------------------
            0.03805472456 + 0.3119505612 I      -0.1137334365 + 0.2590698828 I
            0.03805472456 - 0.3119505612 I      -0.1137334365 - 0.2590698828 I
            -12.40629272 + 11.65358421 I        -1.063882999
            -12.40629272 - 11.65358421 I        -13. + 15.19868415 I
            -15.00541525 + 42.4492691 I         -13. - 15.19868415 I
            -15.00541525 - 42.4492691 I         -14.924 + 33.19991301 I
            -50.55178724 + 50.69632917 I        -14.924 - 33.19991301 I
            -50.55178724 - 50.69632917 I        -44.25 + 60.55524337 I
            -54.36332368 + 83.74882852 I        -44.25 - 60.55524337 I
            -54.36332368 - 83.74882852 I        -49.68 + 52.11427444 I
                                                -49.68 - 52.11427444 I
                                                -62.127 + 85.0195617 I
```

```
                                                -62.127 - 85.0195617 I
        Factored form gain multiplier: -624.8642066

Plant Case: 4  Element: {3, 2}
        Roots of Numerator              Roots of Denominator
        ------------------              --------------------
        2.866812795e13                  -0.1137334365 + 0.2590698828 I
        -1.485201811                    -0.1137334365 - 0.2590698828 I
        -14.76581091 + 21.99367018 I    -1.063882999
        -14.76581091 - 21.99367018 I    -13. + 15.19868415 I
        -17.15376289 + 86.63948955 I    -13. - 15.19868415 I
        -17.15376289 - 86.63948955 I    -14.924 + 33.19991301 I
                                        -14.924 - 33.19991301 I
                                        -62.127 + 85.0195617 I
                                        -62.127 - 85.0195617 I

                                                     -12
        Factored form gain multiplier: -1.245493544 10


Plant Case: 4  Element: {3, 3}
        Roots of Numerator              Roots of Denominator
        ------------------              --------------------
        -0.3634122948 + 0.1618778524 I  -0.1137334365 + 0.2590698828 I
        -0.3634122948 - 0.1618778524 I  -0.1137334365 - 0.2590698828 I
        -13.80346364 + 18.557098 I      -1.063882999
        -13.80346364 - 18.557098 I      -13. + 15.19868415 I
        -15.94704047 + 39.43184461 I    -13. - 15.19868415 I
        -15.94704047 - 39.43184461 I    -14.924 + 33.19991301 I
        -48.71358198 + 53.64892893 I    -14.924 - 33.19991301 I
        -48.71358198 - 53.64892893 I    -44.25 + 60.55524337 I
        -57.64123543 + 84.21130887 I    -44.25 - 60.55524337 I
        -57.64123543 - 84.21130887 I    -49.68 + 52.11427444 I
                                        -49.68 - 52.11427444 I
                                        -62.127 + 85.0195617 I
                                        -62.127 - 85.0195617 I
        Factored form gain multiplier: -2579.738509


Plant Case: 5  Element: {1, 1}
        Roots of Numerator              Roots of Denominator
        ------------------              --------------------
        -0.1126673471                   -0.06201210412
        -13.15110836 + 15.94448679 I    -0.997365568
        -13.15110836 - 15.94448679 I    -13. + 15.19868415 I
        -15.73743682 + 42.03080543 I    -13. - 15.19868415 I
        -15.73743682 - 42.03080543 I    -14.924 + 33.19991301 I
        -49.65339301 + 52.15007315 I    -14.924 - 33.19991301 I
        -49.65339301 - 52.15007315 I    -44.25 + 60.55524337 I
        -55.2784838 + 83.79977156 I     -44.25 - 60.55524337 I
        -55.2784838 - 83.79977156 I     -49.68 + 52.11427444 I
                                        -49.68 - 52.11427444 I
                                        -62.127 + 85.0195617 I
                                        -62.127 - 85.0195617 I
        Factored form gain multiplier: 1135.56275

Plant Case: 5  Element: {1, 2}
        Roots of Numerator              Roots of Denominator
        ------------------              --------------------
        Factored form gain multiplier: 0

Plant Case: 5  Element: {1, 3}
        Roots of Numerator              Roots of Denominator
        ------------------              --------------------
        0.2385145022                    -0.06201210412
        -12.74971151 + 13.7726672 I     -0.997365568
        -12.74971151 - 13.7726672 I     -13. + 15.19868415 I
        -15.27249035 + 39.85762199 I    -13. - 15.19868415 I
        -15.27249035 - 39.85762199 I    -14.924 + 33.19991301 I
        -49.71988084 + 52.05911201 I    -14.924 - 33.19991301 I
        -49.71988084 - 52.05911201 I    -44.25 + 60.55524337 I
        -56.71481482 + 84.1592048 I     -44.25 - 60.55524337 I
        -56.71481482 - 84.1592048 I     -49.68 + 52.11427444 I
                                        -49.68 - 52.11427444 I
                                        -62.127 + 85.0195617 I
                                        -62.127 - 85.0195617 I
        Factored form gain multiplier: 3138.264615
```

Plant Case: 5 Element: {2, 1}
    Roots of Numerator   Roots of Denominator
    ------------------   --------------------
    Factored form gain multiplier: 0

Plant Case: 5 Element: {2, 2}
    Roots of Numerator   Roots of Denominator
    ------------------   --------------------
    -14.76364568 + 21.98417326 I   -0.1366001171
    -14.76364568 - 21.98417326 I   -13. + 15.19868415 I
    -17.13211925 + 86.63467236 I   -13. - 15.19868415 I
    -17.13211925 - 86.63467236 I   -14.924 + 33.19991301 I
                                   -14.924 - 33.19991301 I
                                   -62.127 + 85.0195617 I
                                   -62.127 - 85.0195617 I
    Factored form gain multiplier: -205.312979

Plant Case: 5 Element: {2, 3}
    Roots of Numerator   Roots of Denominator
    ------------------   --------------------
    Factored form gain multiplier: 0

Plant Case: 5 Element: {3, 1}
    Roots of Numerator   Roots of Denominator
    ------------------   --------------------
    0.2210511777   -0.06201210412
    -12.38008903 + 11.5545971 I   -0.997365568
    -12.38008903 - 11.5545971 I   -13. + 15.19868415 I
    -14.99454494 + 42.44663728 I   -13. - 15.19868415 I
    -14.°9454494 - 42.44663728 I   -14.924 + 33.19991301 I
    -50.__11786 + 50.6784398 I   -14.924 - 33.19991301 I
    -50.5611786 - 50.6784398 I   -44.25 + 60.55524337 I
    -54.3552077 + 83.7490214 I   -44.25 - 60.55524337 I
    -54.3552077 - 83.7490214 I   -49.68 + 52.11427444 I
                                     -49.68 - 52.11427444 I
                                   -62.127 + 85.0195617 I
                                   -62.127 - 85.0195617 I
    Factored form gain multiplier: -612.7048551

Plant Case: 5 Element: {3, 2}
    Roots of Numerator   Roots of Denominator
    ------------------   --------------------
    Factored form gain multiplier: 0

Plant Case: 5 Element: {3, 3}
    Roots of Numerator   Roots of Denominator
    ------------------   --------------------
    -0.536633144   -0.06201210412
    -13.82385478 + 18.61043872 I   -0.997365568
    -13.82385478 - 18.61043872 I   -13. + 15.19868415 I
    -15.95495777 + 39.42818093 I   -13. - 15.19868415 I
    -15.95495777 - 39.42818093 I   -14.924 + 33.19991301 I
    -48.70565529 + 53.66243292 I   -14.924 - 33.19991301 I
    -48.70565529 - 53.66243292 I   -44.25 + 60.55524337 I
    -57.65121702 + 84.21232942 I   -44.25 - 60.55524337 I
    -57.65121702 - 84.21232942 I   -49.68 + 52.11427444 I
                                     -49.68 - 52.°1427444 I
                                     -62.127 + 85.0195617 I
                                   -62.127 - 85.0195617 I
    Factored form gain multiplier: -2540.565597

Plant Case: 6 Element: {1, 1}
    Roots of Numerator   Roots of Denominator
    ------------------   --------------------
    -0.1246591708 + 0.07467766531 I   -0.1001018991 + 0.07866949412 I
    -0.1246591708 - 0.07467766531 I   -0.1001018991 - 0.07866949412 I
    -13.15108234 + 15.94449866 I   -0.9957739909
    -13.15108234 - 15.94449866 I   -13. + 15.19868415 I
    -15.73743823 + 42.0308056 I   -13. - 15.19868415 I
    -15.73743823 - 42.0308056 I   -14.924 + 33.19991301 I
    -49.65339207 + 52.15007262 I   -14.924 - 33.19991301 I
    -49.65339207 - 52.15007262 I   -44.25 + 60.55524337 I
    -55.2784839 + 83.79977184 I   -44.25 - 60.55524337 I
    -55.2784839 - 83.79977184 I   -49.68 + 52.11427444 I
                                     -49.68 - 52.11427444 I
                                     -62.127 + 85.0195617 I
                                   -62.127 - 85.0195617 I
    Factored form gain multiplier: 1135.56275

```
Plant Case: 6  Element: (1, 2)
        Roots of Numerator              Roots of Denominator
        -------------------             -------------------
        5.169088345e13                  -0.1001018991 + 0.07866949412 I
        -0.4884913722                   -0.1001018991 - 0.07866949412 I
        -14.76364568 + 21.98417326 I    -0.9957739909
        -14.76364568 - 21.98417326 I    -13. + 15.19868415 I
        -17.13211925 + 86.63467236 I    -13. - 15.19868415 I
        -17.13211925 - 86.63467236 I    -14.924 + 33.19991301 I
                                        -14.924 - 33.19991301 I
                                        -62.127 + 85.0195617 I
                                        -62.127 - 85.0195617 I

                                              -13
        Factored form gain multiplier: -3.579951987 10

Plant Case: 6  Element: (1, 3)
        Roots of Numerator              Roots of Denominator
        -------------------             -------------------
        0.2066927034                    -0.1001018991 + 0.07866949412 I
        -0.1046292009                   -0.1001018991 - 0.07866949412 I
        -12.74978653 + 13.77264691 I    -0.9957739909
        -12.74978653 - 13.77264691 I    -13. + 15.19868415 I
        -15.27248857 + 39.85762151 I    -13. - 15.19868415 I
        -15.27248857 - 39.85762151 I    -14.924 + 33.19991301 I
        -49.71988229 + 52.0591128 I     -14.924 - 33.19991301 I
        -49.71988229 - 52.0591128 I     -44.25 + 60.55524337 I
        -56.71481468 + 84.15920442 I    -44.25 - 60.55524337 I
        -56.71481468 - 84.15920442 I    -49.68 + 52.11427444 I
                                        -49.68 - 52.11427444 I
                                        -62.127 + 85.0195617 I
                                        -62.127 - 85.0195617 I
        Factored form gain multiplier: 3138.264615

Plant Case: 6  Element: (2, 1)
        Roots of Numerator              Roots of Denominator
        -------------------             ----------- --------
        1.786836745e13                  -0.1001018991 + 0.07866949412 I
        -0.3210353119                   -0.1001018991 - 0.07866949412 I
        -14.28636138 + 20.61043488 I    -0.9957739909
        -14.28636138 - 20.61043488 I    -13. + 15.19868415 I
        -16.85701882 + 41.0898694 I     -13. - 15.19868415 I
        -16.85701882 - 41.0898694 I     -14.924 + 33.19991301 I
        -48.21095518 + 54.34137954 I    -14.924 - 33.19991301 I
        -48.21095518 - 54.34137954 I    -44.25 + 60.55524337 I
        -56.77048907 + 83.9297526? I    -44.25 - 60.55524337 I
        -56.77048907 - 83.9297... .     -49.68 + 52.11427444 I
                                        -49.68 - 52.11427444 I
                                        -62.127 + 85.0195617 I
                                        -62.127 - 85.0195617 I

                                              -12
        Factored form gain multiplier: -1.541480311 10

Plant Case: 6  Element: (2, 2)
        Roots of Numerator              Roots of Denominator
        -------------------             -------------------
        -0.06201210412                  -0.1001018991 + 0.07866949412 I
        -0.997365568                    -0.1001018991 - 0.07866949412 I
        -14.76364568 + 21.98417326 I    -0.9957739909
        -14.76364568 - 21.98417326 I    -13. + 15.19868415 I
        -17.13211925 + 86.63467236 I    -13. - 15.19868415 I
        -17.13211925 - 86.63467236 I    -14.924 + 33.19991301 I
                                        -14.924 - 33.19991301 I
                                        -62.127 + 85.0195617 I
                                        -62.127 - 85.0195617 I
        Factored form gain multiplier: -205.312979

Plant Case: 6  Element: (2, 3)
        Roots of Numerator              Roots of Denominator
        -------------------             -------------------
        2.851382737e12                  -0.1001018991 + 0.07866949412 I
        39.54079128                     -0.1001018991 - 0.07866949412 I
        -2.315207499                    -0.9957739909
        -12.63819681 + 39.90321185 I    -13. + 15.19868415 I
        -12.63819681 - 39.90321185 I    -13. - 15.19868415 I
        -37.38993011                    -14.924 + 33.19991301 I
```

145

```
        -52.37118734 + 84.09773695 I      -14.924 - 33.19991301 I
        -52.37118734 - 84.09773695 I      -44.25 + 60.55524337 I
        -54.03931775 + 42.52656698 I      -44.25 - 60.55524337 I
        -54.03931775 - 42.52656698 I      -49.68 + 52.11427444 I
                                          -49.68 - 52.11427444 I
                                          -62.127 + 85.0195617 I
                                          -62.127 - 85.0195617 I
```

$$\text{Factored form gain multiplier: } -7.728325299 \ 10^{-12}$$

Plant Case: 6 Element: {3, 1}
```
        Roots of Numerator               Roots of Denominator
        -------------------              -------------------
        0.1735209802                     -0.1001018991 + 0.07866949412 I
        -0.08884012941                   -0.1001018991 - 0.07866949412 I
        -12.38020474 + 11.55459044 I     -0.9957739909
        -12.38020474 - 11.55459044 I     -13. + 15.19868415 I
        -14.99454255 + 42.44663668 I     -13. - 15.19868415 I
        -14.99454255 - 42.44663668 I     -14.924 + 33.19991301 I
        -50.56118038 + 50.67844086 I     -14.924 - 33.19991301 I
        -50.56118038 + 50.67844086 I     -44.25 + 60.55524337 I
        -54.3552075 + 83.74902089 I      -44.25 - 60.55524337 I
        -54.3552075 - 83.74902089 I      -49.68 + 52.11427444 I
                                         -49.68 - 52.11427444 I
                                         -62.127 + 85.0195617 I
                                         -62.127 - 85.0195617 I
        Factored form gain multiplier: -612.7048551
```

Plant Case: 6 Element: {3, 2}
```
        Roots of Numerator               Roots of Denominator
        -------------------              -------------------
        -1.374299119                     -0.1001018991 + 0.07866949412 I
        -14.76364568 + 21.98417326 I     -0.1001018991 - 0.07866949412 I
        -14.76364568 - 21.98417326 I     -0.9957739909
        -17.13211925 + 86.63467236 I     -13. + 15.19868415 I
        -17.13211925 - 86.63467236 I     -13. - 15.19868415 I
                                         -14.924 + 33.19991301 I
                                         -14.924 - 33.19991301 I
                                         -62.127 + 85.0195617 I
                                         -62.127 - 85.0195617 I
        Factored form gain multiplier: 11.95465082
```

Plant Case: 6 Element: {3, 3}
```
        Roots of Numerator               Roots of Denominator
        -------------------              -------------------
        -0.1577260214                    -0.1001018991 + 0.07866949412 I
        -0.5155635944                    -0.1001018991 - 0.07866949412 I
        -13.82382577 + 18.61045683 I     -0.9957739909
        -13.82382577 - 18.61045683 I     -13. + 15.19868415 I
        -15.95495988 + 39.42818116 I     -13. - 15.19868415 I
        -15.95495988 - 39.42818116 I     -14.924 + 33.19991301 I
        -48.70565389 + 53.6624322 I      -14.924 - 33.19991301 I
        -48.70565389 - 53.6624322 I      -44.25 + 60.55524337 I
        -57.65121713 + 84.2123298 I      -44.25 - 60.55524337 I
        -57.65121713 - 84.2123298 I      -49.68 + 52.11427444 I
                                         -49.68 - 52.11427444 I
                                         -62.127 + 85.0195617 I
                                         -62.127 - 85.0195617 I
        Factored form gain multiplier: -2540.565597
```

Plant Case: 7 Element: {1, 1}
```
        Roots of Numerator               Roots of Denominator
        ----------- ------               -------------------
        -0.1247354898 + 0.1507867306 I   -0.1024173959 + 0.1705245196 I
        -0.1247354898 - 0.1507867306 I   -0.1024173959 - 0.1705245196 I
        -13.15100429 + 15.94453429 I     -0.9911429974
        -13.15100429 - 15.94453429 I     -13. + 15.19868415 I
        -15.73744247 + 42.0308061 I      -13. - 15.19868415 I
        -15.73744247 - 42.0308061 I      -14.924 + 33.19991301 I
        -49.65338926 + 52.15007105 I     -14.924 - 33.19991301 I
        -49.65338926 - 52.15007105 I     -44.25 + 60.55524337 I
        -55.27848421 + 83.7997727 I      -44.25 - 60.55524337 I
        -55.27848421 - 83.7997727 I      -49.68 + 52.11427444 I
                                         -49.68 - 52.11427444 I
                                         -62.127 + 85.0195617 I
                                         -62.127 - 85.0195617 I
        Factored form gain multiplier: 1135.56275
```

```
Plant Case: 7  Element: {1, 2}
        Roots of Numerator              Roots of Denominator
        -------------------             --------------------
        1.492469696e15                  -0.1024173959 + 0.1705245196 I
        -0.4884913722                   -0.1024173959 - 0.1705245196 I
        -14.76364568 + 21.98417326 I    -0.9911429974
        -14.76364568 - 21.98417326 I    -13. + 15.19868415 I
        -17.13211925 + 86.63467236 I    -13. - 15.19868415 I
        -17.13211925 - 86.63467236 I    -14.924 + 33.19991301 I
                                        -14.924 - 33.19991301 I
                                        -62.127 + 85.0195617 I
                                        -62.127 - 85.0195617 I

                                             -14
        Factored form gain multiplier: -2.479794148 10

Plant Case: 7  Element: {1, 3}
        Roots of Numerator              Roots of Denominator
        -------------------             --------------------
        0.05125543325 + 0.09279727562 I -0.1024173959 + 0.1705245196 I
        0.05125543325 - 0.09279727562 I -0.1024173959 - 0.1705245196 I
        -12.7500116 + 13.77258605 I     -0.9911429974
        -12.7500116 - 13.77258605 I     -13. + 15.19868415 I
        -15.27248324 + 39.85762008 I    -13. - 15.19868415 I
        -15.27248324 - 39.85762008 I    -14.924 + 33.19991301 I
        -49.71988665 + 52.05911519 I    -14.924 - 33.19991301 I
        -49.71988665 - 52.05911519 I    -44.25 + 60.55524337 I
        -56.71481427 + 84.15920329 I    -44.25 - 60.55524337 I
        -56.71481427 - 84.15920329 I    -49.68 + 52.11427444 I
                                        -49.68 - 52.11427444 I
                                        -62.127 + 85.0195617 I
                                        -62.127 - 85.0195617 I
        Factored form gain multiplier: 3138.264615

Plant Case: 7  Element: {2, 1}
        Roots of Numerator              Roots of Denominator
        -------------------             --------------------
        4.55231746e13                   -0.1024173959 + 0.1705245196 I
        -0.3210353119                   -0.1024173959 - 0.1705245196 I
        -14.28636138 + 20.61043488 I    -0.9911429974
        -14.28636138 - 20.61043488 I    -13. + 15.19868415 I
        -16.85701882 + 41.0898694 I     -13. - 15.19868415 I
        -16.85701882 - 41.0898694 I     -14.924 + 33.19991301 I
        -48.21095518 + 54.34137954 I    -14.924 - 33.19991301 I
        -48.21095518 - 54.34137954 I    -44.25 + 60.55524337 I
        -56.77048907 + 83.92975261 I    -44.25 - 60.55524337 I
        -56.77048907 - 83.92975261 I    -49.68 + 52.11427444 I
                                        -49.68 - 52.11427444 I
                                        -62.127 + 85.0195617 I
                                        -62.127 - 85.0195617 I

                                             -12
        Factored form gain multiplier: -1.210097356 10

Plant Case: 7  Element: {2, 2}
        Roots of Numerator              Roots of Denominator
        -------------------             --------------------
        -0.06201210412                  -0.1024173959 + 0.1705245196 I
        -0.997365568                    -0.1024173959 - 0.1705245196 I
        -14.76364568 + 21.98417326 I    -0.9911429974
        -14.76364568 - 21.98417326 I    -13. + 15.19868415 I
        -17.13211925 + 86.63467236 I    -13. - 15.19868415 I
        -17.13211925 - 86.63467236 I    -14.924 + 33.19991301 I
                                        -14.924 - 33.19991301 I
                                        -62.127 + 85.0195617 I
                                        -62.127 - 85.0195617 I
        Factored form gain multiplier: -205.31297

Plant Case: 7  Element: {2, 3}
        Roots of Numerator              Roots of Denominator
        -------------------             --------------------
        1.173908901e13                  -0.1024173959 + 0.1705245196 I
        39.54079128                     -0.1024173959 - 0.1705245196 I
        -2.315207499                    -0.9911429974
        -12.63819681 + 39.90321185 I    -13. + 15.19868415 I
        -12.63819681 - 39.90321185 I    -13. - 15.19868415 I
        -37.38993011                    -14.924 + 33.19991301 I
```

147

```
        -52.37118734 + 84.09773695 I       -14.924 - 33.19991301 I
        -52.37118734 - 84.09773695 I       -44.25 + 60.55524337 I
        -54.03931775 + 42.52656698 I       -44.25 - 60.55524337 I
        -54.03931775 - 42.52656698 I       -49.68 + 52.11427444 I
                                           -49.68 - 52.11427444 I
                                           -62.127 + 85.0195617 I
                                           -62.127 - 85.0195617 I

                                                          -12
        Factored form gain multiplier: -3.754365152 10
```

Plant Case: 7 Element: {3, 1}

```
        Roots of Numerator                 Roots of Denominator
        ------------------                 --------------------
        0.04268509635 + 0.164622761 I      -0.1024173959 + 0.1705245196 I
        0.04268509635 - 0.164622761 I      -0.1024173959 - 0.1705245196 I
        -12.38055187 + 11.55457052 I       -0.9911429974
        -12.38055187 - 11.55457052 I       -13. + 15.19868415 I
        -14.99453537 + 42.44663486 I       -13. - 15.19868415 I
        -14.99453537 - 42.44663486 I       -14.924 + 33.19991301 I
        -50.56118572 + 50.67844403 I       -14.924 - 33.19991301 I
        -50.56118572 - 50.67844403 I       -44.25 + 60.55524337 I
        -54.3552069 + 83.74901933 I        -44.25 - 60.55524337 I
        -54.3552069 - 83.74901933 I        -49.68 + 52.11427444 I
                                           -49.68 - 52.11427444 I
                                           -62.127 + 85.0195617 I
                                           -62.127 - 85.0195617 I
        Factored form gain multiplier: -612.7048551
```

Plant Case: 7 Element: {3, 2}

```
        Roots of Numerator                 Roots of Denominator
        ------------------                 --------------------
        3.942324224e13                     -0.1024173959 + 0.1705245196 I
        -1.374299119                       -0.1024173959 - 0.1705245196 I
        -14.76364568 + 21.98417326 I       -0.9911429974
        -14.76364568 - 21.98417326 I       -13. + 15.19868415 I
        -17.13211925 + 86.63467236 I       -13. - 15.19868415 I
        -17.13211925 - 86.63467236 I       -14.924 + 33.19991301 I
                                           -14.924 - 33.19991301 I
                                           -62.127 + 85.0195617 I
                                           -62.127 - 85.0195617 I

                                                          -13
        Factored form gain multiplier: -6.064773032 10
```

Plant Case: 7 Element: {3, 3}

```
        Roots of Numerator                 Roots of Denominator
        ------------------                 --------------------
        -0.24713078                        -0.1024173959 + 0.1705245196 I
        -0.4263279097                      -0.1024173959 - 0.1705245196 I
        -13.82373875 + 18.61051116 I       -0.9911429974
        -13.82373875 - 18.61051116 I       -13. + 15.19868415 I
        -15.95496621 + 39.42818184 I       -13. - 15.19868415 I
        -15.95496621 - 39.42818184 I       -14.924 + 33.19991301 I
        -48.70564969 + 53.66243002 I       -14.924 - 33.19991301 I
        -48.70564969 - 53.66243002 I       -44.25 + 60.55524337 I
        -57.65121749 + 84.21233096 I       -44.25 - 60.55524337 I
        -57.65121749 - 84.21233096 I       -49.68 + 52.11427444 I
                                           -49.68 - 52.11427444 I
                                           -62.127 + 85.0195617 I
                                           -62.127 - 85.0195617 I
        Factored form gain multiplier: -2540.565597
```

Plant Case: 8 Element: {1, 1}

```
        Roots of Numerator                 Roots of Denominator
        ------------------                 --------------------
        -0.1248626979 + 0.2265757703 I     -0.1060454906 + 0.2602021439 I
        -0.1248626979 - 0.2265757703 I     -0.1060454906 - 0.2602021439 I
        -13.15087419 + 15.94459366 I       -0.983886808
        -13.15087419 - 15.94459366 I       -13. + 15.19868415 I
        -15.73744953 + 42.03080694 I       -13. - 15.19868415 I
        -15.73744953 - 42.03080694 I       -14.924 + 33.19991301 I
        -49.65338458 + 52.15006843 I       -14.924 - 33.19991301 I
        -49.65338458 - 52.15006843 I       -44.25 + 60.55524337 I
        -55.27848472 + 83.79977412 I       -44.25 - 60.55524337 I
```

148

```
           -55.27848472 - 83.79977412 I       -49.68 + 52.11427444 I
                                               -49.68 - 52.11427444 I
                                               -62.127 + 85.0195617 I
                                               -62.127 - 85.0195617 I
           Factored form gain multiplier: 1135.56275

Plant Case: 8  Element: {1, 2}
            Roots of Numerator                Roots of Denominator
            -- ----------------               --------------------
            -0.4884913722                     -0.1060454906 + 0.2602021439 I
            -14.76364568 + 21.98417326 I      -0.1060454906 - 0.2602021439 I
            -14.76364568 - 21.98417326 I      -0.983886808
            -17.13211925 + 86.63467236 I      -13. + 15.19868415 I
            -17.13211925 - 86.63467236 I      -13. - 15.19868415 I
            -1.02445188e14                    -14.924 + 33.19991301 I
                                              -14.924 - 33.19991301 I
                                              -62.127 + 85.0195617 I
                                              -62.127 - 85.0195617 I
                                                    -13
            Factored form gain multiplier: 5.419021174 10

Plant Case: 8  Element: {1, 3}
            Roots of Numerator                Roots of Denominator
            ------------------                --------------------
            0.05162825669 + 0.251685402 I     -0.1060454906 + 0.2602021439 I
            0.05162825669 - 0.251685402 I     -0.1060454906 - 0.2602021439 I
            -12.75038674 + 13.77248472 I      -0.983886808
            -12.75038674 - 13.77248472 I      -13. + 15.19868415 I
            -15.27247434 + 39.85761769 I      -13. - 15.19868415 I
            -15.27247434 - 39.85761769 I      -14.924 + 33.19991301 I
            -49.71989391 + 52.05911916 I      -14.924 - 33.19991301 I
            -49.71989391 - 52.05911916 I      -44.25 + 60.55524337 I
            -56.71481358 + 84.15920141 I      -44.25 - 60.55524337 I
            -56.71481358 - 84.15920141 I      -49.68 + 52.11427444 I
                                              -49.68 - 52.11427444 I
                                              -62.127 + 85.0195617 I
                                              -62.127 - 85.0195617 I
            Factored form gain multiplier: 3138.264615

Plant Case: 8  Element: {2, 1}
            Roots of Numerator                Roots of Denominator
            ------------------                --------------------
            -0.3210353119                     -0.1060454906 + 0.2602021439 I
            -14.28636138 + 20.61043488 I      -0.1060454906 - 0.2602021439 I
            -14.28636138 - 20.61043488 I      -0.983886808
            -16.85701882 + 41.0898694 I       -13. + 15.19868415 I
            -16.85701882 - 41.0898694 I       -13. - 15.19868415 I
            -48.21095518 + 54.34137954 I      -14.924 + 33.19991301 I
            -48.21095518 - 54.34137954 I      -14.924 - 33.19991301 I
            -56.77048907 + 83.92975261 I      -44.25 + 60.55524337 I
            -56.77048907 - 83.92975261 I      -44.25 - 60.55524337 I
            -9.235012632e13                   -49.68 + 52.11427444 I
                                              -49.68 - 52.11427444 I
                                              -62.127 + 85.0195617 I
                                              -62.127 - 85.0195617 I
                                                    -13
            Factored form gain multiplier: 8.947601167 10

Plant Case: 8  Element: {2, 2}
            Roots of Numerator                Roots of Denominator
            ------------------                --------------------
            -0.06201210412                    -0.1060454906 + 0.2602021439 I
            -0.997365568                       -0.1060454906 - 0.2602021439 I
            -14.76364568 + 21.98417326 I      -0.983886808
            -14.76364568 - 21.98417326 I      -13. + 15.19868415 I
            -17.13211925 + 86.63467236 I      -13. - 15.19868415 I
            -17.13211925 - 86.63467236 I      -14.924 + 33.19991301 I
                                              -14.924 - 33.19991301 I
                                              -62.127 + 85.0195617 I
                                              -62.127 - 85.0195617 I
            Factored form gain multiplier: -205.312979

Plant Case: 8  Element: {2, 3}
            Roots of Numerator                Roots of Denominator
            ------------------                --------------------
            39.54079128                       -0.1060454906 + 0.2602021439 I
```

```
         -2.315207499                    -0.1060454906 - 0.2602021439 I
         -12.63819681 + 39.90321185 I    -0.983886808
         -12.63819681 - 39.90321185 I    -13. + 15.19868415 I
         -37.38993011                    -13. - 15.19868415 I
         -52.37118734 + 84.09773695 I    -14.924 + 33.19991301 I
         -52.37118734 - 84.09773695 I    -14.924 - 33.19991301 I
         -54.03931775 + 42.52656698 I    -44.25 + 60.55524337 I
         -54.03931775 - 42.52656698 I    -44.25 - 60.55524337 I
         -5.79471861e12                  -49.68 + 52.11427444 I
                                         -49.68 - 52.11427444 I
                                         -62.127 + 85.0195617 I
                                         -62.127 - 85.0195617 I
```

                                         -11
         Factored form gain multiplier: 1.140853327 10

Plant Case: 8 Element: {3, 1}
         Roots of Numerator   Roots of Denominator
         ------------------   --------------------

```
         0.04325950035 + 0.3177150712 I  -0.1060454906 + 0.2602021439 I
         0.04325950035 - 0.3177150712 I  -0.1060454906 - 0.2602021439 I
         -12.38113035 + 11.55453759 I    -0.983886808
         -12.38113035 - 11.55453759 I    -13. + 15.19868415 I
         -14.9945234 + 42.44663183 I     -13. - 15.19868415 I
         -14.9945234 - 42.44663183 I     -14.924 + 33.19991301 I
         -50.56119461 + 50.67844933 I    -14.924 - 33.19991301 I
         -50.56119461 - 50.67844933 I    -44.25 + 60.55524337 I
         -54.35520589 + 83.74901675 I    -44.25 - 60.55524337 I
         -54.35520589 - 83.74901675 I    -49.68 + 52.11427444 I
                                         -49.68 - 52.11427444 I
                                         -62.127 + 85.0195617 I
                                         -62.127 - 85.0195617 I
```
         Factored form gain multiplier: -612.7048551

Plant Case: 8 Element: {3, 2}
         Roots of Numerator   Roots of Denominator
         ------------------   --------------------

```
         7.433134606e13                  -0.1060454906 + 0.2602021439 I
         -1.374299119                    -0.1060454906 - 0.2602021439 I
         -14.76364568 + 21.98417326 I    -0.983886808
         -14.76364568 - 21.98417326 I    -13. + 15.19868415 I
         -17.13211925 + 86.63467236 I    -13. - 15.19868415 I
         -17.13211925 - 86.63467236 I    -14.924 + 33.19991301 I
                                         -14.924 - 33.19991301 I
                                         -62.127 + 85.0195617 I
                                         -62.127 - 85.0195617 I
```

                                         -13
         Factored form gain multiplier: -4.824875958 10

Plant Case: 8 Element: {3, 3}
         Roots of Numerator   Roots of Denominator
         ------------------   --------------------

```
         -0.3368702557 + 0.1787330665 I  -0.1060454906 + 0.2602021439 I
         -0.3368702557 - 0.1787330665 I  -0.1060454906 - 0.2602021439 I
         -13.8235937 + 18.61060169 I     0.983886808
         -13.8235937 - 18.61060169 I     -13. + 15.19868415 I
         -15.95497676 + 39.42818298 I    -13. - 15.19868415 I
         -15.95497676 - 39.42818298 I    -14.924 + 33.19991301 I
         -48.7056427 + 53.6624264 I      -14.924 - 33.19991301 I
         -48.7056427 - 53.6624264 I      -44.25 + 60.55524337 I
         -57.65121807 + 84.21233289 I    -44.25 - 60.55524337 I
         -57.65121807 - 84.21233289 I    -49.68 + 52.11427444 I
                                         -49.68 - 52.11427444 I
                                         -62.127 + 85.0195617 I
                                         -62.127 - 85.0195617 I
```
         Factored form gain multiplier: -2540.565597

Plant Case: 9 Element: {1, 1}
         Roots of Numerator   Roots of Denominator
         ------------------   --------------------

```
         -0.1074664032                   -0.05808085747
         -13.15738138 + 15.96338795 I    -0.9222246199
         -13.15738138 - 15.96338795 I    -13. + 15.19868415 I
         -15.73875728 + 42.0259814 I     -13. - 15.19868415 I
         -15.73875728 - 42.0259814 I     -14.924 + 33.19991301 I
         -49.65523805 + 52.14751366 I    -14.924 - 33.19991301 I
```

```
          -49.65523805 - 52.14751366 I      -44.25 + 60.55524337 I
          -55.28583411 + 83.80254913 I      -44.25 - 60.55524337 I
          -55.28583411 - 83.80254913 I      -49.68 + 52.11427444 I
                                            -49.68 - 52.11427444 I
                                            -62.127 + 85.0195617 I
                                            -62.127 - 85.0195617 I
          Factored form gain multiplier: 1114.772272

Plant Case: 9  Element: (1, 2)
          Roots of Numerator             Roots of Denominator
          ------------------             --------------------
          Factored form gain multiplier: 0

Plant Case: 9  Element: (1, 3)
          Roots of Numerator             Roots of Denominator
          ------------------             ------ -------------
          0.2267657372                   -0.05808085747
          -12.73774686 + 13.7320958 I    -0.9222246199
          -12.73774686 - 13.7320958 I    -13. + 15.19868415 I
          -15.26905449 + 39.84154152 I   -13. - 15.19868415 I
          -15.26905449 - 39.84154152 I   -14.924 + 33.19991301 I
          -49.71707966 + 52.06308354 I   -14.924 - 33.19991301 I
          -49.71707966 - 52.06308354 I   -44.25 + 60.55524337 I
          -56.7232334 + 84.1603752 I     -44.25 - 60.55524337 I
          -56.7232334 - 84.1603752 I     -49.68 + 52.11427444 I
                                         -49.68 - 52.11427444 I
                                         -62.127 + 85.0195617 I
                                         -62.127 - 85.0195617 I
          Factored form gain multiplier: 3081.532346

Plant Case: 9  Element: (2, 1)
          Roots of Numerator             Roots of Denominator
          ------------------             --------------- ------
          Factored form gain multiplier: 0

Plant Case: 9  Element: (2, 2)
          Roots of Numerator             Roots of Denominator
          ------------------             --------------------
          -14.75644431 + 21.95264007 I   -0.1252573635
          -14.75644431 - 21.95264007 I   -13. + 15.19868415 I
          -17.06037998 + 86.61864862 I   -13. - 15.19866415 I
          -17.06037998 - 86.61864862 I   -14.924 + 33.19991301 I
                                         -14.924 - 33.19991301 I
                                         -62.127 + 85.0195617 I
                                         -62.127 - 85.0195617 I
          Factored form gain multiplier: -207.0716183

Plant Case: 9  Element: (2, 3)
          Roots of Numerator             Roots of Denominator
          ------------------             ----- --------------
          Factored form gain multiplier: 0

Plant Case: 9  Element: (3, 1)
          Roots of Numerator             Roots of Denominator
          ------------------             --------------------
          0.2186105805                   -0.05808085747
          -12.35458828 + 11.45254297 I   -0.9222246199
          -12.35458828 - 11.45254297 I   -13. + 15.19868415 I
          -14.98296916 + 42.43676453 I   -13. - 15.19868415 I
          -14.98296916 - 42.43676453 I   -14.924 + 33.19991301 I
          -50.57188104 + 50.65834723 I   -14.924 - 33.19991301 I
          -50.57188104 - 50.65834723 I   -44.25 + 60.55524337 I
          -54.35317582 + 83.75141081 I   -44.25 - 60.55524337 I
          -54.35317582 - 83.75141081 I   -49.68 + 52.11427444 I
                                         -49.68 - 52.11427444 I
                                         -62.127 + 85.0195617 I
                                         -62.127 - 85.0195617 I
          Factored form gain multiplier: -601.1576115

Plant Case: 9  Element: (3, 2)
          Roots of Numerator             Roots of Denominator
          ------------------             --------------------
          Factored form gain multiplier: 0

Plant Case: 9  Element: (3, 3)
          Roots of Numerator             Roots of Denominator
          ------------ -------           ------ -------------
          -0.4972344919                  -0.05808085747
```

```
          -13.84370684 + 18.6632871 I        -0.9222246199
          -13.84370684 - 18.6632871 I        -13. + 15.19868415 I
          -15.96173093 + 39.41716877 I       -13. - 15.19868415 I
          -15.96173093 - 39.41716877 I       -14.924 + 33.19991301 I
          -48.6967764 + 53.67744786 I        -14.924 - 33.19991301 I
          -48.6967764 - 53.67744786 I        -44.25 + 60.55524337 I
          -57.66651368 + 84.21444127 I       -44.25 - 60.55524337 I
          -57.66651368 - 84.21444127 I       -49.68 + 52.11427444 I
                                             -49.68 - 52.11427444 I
                                             -62.127 + 85.0195617 I
                                             -62.127 - 85.0195617 I
          Factored form gain multiplier: -2504.666237


Plant Case: 10  Element: (1, 1)
          Roots of Numerator                 Roots of Denominator
          ------------------                 --------------------
          -0.1163877828 + 0.07493670829 I    -0.09251651137 + 0.08045818654 I
          -0.1163877828 - 0.07493670829 I    -0.09251651137 - 0.08045818654 I
          -13.1573549 + 15.96340009 I        -0.9205298181
          -13.1573549 - 15.96340009 I        -13. + 15.19868415 I
          -15.73875871 + 42.02598158 I       -13. - 15.19868415 I
          -15.73875871 - 42.02598158 I       -14.924 + 33.19991301 I
          -49.65523711 + 52.14751313 I       -14.924 - 33.19991301 I
          -49.65523711 - 52.14751313 I       -44.25 + 60.55524337 I
          -55.28583421 + 83.80254941 I       -44.25 - 60.55524337 I
          -55.28583421 - 83.80254941 I       -49.68 + 52.11427444 I
                                             -49.68 - 52.11427444 I
                                             -62.127 + 85.0195617 I
                                             -62.127 - 85.0195617 I
          Factored form gain multiplier: 1114.772272


Plant Case: 10  Element: (1, 2)
          Roots of Numerator                 Roots of Denominator
          ------------------                 --------------------
          3.577031451e14                     -0.09251651137 + 0.08045818654 I
          -0.4559228663                      -0.09251651137 - 0.08045818654 I
          -14.75644431 + 21.95264007 I       -0.9205298181
          -14.75644431 - 21.95264007 I       -13. + 15.19868415 I
          -17.06037998 + 86.61864862 I       -13. - 15.19868415 I
          -17.06037998 - 86.61864862 I       -14.924 + 33.19991301 I
                                             -14.924 - 33.19991301 I
                                             -62.127 + 85.0195617 I
                                             -62.127 - 85.0195617 I

                                                       -14
          Factored form gain multiplier: -5.217621504 10


Plant Case: 10  Element: (1, 3)
          Roots of Numerator                 Roots of Denominator
          ------------------                 --------------------
          0.1920289011                       -0.09251651137 + 0.08045818654 I
          -0.0903665771                      -0.09251651137 - 0.08045818654 I
          -12.7378243 + 13.73207494 I        -0.9205298181
          -12.7378243 - 13.73207494 I        -13. + 15.19868415 I
          -15.2690527 + 39.84154101 I        -13. - 15.19868415 I
          -15.2690527 - 39.84154101 I        -14.924 + 33.19991301 I
          -49.71708113 + 52.06308434 I       -14.924 - 33.19991301 I
          -49.71708113 - 52.06308434 I       -44.25 + 60.55524337 I
          -56.72323326 + 84.16037482 I       -44.25 - 60.55524337 I
          -56.72323326 - 84.16037482 I       -49.68 + 52.11427444 I
                                             -49.68 - 52.11427444 I
                                             -62.127 + 85.0195617 I
                                             -62.127 - 85.0195617 I
          Factored form gain multiplier: 3081.532346


Plant Case: 10  Element: (2, 1)
          Roots of Numerator                 Roots of Denominator
          ------------------                 --------------------
          4.229210323e13                     -0.09251651137 + 0.08045818654 I
          -0.3067093734                      -0.09251651137 - 0.08045818654 I
          -14.32930562 + 20.71139526 I       -0.9205298181
          -14.32930562 - 20.71139526 I       -13. + 15.19868415 I
          -16.8808181 + 41.08160672 I        -13. - 15.19868415 I
          -16.8808181 - 41.08160672 I        -14.924 + 33.19991301 I
          -48.19685605 + 54.36637579 I       -14.924 - 33.19991301 I
          -48.19685605 - 54.36637579 I       -44.25 + 60.55524337 I
          -56.79467608 + 83.93352453 I       -44.25 - 60.55524337 I
```

152

```
  -56.79467608 - 83.93352453 I        -49.68 + 52.11427444 I
                                       -49.68 - 52.11427444 I
                                       -62.127 + 85.0195617 I
                                       -62.127 - 85.0195617 I

                                            -13
        Factored form gain multiplier: -6.398472426 10

Plant Case: 10  Element: {2, 2}
        Roots of Numerator            Roots of Denominator
        -------------------           --------------------
        -0.05808085747                -0.09251651137 + 0.08045818654 I
        -0.9222246199                 -0.09251651137 - 0.08045818654 I
        -14.75644431 + 21.95264007 T  -0.9205298181
        -14.75644431 - 21.95264007 I  -13. + 15.19868415 I
        -17.06037998 + 86.61864862 I  -13. - 15.19868415 I
        -17.06037998 - 86.61864862 I  -14.924 + 33.19991301 I
                                      -14.924 - 33.19991301 I
                                      -62.127 + 85.0195617 I
                                      -62.127 - 85.0195617 I
        Factored form gain multiplier: -207.0716183

Plant Case: 10  Element: {2, 3}
        Roots of Numerator            Roots of Denominator
        -------------------           --------------------
        41.37265586                   -0.09251651137 + 0.08045818654 I
        -2.106815802                  -0.09251651137 - 0.08045818654 I
        -12.60304461 + 39.82989704 I  -0.9205298181
        -12.60304461 - 39.82989704 I  -13. + 15.19868415 I
        -38.33750044                  -13. - 15.19868415 I
        -52.26776194 + 84.09718122 I  -14.924 + 33.19991301 I
        -52.26776194 - 84.09718122 I  -14.924 - 33.19991301 I
        -54.06240993 + 42.18963712 I  -44.25 + 60.55524337 I
        -54.06240593 - 42.18963712 I  -44.25 - 60.55524337 I
        -2.10325088e13                -49.68 + 52.11427444 I
                                      -49.68 - 52.11427444 I
                                      -62.127 + 85.0195617 I
                                      -62.127 - 85.0195617 I

                                           -13
        Factored form gain multiplier: 9.983564129 10

Plant Case: 10  Element: {3, 1}
        Roots of Numerator            Roots of Denominator
        -------------------           --------------------
        0.1678720891                  -0.09251651137 + 0.08045818654 I
        -0.07427813514                -0.09251651137 - 0.08045818654 I
        -12.35470947 + 11.45253655 I  -0.9205298181
        -12.35470947 - 11.45253655 I  -13. + 15.19868415 I
        -14.98296676 + 42.43676389 I  -13. - 15.19868415 I
        -14.98296676 - 42.43676389 I  -14.924 + 33.19991301 I
        -50.57188284 + 50.6583483 I   -14.924 - 33.19991301 I
        -50.57188284 - 50.6583483 I   -44.25 + 60.55524337 I
        -54.35317562 + 83.75141029 I  -44.25 - 60.55524337 I
        -54.35317562 - 83.75141029 I  -49.68 + 52.11427444 I
                                      -49.68 - 52.11427444 I
                                      -62.127 + 85.0195617 I
                                      -62.127 - 85.0195617 I
        Factored form gain multiplier: -601.1576115

Plant Case: 10  Element: {3, 2}
        Roots of Numerator            Roots of Denominator
        -------------------           --------------------
        -1.269098079                  -0.09251651137 + 0.08045818654 I
        -14.75644431 + 21.95264007 I  -0.09251651137 - 0.08045818654 I
        -14.75644431 - 21.95264007 I  -0.9205298181
        -17.06037998 + 86.61864862 I  -13. + 15.19868415 I
        -17.06037998 - 86.61864862 I  -13. - 15.19868415 I
        -2.483068322e14               -14.924 + 33.19991301 I
                                      -14.924 - 33.19991301 I
                                      -62.127 + 85.0195617 I
                                      -62.127 - 85.0195617 I

                                           -14
        Factored form gain multiplier: 4.855706176 10
```

Plant Case: 10 Element: {3, 3}
```
         Roots of Numerator              Roots of Denominator
         -------------------              --------------------
         -0.1480793875                    -0.09251651137 + 0.08045818654 I
         -0.474469106                     -0.09251651137 - 0.08045818654 I
         -13.84367768 + 18.66330543 I     -0.9205298181
         -13.84367768 - 18.66330543 I     -13. + 15.19868415 I
         -15.96173305 + 39.41716903 I     -13. - 15.19868415 I
         -15.96173305 - 39.41716903 I     -14.924 + 33.19991301 I
         -48.696775 + 53.67744713 I       -14.924 - 33.19991301 I
         -48.696775 - 53.67744713 I       -44.25 + 60.55524337 I
         -57.6665138 + 84.21444165 I      -44.25 - 60.55524337 I
         -57.6665138 - 84.21444165 I      -49.68 + 52.11427444 I
                                          -49.68 - 52.11427444 I
                                          -62.127 + 85.0195617 I
                                          -62.127 - 85.0195617 I
         Factored form gain multiplier: -2504.666237
```

Plant Case: 11 Element: {1, 1}
```
         Roots of Numerator              Roots of Denominator
         -------------------              --------------------
         -0.1164654839 + 0.1506634327 I   -0.09496889422 + 0.1716153858 I
         -0.1164654839 - 0.506634327 I    -0.09496889422 - 0.1716153858 I
         -13.15727545 + 15.96343649 I     -0.9156250524
         -13.15727545 - 15.96343649 I     -13. + 15.19868415 I
         -15.73876299 + 42.02598215 I     -13. - 15.19868415 I
         -15.73876299 - 42.02598215 I     -14.924 + 33.19991301 I
         -49.65523427 + 52.14751154 I     -14.924 - 33.19991301 I
         -49.65523427 - 52.14751154 I     -44.25 + 60.55524337 I
         -55.28583452 + 83.80255028 I     -44.25 - 60.55524337 I
         -55.28583452 - 83.80255028 I     -49.68 + 52.11427444 I
                                          -49.68 - 52.11427444 I
                                          -62.127 + 85.0195617 I
                                          -62.127 - 85.0195617 I
         Factored form gain multiplier: 1114.772272
```

Plant Case: 11 Element: {1, 2}
```
         Roots of Numerator              Roots of Denominator
         -------------------              --------------------
         -0.4559228663                    -0.09496889422 + 0.1716153858 I
         -14.75644431 + 21.95264007 I     -0.09496889422 - 0.1716153858 I
         -14.75644431 - 21.95264007 I     -0.9156250524
         -17.06037998 + 86.61864862 I     -13. + 15.19868415 I
         -17.06037998 - 86.61864862 I     -13. - 15.19868415 I
         -1.581103735e14                  -14.924 + 33.19991301 I
                                          -14.924 - 33.19991301 I
                                          -62.127 + 85.0195617 I
                                          -62.127 - 85.0195617 I

                                         -13
         Factored form gain multiplier: 2.360831337 10
```

Plant Case: 11 Element: {1, 3}
```
         Roots of Numerator              Roots of Denominator
         -------------------              --------------------
         0.05106210417 + 0.1148581251 I   -0.09496889422 + 0.1716153858 I
         0.05106210417 - 0.1148581251 I   -0.09496889422 - 0.1716153858 I
         -12.73805662 + 13.7320124 I      -0.9156250524
         -12.73805662 - 13.7320124 I      -13. + 15.19868415 I
         -15.26904733 + 39.84153948 I     -13. - 15.19868415 I
         -15.26904733 - 39.84153948 I     -14.924 + 33.19991301 I
         -49.71708553 + 52.06308674 I     -14.924 - 33.19991301 I
         -49.71708553 - 52.06308674 I     -44.25 + 60.55524337 I
         -56.72323285 + 84.16037367 I     -44.25 - 60.55524337 I
         -56.72323285 - 84.16037367 I     -49.68 + 52.11427444 I
                                          -49.68 - 52.11427444 I
                                          -62.127 + 85.0195617 I
                                          -62.127 - 85.0195617 I
         Factored form gain multiplier: 3081.532346
```

Plant Case: 11 Element: {2, 1}
```
         Roots of Numerator              Roots of Denominator
         -------------------              --------------------
         6.109969385e13                   -0.09496889422 + 0.1716153858 I
         -0.3067093734                    -0.09496889422 - 0.1716153858 I
         -14.32930562 + 20.71139526 I     -0.9156250524
         -14.32930562 - 20.71139526 I     -13. + 15.19868415 I
         -16.8808181 + 41.08160672 I      -13. - 15.19868415 I
```

```
         -16.8808181 - 41.08160672 I        -14.924 + 33.19991301 I
         -48.19685605 + 54.36637579 I       -14.924 - 33.19991301 I
         -48.19685605 - 54.36637579 I       -44.25 + 60.55524337 I
         -56.79467608 + 83.93352453 I       -44.25 - 60.55524337 I
         -56.79467608 - 83.93352453 I       -49.68 + 52.11427444 I
                                            -49.68 - 52.11427444 I
                                            -62.127 + 85.0195617 I
                                            -62.127 - 85.0195617 I

                                          -13
         Factored form gain multiplier: -8.857813824 10

Plant Case: 11  Element: (2, 2)
         Roots of Numerator                Roots of Denominator
         ------------------                --------------------
         -0.05808085747                    -0.09496889422 + 0.1716153858 I
         -0.9222246199                     -0.09496889422 - 0.1716153858 I
         -14.75644431 + 21.95264007 I      -0.9156250524
         -14.75644431 - 21.95264007 I      -13. + 15.19868415 I
         -17.06037998 + 86.61864862 I      -13. - 15.19868415 I
         -17.06037998 - 86.61864862 I      -14.924 + 33.19991301 I
                                           -14.924 - 33.19991301 I
                                           -62.127 + 85.0195617 I
                                           -62.127 - 85.0195617 I
         Factored form gain multiplier: -207.0716183


Plant Case: 11  Element: (2, 3)
         Roots of Numerator                Roots of Denominator
         ------------------                --------------------
         8.842029721e12                    -0.09496889422 + 0.1716153858 I
         41.37265586                       -0.09496889422 - 0.1716153858 I
         -2.106815802                      -0.9156250524
         -12.60304461 + 39.82989704 I      -13. + 15.19868415 I
         -12.60304461 - 39.82989704 I      -13. - 15.19868415 I
         -38.33750044                      -14.924 + 33.19991301 I
         -52.26776194 + 84.09718122 I      -14.924 - 33.19991301 I
         -52.26776194 - 84.09718122 I      -44.25 + 60.55524337 I
         -54.06240993 + 42.18963712 I      -44.25 - 60.55524337 I
         -54.06240993 - 42.18963712 I      -49.68 + 52.11427444 I
                                           -49.68 - 52.11427444 I
                                           -62.127 + 85.0195617 I
                                           -62.127 - 85.0195617 I

                                          -12
         Factored form gain multiplier: -4.749574635 10


Plant Case: 11  Element: (3, 1)
         Roots of Numerator                Roots of Denominator
         ------------------                --------------------
         0.04715806566 + 0.1733354442 I    -0.09496889422 + 0.1716153858 I
         0.04715806566 - 0.1733354442 I    -0.09496889422 - 0.1716153858 I
         -12.35507299 + 11.45251738 I      -0.9156250524
         12.35507299 - 11.45251738 I       -13. + 15.19868415 I
         -14.98295953 + 42.43676196 I      -13. - 15.19868415 I
         -14.98295953 - 42.43676196 I      -14.924 + 33.19991301 I
         -50.57188823 + 50.65835151 I      -14.924 - 33.19991301 I
         -50.57188823 - 50.65835151 I      -44.25 + 60.55524337 I
         -54.35317501 + 83.75140872 I      -44.25 - 60.55524337 I
         -54.35317501 - 83.75140872 I      -49.68 + 52.11427444 I
                                           -49.68 - 52.11427444 I
                                           -62.127 + 85.0195617 I
                                           -62.127 - 85.0195617 I
         Factored form gain multiplier: -601.1576115


Plant Case: 11  Element: (3, 2)
         Roots of Numerator                Roots of Denominator
         ------------------                --------------------
         -1.269098079                      -0.09496889422 + 0.1716153858 I
         -14.75644431 + 21.95264007 I      -0.09496889422 - 0.1716153858 I
         -14.75644431 - 21.9526400/ I      -0.9156250524
         -17.06037998 + 86.61864862 I      -13. + 15.19868415 I
         -17.06037998 - 86.61864862 I      -13. - 15.19868415 I
         -2.899247865e14                   -14.924 + 33.19991301 I
                                           -14.924 - 33.19991301 I
                                           -62.127 + 85.0195617 I
```

155

```
                                    -62.127 - 85.0195617 I

                                              -14
        Factored form gain multiplier: 8.317364189 10

Plant Case: 11  Element: {3, 3}
        Roots of Numerator              Roots of Denominator
        -------------------             --------------------
        -0.2588710912                   -0.09496889422 + 0.1716153858 I
        -0.3638473257                   -0.09496889422 - 0.1716153858 I
        -13.84359022 + 18.66336039 I    -0.9156250524
        -13.84359022 - 18.66336039 I    -13. + 15.19868415 I
        -15.96173941 + 39.41716979 I    -13. - 15.19868415 I
        -15.96173941 - 39.41716979 I    -14.924 + 33.19991301 I
        -48.69677078 + 53.67744495 I    -14.924 - 33.19991301 I
        -48.69677078 - 53.67744495 I    -44.25 + 60.55524337 I
        -57.66651415 + 84.21444281 I    -44.25 - 60.55524337 I
        -57.66651415 - 84.21444281 I    -49.68 + 52.11427444 I
                                        -49.68 - 52.11427444 I
                                        -62.127 + 85.0195617 I
                                        -62.127 - 85.0195617 I
        Factored form gain multiplier: -2504.666237

Plant Case: 12  Element: {1, 1}
        Roots of Numerator              Roots of Denominator
        -------------------             --------------------
        -0.1165949957 + 0.2262142133 I  -0.0987696648 + 0.2613288017 I
        -0.1165949957 - 0.2262142133 I  -0.0987696648 - 0.2613288017 I
        -13.15714302 + 15.96349716 I    -0.9080235113
        -13.15714302 - 15.96349716 I    -13. + 15.19868415 I
        -15.73877012 + 42.02598308 I    -13. - 15.19868415 I
        -15.73877012 - 42.02598308 I    -14.924 + 33.19991301 I
        -49.65522953 + 52.14750889 I    -14.924 - 33.19991301 I
        -49.65522953 - 52.14750889 I    -44.25 + 60.55524337 I
        -55.28583503 + 83.80255171 I    -44.25 - 60.55524337 I
        -55.28583503 - 83.80255171 I    -49.68 + 52.11427444 I
                                        -49.68 - 52.11427444 I
                                        -62.127 + 85.0195617 I
                                        -62.127 - 85.0195617 I
        Factored form gain multiplier: 1114.772272

Plant Case: 12  Element: {1, 2}
        Roots of Numerator              Roots of Denominator
        -------------------             --------------------
        4.795727355e14                  -0.0987696648 + 0.2613288017 I
        -0.4559228663                   -0.0987696648 - 0.2613288017 I
        -14.75644431 + 21.95264007 I    -0.9080235113
        -14.75644431 - 21.95264007 I    -13. + 15.19868415 I
        -17.06037998 + 86.61864862 I    -13. - 15.19868415 I
        -17.06037998 - 86.61864862 I    -14.924 + 33.19991301 I
                                        -14.924 - 33.19991301 I
                                        -62.127 + 85.0195617 I
                                        -62.127 - 85.0195617 I

                                              -13
        Factored form gain multiplier: -1.167514008 10

Plant Case: 12  Element: {1, 3}
        Roots of Numerator              Roots of Denominator
        -------------------             --------------------
        0.05144702817 + 0.2615448508 I  -0.0987696648 + 0.2613288017 I
        0.05144702817 - 0.2615448508 I  -0.0987696648 - 0.2613288017 I
        -12.73844385 + 13.73190828 I    -0.9080235113
        -12.73844385 - 13.73190828 I    -13. + 15.19868415 I
        -15.26903839 + 39.84153694 I    -13. - 15.19868415 I
        -15.26903839 - 39.84153694 I    -14.924 + 33.19991301 I
        -49.71709287 + 52.06309075 I    -14.924 - 33.19991301 I
        -49.71709287 - 52.06309075 I    -44.25 + 60.55524337 I
        -56.72323216 + 84.16037177 I    -44.25 - 60.55524337 I
        -56.72323216 - 84.16037177 I    -49.68 + 52.11427444 I
                                        -49.68 - 52.11427444 I
                                        -62.127 + 85.0195617 I
                                        -62.127 - 85.0195617 I
        Factored form gain multiplier: 3081.532346

Plant Case: 12  Element: {2, 1}
        Roots of Numerator              Roots of Denominator
        -------------------             --------------------
```

```
         -0.3067093734                        -0.0987696648 + 0.2613288017 I
         -14.32930562 + 20.71139526 I         -0.0987696648   0.2613288017 I
         -14.32930562 - 20.71139526 I         -0.9080235113
         -16.8808181 + 41.08160672 I           13. + 15.19868415 I
         -16.8808181 - 41.08160672 I          -13. - 15.19868415 I
         -48.19685605 + 54.36637579 I         -14.924 + 33.19991301 I
         -48.19685605 - 54.36637579 I         -14.924 - 33.19991301 I
         -56.79467608 + 83.93352453 I         -44.25 + 60.55524337 I
         -56.79467608 - 83.93352453 I         -44.25 - 60.55524337 I
         -4.825427599e13                      -49.68 + 52.11427444 I
                                              -49.68 - 52.11427444 I
                                              -62.127 + 85.0195617 I
                                              -62.127 - 85.0195617 I
                                         -12
      Factored form gain multiplier: 1.682368148 10

Plant Case: 12  Element: (2, 2)
         Roots of Numerator               Roots of Denominator
         ------------------               -------------------
         -0.05808085747                       -0.0987696648 + 0.2613288017 I
         -0.9222246199                        -0.0987696648 - 0.2613288017 I
         -14.75644431 + 21.95264007 I         -0.9080235113
         -14.75644431 - 21.95264007 I         -13. + 15.19868415 I
         -17.06037998 + 86.61864862 I         -13. - 15.19868415 I
         -17.06037998 - 86.61864862 I         -14.924 + 33.19991301 I
                                              -14.924 - 33.19991301 I
                                              -62.127 + 85.0195617 I
                                              -62.127 - 85.0195617 I
      Factored form gain multiplier: -207.0716183

Plant Case: 12  Element: (2, 3)
         Roots of Numerator               Roots of Denominator
         ------------------               -------------------
         5.937054509e13                       -0.0987696648 + 0.2613288017 I
         41.37265586                          -0.0987696648 - 0.2613288017 I
         -2.106815802                         -0.9080235113
         -12.60304461 + 39.82989704 I         -13. + 15.19868415 I
         -12.60304461 - 39.82989704 I         -13. - 15.19868415 I
         -38.33750044                         -14.924 + 33.19991301 I
         -52.26776194 + 84.09718122 I         -14.924 - 33.19991301 I
         -52.26776194 - 84.09718122 I         -44.25 + 60.55524337 I
         -54.06240993 + 42.18963712 I         -44.25 - 60.55524337 I
         -54 06240993 - 42.18963712 I         -49.68 + 52.11427444 I
                                              -49.68 - 52.11427444 I
                                              -62.127 + 85.0195617 I
                                              -62.127 - 85.0195617 I
                                         -12
      Factored form gain multiplier: -1.061028158 10

Plant Case: 12  Element: (3, 1)
         Roots of Numerator               Roots of Denominator
         ------------------               ------- ------------
         0.04775982445 + 0.3233355681 I   -0.0987696648 + 0.2613288017 I
         0.04775982445 - 0.3233355681 I   -0.0987696648 - 0.2613288017 I
         -12.35567882 + 11.45248572 I     -0.9080235113
         -12.35567882 - 11.45248572 I     -13. + 15.19868415 I
         -14.98294748 + 42.43675873 I     -13. - 15.19368415 I
         -14.98294748 - 42.43675873 I     -14.924 + 33.19991301 I
         -50.57189723 + 50.65835636 I     -14.924 - 33.19991301 I
         -50.57189723 - 50.65835686 I     -44.25 + 60.55524337 I
         -54.35317399 + 83.75140611 I     -44.25 - 60.55524337 I
         -54.35317399 - 83.75140611 I     -49.68 + 52.11427444 I
                                          -49.68 - 52.11427444 I
                                          -62.127 + 85.0195617 I
                                          -62.127 - 85.0195617 I
      Factored form gain multiplier: -601.1576115

Plant Case: 12  Element: (3, 2)
         Roots of Numerator               Roots of Denominator
         ------------------               -------------------
         3.031142654e14                       -0.0987696648 + 0.2613288017 I
         -1.269098079                         -0.0987696648 - 0.2613288017 I
         -14.75644431 + 21.95264007 I         -0.9080235113
         -14.75644431 - 21.95264007 I         -13. + 15.19868415 I
         -17.06037998 + 86.61864862 I         -13. - 15.19868415 I
         -17.06037998 - 86.61864862 I          14.924 + 33.19991301 I
```

157

```
                                        -14.924 - 33.19991301 I
                                        -62.127 + 85.0195617 I
                                        -62.127 - 85.0195617 I

                                               -13
         Factored form gain multiplier: -1.193317329 10

Plant Case: 12   Element: {3, 3}
         Roots of Numerator                Roots of Denominator
         ------------------                --------------------
         -0.3115008272 + 0.1924602727 I    -0.0987696648 + 0.2613288017 I
         -0.3115008272 - 0.1924602727 I    -0.0987696648 - 0.2613288017 I
         -13.84344444 + 18.66345199 I      -0.9080235113
         -13.84344444 - 18.66345199 I      -13. + 15.19868415 I
         -15.96175001 + 39.41717105 I      -13. - 15.19868415 I
         -15.96175001 - 39.41717105 I      -14.924 + 33.19991301 I
         -48.69676376 + 53.67744132 I      -14.924 - 33.19991301 I
         -48.69676376 - 53.67744132 I      -44.25 + 60.55524337 I
         -57.66651474 + 84.21444475 I      -44.25 - 60.55524337 I
         -57.66651474 - 84.21444475 I      -49.68 + 52.11427444 I
                                           -49.68 - 52.11427444 I
                                           -62.127 + 85.0195617 I
                                           -62.127 - 85.0195617 I
         Factored form gain multiplier: -2504.666237
```

C.2. Effective Plant Bode Plot
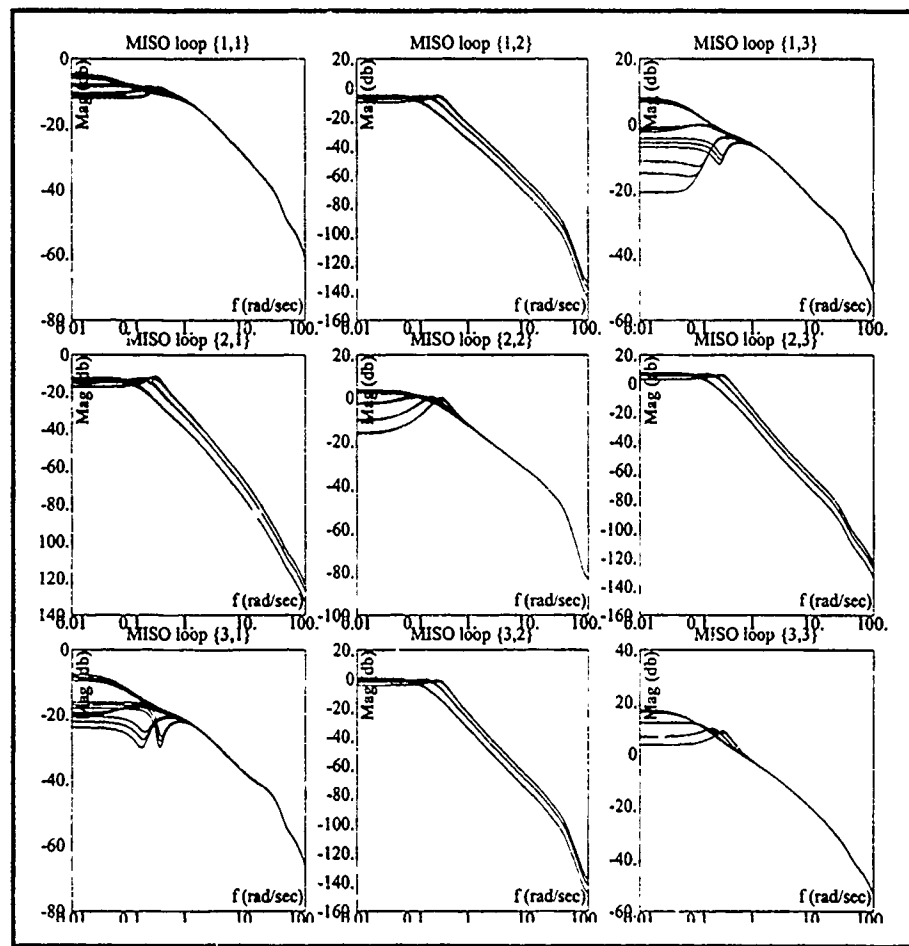
Figure 80. Effective Plant Bode Plot

158

This chapter presents the Q matrix transfer functions for each of the twelve plant cases, after pole-zero cancellation. The twelve cases are defined in the MIMO QFT CAD Package as:

```
                Current List of Plant Models

    Plant    Comments                        Parameter    Value
    -----    --------                        ---------    ----------
    #1                                       h            10000
                                             P            0

    #2                                       h            10000
                                             P            8

    #3                                       h            10000
                                             P            16

    #4                                       h            10000
                                             P            24

    #5                                       h            15000
                                             P            0

    #6                                       h            15000
                                             P            8

    #7                                       h            15000
                                             P            16

    #8                                       h            15000
                                             P            24

    #9                                       h            20000
                                             P            0

    #10                                      h            20000
                                             P            8

    #11                                      h            20000
                                             P            16

    #12                                      h            20000
                                             P            24
```

D.1. Q matrix Transfer Functions

```
Choice> 2  Q Matrix s-Domain Transfer Functions

Plant Case: 1  Element: {1, 1}

        Roots of Numerator              Roots of Denominator
        ------------------              --------------------
        -15.59512403 + 41.20031139 I    -0.57779199
        -15.59512403 - 41.20031139 I    -13.80372315 + 18.55693714 I
        -21.79695528 + 32.80306822 I    -13.80372315 - 18.55693714 I
        -21.79695528 - 32.80306822 I    -15.94702152 + 39.43184289 I
        -55.80497644 + 83.93079561 I    -15.94702152 - 39.43184289 I
        -55.80497644 - 83.93079561 I    -48.71359453 + 53.64893544 I
                                        -48.71359453 - 53.64893544 I
                                        -57.64123437 + 84.21130541 I
                                        -57.64123437 - 84.21130541 I
        Factored form gain multiplier: 382.6380294

Plant Case: 1  Element: {1, 2}

        Roots of Numerator              Roots of Denominator
        ------------------              --------------------
        Factored form gain multiplier: Infinity

Plant Case: 1  Element: {1. 3}

        Roots of Numerator              Roots of Denominator
        ------------------              --------------------
        -15.59512403 + 41.20031139 I    0.250583541
        -15.59512403 - 41.20031139 I    -12.76209141 + 13.81487535 I
        -21.79695528 + 32.80306822 I    -12.76209141 - 13.81487535 I
        -21.79695528 - 32.80306822 I    -15.27589594 + 39.8708367 I
        -55.80497644 + 83.93079561 I    -15.27589594 - 39.8708367 I
        -55.80497644 - 83.93079561 I    -49.72241744 + 52.05562842 I
                                        -49.72241744 - 52.05562842 I
                                        -56.7089719 + 84.15858497 I
                                        -56.7089719 - 84.15858497 I
        Factored form gain multiplier: 308.7019259

Plant Case: 1  Element: {2, 1}

        Roots of Numerator              Roots of Denominator
        ------------------              --------------------
        Factored form gain multiplier: Infinity

Plant Case: 1  Element: {2, 2}

        Roots of Numerator              Roots of Denominator
        ------------------              --------------------
        -14.76581091 + 21.99367018 I    -0.1485284702
        -14.76581091 - 21.99367018 I    -13. + 15.19868415 I
        -17.15376289 + 86.63948955 I    -13. - 15.19868415 I
        -17.15376289 - 86.63948955 I    -14.924 + 33.19991301 I
                                        -14.924 - 33.19991301 I
                                        -62.127 + 85.0195617 I
                                        -62.127 - 85.0195617 I
        Factored form gain multiplier: -204.4085555

Plant Case: 1  Element: {2, 3}

        Roots of Numerator              Roots of Denominator
        ------------------              --------------------
        Factored form gain multiplier: Infinity

Plant Case: 1  Element: {3, 1}

        Roots of Numerator              Roots of Denominator
        ------------------              --------------------
        -15.59512403 + 41.20031139 I    0.2226635869
        -15.59512403 - 41.20031139 I    -12.40529826 + 11.65364509 I
        -21.79695528 + 32.80306822 I    -12.40529826 - 11.65364509 I
        -21.79695528 - 32.80306822 I    -15.00543659 + 42.44927428 I
        -55.80497644 + 83.93079561 I    -15.00543659 - 42.44927428 I
        -55.80497644 - 83.93079561 I    -50.55177141 + 50.69631972 I
                                        -50.55177141 - 50.69631972 I
                                        -54.36332547 + 83.74883311 I
                                        -54.36332547 - 83.74883311 I
```

Factored form gain multiplier: -1579.712919

Plant Case: 1   Element: (3, 2)

　　　　Roots of Numerator　　　　　　Roots of Denominator
　　　　-------------------　　　　　　--------------------
　　　　Factored form gain multiplier: Infinity

Plant Case: 1   Element: (3, 3)

　　　　Roots of Numerator　　　　　　Roots of Denominator
　　　　-------------------　　　　　　--------------------
　　　　-15.59512403 + 41.20031139 I　　-0.1180659113
　　　　-15.59512403 - 41.20031139 I　　-13.1445853 + 15.92479066 I
　　　　-21.79695528 + 32.80306822 I　　-13.1445853 - 15.92479066 I
　　　　-21.79695528 - 32.80306822 I　　-15.73553132 + 42.03227768 I
　　　　-55.80497644 + 83.93079561 I　　-15.73553132 - 42.03227768 I
　　　　-55.80497644 - 83.93079561 I　　-49.65172678 + 52.15231675 I
　　　　　　　　　　　　　　　　　　　　-49.65172678 - 52.15231675 I
　　　　　　　　　　　　　　　　　　　　-55.27372311 + 83.79775981 I
　　　　　　　　　　　　　　　　　　　　-55.27372311 - 83.79775981 I
　　　　Factored form gain multiplier: -853.041063

Plant Case: 2   Element: (1, 1)

　　　　Roots of Numerator　　　　　　Roots of Denominator
　　　　-------------------　　　　　　--------------------
　　　　-15.59512403 + 41.20031139 I　　-0.57779199
　　　　-15.59512403 - 41.20031139 I　　-13.80372315 + 18.55693714 I
　　　　-21.79695528 + 32.80306822 I　　-13.80372315 - 18.55693714 I
　　　　-21.79695528 - 32.80306822 I　　-15.94702152 + 39.43184289 I
　　　　-55.80497643 + 83.9307956 I　　-15.94702152 - 39.43184289 I
　　　　-55.80497643 - 83.9307956 I　　-48.71359453 + 53.64893544 I
　　　　　　　　　　　　　　　　　　　　-48.71359453 - 53.64893544 I
　　　　　　　　　　　　　　　　　　　　-57.64123437 + 84.21130541 I
　　　　　　　　　　　　　　　　　　　　-57.64123437 - 84.21130541 I
　　　　Factored form gain multiplier: 382.6380294

Plant Case: 2   Element: (1, 2)

　　　　Roots of Numerator　　　　　　Roots of Denominator
　　　　-------------------　　　　　　--------------------
　　　　-15.59512403 + 41.20031139 I　　-13.35678088 + 16.63402383 I
　　　　-15.5y512403 - 41.20031139 I　　-13.35678088 - 16.63402383 I
　　　　-21.79695528 + 32.80306822 I　　-15.63942316 + 39.65306512 I
　　　　-21.79695528 - 32.80306822 I　　-15.63942316 - 39.65306512 I
　　　　-55.80497643 + 83.9307956 I　　-49.17612021 + 52.93500268 I
　　　　-55.80497643 - 83.9307956 I　　-49.17612021 - 52.93500268 I
　　　　　　　　　　　　　　　　　　　　-57.21442398 + 84.18185775 I
　　　　　　　　　　　　　　　　　　　　-57.21442398 - 84.18185775 I
　　　　Factored form gain multiplier: 2357.550639

Plant Case: 2   Element: (1, 3)

　　　　Roots of Numerator　　　　　　Roots of Denominator
　　　　-------------------　　　　　　--------------------
　　　　-15.59512403 + 41.20031139 I　　0.250583541
　　　　-15.59512403 - 41.20031139 I　　-12.76209141 + 13.81487535 I
　　　　-21.79695528 + 32.80306822 I　　-12.76209141 - 13.81487535 I
　　　　-21.79695528 - 32.80306822 I　　-15.27589594 + 39.8708367 I
　　　　-55.80497643 + 83.9307956 I　　-15.27589594 - 39.8708367 I
　　　　-55.80497643 - 83.9307956 I　　-49.72241744 + 52.05562842 I
　　　　　　　　　　　　　　　　　　　　-49.72241744 - 52.05562842 I
　　　　　　　　　　　　　　　　　　　　-56.7089719 + 84.15858497 I
　　　　　　　　　　　　　　　　　　　　-56.7089719 - 84.15858497 I
　　　　Factored form gain multiplier: 308.7019259

Plant Case: 2   Element: (2, 1)

　　　　Roots of Numerator　　　　　　Roots of Denominator
　　　　-------------------　　　　　　--------------------
　　　　-14.76581091 + 21.99367018 I　　-13. + 15.19868415 I
　　　　-14.76581091 - 21.99367018 I　　-13. - 15.19868415 I
　　　　-17.15376289 + 86.63948955 I　　-14.924 + 33.19991301 I
　　　　-17.15376289 - 86.63948955 I　　-14.924 - 33.19991301 I
　　　　　　　　　　　　　　　　　　　　-62.127 + 85.0195617 I
　　　　　　　　　　　　　　　　　　　　-62.127 - 85.0195617 I

161

Factored form gain multiplier: 3482.434837

Plant Case: 2   Element: (2, 2)

```
       Roots of Numerator              Roots of Denominator
       -------------------             --------------------
       -14.76581091 + 21.99367018 I    -0.1485284702
       -14.76581091 - 21.99367018 I    -13. + 15.19868415 I
       -17.15376289 + 86.63948955 I    -13. - 15.19868415 I
       -17.15376289 - 86.63948955 I    -14.924 + 33.19991301 I
                                       -14.924 - 33.19991301 I
                                       -62.127 + 85.0195617 I
                                       -62.127 - 85.0195617 I
       Factored form gain multiplier: -204.4085555
```

Plant Case: 2   Element: (2, 3)

```
       Roots of Numerator              Roots of Denominator
       -------------------             --------------------
       -14.76581091 + 21.99367018 I    -13. + 15.19868415 I
       -14.76581091 - 21.99367018 I    -13. - 15.19868415 I
       -17.15376289 + 86.63948955 I    -14.924 + 33.19991301 I
       -17.15376289 - 86.63948955 I    -14.924 - 33.19991301 I
                                       -62.127 + 85.0195617 I
                                       -62.127 - 85.0195617 I
       Factored form gain multiplier: 3202.270107
```

Plant Case: 2   Element: (3, 1)

```
       Roots of Numerator              Roots of Denominator
       -------------------             --------------------
       -15.59512403 + 41.20031139 I    0.2226635869
       -15.59512403 - 41.20031139 I    -12.40529826 + 11.65364509 I
       -21.79695528 + 32.80306822 I    -12.40529826 - 11.65364509 I
       -21.79695528 - 32.80306822 I    -15.00543659 + 42.44927428 I
       -55.80497643 + 83.9307956 I     -15.00543659 - 42.44927428 I
       -55.80497643 - 83.9307956 I     -50.55177141 + 50.69631972 I
                                       -50.55177141 - 50.69631972 I
                                       -54.36332547 + 83.74883311 I
                                       -54.36332547 - 83.74883311 I
       Factored form gain multiplier: -1579.712919
```

Plant Case: 2   Element: (3, 2)

```
       Roots of Numerator              Roots of Denominator
       -------------------             --------------------
       -15.59512403 + 41.20031139 I    -12.74972514 + 14.11765519 I
       -15.59512403 - 41.20031139 I    -12.74972514 - 14.11765519 I
       -21.79695528 + 32.80306822 I    -15.39829491 + 42.24727899 I
       -21.79695528 - 32.80306822 I    -15.39829491 - 42.24727899 I
       -55.80497643 + 83.9307956 I     -50.0716342 + 51.4766149 I
       -55.80497643 - 83.9307956 I     -50.0716342 - 51.4766149 I
                                       -54.84580086 + 83.7743349 I
                                       -54.84580086 - 83.7743349 I
       Factored form gain multiplier: -7980.02408
```

Plant Case: 2   Element: (3, 3)

```
       Roots of Numerator              Roots of Denominator
       -------------------             --------------------
       -15.59512403 + 41.20031139 I    -0.1180659113
       -15.59512403 - 41.20031139 I    -13.1445853 + 15.92479066 I
       -21.79695528 + 32.80306822 I    -13.1445853 - 15.92479066 I
       -21.79695528 - 32.80306822 I    -15.73553132 + 42.03227768 I
       -55.80497643 + 83.9307956 I     -15.73553132 - 42.03227768 I
       -55.80497643 - 83.9307956 I     -49.65172678 + 52.15231675 I
                                       -49.65172678 - 52.15231675 I
                                       -55.27372311 + 83.79775981 I
                                       -55.27372311 - 83.79775981 I
       Factored form gain multiplier: -853.0410631
```

Plant Case: 3   Element: (1, 1)

```
       Roots of Numerator              Roots of Denominator
       -------------------             --------------------
       -15.59512403 + 41.20031139 I    -0.57779199
       -15.59512403 - 41.20031139 I    -13.80372315 + 18.55693714 I
```

162

```
         -21.79695528 + 32.80306822 I        -13.80372315 - 18.55693714 I
         -21.79695528 - 32.80306822 I        -15.94702152 + 39.43184289 I
         -55.80497644 + 83.93079561 I        -15.94702152 - 39.43184289 I
         -55.80497644 - 83.93079561 I        -48.71359453 + 53.64893544 I
                                             -48.71359453 - 53.64893544 I
                                             -57.64123437 + 84.21130541 I
                                             -57.64123437 - 84.21130541 I
         Factored form gain multiplier: 382.6380294
```

Plant Case: 3 Element: (1, 2)

```
    Roots of Numerator                  Roots of Denominator
    ------------------                  --------------------
    -15.59512403 + 41.20031139 I        -13.35678088 + 16.63402383 I
    -15.59512403 - 41.20031139 I        -13.35678088 - 16.63402383 I
    -21.79695528 + 32.80306822 I        -15.63942316 + 39.65306512 I
    -21.79695528 - 32.80306822 I        -15.63942316 - 39.65306512 I
    -55.80497644 + 83.93079561 I        -49.17612021 + 52.93500268 I
    -55.80497644 - 83.93079561 I        -49.17612021 - 52.93500268 I
                                        -57.21442398 + 84.18185775 I
                                        -57.21442398 - 84.18185775 I
    Factored form gain multiplier: 1178.775319
```

Plant Case: 3 Element: (1, 3)

```
    Roots of Numerator                  Roots of Denominator
    ------------------                  --------------------
    -15.59512403 + 41.20031139 I        0.250583541
    -15.59512403 - 41.20031139 I        -12.76209141 + 13.81487535 I
    -21.79695528 + 32.80306822 I        -12.76209141 - 13.81487535 I
    -21.79695528 - 32.80306822 I        -15.27589594 + 39.8708367 I
    -55.80497644 + 83.93079561 I        -15.27589594 - 39.8708367 I
    -55.80497644 - 83.93079561 I        -49.72241744 + 52.05562842 I
                                        -49.72241744 - 52.05562842 I
                                        -56.7089719 + 84.15858497 I
                                        -56.7089719 - 84.15858497 I
    Factored form gain multiplier: 308.7019259
```

Plant Case: 3 Element: (2, 1)

```
    Roots of Numerator                  Roots of Denominator
    ------------------                  --------------------
    -14.76581091 + 21.99367018 I        -13. + 15.19868415 I
    -14.76581091 - 21.99367018 I        -13. - 15.19868415 I
    -17.15376289 + 86.63948955 I        -14.924 + 33.19991301 I
    -17.15376289 - 86.63948955 I        -14.924 - 33.19991301 I
                                        -62.127 + 85.0195617 I
                                        -62.127 - 85.0195617 I
    Factored form gain multiplier: 1741.217419
```

Plant Case: 3 Element: (2, 2)

```
    Roots of Numerator                  Roots of Denominator
    ------------------                  --------------------
    -14.76581091 + 21.99367018 I        -0.1485284702
    -14.76581091 - 21.99367018 I        -13. + 15.19868415 I
    -17.15376289 + 86.63948955 I        -13. - 15.19868415 I
    -17.15376289 - 86.63948955 I        -14.924 + 33.19991301 I
                                        -14.924   33.19991301 I
                                        -62.127 + 85.0195617 I
                                        -62.127 - 85.0195617 I
    Factored form gain multiplier: -204.4085555
```

Plant Case: 3 Element: (2, 3)

```
    Roots of Numerator                  Roots of Denominator
    ------------------                  --------------------
    -14.76581091 + 21.99367018 I        -13. + 15.19868415 I
    -14.76581091 - 21.99367018 I        -13. - 15.19868415 I
    -17.15376289 + 86.63948955 I        -14.924 + 33.19991301 I
    -17.15376289 - 86.63948955 I        -14.924 - 33.19991301 I
                                        -62.127 + 85.0195617 I
                                        -62.127 - 85.0195617 I
    Factored form gain multiplier: 1601.135053
```

Plant Case: 3 Element: (3, 1)

```
    Roots of Numerator                  Roots of Denominator
```

```
        ------------------              --------------------
        -15.59512403 + 41.20031139 I    0.2226635869
        -15.59512403 - 41.20031139 I    -12.40529826 + 11.65364509 I
        -21.79695528 + 32.80306822 I    -12.40529826 - 11.65364509 I
        -21.79695528 - 32.80306822 I    -15.00543659 + 42.44927428 I
        -55.80497644 + 83.93079561 I    -15.00543659 - 42.44927428 I
        -55.80497644 - 83.930  :51 I    -50.55177141 + 50.69631972 I
                                        -50.55177141 - 50.69631972 I
                                        -54.36332547 + 83.74883311 I
                                        -54.36332547 - 83.74883311 I
        Factored form gain multiplier: -1579.712919

Plant Case: 3  Element: (3, 2)

        Roots of Numerator              Roots of Denominator
        ------------------              --------------------
        -15.59512403 + 41.20031139 I    -12.74972514 + 14.11765519 I
        -15.59512403 - 41.20031139 I    -12.74972514 - 14.11765519 I
        -21.79695528 + 32.80306822 I    -15.39829491 + 42.24727899 I
        -21.79695528 - 32.80306822 I    -15.39829491 - 42.24727899 I
        -55.80497644 + 83.93079561 I    -50.0716342 + 51.4766149 I
        -55.80497644 - 83.93079561 I    -50.0716342 - 51.4766149 I
                                        -54.84580086 + 83.7743349 I
                                        -54.84580086 - 83.7743349 I
        Factored form gain multiplier: -3990.01204

Plant Case: 3  Element: (3, 3)

        Roots of Numerator              Roots of Denominator
        ------------------              --------------------
        -15.59512403 + 41.20031139 I    -0.1180659113
        -15.59512403 - 41.20031139 I    -13.1445853 + 15.92479066 I
        -21.79695528 + 32.80306822 I    -13.1445853 - 15.92479066 I
        -21.79695528 - 32.80306822 I    -15.73553132 + 42.03227768 I
        -55.80497644 + 83.93079561 I    -15.73553132 - 42.03227768 I
        -55.80497644 - 83.93079561 I    -49.65172678 + 52.15231675 I
                                        -49.65172678 - 52.15231675 I
                                        -55.27372311 + 83.79775981 I
                                        -55.27372311 - 83.79775981 I
        Factored form gain multiplier: -853.041063


Plant Case: 4  Element: (1, 1)

        Roots of Numerator              Roots of Denominator
        ------------------              --------------------
        -15.59512403 + 41.20031139 I    -0.57779199
        -15.59512403 - 41.20031139 I    -13.80372315 + 18.55693714 I
        -21.79695528 + 32.80306822 I    -13.80372315 - 18.55693714 I
        -21.79695528 - 32.80306822 I    -15.94702152 + 39.43184289 I
        -55.80497644 + 83.93079561 I    -15.94702152 - 39.43184289 I
        -55.80497644 - 83.93079561 I    -48.71359453 + 53.64893544 I
                                        -48.71359453 - 53.64893544 I
                                        -57.64123437 + 84.21130541 I
                                        -57.64123437 - 84.21130541 I
        Factored form gain multiplier: 382.6380294

Plant Case: 4  Element: (1, 2)

        Roots of Numerator              Roots of Denominator
        ------------------              --------------------
        -15.59512403 + 41.20031139 I    -13.35678088 + 16.63402383 I
        -15.59512403 - 41.20031139 I    -13.35678088 - 16.63402383 I
        -21.79695528 + 32.80306822 I    -15.63942316 + 39.65306512 I
        -21.79695528 - 32.80306822 I    -15.63942316 - 39.65306512 I
        -55.80497644 + 83.93079561 I    -49.17612021 + 52.93500268 I
        -55.80497644 - 83.93079561 I    -49.17612021 - 52.93500268 I
                                        -57.21442398 + 84.18185775 I
                                        -57.21442398 - 84.18185775 I
        Factored form gain multiplier: 785.8502129

Plant Case: 4  Element: (1, 3)

        Roots of Numerator              Roots of Denominator
        ------------------              --------------------
        -15.59512403 + 41.20031139 I    0.250583541
        -15.59512403 - 41.20031139 I    -12.76209141 + 13.81487535 I
        -21.79695528 + 32.80306822 I    -12.76209141 - 13.81487535 I
```

164

```
      -21.79695528 - 32.80306822 I        -15.27589594 + 39.8708367 I
      -55.80497644 + 83.93079561 I        -15.27589594 - 39.8708367 I
      -55.80497644 - 83.93079561 I        -49.72241744 + 52.05562842 I
                                           -49.72241744 - 52.05562842 I
                                           -56.7089719 + 84.15858497 I
                                           -56.7089719 - 84.15858497 I
          Factored form gain multiplier: 308.7019259
```

Plant Case: 4   Element: (2, 1)

```
          Roots of Numerator                Roots of Denominator
          ------------------                --------------------
          -14.76581091 + 21.99367018 I      -13. + 15.19868415 I
          -14.76581091 - 21.99367018 I      -13. - 15.19868415 I
          -17.15376289 + 86.63948955 I      -14.924 + 33.19991301 I
          -17.15376289 - 86.63948955 I      -14.924 - 33.19991301 I
                                            -62.127 + 85.0195617 I
                                            -62.127 - 85.0195617 I
          Factored form gain multiplier: 1160.811612
```

Plant Case: 4   Element: (2, 2)

```
          Roots of Numerator                Roots of Denominator
          ------------------                --------------------
          -14.76581091 + 21.99367018 I      -0.1485284702
          -14.76581091 - 21.99367018 I      -13. + 15.19868415 I
          -17.15376289 + 86.63948955 I      -13. - 15.19868415 I
          -17.15376289 - 86.63948955 I      -14.924 + 33.19991301 I
                                            -14.924 - 33.19991301 I
                                            -62.127 + 85.0195617 I
                                            -62.127 - 85.0195617 I
          Factored form gain multiplier: -204.4085555
```

Plant Case: 4   Element: (2, 3)

```
          Roots of Numerator                Roots of Denominator
          ------------------                --------------------
          -14.76581091 + 21.99367018 I      -13. + 15.19868415 I
          -14.76581091 - 21.99367018 I      -13. - 15.19868415 I
          -17.15376289 + 86.63948955 I      -14.924 + 33.19991301 I
          -17.15376289 - 86.63948955 I      -14.924 - 33.19991301 I
                                            -62.127 + 85.0195617 I
                                            -62.127 - 85.0195617 I
          Factored form gain multiplier: 1067.423769
```

Plant Case: 4   Element: (3, 1)

```
          Roots of Numerator                Roots of Denominator
          ------------------                --------------------
          -15.59512403 + 41.20031139 I      0.2226635869
          -15.59512403 - 41.20031139 I      -12.40529826 + 11.65364509 I
          -21.79695528 + 32.80306822 I      -12.40529826 - 11.65364509 I
          -21.79695528 - 32.80306822 I      -15.00543659 + 42.44927428 I
          -55.80497644 + 83.93079561 I      -15.00543659 - 42.44927428 I
          -55.80497644 - 83.93079561 I      -50.55177141 + 50.69631972 I
                                            -50.55177141 - 50.69631972 I
                                            -54.36332547 + 83.74883311 I
                                            -54.36332547 - 83.74883311 I
          Factored form gain multiplier: -1579.712919
```

Plant Case: 4   Element: (3, 2)

```
          Roots of Numerator                Roots of Denominator
          ------------------                --------------------
          -15.59512403 + 41.20031139 I      -12.74972514 + 14.11765519 I
          -15.59512403 - 41.20031139 I      -12.74972514 - 14.11765519 I
          -21.79695528 + 32.80306822 I      -15.39829491 + 42.24727899 I
          -21.79695528 - 32.80306822 I      -15.39829491 - 42.24727899 I
          -55.80497644 + 83.93079561 I      -50.0716342 + 51.4766149 I
          -55.80497644 - 83.93079561 I      -50.0716342 - 51.4766149 I
                                            -54.84580086 + 83.7743349 I
                                            -54.84580086 - 83.7743349 I
          Factored form gain multiplier: -2660.008027
```

Plant Case: 4   Element: (3, 3)

```
          Roots of Numerator                Roots of Denominator
          ------------------                --------------------
```

```
        -15.59512403 + 41.20031139 I    -0.1180659113
        -15.59512403 - 41.20031139 I    -13.1445853 + 15.92479066 I
        -21.79695528 + 32.80306822 I    -13.1445853 - 15.92479066 I
        -21.79695528 - 32.80306822 I    -15.73553132 + 42.03227768 I
        -55.80497644 + 83.93079561 I    -15.73553132 - 42.03227768 I
        -55.80497644 - 83.93079561 I    -49.65172678 + 52.15231675 I
                                         -49.65172678 - 52.15231675 I
                                         -55.27372311 + 83.79775981 I
                                         -55.27372311 - 83.79775981 I
        Factored form gain multiplier: -853.041063


Plant Case: 5  Element: {1, 1}

        Roots of Numerator              Roots of Denominator
        -------------------             --------------------
        -15.59067855 + 41.19171381 I    -0.536633144
        -15.59067855 - 41.19171381 I    -13.82385478 + 18.61043872 I
        -21.88667475 + 32.91844932 I    -13.82385478 - 18.61043872 I
        -21.88 67475 - 32.91844932 I    -15.95495777 + 39.42818093 I
        -55.81 27537 + 83.93326683 I    -15.95495777 - 39.42818093 I
        -55.81227537 - 83.93326683 I    -48.70565529 + 53.66243292 I
                                         -48.70565529 - 53.66243292 I
                                         -57.65121702 + 84.21232942 I
                                         -57.65121702 - 84.21232942 I
        Factored form gain multiplier: 378.7116103


Plant Case: 5  Element: {1, 2}

        Roots of Numerator              Roots of Denominator
        -------------------             --------------------
        Factored form gain multiplier: Infinity


Plant Case: 5  Element: {1, 3}

        Roots of Numerator              Roots of Denominator
        -------------------             --------------------
        -15.59067855 + 41.19171381 I    0.2385145022
        -15.59067855 - 41.19171381 I    -12.74971151 + 13.7726672 I
        -21.88667475 + 32.91844932 I    -12.74971151 - 13.7726672 I
        -21.88667475 - 32.91844932 I    -15.27249035 + 39.85762199 I
        -55.81227537 + 83.93326683 I    -15.27249035 - 39.85762199 I
        -55.81227537 - 83.93326683 I    -49.68 + 52.11427444 I
                                         -49.68 - 52.11427444 I
                                         -56.71481482 + 84.1592048 I
                                         -56.71481482 - 84.1592048 I
        Factored form gain multiplier: 306.6894329


Plant Case: 5  Element: {2, 1}

        Roots of Numerator              Roots of Denominator
        -------------------             --------------------
        Factored form gain multiplier: Infinity


Plant Case: 5  Element: {2, 2}

        Roots of Numerator              Roots of Denominator
        -------------------             --------------------
        -14 76364568 + 21.98417326 I    -0.1366001171
        -14.76364568 - 21.98417326 I    -13. + 15.19 8415 I
        -17.13211925 + 86.63467236 I    -13. - 15.19868415 I
        -17.13211925 - 86.63467236 I    -14.924 + 33.19991301 I
                                         -14.924 - 33.19991301 I
                                         -62.127 + 85.0195617 I
                                         -62.127 - 85.0195617 I
        Factored form gain multiplier: -205.312979


Plant Case: 5  Element: {2, 3}

        Roots of Numerator              Roots of Denominator
        -------------------             --------------------
        Factor. form gain multiplier: Infinity


Plant Case: 5  Element: {3, 1}

        Roots of Numerator              Roots of Denominator
        -------------------             --------------------
        -15.59067855 + 41.19171381 I    0.2210511777
```

```
        -15.59067855 - 41.19171381 I      -12.38008903 + 11.5545971 I
        -21.88667475 + 32.91844932 I      -12.38008903 - 11.5545971 I
        -21.88667475 - 32.91844932 I      -14.99454494 + 42.44663728 I
        -55.81227537 + 83.93326683 I      -14.99454494 - 42.44663728 I
        -55.81227537 - 83.93326683 I      -50.5611786 + 50.6784398 I
                                          -50.5611786 - 50.6784398 I
                                          -54.3552077 + 83.7490214 I
                                          -54.3552077 - 83.7490214 I
        Factored form gain multiplier: -1570.318368

Plant Case: 5  Element: (3, 2)

        Roots of Numerator              Roots of Denominator
        ------------------              --------------------
        Factored form gain multiplier: Infinity

Plant Case: 5  Element: (3, 3)

        Roots of Numerator              Roots of Denominator
        ------------------              --------------------
        -15.59067855 + 41.19171381 I      -0.1126673471
        -15.59067855 - 41.19171381 I      -13.15110836 + 15.94448679 I
        -21.88667475 + 32.91844932 I      -13.15110836 - 15.94448679 I
        -21.88667475 - 32.91844932 I      -15.73743682 + 42.03080543 I
        -55.81227537 + 83.93326683 I      -15.73743682 - 42.03080543 I
        -55.81227537 - 83.93326683 I      -49.65339301 + 52.15007315 I
                                          -49.65339301 - 52.15007315 I
                                          -55.2784838 + 83.79977156 I
                                          -55.2784838 - 83.79977156 I
        Factored form gain multiplier: -847.2818334


Plant Case: 6  Element: (1, 1)

        Roots of Numerator              Roots of Denominator
        ------------------              --------------------
        -15.59067855 + 41.19171381 I      -0.536633144
        -15.59067855 - 41.19171381 I      -13.82385478 + 18.61043872 I
        -21.88667476 + 32.91844932 I      -13.82385478 - 18.61043872 I
        -21.88667476 - 32.91844932 I      -15.95495777 + 39.42818093 I
        -55.81227537 + 83.93326683 I      -15.95495777 - 39.42818093 I
        -55.81227537 - 83.93326683 I      -48.70565529 + 53.66243292 I
                                          -48.70565529 - 53.66243292 I
                                          -57.65121702 + 84.21232942 I
                                          -57.65121702 - 84.21232942 I
        Factored form gain multiplier: 378.7116103

Plant Case: 6  Element: (1, 2)

        Roots of Numerator              Roots of Denominator
        ------------------              --------------------
        -15.59067855 + 41.19171381 I      -13.36268454 + 16.65678236 I
        -15.59067855 - 41.19171381 I      -13.36268454 - 16.65678236 I
        -21.88667476 + 32.91844932 I      -15.64223442 + 39.64547173 I
        -21.88667476 - 32.91844932 I      -15.64223442 - 39.64547173 I
        -55.81227537 + 83.93326683 I      -49.17003703 + 52.94480699 I
        -55.81227537 - 83.93326683 I      -49.17003703 - 52.94480699 I
                                          -57.22306713 + 84.18279199 I
                                          -57.22306713 - 84.19279199 I
        Factored form gain multiplier: 2336.917036

Plant Case: 6  Element: (1, 3)

        Roots of Numerator              Roots of Denominator
        --- ----------------            --------------------
        -15.59067855 + 41.19171381 I      0.2385145022
        -15.59067855 - 41.19171381 I      -12.74971151 + 13.7726672 I
        -21.88667476 + 32.91844932 I      -12.74971151 - 13.7726672 I
        -21.88667476 - 32.91844932 I      -15.27249035 + 39.85762199 I
        -55.81227537 + 83.93326683 I      -15.27249035 - 39.85762199 I
        -55.81227537 - 83.93326683 I      -49.68 + 52.11427444 I
                                          -49.68 - 52.11427444 I
                                          -56.71481482 + 84.1592048 I
                                          -56.71481482 - 84.1592048 I
        Factored form gain multiplier: 306.6894329


Plant Case: 6  Element: (2, 1)
```

167

```
          Roots of Numerator           Roots of Denominator
          -------------------           --------------------
          -14.76364568 + 21.98417326 I   -13. + 15.19868415 I
          -14.76364568 - 21.98417326 I   -13. - 15.19868415 I
          -17.13211925 + 86.63467236 I   -14.924 + 33.19991301 I
          -17.13211925 - 86.63467236 I   -14.924 - 33.19991301 I
                                         -62.127 + 85.0195617 I
                                         -62.127 - 85.0195617 I
          Factored form gain multiplier: 3497.843174

Plant Case: 6  Element: (2, 2)

          Roots of Numerator           Roots of Denominator
          -------------------           --------------------
          -14.76364568 + 21.98417326 I   -0.1366001171
          -14.76364568 - 21.98417326 I   -13. + 15.19868415 I
          -17.13211925 + 86.63467236 I   -13. - 15.19868415 I
          -17.13211925 - 86.63467236 I   -14.924 + 33.19991301 I
                                         -14.924 - 33.19991301 I
                                         -62.127 + 85.0195617 I
                                         -62.127 - 85.0195617 I
          Factored form gain multiplier: -205.312979

Plant Case: 6  Element: (2, 3)

          Roots of Numerator           Roots of Denominator
          -------------------           --------------------
          -14.76364568 + 21.98417326 I   -13. + 15.19868415 I
          -14.76364568 - 21.98417326 I   -13. - 15.19868415 I
          -17.13211925 + 86.63467236 I   -14.924 + 33.19991301 I
          -17.13211925 - 86.63467236 I   -14.924 - 33.19991301 I
                                         -62.127 + 85.0195617 I
                                         -62.127 - 85.0195617 I
          Factored form gain multiplier: 3216.43883

Plant Case: 6  Element: (3, 1)

          Roots of Numerator           Roots of Denominator
          -------------------           --------------------
          -15.59067855 + 41.19171381 I   0.2210511777
          -15.59067855 - 41.19171381 I   -12.38008903 + 11.5545971 I
          -21.88667476 + 32.91844932 I   -12.38008903 - 11.5545971 I
          -21.88667476 - 32.91844932 I   -14.99454494 + 42.44663728 I
          -55.81227537 + 83.93326683 I   -14.99454494 - 42.44663728 I
          -55.81227537 - 83.93326683 I   -50.5611786 + 50.6784398 I
                                         -50.5611786 - 50.6784398 I
                                         -54.3552077 + 83.7490214 I
                                         -54.3552077 - 83.7490214 I
          Factored form gain multiplier: -1570.318368

Plant Case: 6  Element: (3, 2)

          Roots of Numerator           Roots of Denominator
          -------------------           --------------------
          -15.59067855 + 41.19171381 I   -12.74494582 + 14.09618803 I
          -15.59067855 - 41.19171381 I   -12.74494582 - 14.09618803 I
          -21.88667476 + 32.91844932 I   -15.39404714 + 42.2455865 I
          -21.88667476 - 32.91844932 I   -15.39404714 - 42.2455865 I
          -55.81227537 + 83.93326683 I   -50.07711236 + 51.46758105 I
          -55.81227537 - 83.93326683 I   -50.07711236 - 51.46758105 I
                                         -54.84457175 + 83.77539572 I
                                         -54.84457175 - 83.77539572 I
          Factored form gain multiplier: -7929.069071

Plant Case: 6  Element: (3, 3)

          Roots of Numerator           Roots of Denominator
          -------------------           --------------------
          -15.59067855 + 41.19171381 I   -0.1126673471
          -15.59067855 - 41.19171381 I   -13.15110836 + 15.94448679 I
          -21.88667476 + 32.91844932 I   -13.15110836 - 15.94448679 I
          -21.88667476 - 32.91844932 I   -15.73743682 + 42.03080543 I
          -55.81227537 + 83.93326683 I   -15.73743682 - 42.03080543 I
          -55.81227537 - 83.93326683 I   -49.65339301 + 52.15007315 I
                                         -49.65339301 - 52.15007315 I
                                         -55.2784838   83.79977156 I
                                         -55.2784838   83.79977155 I
```

Factored form gain multiplier: -847.2818333

Press RETURN for next plant, enter a plant number, or 0 if done:

Plant Case: 7 Element: (1, 1)

```
        Roots of Numerator            Roots of Denominator
        -------------------            -------------------
        -15.59067855 + 41.19171381 I   -0.536633144
        -15.59067855 - 41.19171381 I   -13.82385478 + 18.61043872 I
        -21.88667476 + 32.91844932 I   -13.82385478 - 18.61043872 I
        -21.88667476 - 32.91844932 I   -15.95495777 + 39.42818093 I
        -55.81227536 + 83.93326683 I   -15.95495777 - 39.42818093 .
        -55.81227536 - 83.93326683 I   -48.70565529 + 53.66243292 I
                                       -48.70565529 - 53.66243292 I
                                       -57.65121702 + 84.21232942 I
                                       -57.65121702 - 84.21232942 I
        Factored form gain multiplier: 378.7116103
```

Plant Case: 7 Element: (1, 2)

```
        Roots of Numerator            Roots of Denominator
        -------------------            -------------------
        -15.59067855 + 41.19171381 I   -13.35268454 + 16.65678236 I
        -15.59067855 - 41.19171381 I   -13.36268454 - 16.65678236 I
        -21.88667476 + 32.91844932 I   -15.64223442 + 39.64547173 I
        -21.88667476 - 32.91844932 I   -15.64223442 - 39.64547173 I
        -55.81227536 + 83.93326683 I   -49.17003703 + 52.94480699 I
        -55.81227536 - 83.93326683 I   -49.17003703 - 52.94480699 I
                                       -57.22306713 + 84.18279199 I
                                       -57.22306713 - 84.18279199 I
        Factored form gain multiplier: 1168.458518
```

Plant Case: 7 Element: (1, 3)

```
        Roots of Numerator            Roots of Denominator
        -------------------            -------------------
        -15.59067855 + 41.19171381 I   0.2385145022
        -15.59067855 - 41.19171381 I   -12.74971151 + 13.7726672 I
        -21.88667476 + 32.91844932 I   -12.74971151 - 13.7726672 I
       -21.88667476 - 32.91844932 I    -15.27249035 + 39.85762199 I
        -55.81227536 + 83.93326683 I   -15.27249035 - 39.85762199 I
        -55.81227536 - 83.93326683 I   -49.68 + 52.11427444 I
                                       -49.68 - 52.11427444 I
                                       -56.71481482 + 84.1592048 I
                                       -56.71481482 - 84.1592048 I
        Factored form gain multiplier: 306.6894329
```

Plant Case: 7 Element: (2, 1)

```
        Roots of Numerator            Roots of Denominator
        -------------------            -------------------
        -14.76364568 + 21.98417326 I   -13. + 15.19868415 I
        -14.76364568 - 21.98417326 I   -13. - 15.19868415 I
        -17.13211925 + 86.63467236 I   -14.924 + 33.19991301 I
        -17.13211925 - 86.63467236 I   -14.924 - 33.19991301 I
                                       -62.127 + 85.0195617 I
                                       -62.127 - 85.0195617 I
        Factored form gain multiplier: 1748.921587
```

Plant Case: 7 Element: (2, 2)

```
        Roots of Numerator            Roots of Denominator
        -------------------            -------------------
        -14.76364568 + 21.98417326 I   -0.1366001171
        -14.76364568 - 21.98417326 I   -13. + 15.19868415 I
        -17.13211925 + 86.63467236 I   -13. - 15.19868415 I
        -17.13211925 - 86.63467236 I   -14.924 + 33.19991301 I
                                       -14.924 - 33.19991301 I
                                       -62.127 + 85.0195617 I
                                       -62.127 - 85.0195617 I
        Factored form gain multiplier: -205.312979
```

Plant Case: 7 Element: (2, 3)

```
        Roots of Numerator            Roots of Denominator
        -------------------            -------------------
        -14.76364568 + 21.98417326 I   -13. + 15.19868415 I
```

```
     -14.76364568 - 21.98417326 I      -13. - 15.19868415 I
     -17.13211925 + 86.63467236 I      -14.924 + 33.19991301 I
     -17.13211925 - 86.63467236 I      -14.924 - 33.19991301 I
                                        -62.127 + 85.0195617 I
                                        -62.127 - 85.0195617 I
        Factored form gain multiplier: 1608.219415
```

Plant Case: 7 Element: {3, 1}

```
        Roots of Numerator              Roots of Denominator
        -------------------             --------------------
        -15.59067855 + 41.19171381 I    0.2210511777
        -15.59067855 - 41.19171381 I    -12.38008903 + 11.5545971 I
        -21.88667476 + 32.91844932 I    -12.38008903 - 11.5545971 I
        -21.88667476 - 32.91844932 I    -14.99454494 + 42.44663728 I
        -55.81227536 + 83.93326683 I    -14.99454494 - 42.44663728 I
        -55.81227536 - 83.93326683 I    -50.5611786 + 50.6784398 I
                                        -50.5611786 - 50.6784398 I
                                        -54.3552077 + 83.7490214 I
                                        -54.3552077 - 83.7490214 I
        Factored form gain multiplier: -1570.318368
```

Plant Case: 7 Element: {3, 2}

```
        Roots of Numerator              Roots of Denominator
        -------------------             --------------------
        -15.59067855 + 41.19171381 I    -12.74494582 + 14.09618803 I
        -15.59067855 - 41.19171381 I    -12.74494582 - 14.09618803 I
        -21.88667476 + 32.91844932 I    -15.39404714 + 42.2455865 I
        -21.88667476 - 32.91844932 I    -15.39404714 - 42.2455865 I
        -55.81227536 + 83.93326683 I    -50.07711236 + 51.46758105 I
        -55.81227536 - 83.93326683 I    -50.07711236 - 51.46758105 I
                                        -54.84457175 + 83.77539572 I
                                        -54.84457175 - 83.77539572 I
        Factored form gain multiplier: -3964.534536
```

Plant Case: 7 Element: {3, 3}

```
        Roots of Numerator              Roots of Denominator
        -------------------             --------------------
        -15.59067855 + 41.19171381 I    -0.1126673471
        -15.59067855 - 41.19171381 I    -13.15110836 + 15.94448679 I
        -21.88667476 + 32.91844932 I    -13.15110836 - 15.94448679 I
        -21.88667476 - 32.91844932 I    -15.73743682 + 42.03080543 I
        -55.81227536 + 83.93326683 I    -15.73743682 - 42.03080543 I
        -55.81227536 - 83.93326683 I    -49.65339301 + 52.15007315 I
                                        -49.65339301 - 52.15007315 I
                                        -55.2784838 + 83.79977156 I
                                        -55.2784838 - 83.79977156 I
        Factored form gain multiplier: -847.2818333
```

Plant Case: 8 Element: {1, 1}

```
        Roots of Numerator              Roots of Denominator
        -------------------             --------------------
        -15.59067855 + 41.19171381 I    -0.536633144
        -15.59067855 - 41.19171381 I    -13.82385478 + 18.61043872 I
        -21.88667476 + 32.91844932 I    -13.82385478 - 18.61043372 I
        -21.88667476 - 32.91844932 I    -15.95495777 + 39.42818093 I
        -55.81227537 + 83.93326683 I    -15.95495777 - 39.42818093 I
        -55.81227537 - 83.93326683 I    -48.70565529 + 53.66243292 I
                                        -48.70565529 - 53.66243292 I
                                        -57.65121702 + 84.21232942 I
                                        -57.65121702 - 84.21232942 I
        Factored form gain multiplier: 378.7116103
```

Plant Case: 8 Element: {1, 2}

```
        Roots of Numerator              Roots of Denominator
        -------------------             --------------------
        -15.59067855 + 41.19171381 I    -13.36268454 + 16.65678236 I
        -15.59067855 - 41.19171381 I    -13.36268454 - 16.65678236 I
        -21.88667476 + 32.91844932 I    -15.64223442 + 39.64547173 I
        -21.88667476 - 32.91844932 I    -15.64223442 - 39.64547173 I
```

```
        -55.81227537 + 83.93326683 I      -49.17003703 + 52.9448069? I
        -55.81227537 - 83.93326683 I      -49.17003703 - 32.94480o99 I
                                          -57.22306713 + 84.182"919? I
                                          -57.22306713 - 84.10279109 I
        Factored form gain multiplier: 778.9723453

Plant Case: 8  Element: {1, 3}

        Roots of Numerator              Roots of Denominator
        -------------------             --------------------
        -15.59067855 + 41.19171381 I     0.2385145022
        -15.59067855 - 41.19171381 I    -12.74971151 + 13.7726672 I
        -21.88667476 + 32.91844932 I    -12.74971151 - 13.7726672 I
        -21.88667476 - 32.91844932 I    -15.27249035 + 39.85762199 I
        -55.81227537 + 83.93326683 I    -15.27249035 - 39.85762199 I
        -55.81227537 - 83.93326683 I    -49.68 + 52.11427444 I
                                        -49.68 - 52.11427444 I
                                        -56.71481482 + 84.1592048 I
                                        -56.71481482 - 84.1592048 I
        Factored form gain multiplier: 306.6894329

Plant Case: 8  Element: {2, 1}

        Roots of Numerator              Roots of Denominator
        -------------------             --------------------
        -14.76364568 + 21.98417326 I    -13. + 15.19868415 I
        -14.76364568 - 21.98417326 I    -13. - 15.19868415 I
        -17.13211925 + 86.63467236 I    -14.924 + 33.19991301 I
        -17.13211925 - 86.63467236 I    -14.924 - 33.19991301 I
                                        -62.127 + 85.0195617 I
                                        -62.127 - 85.0195617 I
        Factored form gain multiplier: 1165.947725

Plant Case: 8  Element: {2, 2}

        Roots of Numerator              Roots of Denominator
        -------------------             --------------------
        -14.76364568 + 21.98417326 I    -0.1366001171
        -14.76364568 - 21.98417326 I    -13. + 15.19868415 I
        -17.13211925 + 86.63467236 I    -13. - 15.19868415 I
        -17.13211925 - 86.63467236 I    -14.924 + 33.19991301 I
                                        -14.924 - 33.19991301 I
                                        -62.127 + 85.0195617 I
                                        -62.127 - 85.0195617 I
        Factored form gain multiplier: -205.312979

Plant Case: 8  Element: {2, 3}

        Roots of Numerator              Roots of Denominator
        -------------------             --------------------
        -14.76364568 + 21.98417326 I     -13. + 15.19868415 I
        -14.76364568 - 21.98417326 I     -13. - 15.19868415 I
        -17.13211925 + 86.63467236 I     -14.924 + 33.19991301 I
        -17.13211925 - 86.63467236 I     -14.924 - 33.19991301 I
                                         -62.127 + 85.0195617 I
                                         -62.127 - 85.0195617 I
        Factored form gain multiplier: 1072.146277

Plant Case: 8  Element: {3, 1}

        Roots of Numerator              Roots of Denominator
        -------------------             --------------------
        -15.59067855 + 41.19171381 I     0.2210511777
        -15.59067855 - 41.19171381 I    -12.38008903 + 11.5545971 I
        -21.88667476 + 32.91844932 I    -12.38008903 - 11.5545971 I
        -21.88667476 - 32.91844932 I    -14.99454494 + 42.44663728 I
        -55.81227537 + 83.93326683 I    -14.99454494 - 42.44663728 I
        -55.81227537 - 83.93326683 I    -50.5611786 + 50.6784393 I
                                        -50.5611786 - 50.6784398 I
                                        -54.3552077 + 83.7490214 I
                                        -54.3552077 - 83.7490214 I
        Factored form gain multiplier: -1570.318368

Plant Case: 8  Element: {3, 2}

        Roots of Numerator              Roots of Denominator
        -------------------             --------------------
        -15.59067855 + 41.19171381 I    -12.74494582 + 14.09618803 I
```

```
    -15.59067855 - 41.19171381 I        -12.74494582 - 14.09618803 I
    -21.88667476 + 32.91844932 I        -15.39404714 + 42.2455865 I
    -21.88667476 - 32.91844932 I        -15.39404714 - 42.2455865 I
    -55.81227537 + 83.93326683 I        -50.07711236 + 51.46758105 I
    -55.81227537 - 83.93326683 I        -50.07711236 - 51.46758105 I
                                        -54.84457175 + 83.77539572 I
                                        -54.84457175 - 83.77539572 I
    Factored form gain multiplier: -2643.023024
```

Plant Case: 8 Element: {3, 3}

```
        Roots of Numerator              Roots of Denominator
        ------------------              --------------------
    -15.59067855 + 41.19171381 I        -0.1126673471
    -15.59067855 - 41.19171381 I        -13.15110836 + 15.94448679 I
    -21.88667476 + 32.91844932 I        -13.15110836 - 15.94448679 I
    -21.88667476 - 32.91844932 I        -15.73743682 + 42.03080543 I
    -55.81227537 + 83.93326683 I        -15.73743682 - 42.03080543 I
    -55.81227537 - 83.93326683 I        -49.65339301 + 52.15007315 I
                                        -49.65339301 - 52.15007315 I
                                        -55.2784838 + 83.79977156 I
                                        -55.2784838 - 83.79977156 I
    Factored form gain multiplier: -847.2818333
```

Plant Case: 9 Element: {1, 1}

```
        Roots of Numerator              Roots of Denominator
        ------------------              --------------------
    -15.59093272 + 41.1814354 I         -0.4972344919
    -15.59093272 - 41.1814354 I         -13.84370684 + 18.6632871 I
    -21.95984556 + 33.01640834 I        -13.84370684 - 18.6632871 I
    -21.95984556 - 33.01640834 I        -15.96173093 + 39.41716877 I
    -55.8198473 + 83.9352645 I          -15.96173093 - 39.41716877 I
    -55.8198473 - 83.9352645 I          -48.6967764 + 53.67744786 I
                                        -48.6967764 - 53.67744786 I
                                        -57.66651368 + 84.21444127 I
                                        -57.66651368 - 84.21444127 I
    Factored form gain multiplier: 375.1581079
```

Plant Case: 9 Element: {1, 2}

```
        Roots of Numerator              Roots of Denominator
        ------------------              --------------------
    Factored form gain multiplier: Infinity
```

Plant Case: 9 Element: {1, 3}

```
        Roots of Numerator              Roots of Denominator
        ------------------              --------------------
    -15.59093272 + 41.1814354 I         0.2267657302
    -15.59093272 - 41.1814354 I         -12.73774686 + 13.7320958 I
    -21.95984556 + 33.01640834 I        -12.73774686 - 13.7320958 I
    -21.95984556 - 33.01640834 I        -15.26905449 + 39.84154152 I
    -55.8199473 + 83.9352645 I          -15.26905449 - 39.84154152 I
    -55.8159473 - 83.9352645 I          -49.68 + 52.11427444 I
                                        -49.68 - 52.11427444 I
                                        -56.7232334 + 84.1603752 I
                                        -56.7232334 - 84.1603752 I
    Factored form gain multiplier: 305.0250419
```

Plant Case: 9 Element: {2, 1}

```
        Roots of Numerator              Roots of Denominator
        ------------------              --------------------
    Factored form gain multiplier: Infinity
```

Plant Case: 9 Element: {2, 2}

```
        Roots of Numerator              Roots of Denominator
        ------------------              --------------------
    -14.75644431 + 21.95264007 I        -0.1252573635
    -14.75644431 - 21.95264007 I        -13. + 15.19868415 I
    -17.06037998 + 86.61864862 I        -13. - 15.19868415 I
    -17.06037998 - 86.61864862 I        -14.924 + 33.19991301 I
```

172

```
                                   -14.924 - 33.19991301 I
                                   -62.127 + 85.0195617 I
                                   -62.127 - 85.0195617 I
          Factored form gain multiplier: -207.0716183

Plant Case: 9  Element: {2, 3}

          Roots of Numerator          Roots of Denominator
          -------------------         -------------------
          Factored form gain multiplier: Infinity


Plant Case: 9  Element: {3, 1}

          Roots of Numerator          Roots of Denominator
          -------------------         -------------------
          -15.59093272 + 41.1814354 I   0.2186105805
          -15.59093272 - 41.1814354 I   -12.35458828 + 11.45254297 I
          -21.95984556 + 33.01640834 I  -12.35458828 - 11.45254297 I
          -21.95984556 - 33.01640834 I  -14.98296916 + 42.43676453 I
          -55.8198473 + 83.9352645 I    -14.98296916 - 42.43676453 I
          -55.8198473 - 83.9352645 I    -50.57188104 + 50.65834723 I
                                        -50.57188104 - 50.65834723 I
                                        -54.35317582 + 83.75141081 I
                                        -54.35317582 - 83.75141081 I
          Factored form gain multiplier: -1563.060716

Plant Case: 9  Element: {3, 2}

          Roots of Numerator          Roots of Denominator
          -------------------         -------------------
          Factored form gain multiplier: Infinity

Plant Case: 9  Element: {3, 3}

          Roots of Numerator          Roots of Denominator
          -------------------         -------------------
          -15.59093272 + 41.1814354 I   -0.1074664032
          -15.59093272 - 41.1814354 I   -13.15738138 + 15.96338795 I
          -21.95984556 + 33.01640834 I  -13.15738138 - 15.96338795 I
          -21.95984556 - 33.01640834 I  -15.73875728 + 42.0259814 I
          -55.8198473 + 83.9352645 I    -15.73875728 - 42.0259814 I
          -55.8198473 - 83.9352645 I    -49.65523805 + 52.14751366 I
                                        -49.65523805 - 52.14751366 I
                                        -55.28583411 + 83.80254913 I
                                        -55.28583411 - 83.80254913 I
          Factored form gain multiplier: -612.9038558


Plant Case: 10  Element: {1, 1}

          Roots of Numerator          Roots of Denominator
          -------------------         -------------------
          -15.59093272 + 41.1814354 I   -0.4972344919
          -15.59093272 - 41.1814354 I   -13.84370684 + 18.6632871 I
          -21.95984556 + 33.01640834 I  -13.84370684 - 18.6632871 I
          -21.95984556 - 33.01640834 I  -15.96173093 + 39.41716877 I
          -55.8198473 + 83.9352645 I    -15.96173093 - 39.41716877 I
          -55.8198473 - 83.9352645 I    -48.6967764 + 53.67744786 I
                                        -48.6967764 - 53.67744785 I
                                        -57.66651368 + 84.21444127 I
                                        -57.66651368 - 84.21444127 I
          Factored form gain multiplier: 375.1581079

Plant Case: 10  Element: {1, 2}

          Roots of Numerator          Roots of Denominator
          -------------------         -------------------
          -15.59093272 + 41.1814354 I   -13.36883211 + 16.680463 I
          -15.59093272 - 41.1814354 I   -13.36883211 - 16.680463 I
          -21.95984556 + 33.01640834 I  -15.64460511 + 39.63256137 I
          -21.95984556 - 33.01640834 I  -15.64460511 - 39.63256137 I
          -55.8198473 + 83.9352645 I    -49.16313728 + 52.95596268 I
          -55.8198473 - 83.9352645 I    -49.16313728 - 52.95596268 I
                                        -57.23592922 + 84.18455711 I
                                        -57.23592922 - 84.18455711 I
          Factored form gain multiplier: 231  10383
```

Plant Case: 10   Element: (1, 3)

```
        Roots of Numerator              Roots of Denominator
        ------------------              --------------------
        -15.59093272 + 41.1814354 I     0.2267657302
        -15.59093272 - 41.1814354 I     -12.73774686 + 13.7320958 I
        -21.95984556 + 33.01640834 I    -12.73774686 - 13.7320958 I
        -21.95984556 - 33.01640834 I    -15.26905449 + 39.84154152 I
        -55.8198473 + 83.9352645 I      -15.26905449 - 39.84154152 I
        -55.8198473 - 83.9352645 I      -49.68 + 52.11427444 I
                                        -49.68 - 52.11427444 I
                                        -56.7232334 + 84.1603752 I
                                        -56.7232334 - 84.1603752 I
        Factored form gain multiplier: 305.0250419
```

Plant Case: 10   Element: (2, 1)

```
        Roots of Numerator              Roots of Denominator
        ------------------              --------------------
        -14.75644431 + 21.95264007 I    -13. + 15.19868415 I
        -14.75644431 - 21.95264007 I    -13. - 15.19868415 I
        -17.06037998 + 86.61864862 I    -14.924 + 33.19991301 I
        -17.06037998 - 86.61864862 I    -14.924 - 33.19991301 I
                                        -62.127 + 85.0195617 I
                                        -62.127 - 85.0195617 I
        Factored form gain multiplier: 3527.804478
```

Plant Case: 10   Element: (2, 2)

```
        Roots of Numerator              Roots of Denominator
        ------------------              --------------------
        -14.75644431 + 21.95264007 I    -0.1252573635
        -14.75644431 - 21.95264007 I    -13. + 15.19868415 I
        -17.06037998 + 86.61864862 I    -13. - 15.19868415 I
        -17.06037998 - 86.61864862 I    -14.924 + 33.19991301 I
                                        -14.924 - 33.19991301 I
                                        -62.127 + 85.0195617 I
                                        -62.127 - 85.0195617 I
        Factored form gain multiplier: -207.0716183
```

Plant Case: 10   Element: (2, 3)

```
        Roots of Numerator              Roots of Denominator
        ------------------              --------------------
        -14.75644431 + 21.95264007 I    -13. + 15.19868415 I
        -14.75644431 - 21.95264007 I    -13. - 15.19868415 I
        -17.06037998 + 86.61864862 I    -14.924 + 33.19991301 I
        -17.06037998 - 86.61864862 I    -14.924 - 33.19991301 I
                                        -62.127 + 85.0195617 I
                                        -62.127 - 85.0195617 I
        Factored form gain multiplier: 3243.989723
```

Plant Case: 10   Element: (3, 1)

```
        Roots of Numerator              Roots of Denominator
        ------------------              --------------------
        -15.59093272 + 41.1814354 I     0.2186105805
        -15.59093272 - 41.1814354 I     -12.35458828 + 11.45254297 I
        -21.95984556 + 33.01640834 I    -12.35458828 - 11.45254297 I
        -21.95984556 - 33.01640834 I    -14.98296916 + 42.43676453 I
        -55.8198473 + 83.9352645 I      -14.98296916 - 42.43676453 I
        -55.8198473 - 83.9352645 I      -50.57188104 + 50.65834723 I
                                        -50.57188104 - 50.65834723 I
                                        -54.35317582 + 83.75141081 I
                                        -54.35317582 - 83.75141081 I
        Factored form gain multiplier: -1563.060716
```

Plant Case: 10   Element: (3, 2)

```
        Roots of Numerator              Roots of Denominator
        ------------------              --------------------
        -15.59093272 + 41.1814354 I     -12.73989941 + 14.07341303 I
        -15.59093272 - 41.1814354 I     -12.73989941 - 14.07341303 I
        -21.95984556 + 33.01640834 I    -15.38902306 + 42.23875741 I
        -21.95984556 - 33.01640834 I    -15.38902306 - 42.23875741 I
        -55.8198473 + 83.9352645 I      -50.08336965 + 51.4572361 I
```

```
        -55.8198473 - 83.9352645 I        -50.08336965 - 51.4572361 I
                                           -54.84749847 + 83.77787304 I
                                           -54.84749847 - 83.77787304 I
        Factored form gain multiplier: -7890.066094

Plant Case: 10  Element: (3, 3)

        Roots of Numerator              Roots of Denominator
        ------------------              -------------------
        -15.59093272 + 41.1814354 I     -0.1074664032
        -15.59093272 - 41.1814354 I     -13.15738138 + 15.96338795 I
        -21.95984556 + 33.01640834 I    -13.15738138 - 15.96338795 I
        -21.95984556 - 33.01640834 I    -15.73875728 + 42.0259814 I
        -55.8198473 + 83.9352645 I      -15.73875728 - 42.0259814 I
        -55.8198473 - 83.9352645 I      -49.65523805 + 52.14751366 I
                                        -49.65523805 - 52.14751366 I
                                        -55.28583411 + 83.80254913 I
                                        -55.28583411 - 83.80254913 I
        Factored form gain multiplier: -842.9038558


Plant Case: 11  Element: (1, 1)

        Roots of Numerator              Roots of Denominator
        ------------------              -------------------
        -15.59093272 + 41.1814354 I     -0.4972344919
        -15.59093272 - 41.1814354 I     -13.84370684 + 18.6632871 I
        -21.95984556 + 33.01640834 I    -13.84370684 - 18.6632871 I
        -21.95984556 - 33.01640834 I    -15.96173093 + 39.41716877 I
        -55.8198473 + 83.9352645 I      -15.96173093 - 39.41716877 I
        -55.8198473 - 83.9352645 I      -48.6967764 + 53.67744786 I
                                        -48.6967764 - 53.67744786 I
                                        -57.66651368 + 84.21444127 I
                                        -57.66651368 - 84.21444127 I
        Factored form gain multiplier: 375.1581079

Plant Case: 11  Element: (1, 2)

        Roots of Numerator              Roots of Denominator
        ------------------              -------------------
        -15.59093272 + 41.1814354 I     -13.36883211 + 16.680463 I
        -15.59093272 - 41.1814354 I     -13.36883211 - 16.680463 I
        -21.95984556 + 33.01640834 I    -15.64460511 + 39.63256137 I
        -21.95984556 - 33.01640834 I    -15.64460511 - 39.63256137 I
        -55.8198473 + 83.9352645 I      -49.16313728 + 52.95596268 I
        -55.8198473 - 83.9352645 I      -49.16313728 - 52.95596268 I
                                        -57.23592922 + 84.18455711 I
                                        -57.23592922 - 84.18455711 I
        Factored form gain multiplier: 1159.555192

Plant Case: 11  Element: (1, 3)

        Roots of Numerator              Roots of Denominator
        ------------------              -------------------
        -15.59093272 + 41.1814354 I     0.2267657302
        -15.59093272 - 41.1814354 I     -12.73774686 + 13.7320958 I
        -21.95984556 + 33.01640834 I    -12.73774686 - 13.7320958 I
        -21.95984556 - 33.01640834 I    -15.26905449 + 39.84154152 I
        -55.8198473 + 83.9352645 I      -15.26905449 - 39.84154152 I
        -55.8198473 - 83.9352645 I      -49.68 + 52.11427444 I
                                        -49.68 - 52.11427444 I
                                        -56.7232334 + 84.1603752 I
                                        -56.7232334 - 84.1603752 I
        Factored form gain multiplier: 305.0250419

Plant Case: 11  Element: (2, 1)

        Roots of Numerator              Roots of Denominator
        ------------------              -------------------
        -14.75644431 + 21.95264007 I    -13. + 15.19868415 I
        -14.75644431 - 21.95264007 I    -13. - 15.19868415 I
        -17.06037998 + 86.61864862 I    -14.924 + 33.19991301 I
        -17.06037998 - 86.61864862 I    -14.924 - 33.19991301 I
                                        -62.127 + 85.0195617 I
                                        -62.127 - 85.0195617 I
        Factored form gain multiplier: 1763.902239

Plant Case: 11  Element: (2, 2)
```

```
Rcots of Numerator                    Roots of Dcnominator
------------------                    --------------------
-14.75644431 + 21.95264007 I          -0.1252573635
-14.7564^431 - 21.95264007 I          -13. + 15.19868415 I
-17.06037998 + 86.61864862 I          -13. - 15.19868415 I
-17.06037998 - 86.61864862 I          -14.924 + 33.19991301 I
                                      -14.924 - 33.19991301 I
                                      -62.127 + 85.0195617 I
                                      -62.127 - 85.0195617 I
Factored form gain multiplier: -207.0716183
```

Plant Case: 11 Element: {2, 3}

```
Roots of Numerator                    Roots of Denominator
------------------                    --------------------
-14.75644431 + 21.95264007 I          -13. + 15.19868415 I
-14.75644431 - 21.95264007 I          -13. - 15.19868415 I
-17.06037998 + 86.61864862 I          -14.924 + 33.19991301 I
-17.06037998 - 86.61864862 I          -14.924 - 33.19991301 I
                                      -62.127 + 85.0195617 I
                                      -62.127 - 85.0195617 I
Factored form gain multiplier: 1621.994861
```

Plant Case: 11 Element: {3, 1}

```
Roots of Numerator                    Roots of Denominator
------------------                    --------------------
-15.59093272 + 41.1814354 I           0.2186105805
-15.59093272 - 41.1814354 I           -12.35458828 + 11.45254297 I
-21.95984556 + 33.01640834 I          -12.35458828 - 11.45254297 I
-21.95984556 - 33.01640834 I          -14.98296916 + 42.43676453 I
-55.8198473 + 83.9352645 I            -14.98296916 - 42.43676453 I
-55.8198473 - 83.9352645 I            -50.57188104 + 50.65834723 I
                                      -50.57188104 - 50.65834723 I
                                      -54.35317582 + 83.75141081 I
                                      -54.35317582 - 83.75141081 I
Factored form gain multiplier: -1563.060716
```

Plant Case: 11 Element: {3, 2}

```
Roots of Numerator                    Roots of Denominator
------------------                    --------------------
-15.59093272 + 41.1814354 I           -12.73989941 + 14.07341303 I
-15.59093272 - 41.1814354 I           -12.73989941 - 14.07341303 I
-21.95984556 + 33.01640834 I          -15.38902306 + 42.23875741 I
-21.95984556 - 33.01640834 I          -15.38902306 - 42.23875741 I
-55.8198473 + 83.9352645 I            -50.08336965 + 51.4572361 I
-55.8198473 - 83.9352645 I            -50.08336965 - 51.4572361 I
                                      -54.84749847 + 83.77787304 I
                                      -54.84749847 - 83.77787304 I
Factored form gain multiplier: -3945.033047
```

Plant Case: 11 Element: {3, 3}

```
Roots of Numerator                    Roots of Denominator
------------------                    --------------------
-15.59093272 + 41.1814354 I           -0.1074664032
-15.59093272 - 41.1814354 I           -13.15738138 + 15.96338795 I
-21.95984556 + 33.01640834 I          -13.15738138 - 15.96338795 I
-21.95984556 - 33.01640834 I          -15.73875728 + 42.0259814 I
-55.8198473 + 83.9352645 I            -15.73875728 - 42.0259814 I
-55.8198473 - 83.9352645 I            -49.65523805 + 52.14751366 I
                                      -49.65523805 - 52.14751366 I
                                      -55.28583411 + 83.80254913 I
                                      -55.28583411 - 83.80254913 I
Factored form gain multiplier: -842.9038558
```

Plant Case: 12 Element: {1, 1}

```
Roots of Numerator                    Roots of Denominator
------------------                    --------------------
-15.59093272 + 41.1814354 I           -0.4972344919
```

176

```
        -15.59093272 - 41.1814354 I      -13.84370684 + 18.6632871 I
        -21.95984556 + 33.01640834 I     -13.84370684 - 18.6632871 I
        -21.95984556 - 33.01640834 I     -15.96173093 + 39.41716877 I
        -55.8198473 + 83.9352645 I       -15.96173093 - 39.41716877 I
        -55.8198473 - 83.9352645 I       -48.6967764 + 53.67744786 I
                                         -48.6967764 - 53.67744786 I
                                         -57.66651368 + 84.21444127 I
                                         -57.66651368 - 84.21444127 I
        Factored form gain multiplier: 375.1581079

Plant Case: 12  Element: (1, 2)

        Roots of Numerator               Roots of Denominator
        ------------------               --------------------
        -15.59093272 + 41.1814354 I      -13.36883211 + 16.680463 I
        -15.59093272 - 41.1814354 I      -13.36883211 - 16.680463 I
        -21.95984556 + 33.01640834 I     -15.64460511 + 39.63256137 I
        -21.95984556 - 33.01640834 I     -15.64460511 - 39.63256137 I
        -55.8198473 + 83.9352645 I       -49.16313728 + 52.95596268 I
        -55.8198473 - 83.9352645 I       -49.16313728 - 52.95596268 I
                                         -57.23592922 + 84.18455711 I
                                         -57.23592922 - 84.18455711 I
        Factored form gain multiplier: 773.0367945

Plant Case: 12  Element: (1, 3)

        Roots of Numerator               Roots of Denominator
        ------------------               --------------------
        -15.59093272 + 41.1814354 I      0.2267657302
        -15.59093272 - 41.1814354 I      -12.73774686 + 13.7320958 I
        -21.95984556 + 33.01640834 I     -12.73774686 - 13.7320958 I
        -21.95984556 - 33.01640834 I     -15.26905449 + 39.84154152 I
        -55.8198473 + 83.9352645 I       -15.26905449 - 39.84154152 I
        -55.8198473 - 83.9352645 I       -49.68 + 52.11427444 I
                                         -49.68 - 52.11427444 I
                                         -56.7232334 + 84.1603752 I
                                         -56.7232334 - 84.1603752 I
        Factored form gain multiplier: 305.0250419

Plant Case: 12  Element: (2, 1)

        Roots of Numerator               Roots of Denominator
        ------------------               --------------------
        -14.75644431 + 21.95264007 I     -13. + 15.19868415 I
        -14.75644431 - 21.95264007 I     -13. - 15.19868415 I
        -17.06037998 + 86.61864862 I     -14.924 + 33.19991301 I
        -17.06037998 - 86.61864862 I     -14.924 - 33.19991301 I
                                         -62.127 + 85.0195617 I
                                         -62.127 - 85.0195617 I
        Factored form gain multiplier: 1175.934826

Plant Case: 12  Element: (2, 2)

        Roots of Numerator               Roots of Denominator
        ------------------               --------------------
        -14.75644431 + 21.95264007 I     -0.1252573635
        -14.75644431 - 21.95264007 I     -13. + 15.19868415 I
        -17.06037998 + 86.61864862 I     -13. - 15.19868415 I
        -17.06037998 - 86.61864862 I     -14.924 + 33.19991301 I
                                         -14.924 - 33.19991301 I
                                         -62.127 + 85.0195617 I
                                         -62.127 - 85.0195617 I
        Factored form gain multiplier: -207.0716183

Plant Case: 12  Element: (2, 3)

        Roots of Numerator               Roots of Denominator
        ------------------               --------------------
        -14.75644431 + 21.95264007 I     -13. + 15.19868415 I
        -14.75644431 - 21.95264007 I     -13. - 15.19868415 I
        -17.06037998 + 86.61864862 I     -14.924 + 33.19991301 I
        -17.06037998 - 86.61864862 I     -14.924 - 33.19991301 I
                                         -62.127 + 85.0195617 I
                                         -62.127 - 85.0195617 I
        Factored form gain multiplier: 1081.329908

Plant Case: 12  Element: (3, 1)
```

```
Roots of Numerator              Roots of Denominator
-------------------              --------------------
-15.59093272 + 41.1814354 I      0.2186105805
-15.59093272 - 41.1814354 I      -12.35458828 + 11.45254297 I
-21.95984556 + 33.01640834 I     -12.35458828 - 11.45254297 I
-21.95984556 - 33.01640834 I     -14.98296916 + 42.43676453 I
-55.8198473 + 83.9352645 I       -14.98296916 - 42.43676453 I
-55.8198473 - 83.9352645 I       -50.57188104 + 50.65834723 I
                                 -50.57188104 - 50.65834723 I
                                 -54.35317582 + 83.75141081 I
                                 -54.35317582 - 83.75141081 I
         Factored form gain multiplier: -1563.060716

Plant Case: 12  Element: {3, 2}

Roots of Numerator              Roots of Denominator
-------------------              --------------------
-15.59093272 + 41.1814354 I      -12.73989941 + 14.07341303 I
-15.59093272 - 41.1814354 I      -12.73989941 - 14.07341303 I
-21.95984556 + 33.01640834 I     -15.38902306 + 42.23875741 I
-21.95984556 - 33.01640834 I     -15.38902306 - 42.23875741 I
-55.8198473 + 83.9352645 I       -50.08336965 + 51.4572361 I
-55.8198473 - 83.9352645 I       -50.08336965 - 51.4572361 I
                                 -54.84749847 + 83.77787304 I
                                 -54.84749847 - 83.77787304 I
         Factored form gain multiplier: -2630.022031

Plant Case: 12  Element: {3, 3}

Roots of Numerator              Roots of Denominator
-------------------              --------------------
-15.59093272 + 41.1814354 I      -0.1074664032
-15.59093272 - 41.1814354 I      -13.15738138 + 15.96338795 I
-21.95984556 + 33.01640834 I     -13.15738138 - 15.96338795 I
-21.95984556 - 33.01640834 I     -15.73875728 + 42.0259814 I
-55.8198473 + 83.9352645 I       -15.73875728 - 42.0259814 I
-55.8198473 - 83.9352645 I       -49.65523805 + 52.14751366 I
                                 -49.65523805 - 52.14751366 I
                                 -55.28583411 + 83.80254913 I
                                 -55.28583411 - 83.80254913 I
         Factored form gain multiplier: -842.9038558
```
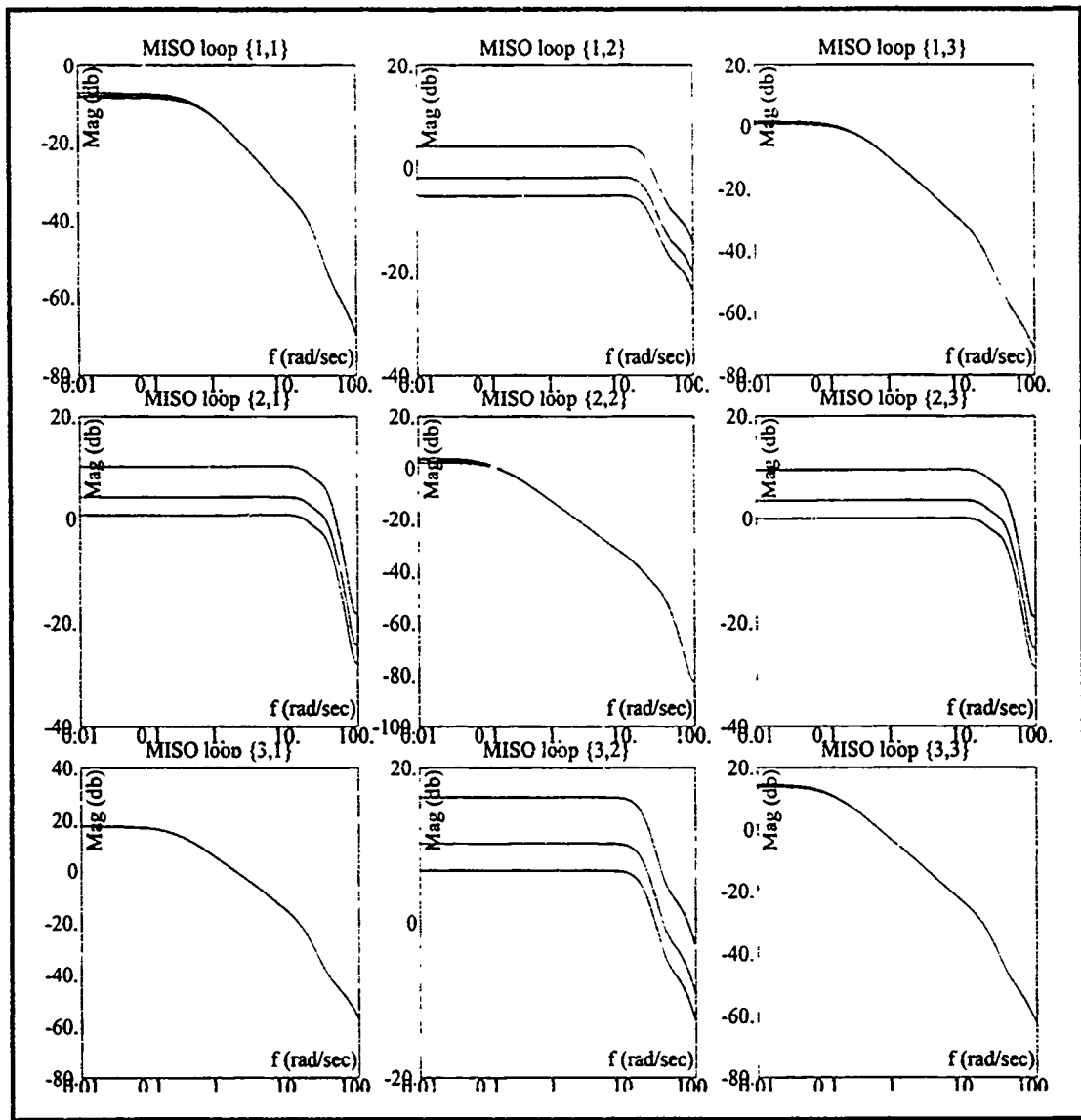
ᴛhis chapter presents the closed-loop simulations used to validate the QFT design. Validation tests are performed on a three DOF model, a six DOF model with no actuator limits, and a six DOF model with actuator limits. Control group deflection commands are also presented for each simulation.
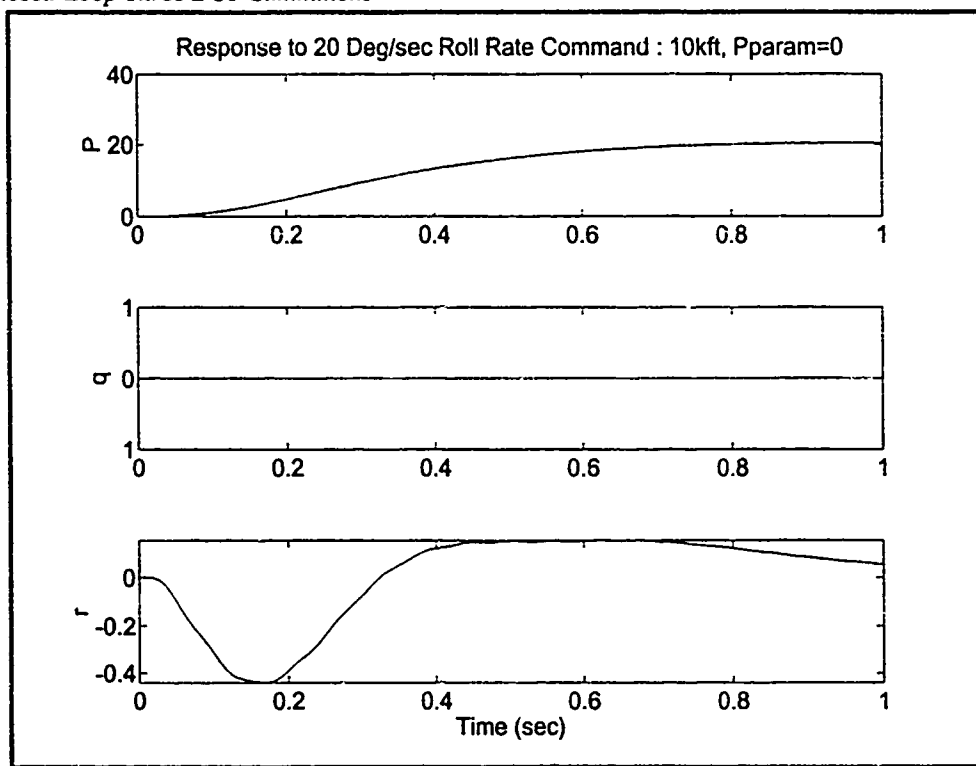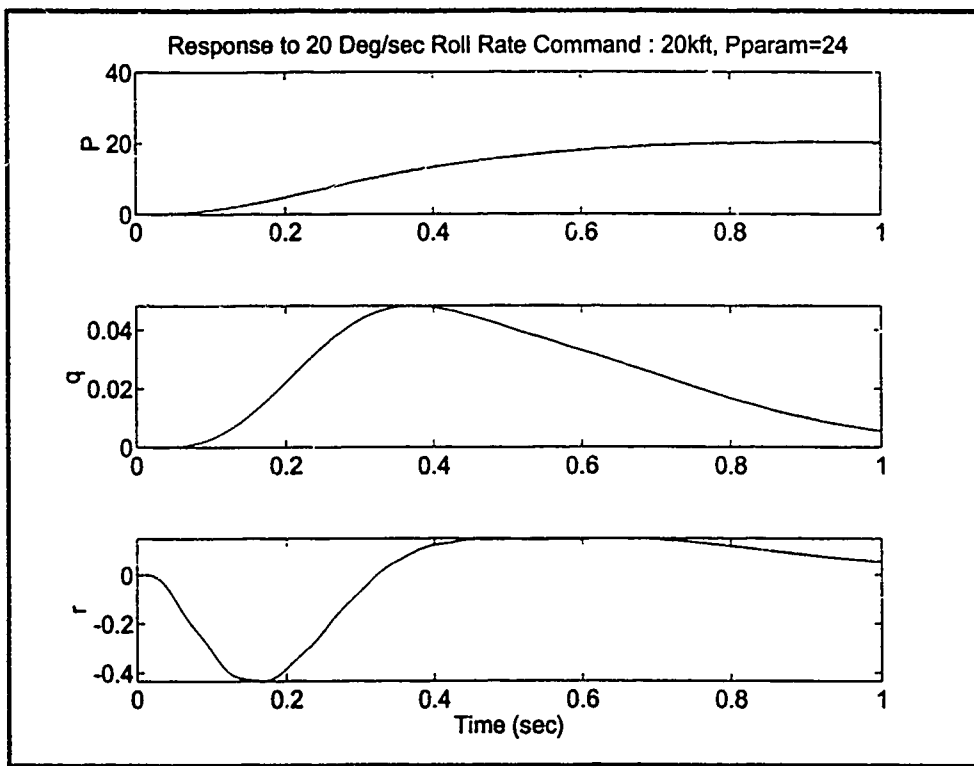
Figure 82. Response to Roll Command, Closed-Loop System, Pparam=0, 10kft
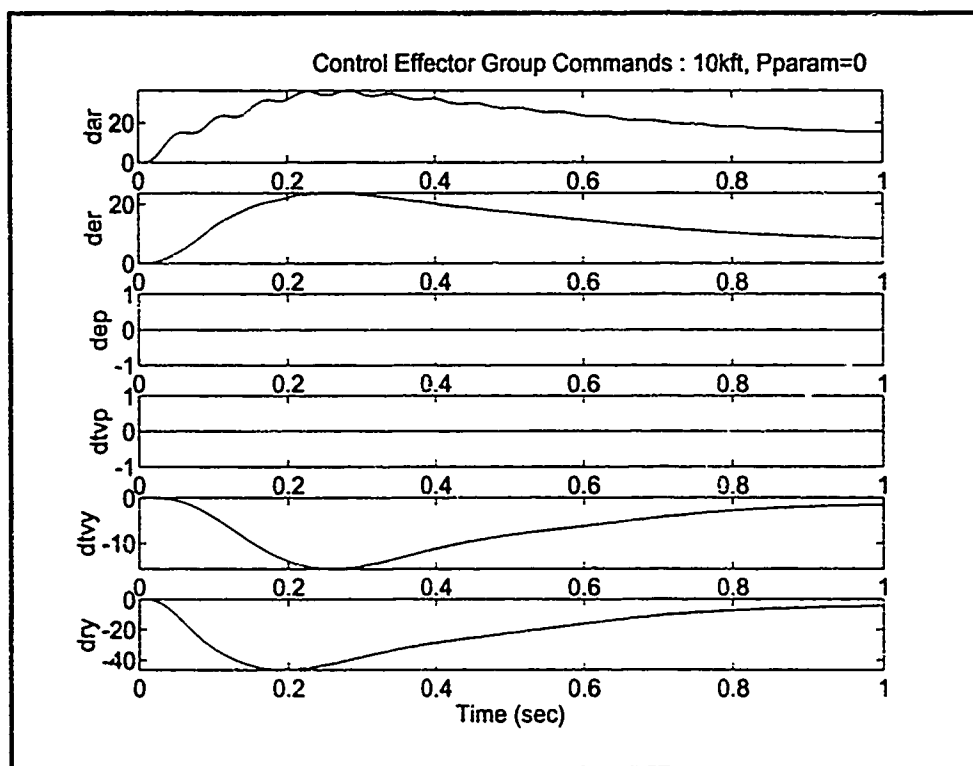
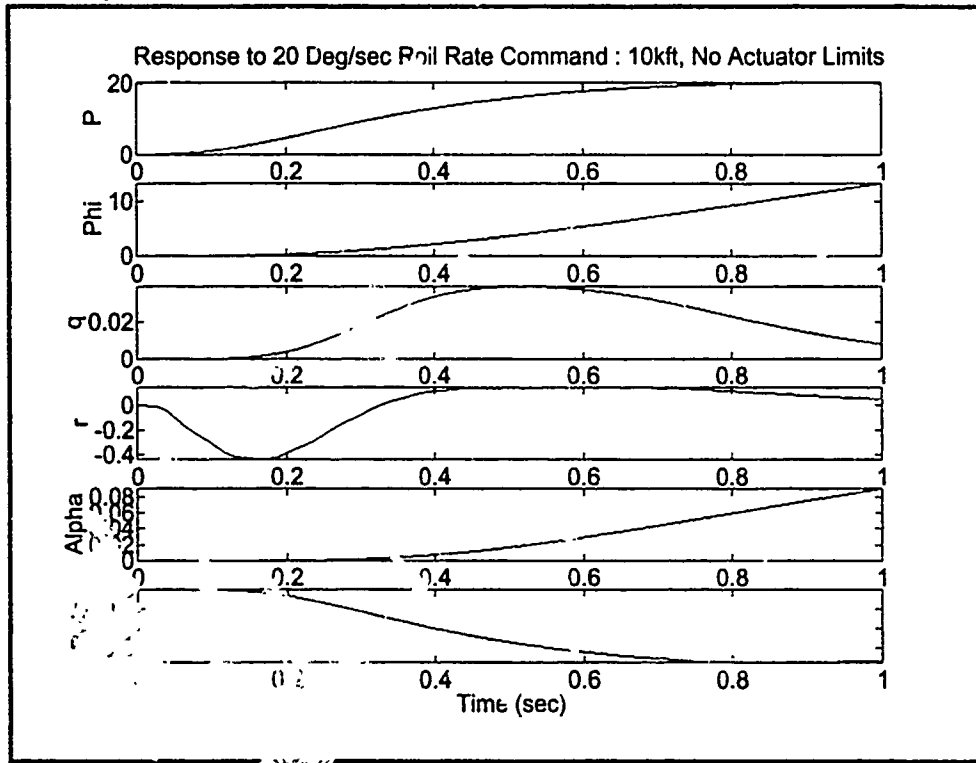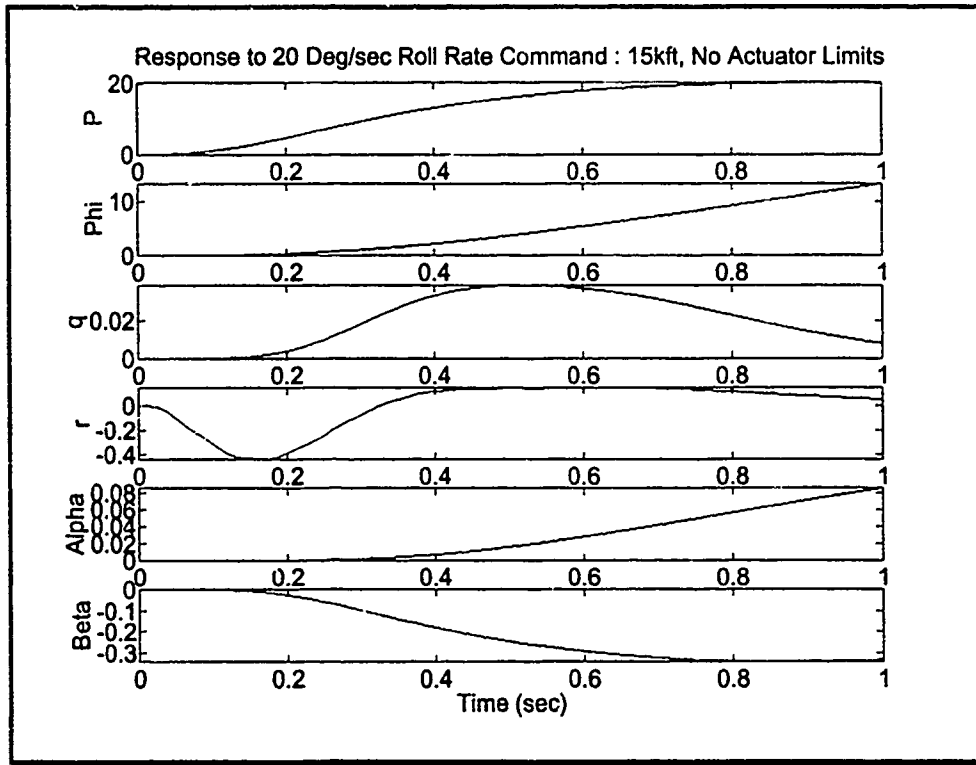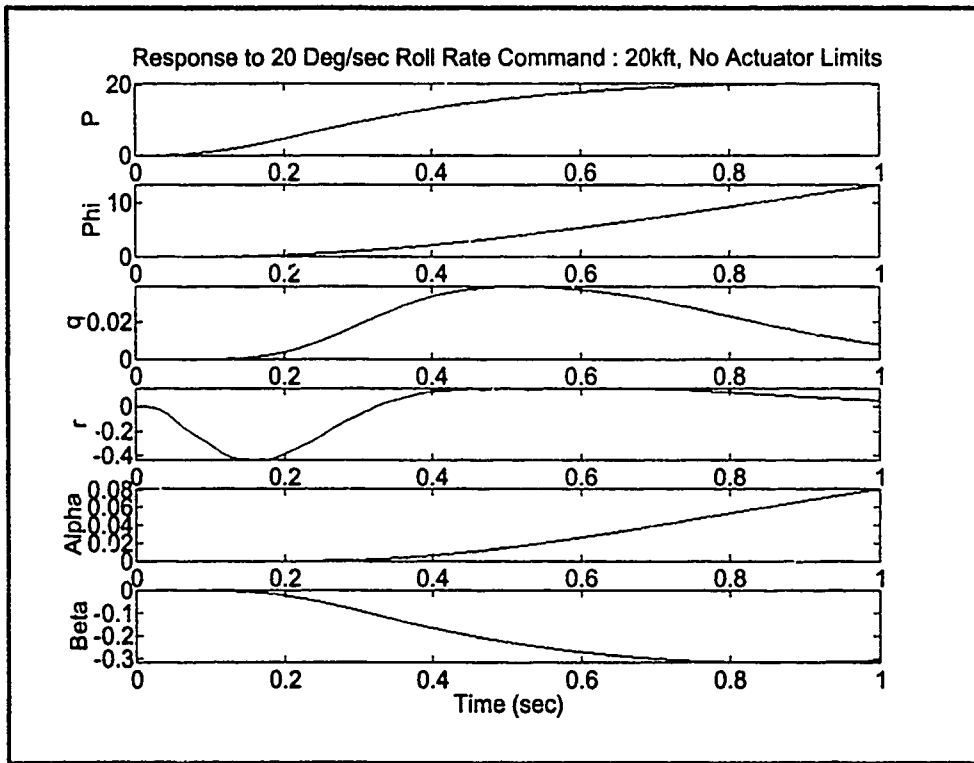Figure 83. Control Effector Group Commands, Closed-Loop System, Pparam=0, 10kft
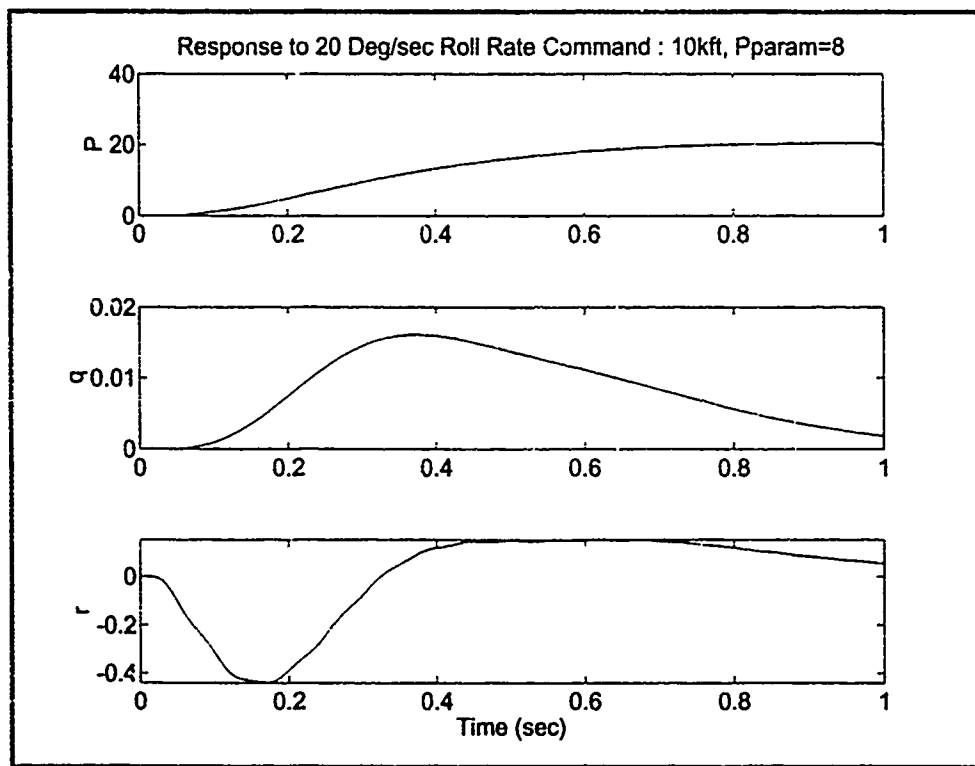
Figure 84. Response to Roll Command, Closed-Loop System, Pparam=8, 10kft
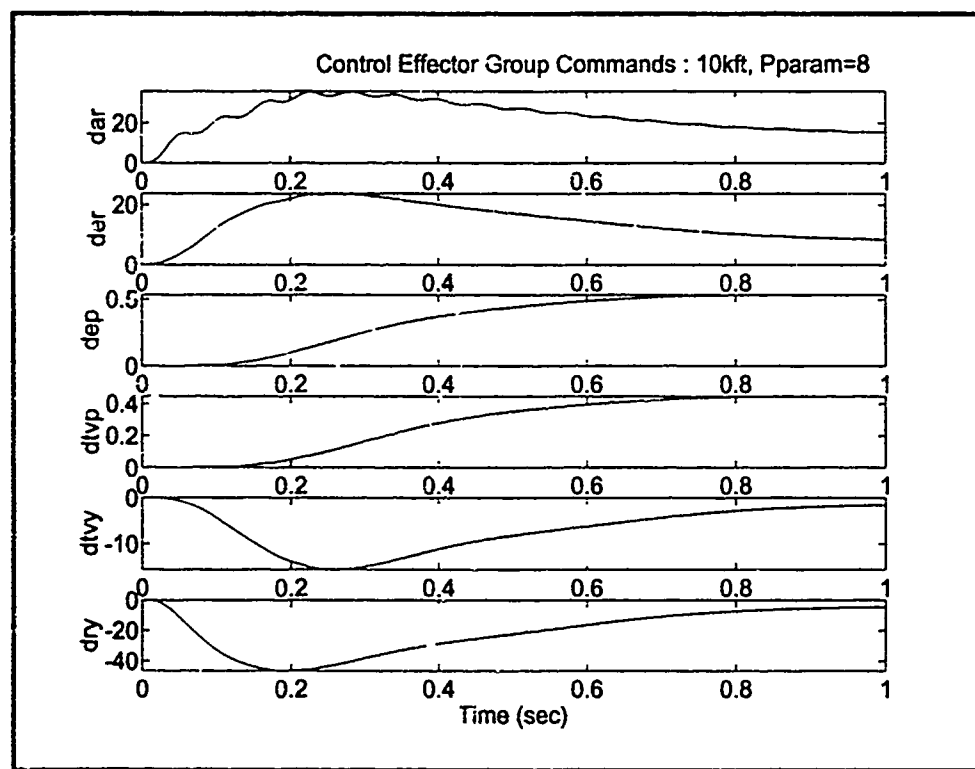
Figure 85. Control Effector Group Commands, Closed-Loop System, Pparam=8, 10kft
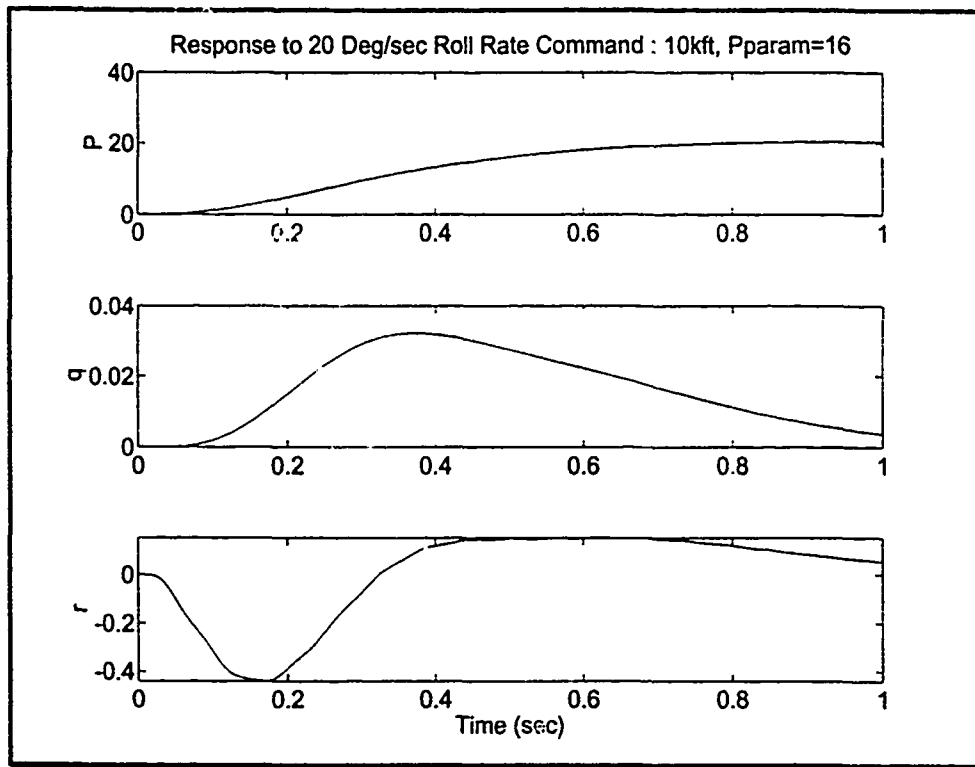
Figure 86. Response to Roll Command, Closed-Loop System, Pparam=16, 10kft
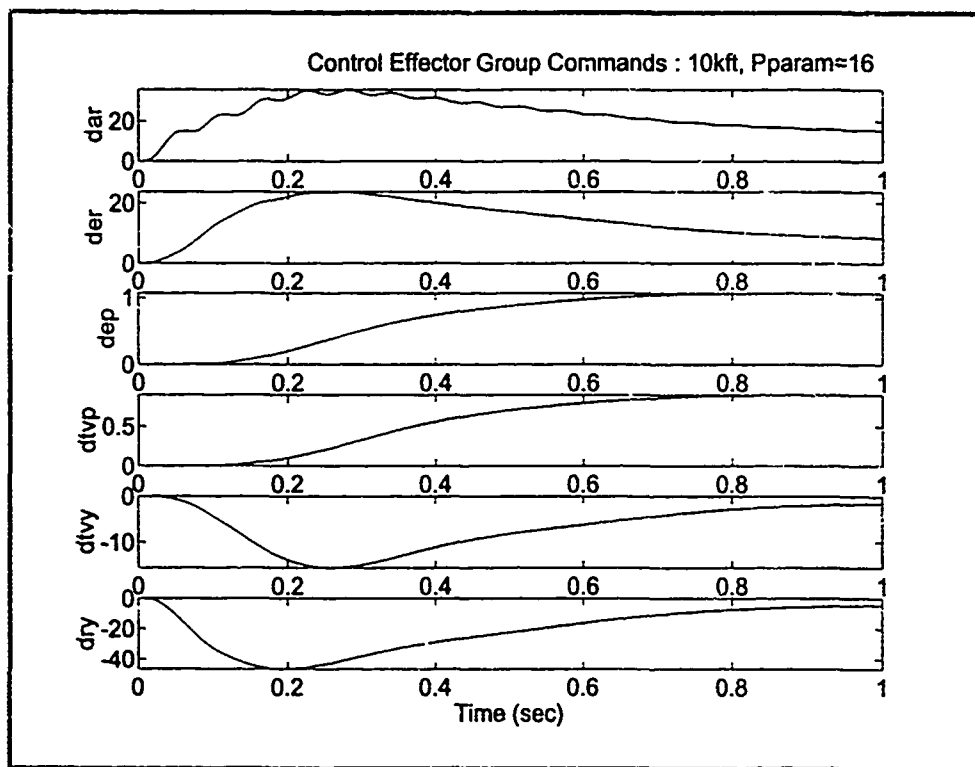
Figure 87. Control Effector Group Commands, Closed-Loop System, Pparam=16, 10kft
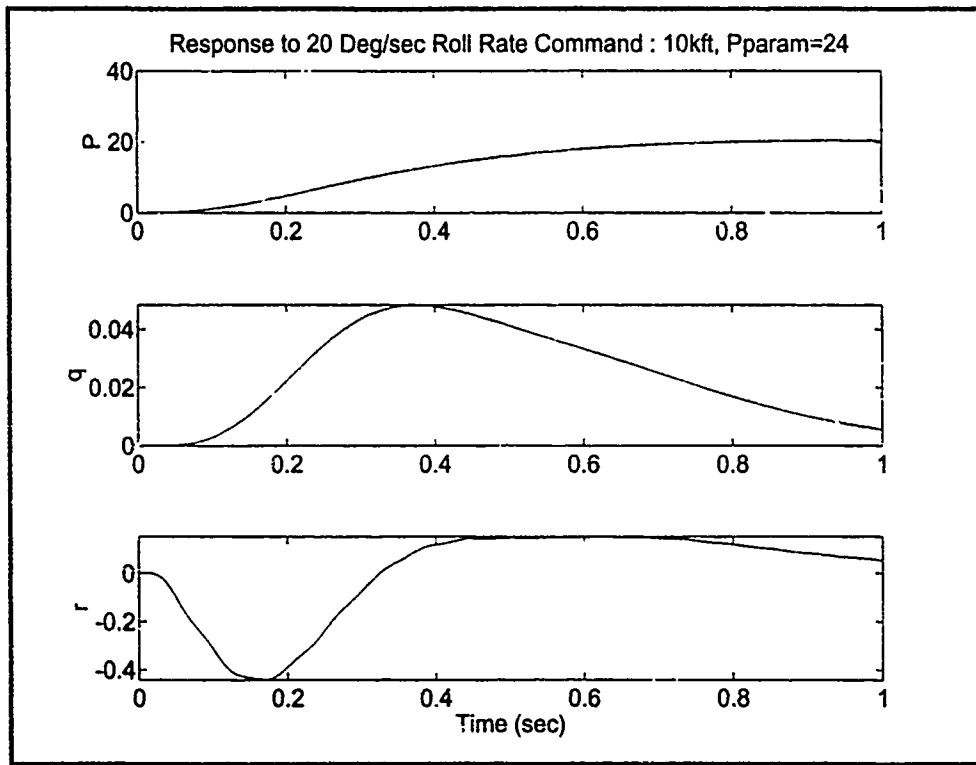
Figure 88. Response to Roll Command, Closed-Loop System, Pparam=24, 10kft
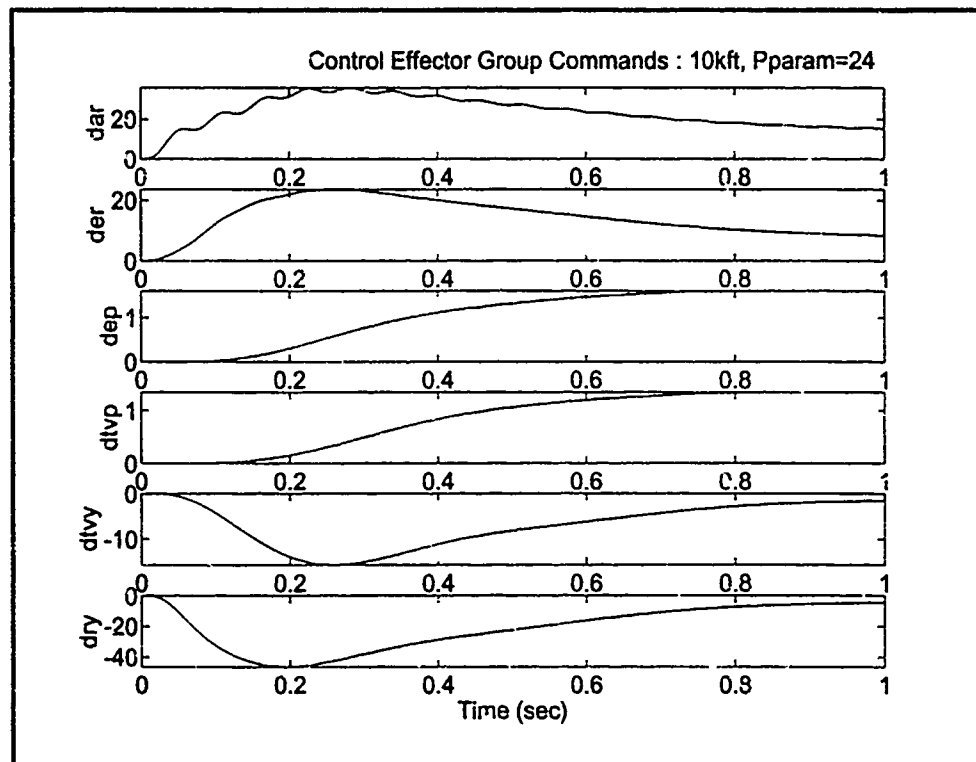
Figure 89. Control Effector Group Commands, Closed-Loop System, Pparam=24, 10kft
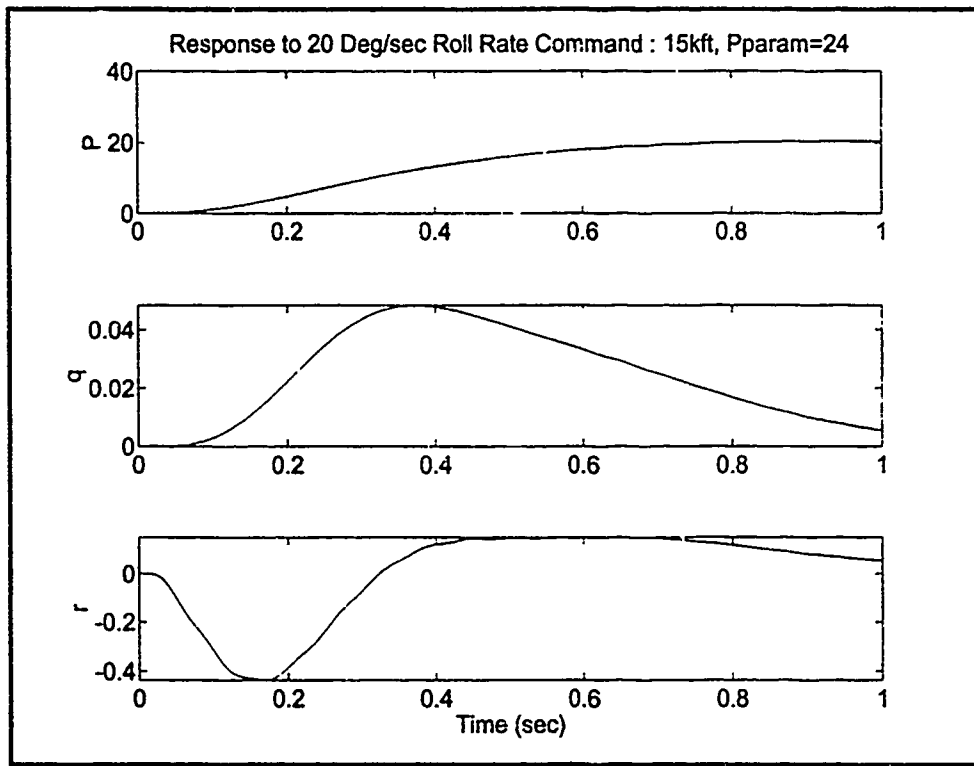
Figure 90. Response to Roll Command, Closed-Loop System, Pparam=24, 15kft
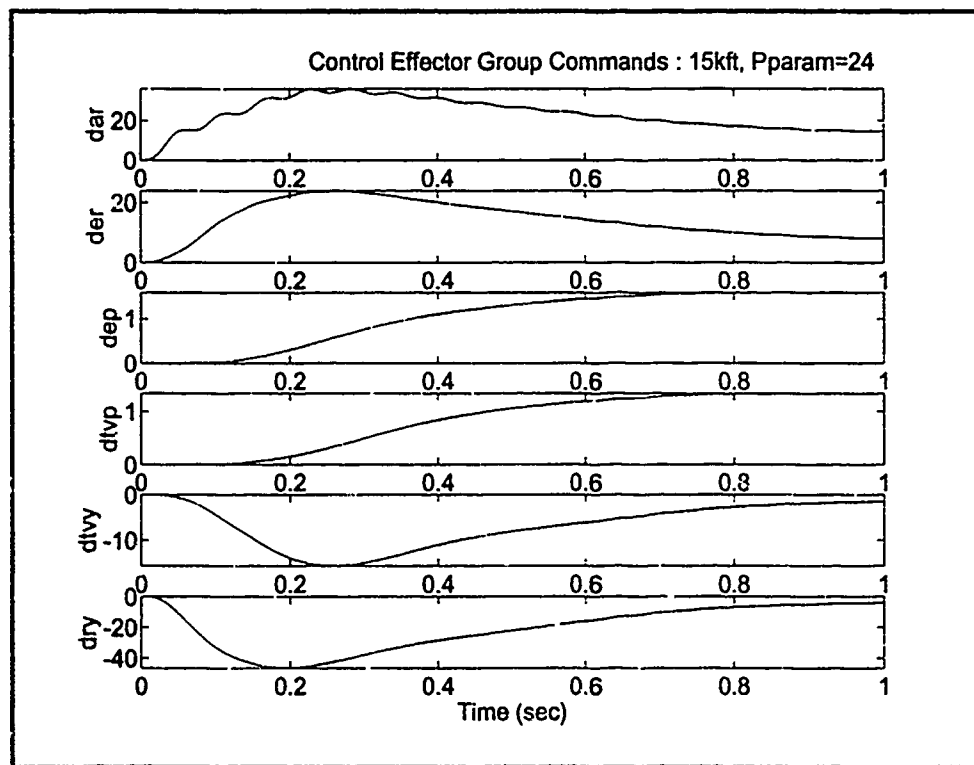
Figure 91. Control Effector Group Commands, Closed-Loop System, Pparam=24, 15kft

Figure 92. Response to Roll Command, Closed-Loop System, Pparam=24, 20kft
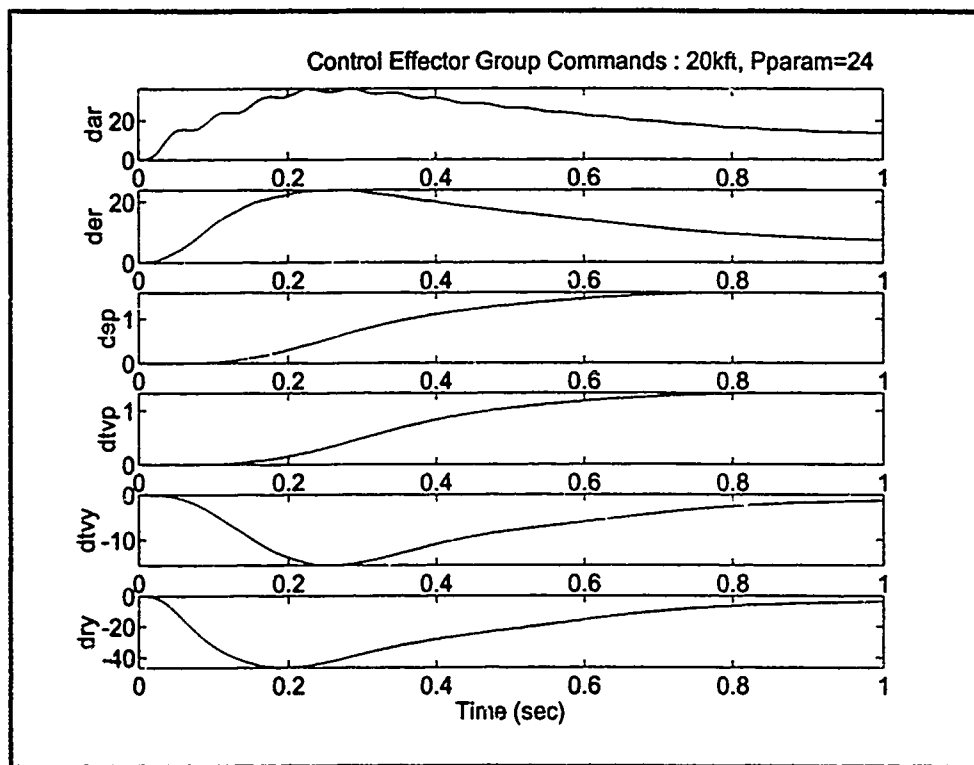
Figure 93. Control Effector Group Commands, Closed-Loop System, Pparam=24, 20kft

Figure 94. Response to Roll Command, Closed-Loop 6 DOF System, 10kft
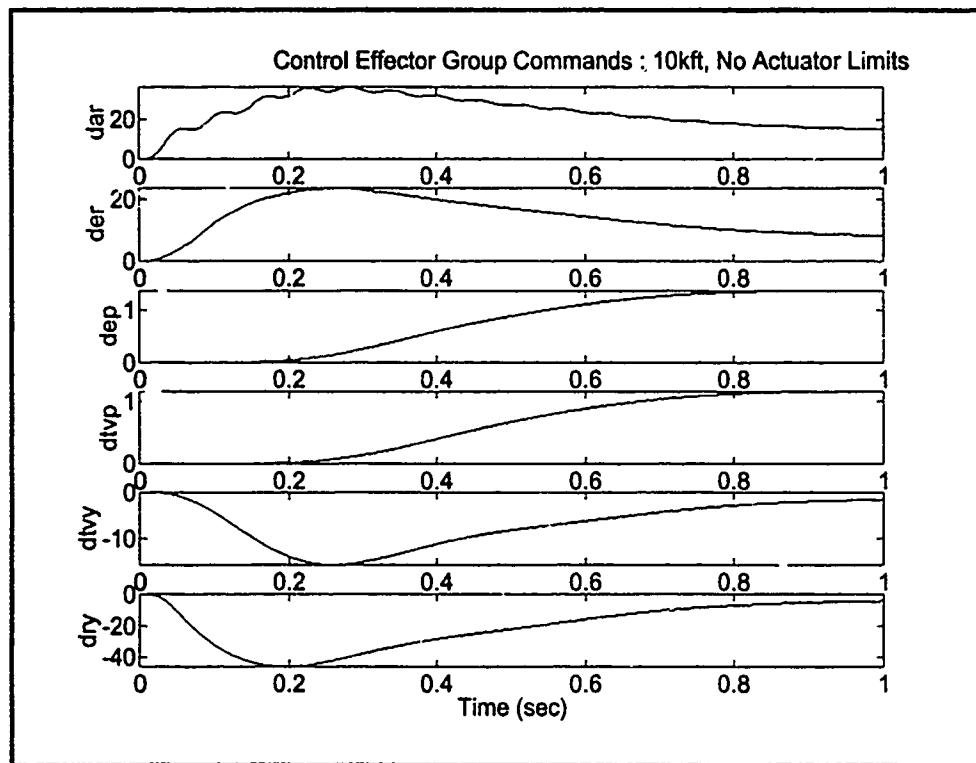
Figure 95. Control Effector Group Commands, Closed-Loop 6 DOF System, 10kft

187

Figure 96. Response to Roll Command, Closed-Loop 6 DOF System, 15kft
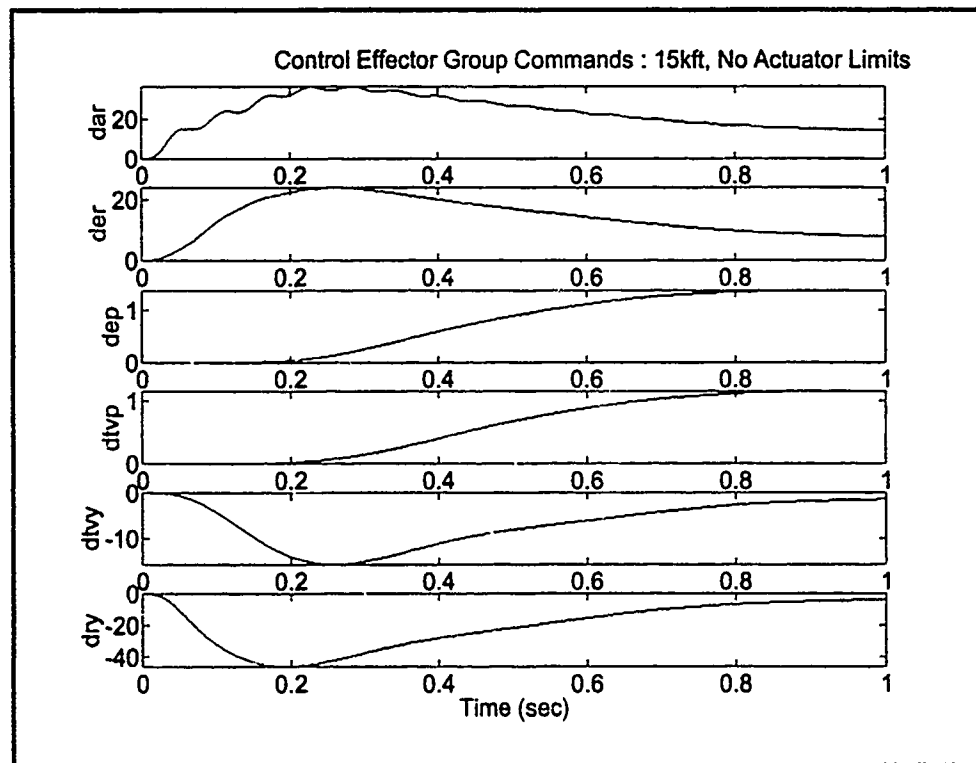
Figure 97. Control Effector Group Commands, Closed-Loop 6 DOF System, 15kft

Figure 98. Response to Roll Command, Closed-Loop 6 DOF System, 20kft
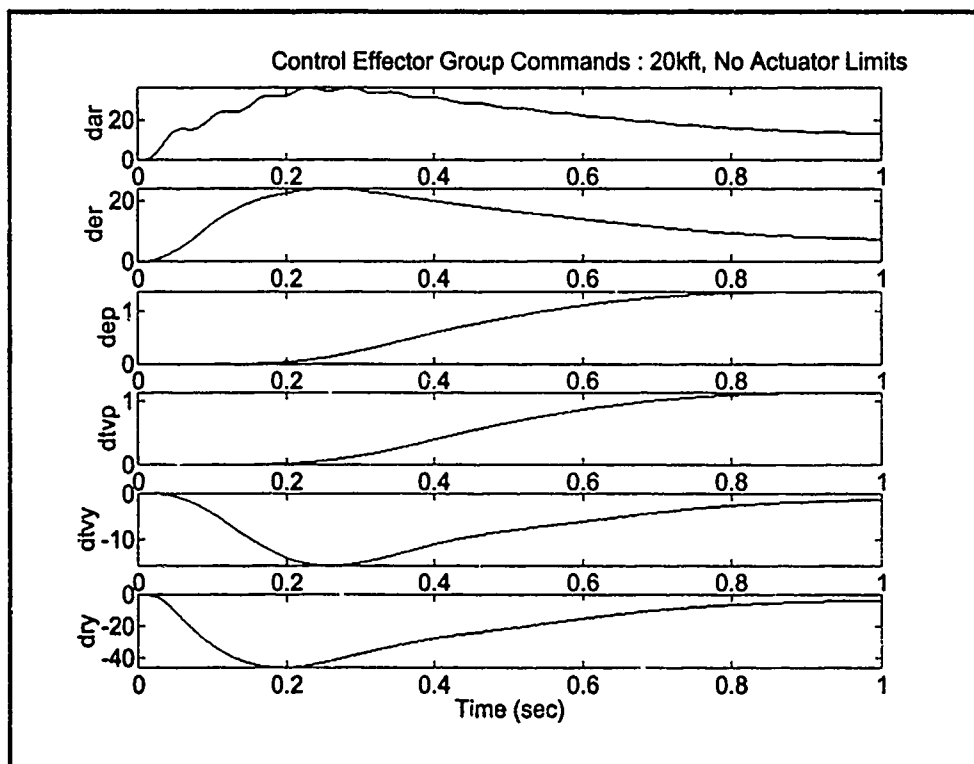
Figure 99. Control Effector Group Commands, Closed-Loop 6 DOF System, 20kft

189

Bibliography

1. Adams, Richard J., James M. Buffington, Andrew G. Sparks and Silva S. Banda. *An Introduction to Multivariable Flight Control System Design*. Technical Report, Flight Dynamics Laboratory, Wright-Patterson AFB, OH, Oct. 1992. WL-TR-92-3110.

2. Arnold, Phillip B. *Flight Control System Reconfiguration Design Using Quantitative Feedback Theory*. MS thesis, Air Force Institute of Technology, Wright-Patterson AFB, OH, Dec. 1984.

3. Buffington, James M., Richard J. Adams and Silva S. Banda. "A Robust, Nonlinear, High Angle of Attack Control Design for a Supermaneuverable Vehicle," *Proceedings 1993 AIAA Guidance, Navigation, and Control Conference.*, Monterey, CA, Aug. 1993, pp. 690-700.

4. Bugajski, Daniel J. and Dale F. Enns. "Nonlinear Control Law with Application to High-Angle-of-Attack Flight," *Journal of Guidance, Control, and Dynamics*, Vol.15, No.3, pp. 761-767, 1992.

5. Chiang, R.Y., Safonov M.G., Haiges, K.R., Madden, K.P., and Tekawy, J.A.. "A Fixed H_∞ Controller for a Supermaneuverable Fighter Performing a Herbst Maneuver," *Automatica*, vol. 29, No. 1, pp. 111-127, 1993.

6. Clough, Bruce T. *Reconfigurable Flight Control System for a STOL Aircraft Using Quantitative Feedback Theory*. MS thesis, Air Force Institute of Technology, Wright-Patterson AFB, OH, Dec. 1985.

7. Connelly, Patrick J. PRC, Inc., NASA Dryden Flight Research Facility, Edwards, CA. Personal Conversation and Electronic Message. May through August 1993.

8. D'Azzo, John J. and Constantine H. Houpis. *Linear Control System Analysis and Design -- Conventional and Modern* (3rd Edition). New York: McGraw-Hill, 1988.

9. Enns, Dale F. and Daniel J. Bugajski. "First Steps Toward a Robust Nonlinear HARV Flight Control Solution," *High-Angle-of-Attack Technology*, NASA Conference Publication 3149, pp. 1241-1256, 1992.

10. Etkin, Bernard. *Dynamics of Atmospheric Flight*. New York: John Wiley & Sons, Inc., 1972.

11. Gangsaas, Dagfin. "A Flight Control System for Post-Stall Maneuvering: The Design and Demonstration," *High-Angle-of-Attack Technology*, NASA Conference Publication 3149, pp. 983-1001, 1992.

12. Hamilton, Steven W. *QFT Digital Controller for an Unmanned Research Vehicle with an Improved Method for Choosing the Control Weightings*. MS thesis, Air Force Institute of Technology, Wright-Patterson AFB, OH, Dec. 1987.

13. Horowitz, Isaac. *Synthesis of Feedback Systems*. New York: Academic Press, 1963.

14. Horowitz, Isaac. "Quantitative Synthesis of Uncertain Multiple Input-Output Feedback Systems," *International Journal of Control*, vol. 30, pp. 81-106, 1979.

190

15. Horowitz, Isaac and Clayton Loecher. "Design of a 3x3 Multivariable Feedback System with Large Plant Uncertainty," *International Journal of Control*, vol. 33, pp. 677-699, 1981.

16. Horowitz Isaac. "Improved Design Technique for Uncertain Multiple-Input-Multiple-Output Feedback Systems," *International Journal of Control*, vol. 36, pp. 977-988, 1982.

17. Houpis, Constantine H. *Quantitative Feedback Theory (QFT) -- Technique for Designing Multivariable Control Systems.* Technical Report, Flight Dynamics Laboratory, Wright-Patterson AFB, OH, Jan. 1987. AFWAL-TR-86-3107.

18. Migyanko, Barry S. *Design of Integrated Flight /Propulsion Control Laws of a STOL Aircraft During Approach and Landing Using Quantitative Feedback Theory.* MS thesis, Air Force Institute of Technology, Wright-Patterson AFB, OH, Dec. 1986.

19. Military Specification -- Flying Qualities of Piloted Aircraft. MIL-STD-1797A. 30 Jan. 1990.

20. Pachter, Meir. Associate Professor of Electrical Engineering, Air Force Institute of Technology, Wright-Patterson AFB, OH. Personal Conversation. Jan. through Oct. 1993.

21. Pahle, Joseph W., Bruce Powers, Victoria Regenie and Vince Chacon. "Research Flight-Control System Development for the F-18 High Alpha Research Vehicle," *High-Angle-of-Attack Technology*, NASA Conference Publication 3149, pp. 1219-1239, 1992.

22. Roskam, J. *Airplane Flight Dynamics and Automatic Flight Controls.* Lawrence, KS: Roskam Aviation and Engineering Corp., 1979.

23. Russell, Harvey H. *Design of Robust Controllers for a Multiple Input-Multiple Output Control System with Uncertain Parameters Application to the Lateral and Longitudinal Modes of the KC-135 Transport Aircraft.* MS thesis, Air Force Institute of Technology, Wright-Patterson AFB, OH, Dec. 1984.

24. Sating, Richard R. *Development of an Analog MIMO Quantitative Feedback Theory (QFT) CAD Package.* MS thesis, Air Force Institute of Technology, Wright-Patterson AFB, OH, Jun. 1992.

25. Sating, Richard R. *MIMO/QFT CAD Program -- User's Manual* (2nd Edition). Air Force Institute of Technology, Wright-Patterson AFB, OH, Jul. 27 1993.

26. Schneider, Dean L. *QFT Digital Flight Control Design as Applied to the AFTI/F16.* MS thesis, Air Force Institute of Technology, Wright-Patterson AFB, OH, Jun. 1986.

27. Scott, William B. and Michael Mecham. "Evaluations of X-29 High-AOA Regime Show Promise for Future Fighters," *Aviation Week & Space Technology*. Jan. 6 1992, pp. 50-51.

28. Snell, S.A., Enns, D.F., and Garrard, W.L. "Nonlinear Inversion Flight Control for a Supermaneuverable Aircraft," *Journal of Guidance, Control, and Dynamics*, Vol.15, No.4, pp.976-984, 1992.

29. Wheaton, David G. *Automatic Flight Control System Design for an Unmanned Research Vehicle using Discrete Quantitative Feedback Theory.* MS thesis, Air Force Institute of Technology, Wright-Patterson AFB, OH, Dec. 1990.

Vita

Captain Kevin E. Boyum was born on 29 April 1967 in Mankato, Minnesota. He graduated from James Madison High School in Vienna, Virginia in 1985, and matriculated to the Virginia Military Institute (VMI) in the same year. He graduated from VMI with a Bachelor of Science Degree in Electrical Engineering and as valedictorian of his class in May 1989. Upon graduation he received a Regular Commission in the United States Air Force and was assigned to the Armament Laboratory, Eglin AFB, Florida, where he performed low-observable air-to-ground missile airframe design, analysis, and flight testing. In May 1992 he entered the Air Force Institute of Technology (AFIT) School of Engineering. Upon graduation from AFIT he will be assigned to the F-22 Systems Program Office, Logistics Support at McClellan AFB, Sacramento, CA.

Permanent Address: 403 Orleans Circle SW
Vienna, VA 22180

1. AGENCY USE ONLY (Leave blank)	2. REPORT DATE	3. REPORT TYPE AND DATES COVERED
	December 1993	Master's Thesis

4. TITLE AND SUBTITLE
EVALUATION OF A MODERATE ANGLE OF ATTACK
ROLL OF A DUAL ENGINE, THRUST VECTORING
AIRCRAFT USING QUANTITATIVE FEEDBACK THEORY

5. FUNDING NUMBERS

6. AUTHOR(S)
Kevin E. Boyum, Captain, USAF

7. PERFORMING ORGANIZATION NAME(S) AND ADDRESS(ES)

Air Force Institute of Technology, WPAFB, OH 45433

8. PERFORMING ORGANIZATION REPORT NUMBER

AFIT/GE/ENG/93D-01

9. SPONSORING / MONITORING AGENCY NAME(S) AND ADDRESS(ES)

Capt. Stuart S. Sheldon
WL/FIGS
Wright-Patterson AFB OH, 45433

10. SPONSORING / MONITORING AGENCY REPORT NUMBER

11. SUPPLEMENTARY NOTES

12a. DISTRIBUTION / AVAILABILITY STATEMENT

Approved for public release; distribution unlimited

12b. DISTRIBUTION CODE

13. ABSTRACT (Maximum 200 words)

This thesis develops an innovative approach to the design of a flight control system for performing the large-amplitude velocity vector roll maneuver at high angles of attack (AOAs). A six degree of freedom aircraft model is developed from the fundamental nine-state equations of motion using a modified linearization technique. The MIMO (multiple-input multiple-output) Quantitative Feedback Theory (QFT) robust control design technique is then used to jointly address the system nonlinearities present in this maneuver and the changes in the system parameters due to changes in flight condition, treating them as structured uncertainty in the design of a three-axis rate-commanded control system. The development of a weighting matrix, based on the fundamentals of the aileron-rudder interconnect, aids in this design process. Nonlinear six degree-of-freedom closed-loop control system simulations demonstrate the accuracy of the developed models, the validity of the QFT designed compensator and prefilter, and the successful initiation and arrest of the velocity vector roll maneuver.

14. SUBJECT TERMS

QFT, Velocity Vector Roll, High Angle of Attack, Flight Control

15. NUMBER OF PAGES
205

16. PRICE CODE

17. SECURITY CLASSIFICATION OF REPORT	18. SECURITY CLASSIFICATION OF THIS PAGE	19. SECURITY CLASSIFICATION OF ABSTRACT	20. LIMITATION OF ABSTRACT
Unclassified	Unclassified	Unclassified	UL